

PYRAZOLYL LIGANDS IN MIXED METAL COMPLEXES

By

EMMANUEL C. ONYIRIUKA

B.S., Adams State Colorado, 1980

M.S., University of California, 1982

A THESIS SUBMITTED IN PARTIAL FULFILLMENT OF

THE REQUIREMENTS FOR THE DEGREE OF

DOCTOR OF PHILOSOPHY

in

THE FACULTY OF GRADUATE STUDIES

(Department of Chemistry)

We accept this thesis as conforming

to the required standard

THE UNIVERSITY OF BRITISH COLUMBIA

September 1986

© Emmanuel C. Onyiriuka, 1986

90

In presenting this thesis in partial fulfilment of the requirements for an advanced degree at the University of British Columbia, I agree that the Library shall make it freely available for reference and study. I further agree that permission for extensive copying of this thesis for scholarly purposes may be granted by the head of my department or by his or her representatives. It is understood that copying or publication of this thesis for financial gain shall not be allowed without my written permission.

Department of CHEMISTRY

The University of British Columbia  
1956 Main Mall  
Vancouver, Canada  
V6T 1Y3

Date Sept 23, 1986

ABSTRACT

The anions  $\text{LMo(CO)}_3^-$  ( $\text{L} = \text{MeGapz}_3$  or  $\text{MeGa(3,5-Me}_2\text{pz)}_3$ ) have been isolated as the  $\text{Na}^+$ ,  $\text{Et}_4\text{N}^+$  or  $\text{HAsPh}_3^+$  salts and the solution structures of the  $\text{Na}^+$  salts in THF have been defined by analysis of the  $\nu_{\text{CO}}$  ir spectra. Ion-pair interaction of the  $\text{LMo(CO)}_3^-$  anion with  $\text{Na}^+$  cation in THF solution is apparent from the spectroscopic evidence obtained. The  $\text{MeGapz}_3\text{Mo(CO)}_3^-$  anion reacted with HCl or EtBr to give the seven-coordinate  $[\text{MeGapz}_3]\text{-Mo(CO)}_3\text{R}$  ( $\text{R} = \text{H}$  or Et) complexes. However, with MeI or PhCOCl complexes of the type  $[\text{MeGapz}_3]\text{Mo(CO)}_2(\eta^2\text{-COR})$  ( $\text{R} = \text{Me}$  or Ph) were obtained.

The reactions of the  $\text{LMo(CO)}_3^-$  ions ( $\text{L} = \text{MeGapz}_3$ ,  $\text{HBpz}_3$  or  $\text{Me}_2\text{Gapz(0-CH}_2\text{CH}_2\text{NMe}_2)$ ) with a variety of transition metal halide species have yielded complexes with transition metal-transition metal bonds. The X-ray crystal structures of two such complexes  $[\text{MeGapz}_3]\text{Mo(CO)}_3\text{Cu(PPh}_3)$  and  $[\text{MeGapz}_3]\text{Mo(CO)}_3\text{Rh(PPh}_3)_2$  have been determined. The former complex provides a rare example of a 3:3:1, or capped octahedral structure, with a short (mean) Mo-Cu distance of 2.513(9)Å. The latter compound displays one terminal and two bridging CO ligands and a Mo-Rh distance of 2.6066(5)Å.

Transition metal-group 14 (Si, Ge or Sn) element bonded complexes of the type  $[\text{MeGapz}_3]\text{Mo(CO)}_3\text{M}'\text{Y}$  ( $\text{Y} = \text{Me}_3$  or  $\text{Ph}_3$ ,  $\text{M}' = \text{Ge}$  or  $\text{Sn}$ ;  $\text{Y} = \text{Me}_3$ ,  $\text{M}' = \text{Si}$ ;  $\text{Y} = \text{Me}_2\text{Cl}$ ,  $\text{M}' = \text{Sn}$ ) have been prepared from the reaction of the  $\text{MeGapz}_3\text{Mo(CO)}_3^-$  anion with the appropriate organo-group 14 chloride. In all the complexes, direct Mo-M' ( $\text{M}' = \text{Si}$ , Ge or Sn) single bonds are featured. The  $[\text{MeGapz}_3]\text{Mo(CO)}_3\text{SnMe}_2\text{Cl}$  complex shows an interesting solution behaviour in which a transition from a 3:4, or piano stool structure, to a 3:3:1, or

capped octahedral arrangement, is thought to occur. The 3:3:1 structure has been demonstrated in the solid state for the  $[\text{MeGapz}_3]\text{Mo}(\text{CO})_3\text{SnPh}_3$  compound by means of a crystal structure determination. The 'Mo-SnPh<sub>3</sub>' and the 'Mo-Cu' compounds discussed in this work are the first examples of such complexes incorporating either the  $\text{MeGapz}_3^-$ ,  $\text{HBpz}_3^-$  or  $\text{C}_5\text{H}_5^-$  ligands in which the 3:3:1 arrangement has been demonstrated unequivocally.

The novel tridentate unsymmetric ligands  $\text{Me}_2\text{GapzO}(\text{C}_5\text{H}_3\text{N})\text{CH}_2\text{NMe}_2^-$  ( $\text{L}_a^-$ ) and  $\text{Me}_2\text{GapzO}(\text{C}_9\text{H}_6\text{N})^-$  ( $\text{L}_q^-$ ) have been prepared and numerous transition metal compounds containing these ligands synthesized. The compounds  $\text{L}_a\text{M}(\text{CO})_3$  (M = Mn or Re) are the first examples of transition metal carbonyl complexes in which both the fac and mer arrangements of the unsymmetric ligand about the central metal have been found to co-exist in solution. The square planar rhodium(I) complex,  $\text{L}_q\text{Rh}(\text{CO})$  has been shown to add MeI oxidatively, followed by facile methyl migration reaction to produce the five-coordinate Rh(III) acetyl derivative,  $\text{L}_q\text{Rh}(\text{COMe})\text{I}$ . In contrast, the reaction of  $\text{L}_a\text{Rh}(\text{CO})$  with MeI, led to the six-coordinate Rh(III) oxidative addition product,  $\text{L}_a\text{Rh}(\text{Me})(\text{I})\text{CO}$ .

TABLE OF CONTENTS

	<u>Page</u>
ABSTRACT.....	ii
TABLE OF CONTENTS.....	iv
LIST OF TABLES.....	x
LIST OF FIGURES.....	xii
LIST OF ABBREVIATIONS.....	xvii
ACKNOWLEDGEMENT.....	xxi
CHAPTER I INTRODUCTION.....	1
1.1 General Introduction.....	1
1.2 General Techniques.....	14
1.2.1 Handling of Reagents.....	14
1.2.2 Starting Materials.....	15
i) Preparation of Trimethylgallium Me <sub>3</sub> Ga.....	15
ii) Preparation of Gallium Trichloride, GaCl <sub>3</sub> ..	16
iii) Preparation of Methylchlorogallane, MeGaCl <sub>2</sub> .....	18
iv) Preparation of the Tricarbonyltris- (acetonitrile)molybdenum(0), (MeCN) <sub>3</sub> Mo(CO) <sub>3</sub>	20
1.3 Physical Measurements.....	21
CHAPTER II THE MOLYBDENUM TRICARBONYL ANION [MeGapz <sub>3</sub> ]Mo(CO) <sub>3</sub> <sup>-</sup> ; SYNTHESIS AND CHARACTERIZATION OF ITS Na <sup>+</sup> , Et <sub>4</sub> N <sup>+</sup> AND HAsPh <sub>3</sub> <sup>+</sup> SALTS, AND INVESTIGATION OF THE REACTIVITY TOWARDS ALKYL HALIDES, PROTONATING SPECIES AND HALOGENS.	23
2.1 Introduction.....	23
2.2 Experimental.....	26

2.2.1	Starting Materials.....	26
2.2.2	Preparation of $\text{Na}^+\text{LMo}(\text{CO})_3^-$ (L = MeGapz <sub>3</sub> , MeGa(3,5-Me <sub>2</sub> pz) <sub>3</sub> ).....	26
2.2.3	Preparation of $[\text{Et}_4\text{N}]^+[\text{MeGapz}_3\text{Mo}(\text{CO})_3]^-$ .....	27
2.2.4	Preparation of $[\text{HAsPh}_3]^+[\text{LMo}(\text{CO})_3]^-$ (L = MeGapz <sub>3</sub> , MeGa(3,5-Me <sub>2</sub> pz) <sub>3</sub> ).....	28
2.2.5	Attempted Preparation of $[\text{MeGapz}_3]\text{Mo}(\text{CO})_3\text{H}$ using Acetic Acid.....	29
2.2.6	Preparation of $[\text{MeGapz}_3]\text{Mo}(\text{CO})_3\text{H}$ using HCl.....	30
2.2.7	Preparation of $[\text{MeGapz}_3]\text{Mo}(\text{CO})_3\text{D}$ .....	31
2.2.8	Preparation of $[\text{MeGapz}_3]\text{Mo}(\text{CO})_2(\eta^2\text{-COMe})$ .....	32
2.2.9	Attempted Preparation of $[\text{MeGapz}_3]\text{Mo}(\text{CO})_2-$ ( $\eta^2\text{-COPh}$ ).....	33
2.2.10	Preparation of $[\text{MeGapz}_3]\text{Mo}(\text{CO})_3\text{Et}$ .....	34
2.2.11	Attempted Preparation of $[\text{MeGapz}_3]\text{Mo}(\text{CO})_3\text{X}$ (X = Br, I).....	35
2.3	Results and Discussion.....	36
2.3.1	$\text{M}^+\text{LMo}(\text{CO})_3^-$ (L = MeGapz <sub>3</sub> , MeGa(3,5-Me <sub>2</sub> pz) <sub>3</sub> ; $\text{M}^+ = \text{Na}^+, \text{Et}_4\text{N}^+, \text{HAsPh}_3^+$ ) Salts.....	36
2.3.2	$[\text{MeGapz}_3]\text{Mo}(\text{CO})_3\text{H}$ .....	45
2.3.3	$[\text{MeGapz}_3]\text{Mo}(\text{CO})_2(\eta^2\text{-COR})$ (R = Me, Ph).....	49
2.3.4	$[\text{MeGapz}_3]\text{Mo}(\text{CO})_3\text{Et}$ .....	56
2.3.5	The $[\text{MeGapz}_3]\text{Mo}(\text{CO})_3\text{X}$ (X = Br, I) Complexes.....	63
2.4	Summary.....	63



CHAPTER IV	TRANSITION METAL-GROUP 14 ELEMENT BONDED COMPLEXES INCORPORATING POLY(1-PYRAZOLYL)GALLATE LIGANDS.....	104
4.1	Introduction.....	104
4.2	Experimental.....	105
4.2.1	Starting Materials.....	105
4.2.2	Preparation of $[\text{MeGapz}_3]\text{Mo}(\text{CO})_3\text{SiMe}_3$ .....	105
4.2.3	Preparation of $[\text{MeGapz}_3]\text{Mo}(\text{CO})_3\text{GeR}_3$ (R = Me, Ph).....	106
4.2.4	Preparation of $[\text{MeGapz}_3]\text{Mo}(\text{CO})_3\text{SnMe}_3$ .....	106
4.2.5	Preparation of $[\text{MeGapz}_3]\text{Mo}(\text{CO})_3\text{SnMe}_2\text{Cl}$ .....	107
4.2.6	Preparation of $[\text{MeGapz}_3]\text{Mo}(\text{CO})_3\text{SnPh}_3$ .....	107
4.2.7	Preparation of $\text{LSnMe}_3$ (L = $[\text{MeGapz}_3]$ or $[\text{MeGa}(3,5\text{-Me}_2\text{pz})_3]$ ).....	108
4.2.8	Preparation of $[\text{MeGapz}_3]\text{SnMe}_2\text{Cl}$ .....	109
4.3	Results and Discussion.....	110
4.3.1	$[\text{MeGapz}_3]\text{Mo}(\text{CO})_3\text{SiMe}_3$ .....	111
4.3.2	$[\text{MeGapz}_3]\text{Mo}(\text{CO})_3\text{GeR}_3$ (R = Me, Ph).....	115
4.3.3.	$[\text{MeGapz}_3]\text{Mo}(\text{CO})_3\text{SnR}_3$ (R = Me, Ph).....	117
4.3.4	$[\text{MeGapz}_3]\text{Mo}(\text{CO})_3\text{SnMe}_2\text{Cl}$ .....	122
4.3.5	$\text{LSnY}$ (L = $[\text{MeGapz}_3]$ , $[\text{MeGa}(3,5\text{-Me}_2\text{pz})_3]$ <sup>-</sup> , Y = $\text{Me}_3$ ; L = $[\text{MeGapz}_3]$ <sup>-</sup> , Y = $\text{Me}_2\text{Cl}$ ).....	129
4.4	Summary.....	130
CHAPTER V	TRANSITION METAL DERIVATIVES OF THE UNSYMMETRIC TRIDENTATE PYRAZOLYLGALLATE LIGANDS $[\text{Me}_2\text{Gapz}\cdot\text{O}(\text{C}_5\text{H}_3\text{N})\text{-}$ $\text{CH}_2\text{NMe}_2]$ <sup>-</sup> AND $[\text{Me}_2\text{GapzO}(\text{C}_9\text{H}_6\text{N})]$ <sup>-</sup> .....	131
5.1	Introduction.....	131

5.2	Experimental.....	133
5.2.1	Starting Materials.....	133
5.2.2	Preparation of $[\text{Me}_2\text{GaO}(\text{C}_5\text{H}_3\text{N})\text{CH}_2\text{NMe}_2]$ .....	133
5.2.3	Preparation of $[\text{Me}_2\text{GaO}(\text{C}_9\text{H}_6\text{N})]_2$ .....	136
5.2.4	Preparation of the ligand $\text{Na}^+[\text{Me}_2\text{GapzO}(\text{C}_5\text{H}_3\text{N})\text{-CH}_2\text{NMe}_2]^-$ ( $\text{Na}^+\text{L}_a^-$ ).....	138
5.2.5	Preparation of the Ligand $\text{Na}^+[\text{Me}_2\text{Gapz}\cdot\text{O}(\text{C}_9\text{H}_6\text{N})]^-$ ( $\text{Na}^+\text{L}_q^-$ ).....	139
5.2.6	Preparation of $\text{L}_a\text{Re}(\text{CO})_3$ .....	140
5.2.7	Preparation of $\text{L}_a\text{Mn}(\text{CO})_3$ .....	140
5.2.8	Preparation of $\text{L}_a\text{Ni}(\text{NO})$ .....	141
5.2.9	Preparation of $\text{L}_q\text{Re}(\text{CO})_3$ .....	141
5.2.10	Preparation of $\text{L}_q\text{Mn}(\text{CO})_3$ .....	142
5.2.11	Attempted Preparation of $\text{L}_q\text{Ni}(\text{NO})$ .....	142
5.2.12	Preparation of $\text{Mo}(\text{MeCN})_2(\eta^2\text{-C}_3\text{H}_5)(\text{CO})_2\text{Br}$ .....	143
5.2.13	Preparation of $\text{L}_a\text{Mo}(\text{CO})_2(\eta^2\text{-C}_3\text{H}_5)$ .....	143
5.2.14	Preparation of $\text{L}_q\text{Mo}(\text{CO})_2(\eta^3\text{-C}_3\text{H}_5)$ .....	144
5.2.15	Preparation of $\text{L}_a\text{Rh}(\text{CO})$ .....	144
5.2.16	Preparation of $\text{L}_q\text{Rh}(\text{CO})$ .....	145
5.2.17	Reaction of $\text{L}_a\text{Rh}(\text{CO})$ with $\text{MeI}$ .....	145
5.2.18	Reaction of $\text{L}_q\text{Rh}(\text{CO})$ with $\text{MeI}$ .....	146
5.2.19	Reaction of $\text{L}^*\text{Rh}(\text{CO})$ ( $\text{L}^* = \text{L}_a, \text{L}_q$ ) with $\text{I}_2$ .....	147
5.3	Results and Discussion.....	148
5.3.1	$[\text{Me}_2\text{GaO}(\text{C}_5\text{H}_3\text{N})\text{CH}_2\text{NMe}_2]$ .....	148

5.3.2	$[\text{Me}_2\text{GaO}(\text{C}_9\text{H}_6\text{N})]_2$ .....	154
5.3.3	$L_a\text{M}(\text{CO})_3$ (M = Mn; Re).....	159
5.3.4	$L_a\text{Ni}(\text{NO})$ .....	167
5.3.5	$L_q\text{M}(\text{CO})_3$ (M = Mn; Re).....	172
5.3.6	$L^*\text{Mo}(\text{CO})_2(\eta^3\text{-C}_3\text{H}_5)$ ( $L^* = L_a, L_q$ ).....	178
5.3.7	$L^*\text{Rh}(\text{CO})$ ( $L^* = L_a, L_q$ ).....	182
5.3.8	Reactivity of $L^*\text{Rh}(\text{CO})$ ( $L^* = L_a, L_q$ )	
	i) With MeI.....	188
	ii) With $\text{I}_2$ .....	195
5.4	Summary.....	197
CHAPTER VI CONCLUSION AND PERSPECTIVES.....		199
BIBLIOGRAPHY.....		203
APPENDIX I	STEREO DIAGRAMS, BOND LENGTHS AND BOND ANGLES OF SOME OF THE PREPARED DERIVATIVES.....	214
APPENDIX II	THEORETICAL INTENSITY PATTERNS FOR MASS SPECTROMETRIC ANALYSIS.....	230

LIST OF TABLES

<u>Table</u>	<u>Page</u>
I $\nu_{CO}$ ( $\text{cm}^{-1}$ ) Infrared data for $M^+L\text{Mo}(\text{CO})_3^-$ ( $L = \text{MeGapz}_3$ , $\text{MeGa}(3,5\text{-Me}_2\text{pz})_3$ , $M^+ = \text{Na}^+$ , $\text{Et}_4\text{N}^+$ , $\text{HAsPh}_3^+$ salts).....	39
II Ir carbonyl stretching frequencies of some $L\text{Mo}(\text{CO})_3\text{Me}$ complexes ( $L = \eta\text{-C}_5\text{H}_5$ , $\eta\text{-C}_5\text{Me}_5$ , $\pi\text{-C}_9\text{H}_7$ , $\text{HBpz}_3$ , $\text{MeGapz}_3$ ).....	51
III Physical data for the complexes $L\text{Mo}(\text{CO})_3\text{MY}$ .....	72
IV Physical data for $[\text{MeGapz}_3]\text{Mo}(\text{CO})_3\text{M}'\text{Y}$ ( $M' = \text{Si}$ , $\text{Ge}$ , $\text{Sn}$ ).....	114
V 400 MHz $^1\text{H}$ nmr data for $\text{HO}(\text{C}_5\text{H}_3\text{N})\text{CH}_2\text{NMe}_2$ in $\text{C}_6\text{D}_6$ solution.....	134
VI 400 MHz $^1\text{H}$ nmr data for $\text{Me}_2\text{GaO}(\text{C}_5\text{H}_3\text{N})\text{CH}_2\text{NMe}_2$ in $\text{C}_6\text{D}_6$ solution.	135
VII 400 MHz $^1\text{H}$ nmr data for $\text{HO}(\text{C}_9\text{H}_6\text{N})$ in $\text{C}_6\text{D}_6$ solution.....	137
VIII 400 MHz $^1\text{H}$ nmr data for $[\text{Me}_2\text{GaO}(\text{C}_9\text{H}_6\text{N})]_2$ in $\text{C}_6\text{D}_6$ solution.....	138
IX Mass spectral data of $[\text{Me}_2\text{GaO}(\text{C}_5\text{H}_3\text{N})\text{CH}_2\text{NMe}_2]$ .....	151
X Mass spectral data of $'[\text{Me}_2\text{GaO}(\text{C}_9\text{H}_6\text{N})]'$ .....	154
XI Comparison of Ga-N and Ga-O bond lengths in four and five coordinate gallium compounds.....	158
XII Physical data for the complexes $L_a\text{MT}$ (where $L_a = \text{Me}_2\text{Gapz}\cdot\text{O}-(\text{C}_5\text{H}_3\text{N})\text{CH}_2\text{NMe}_2$ ).....	161
XIII Mass spectral data of $[\text{Me}_2\text{GapzO}(\text{C}_5\text{H}_3\text{N})\text{CH}_2\text{NMe}_2]\text{Mn}(\text{CO})_3$ .....	165
XIV Mass spectral data of $[\text{Me}_2\text{GapzO}(\text{C}_5\text{H}_3\text{N})\text{CH}_2\text{NMe}_2]\text{Re}(\text{CO})_3$ .....	166
XV Comparison of $\nu_{\text{NO}}$ values in selected four-coordinate $\{\text{MNO}\}^{10}$ complexes.....	169

<u>Table</u>		<u>Page</u>
XVI	Physical data for the complexes $L_qMT$ (where $L_q = Me_2Gapz \cdot O(C_9H_6N)$ ).....	174
XVII	Mass spectral data of $[Me_2Gapz \cdot O(C_9H_6N)]Mn(CO)_3$ .....	176
XVIII	Mass spectral data of $[Me_2Gapz \cdot O(C_9H_6N)]Re(CO)_3$ .....	177
XIX	Comparison of $\nu_{CO}$ values in some $LMO(CO)_2(\eta^3-C_3H_5)$ complexes..	178
XX	Comparison of $\nu_{CO}$ values in some $LRh(CO)$ complexes.....	184
XXI	Mass spectral data of $[Me_2Gapz \cdot O(C_9H_6N)]Rh(CO)$ .....	187
XXII	Mass spectral data of $[Me_2Gapz \cdot O(C_9H_6N)]Rh(COMe)I$ .....	192
XXIII	Mass spectral data of $[Me_2Gapz \cdot O(C_9H_6N)]Rh(COMe)I$ (Cont'd)....	193
XXIV	Comparison of $\nu_{CO}$ values in $LRhI_2(CO)$ complexes.....	196

LIST OF FIGURES

<u>Figure</u>		<u>Page</u>
1	Pyrazole.....	1
2	Deprotonation of pyrazole.....	2
3	Monodentate coordination of pyrazole.....	3
4	Coordination modes of the pyrazolide anion.....	3
5	Preparation of the Poly(1-pyrazolyl)borate ligand systems.....	6
6	Boat conformation of the bis(1-pyrazolyl)borate bidentate metal complex.....	7
7	Preparation of $\text{Me}_2\text{Gapz}_2^-$ ligand.....	9
8	General representation for the unsymmetrical tridentate organogallate ligand.....	12
9	Apparatus for the preparation of $\text{GaCl}_3$ .....	17
10	Apparatus for the preparation of $\text{MeGaCl}_2$ .....	19
11	Ir spectrum of $\text{M}^+\text{MeGapz}_3\text{Mo}(\text{CO})_3^-$ salts in the $\nu_{\text{CO}}$ region. a. $\text{M}^+ = \text{Na}^+$ in THF. b. $\text{M}^+ = \text{Na}^+$ in $\text{CH}_2\text{Cl}_2$ . c. $\text{M}^+ = \text{Et}_4\text{N}^+$ in $\text{CH}_2\text{Cl}_2$ . d. $\text{M}^+ = \text{HAsPh}_3^+$ in $\text{CH}_2\text{Cl}_2$ .....	38
12	Proposed structures for the interactions of $\text{MeGapz}_3\text{Mo}(\text{CO})_3^-$ anion with $\text{Na}^+$ cation in THF solution. a. Unperturbed anion b. Perturbed anion.....	40
13	Proposed cation ( $\text{Na}^+$ ) interaction with $\text{MeGapz}_3\text{Mo}(\text{CO})_3^-$ anion, external to the Mo coordination sphere in THF. a. M.O. description of CO electron density. b. Linear interaction. c. Non-linear interaction.....	42

<u>Figure</u>	<u>Page</u>
14	80 MHz $^1\text{H}$ spectrum of $[\text{HAsPh}_3]^+[\text{MeGapz}_3\text{Mo}(\text{CO})_3]^-$ in $\text{d}_6$ -acetone 44
15	Ir spectra of the carbonyl stretching frequency region observed during the reaction of $\text{MeGapz}_3\text{Mo}(\text{CO})_3^-$ with $\text{MeI}$ ..... 53
16	80 MHz $^1\text{H}$ nmr spectrum of $[\text{MeGapz}_3]\text{Mo}(\text{CO})_2(\eta^2\text{-COME})$ in $\text{d}_6$ -acetone solution..... 55
17	270 MHz $^1\text{H}$ nmr spectrum of $[\text{MeGapz}_3]\text{Mo}(\text{CO})_3\text{Et}$ in $\text{d}_6$ -acetone solution..... 60
18	Various isomers of the seven-coordinate $[\text{MeGapz}_3]\text{Mo}(\text{CO})_3\text{Et}$ .... 62
19	Room temperature 100 MHz $^1\text{H}$ nmr spectrum of $[\text{MeGapz}_3]\text{Mo}(\text{CO})_3\text{Rh}(\text{PPh}_3)_2$ in $\text{C}_6\text{D}_6$ solution..... 80
20	Molecular structure of $[\text{MeGapz}_3]\text{Mo}(\text{CO})_3\text{Rh}(\text{PPh}_3)_2$ ..... 81
21	Proposed bonding scheme for $[\text{MeGapz}_3]\text{Mo}(\text{CO})_3\text{Rh}(\text{PPh}_3)_2$ ..... 82
22	Possible structure of $[\text{MeGapz}_3]\text{Mo}(\text{CO})_3\text{Cu}(\text{PPh}_3)$ as suggested by the ir data..... 84
23	Molecular structures of $[\text{MeGapz}_3]\text{Mo}(\text{CO})_3\text{Cu}(\text{PPh}_3)$ ..... 86
24	Possible interaction between the Mo-Cu $\pi$ bond and the $\pi^*$ orbital of the CO ligand in the complex $[\text{MeGapz}_3]\text{Mo}(\text{CO})_3\text{Cu}(\text{PPh}_3)$ ..... 88
25	The structure of a linear semi-bridging CO type bonding..... 89
26	Proposed bonding scheme for $[\text{MeGapz}_3]\text{Mo}(\text{CO})_3\text{Pt}(\text{Me})(\text{PPh}_3)$ ..... 95
27	80 MHz $^1\text{H}$ nmr spectrum of $[\text{MeGapz}_3]\text{Mo}(\text{CO})_3\text{ZrCl}_3$ in $\text{C}_6\text{D}_6$ solution..... 97
28	Possible molecular arrangements for the $[\text{MeGapz}_3]\text{Mo}(\text{CO})_3\text{M}'\text{Cl}_3$ ( $\text{M}' = \text{Zr}$ or $\text{Hf}$ ) complexes..... 98

<u>Figure</u>	<u>Page</u>
29	Ir spectrum of $[\text{MeGapz}_3]\text{Mo}(\text{CO})_3\text{HfCl}_3$ in $\text{CH}_2\text{Cl}_2$ solution..... 99
30	Possible molecular arrangement for the complex $[\text{MeGapz}_3\text{Mo}(\text{CO})_3]_2\text{Hg}$ ..... 100
31	The $\nu_{\text{CO}}$ region of the ir spectrum of $[\text{MeGapz}_3]\text{Mo}(\text{CO})_3\text{SiMe}_3$ in $\text{CH}_2\text{Cl}_2$ solution..... 113
32	270 MHz $^1\text{H}$ nmr spectrum of $[\text{MeGapz}_3]\text{Mo}(\text{CO})_3\text{GePh}_3$ in $\text{C}_6\text{D}_6$ solution..... 116
33	Room temperature 80 MHz $^1\text{H}$ nmr spectrum of $[\text{MeGapz}_3]\text{-}$ $\text{Mo}(\text{CO})_3\text{SnMe}_3$ in $d_8$ -toluene..... 119
34	Molecular structure of $[\text{MeGapz}_3]\text{Mo}(\text{CO})_3\text{SnPh}_3$ ..... 120
35	Room temperature 80 MHz $^1\text{H}$ nmr spectra of $[\text{MeGapz}_3]\text{Mo}(\text{CO})_3\text{-}$ $\text{SnMe}_2\text{Cl}$ , showing the change with time..... 123
36	Possible molecular arrangements for the $[\text{MeGapz}_3]\text{Mo}(\text{CO})_3\text{-}$ $\text{SnMe}_2\text{Cl}$ complex in solution..... 125
37	Temperature dependent 300 MHz $^1\text{H}$ nmr spectrum of $[\text{MeGapz}_3]\text{Mo}(\text{CO})_3\text{-}$ $\text{SnMe}_2\text{Cl}$ in $d_8$ -toluene solution ..... 126
38	Partial mass spectrum of $[\text{MeGapz}_3]\text{Mo}(\text{CO})_3\text{SnMe}_2\text{Cl}$ ..... 128
39	The unsymmetric organogallate ligands $[\text{Me}_2\text{Gapz}\cdot\text{O}(\text{C}_5\text{H}_3\text{N})\text{-}$ $\text{CH}_2\text{NMe}_2]^-$ ( $\text{L}_a^-$ ), and $[\text{Me}_2\text{Gapz}\cdot\text{O}(\text{C}_9\text{H}_6\text{N})]^-$ ( $\text{L}_q^-$ )..... 132
40	Molecular structure of $[\text{Me}_2\text{Ga}\cdot\text{O}(\text{C}_5\text{H}_3\text{N})\text{CH}_2\text{NMe}_2]$ ..... 149
41	Comparison of the Ga-N bond lengths in the dimethylgallium compounds..... 150
42	80 MHz $^1\text{H}$ nmr spectrum of $\text{HO}(\text{C}_5\text{H}_3\text{N})\text{CH}_2\text{NMe}_2$ in $\text{C}_6\text{D}_6$ solution... 152

<u>Figure</u>	<u>Page</u>	
43	400 MHz $^1\text{H}$ nmr spectrum of $\text{Me}_2\text{GaO}(\text{C}_5\text{H}_3\text{N})\text{CH}_2\text{NMe}_2$ in $\text{C}_6\text{D}_6$ solution.....	153
44	400 MHz $^1\text{H}$ nmr spectrum of $\text{HO}(\text{C}_9\text{H}_6\text{N})$ in $\text{C}_6\text{D}_6$ solution.....	155
45	80 MHz $^1\text{H}$ nmr spectrum of $\text{Me}_2\text{GaO}(\text{C}_9\text{H}_6\text{N})$ in $\text{C}_6\text{D}_6$ solution.....	156
46	Molecular structure of $[\text{Me}_2\text{GaO}(\text{C}_9\text{H}_6\text{N})]_2$ .....	157
47	Ir spectrum in the $\nu_{\text{CO}}$ region of $[\text{Me}_2\text{GapzO}(\text{C}_5\text{H}_3\text{N})\text{CH}_2\text{NMe}_2]\text{Mn}(\text{CO})_3$ in cyclohexane solution.....	160
48	80 MHz $^1\text{H}$ nmr spectrum of $[\text{Me}_2\text{GapzO}(\text{C}_5\text{H}_3\text{N})\text{CH}_2\text{NMe}_2]\text{Re}(\text{CO})_3$ in $\text{C}_6\text{D}_6$ solution.....	162
49	Proposed conformation of $[\text{Me}_2\text{GapzO}(\text{C}_5\text{H}_3\text{N})\text{CH}_2\text{NMe}_2]\text{M}(\text{CO})_3$ (M = Mn or Re).....	163
50	80 MHz room temperature $^1\text{H}$ nmr spectrum of $[\text{Me}_2\text{GapzO}(\text{C}_5\text{H}_3\text{N})\text{CH}_2\text{NMe}_2]\text{Ni}(\text{NO})$ in $\text{CDCl}_3$ solution.....	168
51	Proposed mechanisms for the fluxional process observed for $[\text{Me}_2\text{GapzO}(\text{C}_5\text{H}_3\text{N})\text{CH}_2\text{NMe}_2]\text{Ni}(\text{NO})$ in $\text{CDCl}_3$ solution.....	171
52	Ir spectrum in the $\nu_{\text{CO}}$ region of $[\text{Me}_2\text{GapzO}(\text{C}_9\text{H}_6\text{N})]\text{Mn}(\text{CO})_3$ in cyclohexane solution.....	172
53	80 MHz $^1\text{H}$ nmr spectrum of $[\text{Me}_2\text{GapzO}(\text{C}_9\text{H}_6\text{N})]\text{Re}(\text{CO})_3$ in $\text{C}_6\text{D}_6$ solution.....	175
54	80 MHz $^1\text{H}$ nmr spectrum of $[\text{Me}_2\text{GapzO}(\text{C}_9\text{H}_6\text{N})]\text{Mo}(\text{CO})_2(\eta^3\text{-C}_3\text{H}_5)$ in $\text{C}_6\text{D}_6$ solution.....	180
55	Proposed reaction sequence for the formation of $\text{L}^*\text{Rh}(\text{CO})$ ( $\text{L}^* = \text{L}_a, \text{L}_q$ ) complexes.....	183

<u>Figure</u>		<u>Page</u>
56	80 MHz $^1\text{H}$ nmr spectrum of $[\text{Me}_2\text{GapzO}(\text{C}_9\text{H}_6\text{N})]\text{Rh}(\text{CO})$ in $\text{C}_6\text{D}_6$ solution.....	186
57	Proposed reaction sequence for the formation of $[\text{Me}_2\text{GapzO}(\text{C}_9\text{H}_6\text{N})]\text{Rh}(\text{COMe})\text{I}$ .....	189
58	270 MHz $^1\text{H}$ nmr spectrum of $[\text{Me}_2\text{GapzO}(\text{C}_9\text{H}_6\text{N})]\text{Rh}(\text{COMe})\text{I}$ in $\text{CDCl}_3$ solution.....	191

LIST OF ABBREVIATIONS

The following abbreviations have been used throughout this thesis:

Å	Angstrom
amu	atomic mass unit(s)
Anal.	Analysis
bipy	2,2'-dipyridine, or bipyridine
br	broad
°C	degree Celsius
Calcd.	Calculated
cf	Latin confer (compare)
cm <sup>-1</sup>	wave number (reciprocal centimeters)
COD	cycloocta-1,5-diene
cont'd	continued
Cp	cyclopentadienyl, C <sub>5</sub> H <sub>5</sub>
d	doublet
dd	doublet of doublets
dec.	decrease
dppe	1,2-bis(diphenylphosphino)ethane
dppm	bis(diphenylphosphino)methane
e.g.	Latin exempli gratis (for example)
EHMO	Extended Huckel Molecular Orbital
E.I	electron impact

Et	ethyl
FAB	Fast Atom Bombardment
fac	facial
Fig.	Figure(s)
F.T.	Fourier Transform
g	gram(s)
h	hour(s)
$^1\text{H}$	proton
Hz	Hertz (cycles per second)
i.e.	Latin id est (that is)
inc.	increase
IR	infrared
J	magnetic resonance coupling constant
$L_a$	$\text{Me}_2\text{GapzO}(\text{C}_5\text{H}_3)\text{CH}_2\text{NMe}_2^-$
$L_q$	$\text{Me}_2\text{GapzO}(\text{C}_9\text{H}_6\text{N})^-$
Ltd	limited
m	multiplet
M	central (usually metal) atom in compound
m/e	mass to charge ratio
Me	methyl
3,5-Me <sub>2</sub> pz	3,5-dimethylpyrazolyl, $\text{C}_5\text{H}_7\text{N}_2$
mer	meridional
MHz	megahertz

min	minute(s)
mL	milliliter(s)
mmol	millimole(s)
MS	Mass Spectrometry
n	integer
nmr	nuclear magnetic resonance
P	parent
Ph	phenyl, $C_6H_5$
pKa	$-\log_{10}K_a$ ( $K_a$ =acid dissociation constant)
ppm	parts per million
pz	pyrazolyl, $C_3H_3N_2$
s	singlet
salen	bis-salicylaldehydeethylenediimine
t	triplet
THF	tetrahydrofuran
tmed	N,N,N',N'-tetramethylethylenediamine
U.B.C.	University of British Columbia
UV	ultraviolet
xs	excess
~	approximately
≥	greater than or equal to
Δ	reflux
η	Greek haptain (hapto = to fasten)
η'	monohapto

$\eta^2$	dihapto
$\eta^3$	trihapto
$\eta^5$	pentahapto
$\eta^6$	hexahapto
$\tau$	nmr chemical shift
$\mu$	bridging
$\nu$	IR stretching frequency

## ACKNOWLEDGEMENT

I wish to thank the faculty and technical staff of the Chemistry Department, especially to Dr. Steve Rettig (X-ray crystallography). I would also like to acknowledge the members of my Steering Committee; Drs. B.R. James, D. Dolphin and M. Fryzuk for their very constructive suggestions during the preparation of this thesis. Financial assistance from the Chemistry Department, in the form of a Teaching Assistantship is gratefully acknowledged.

My most sincere thanks are also extended to my family, whose support and patience was a constant source of encouragement. This thesis is dedicated to them.

Finally, I wish to express my gratitude to my research supervisor, Dr. Alan Storr for his guidance and support during the course of this work.

## CHAPTER 1

## INTRODUCTION

1.1 GENERAL INTRODUCTION

The five-membered diazole heterocyclic compound, pyrazole, was first prepared in the late nineteenth century [1]. By conventional heterocyclic nomenclature, numbering begins at the protonated nitrogen and proceeds in the direction of the second unprotonated nitrogen as shown in Figure 1.

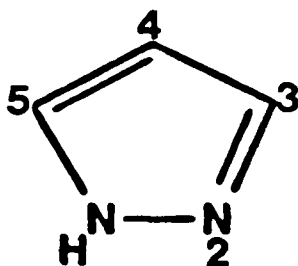


Figure 1. Pyrazole.

The three carbon atoms (C3, C4, C5) and N2 of the pyrazole nucleus contribute four  $\pi$ -electrons, and N1 which is uninvolved in the double bond

formation, donates its electron pair, thus creating an aromatic sextet of  $\pi$ -electrons. The colorless, sweetish smelling (unlike most amines), crystalline solid is hydrolytically, oxidatively, and thermally stable, due partly to its aromatic character, since it may be considered a Huckel '4n + 2' system (n = 1). The considerable aromatic character of the five-membered pyrazole ring has been borne out by molecular orbital calculations by Kaufman et al. [2].

Upon deprotonation of the acidic hydrogen attached to N1 ( $pK_a = 2.53$ ) [3] by appropriate bases, pyrazole becomes the resonance-stabilized pyrazolide anion (Figure 2).

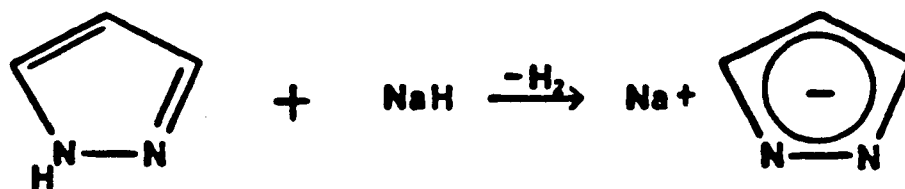


Figure 2. Deprotonation of pyrazole.

As a ligand, pyrazole can act as a neutral, monodentate, two-electron donor ligand via the lone pair on N2 in a similar manner to pyridine as shown in Figure 3.

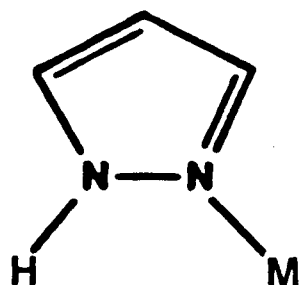


Figure 3. Monodentate coordination of pyrazole.

With the pyrazolide anion, interaction with suitable metals can occur via one of three possible coordination modes - monodentate,  $\eta^2$ -endobidentate and exobidentate modes, respectively (Figure 4).

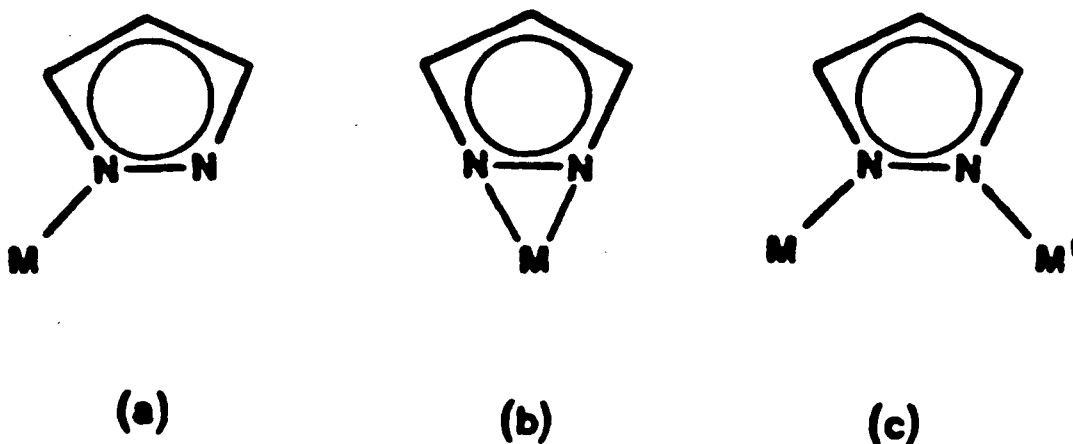


Figure 4. Coordination modes of the pyrazolide anion.

Relatively few examples of monodentate coordination of the pyrazolide anion to transition metals (Fig. 4(a)) have been reported e.g.,  $[M(pz)_2(L-L)]$  ( $M = Pt, Pd$ ;  $L-L = dppe, bipy, COD$ ) [4] and  $(PPh_3)_2(CO)Ir-[3,5-(CF_3)_2pz]$  [5]. On the other hand, only one example of  $\eta^2$ -endobidentate coordination of the pyrazolide anion (Fig. 4(b)), has been reported in the literature. This unusual bonding mode exhibited by the compound structurally characterized as  $pzUCp_3$  [6] was interpreted as being reflective of i) the ionic character of the uranium nitrogen bonds as compared to a d-block transition element, and ii) the larger atomic radius of uranium. The most commonly found coordination mode is where the pyrazolide anion acts as an 'exobidentate' bridge between two metals, which may be identical or different (Fig. 4(c)). Numerous examples of stable compounds containing such 'exobidentate' bridges have been reported in the literature (e.g., [7-11]).

Upon coordination to certain main group elements, monodentate interactions (as depicted in Fig. 4(a)) of the pyrazolide anion become more prevalent. For example, coordination to boron gives the poly(1-pyrazolyl)borates [12]; similarly to carbon, the poly(1-pyrazolyl)-alkanes [13], to gallium the poly(1-pyrazolyl)gallates [14], and recently the tris(1-pyrazolyloethyl)amine were obtained by coordination to nitrogen [15]. The most widely studied of these main group pyrazolyl ligand systems are the uninegative poly(1-pyrazolyl)borates with the general formula  $[R_nB(pz)_{4-n}]^-$  (where  $R = H, alkyl, aryl, pyrazolyl, N_2C_3H_3$ ; and  $n = 0, 1, 2$ ). These are a broad and versatile class of uninegative ligands whose coordinative ability is a consequence of favourable

electronic and geometric factors. The combination of these factors has led to numerous metal complexes incorporating the poly(1-pyrazolyl)borate ligands, an area that has been the subject of a number of review articles [7,16,17].

These fairly robust ligand systems are readily prepared by the reaction of an alkali metal borohydride with pyrazole, the extent of the reaction being dependent on the reaction temperature as shown in Figure 5 [12,18].

Although the salts of all three anions are air-stable and can be stored indefinitely in the solid state, the stability of the poly(1-pyrazolyl)borate species in solution decreases as the number of hydrogens attached to boron is increased.

The uninegative bidentate bispyrazolylborate anion ( $n = 2$ ), is formally analogous to the 1,3-diketónate ion, both being uninegative four-electron donor ligands. A notable difference between both ligand systems is that while various associative equilibria i.e., monomer-dimer-trimer have been observed for the 1,3-diketónate metal complexes [19], the former reacts with metal ions to give monomeric bisbidentate complexes usually with the  $[B-(N-N)_2-M]$  ( $M =$  transition metal) six-membered ring in a boat conformation as shown in Figure 6 (e.g., [20,21]).

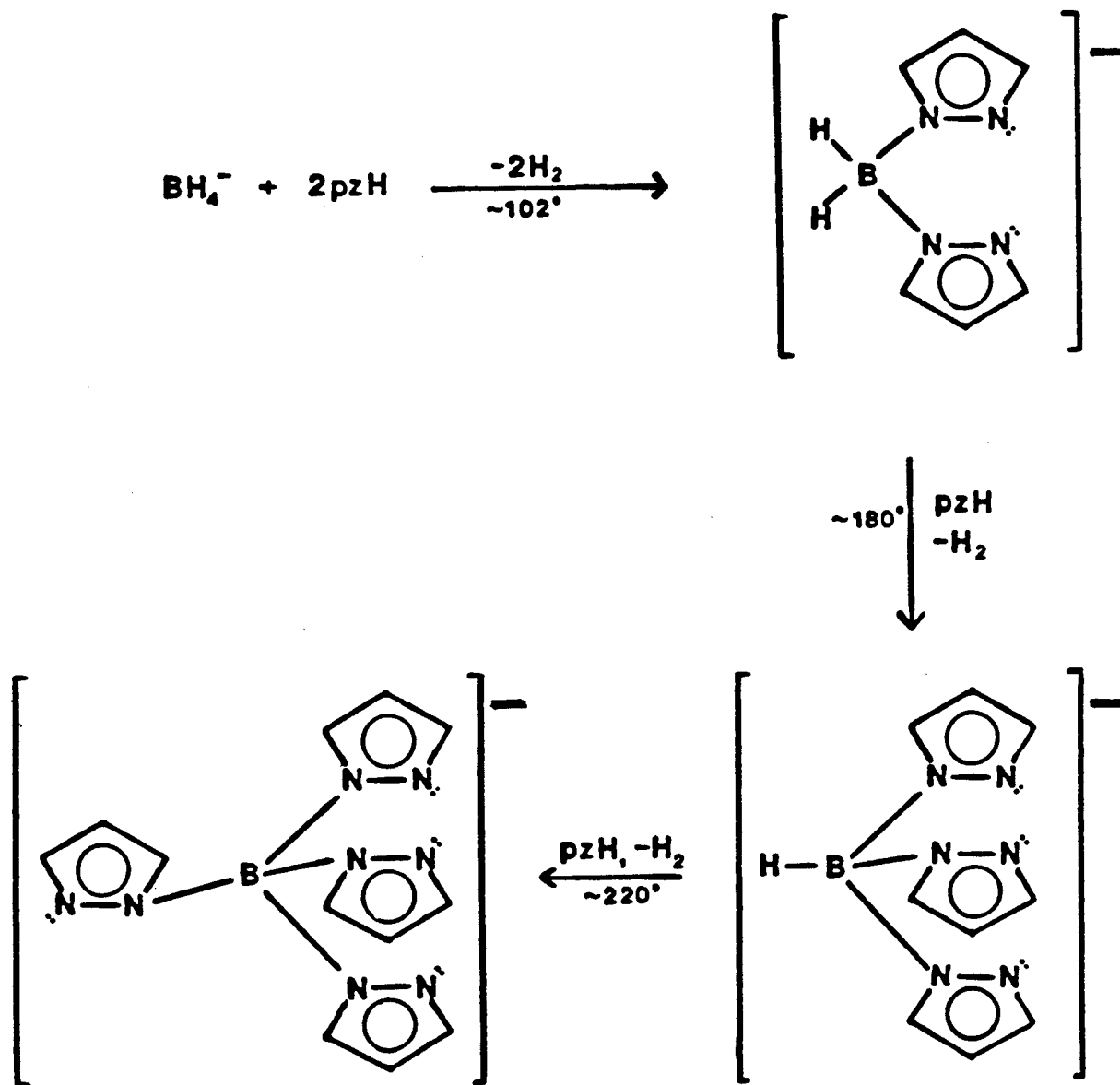


Figure 5. Preparation of the poly(1-pyrazolyl)borate ligand systems.

Of particular interest is the symmetrical uninegative, tridentate tris(1-pyrazolyl)borate anion  $\text{RBpz}_3^-$  ( $n = 1$ ), formally analogous to the



Figure 6. Boat conformation of the bis(1-pyrazolyl)borate bidentate metal complex.

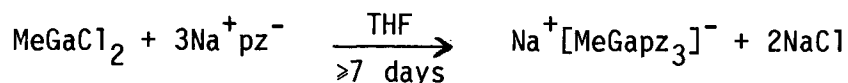
well known cyclopentadienide ion ( $\text{Cp}^-$ ) - both being uninegative, six-electron donor ligands which are considered to occupy three mutually cis positions in their octahedral metal derivatives. The presence of  $\text{RBpz}_3^-$  in place of  $\text{Cp}^-$  ligand has been found to impart unusual stability to the resulting metal derivatives. For example, the compound  $[\text{HBpz}_3]\text{CuCO}$  [22] is heat- and air-stable, while  $(\eta\text{-C}_5\text{H}_5)\text{CuCO}$  [23] is thermally unstable and air-sensitive. In another example, Clark and Manzer have succeeded in stabilizing a series of five-coordinate methylplatinum (II)-acetylene, allene and olefin complexes using the tridentate  $\text{RBpz}_3^-$

(R = H, Me, pyrazolyl,  $N_2C_3H_3$ ) [24,25] ligands. Such five-coordinate platinum(II) complexes are rare [26-30].

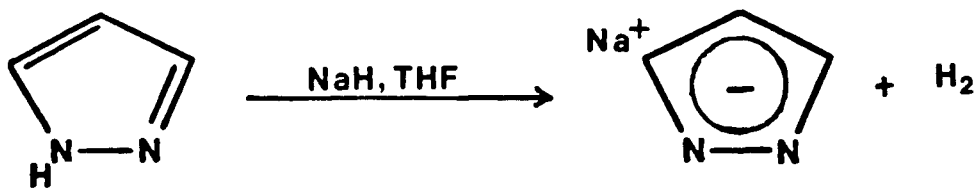
The mode of reactivity of  $RBpz_3^-$  ligand can be altered by the presence of alkyl substituents at the C(3) and C(5) positions of each pz ring. For example, the reaction of  $[HBpz_3]Mo(CO)_3^-$  with aryldiazonium cation  $ArN_2^+$ , gave the substitution product  $[HBpz_3]Mo(CO)_2(N_2Ar)$  (Ar = m- or p-fluorophenyl) [31]. In contrast, the reaction of  $[HB(3,5-Me_2pz)_3]Mo(CO)_3^-$  anion with aryldiazonium cation  $ArN_2^+$ , yielded the novel  $\eta^2$ -aroyl complex  $[HB(3,5-Me_2pz)_3]Mo(CO)_2(\eta^2-COAr)$  in acetonitrile [32], and the chloromethylidene complex  $[HB(3,5-Me_2pz)_3]Mo(CO)_2(\eta^1-CCl)$  in  $CH_2Cl_2$  [33], respectively.

The closely related dimethylbis(1-pyrazolyl)gallate ligand is prepared by the reaction of trimethylgallium with sodium pyrazolide followed by addition of pyrazole [14] as depicted in Figure 7.

The methyltris-(1-pyrazolyl)gallate  $MeGapz_3^-$  ligand is prepared by the reaction of methylchlorogallium with sodium pyrazolide according to the equation below [34].



Alkali metal salts of the poly(1-pyrazolyl)gallate anions are hygroscopic, white solids quite unlike the poly(1-pyrazolyl)borate salts which are air- and moisture-stable solids.



$\text{pzH}$   
 18hr reflux

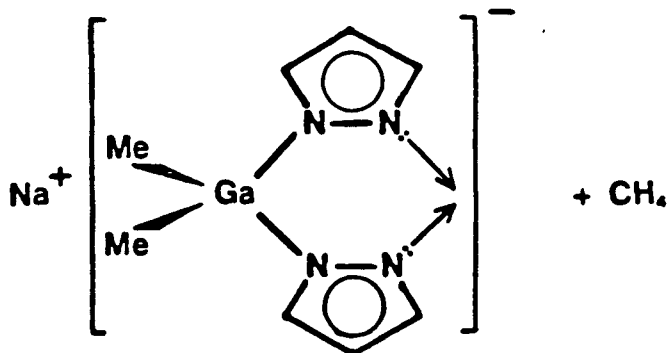


Figure 7. Preparation of  $\text{Me}_2\text{Ga}^-\text{pz}_2^-$  ligand.

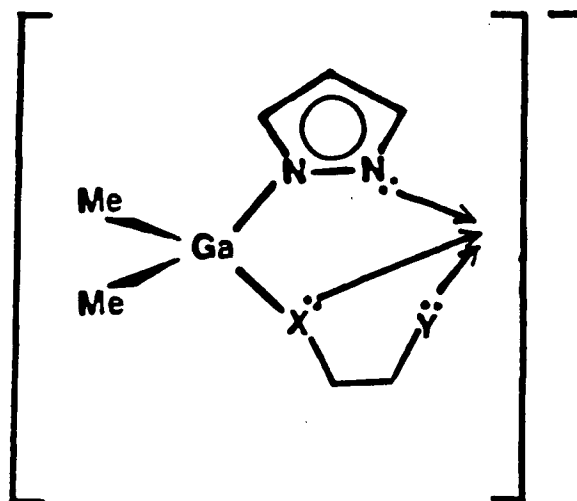
Although the coordination chemistry of the poly(1-pyrazolyl)gallate ligands parallels that of the boron systems, some important differences result from the introduction of gallium for boron in the ligand systems.

A more electron-rich transition metal center is created in the gallium complexes [34], with a greater degree of steric protection afforded the chelated metal due to the longer Ga-N bond ( $\sim 2.0\text{\AA}$  cf.  $\sim 1.5\text{\AA}$  for B-N) [34]. The gallium-based ligands occasionally undergo chemical transformations unknown in the analogous boron systems. For example, the ligand  $[\text{MeGa}(3,5\text{-Me}_2\text{pz})_3]^-$  readily converts to the less sterically demanding tris-chelating 'hydroxy' ligand  $[\text{MeGa}(3,5\text{-Me}_2\text{pz})_2(\text{OH})]^-$  in the attempted syntheses of the ' $\eta^3$ -allyl' complexes,  $[\text{MeGa}(3,5\text{-Me}_2\text{pz})_3]\text{M}(\text{CO})_2(\eta^3\text{-allyl})$  (where  $\text{M} = \text{Mo}$  or  $\text{W}$ , ' $\eta^3$ -allyl' =  $\eta^3\text{-C}_3\text{H}_5$ ,  $\eta^3\text{-C}_4\text{H}_7$ ) [35]. The gallium-based ligand systems are synthetically much easier to prepare since forcing-conditions (i.e., high temperatures) are generally unnecessary. Most importantly, the methyl groups on gallium appear as unique resonances at high fields ( $\sim 9\text{-}11\tau$ ) in the  $^1\text{H}$  nmr spectrum. Not only can these resonances act as  $^1\text{H}$  nmr probes but they also make spectral interpretation less complicated than in the boron systems.

The  $\text{RBpz}_3^-$  and  $\text{MeGapz}_3^-$  ligand systems are unique in themselves, being the only trigonal tridentate, uninegative six-electron donor ligands of approximate  $\text{C}_{3v}$  symmetry. The tripod-like structure of these ligands is ideally suited to occupy three mutually cis positions in octahedral metal complexes. Crystal structure determinations of  $[\text{HBpz}_3]_2\text{Co}$  [36],  $[\text{HBpz}_3]\text{SnMe}_3$  [37],  $[\text{HBpz}_3]\text{Mo}(\text{CO})_3$  radical species [38], and  $[\text{MeGapz}_3]_2\text{Ni}$  [39] do attest to this coordination geometry of the ligands about the metal centers in the above complexes. This uniqueness however poses the problem of finding appropriate known systems for direct comparison. The

various known tridentate donor tripod ligands of  $C_{3v}$  symmetry such as the 1,1,1-tris(aminomethyl)ethane and its N-methyl-substituted derivatives with the general formula  $CH_3-C-(CH_2-Z)_3$  (where  $Z = NH_2, NHMe, NMe_2$ ) [40] are inappropriate, being uncharged and thus, incapable of forming neutral bis-tridentate complexes analogous to the  $[RBpz_3]M$  compounds (where  $M =$  divalent transition metal e.g.,  $Mn^{2+}, Ni^{2+}, Fe^{2+}$ ). The uninegative, electronically tridentate cyclopentadienyl ion ( $Cp^-$ ), even though it forms  $\pi$ - rather than  $\sigma$ -bonded complexes typical of the tris(1-pyrazolyl)borate/-gallate ligands, still provides the closest approximation to the  $RBpz_3^-$ , and  $MeGapz_3^-$  ligands in terms of derivative chemistry. Hence the  $RBpz_3^-$ ,  $MeGapz_3^-$  and  $Cp^-$  ligands are likened to and compared to one another in several "isoelectronic" complexes.

A slight but significant deviation from the  $RBpz_3^-$  and  $MeGapz_3^-$  ligand systems came with the introduction of the novel unsymmetric, uninegative, tridentate, six-electron donor, gallium-containing ligand systems. These unsymmetric ligands incorporating a pyrazolyl moiety, in conjunction with a bifunctional donor group both being attached to a dimethylgallium grouping [41] (Figure 8), have yet no counterparts in the related pyrazolylborate chemistry.



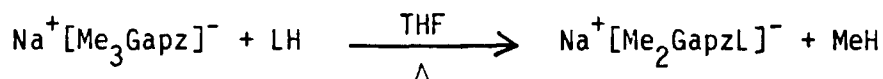
$X = O; Y = N \text{ or } S.$

$X = S; Y = N.$

Figure 8. General representation for the unsymmetrical tridentate organogallate ligand.

The ligand  $[\text{HB}(3,5\text{-Me}_2\text{pz})_2(\text{SAr})]^-$  ( $\text{Ar} = \text{C}_6\text{H}_4\text{-4-CH}_3$ ) [42], reported recently, is the first and the only known example of a poly(1-pyrazolyl)-borate ligand in which an additional donor functionality apart from the pyrazolyl groups is attached to boron.

The unsymmetric gallate ligands are prepared by the reaction of an active hydrogen-containing polyfunctional donor compound with the sodium salt of trimethylgallium pyrazolyl anion to eliminate methane gas according to the equation:-



LH = active hydrogen-containing compound

In contrast to  $\text{RBpz}_3^-$ ,  $\text{MeGapz}_3^-$  or  $\text{Cp}^-$  ligand systems which coordinate exclusively facial to metals, the unsymmetric gallate ligands have the flexibility to coordinate to metals in either a facial or meridional arrangement. Both of these geometries have been confirmed structurally by X-ray crystal analyses of metal complexes incorporating the unsymmetric gallate ligands [43,44].

Chapter II of this thesis reports on the synthesis and characterization of the molybdenum tricarbonyl anions  $\text{LMo}(\text{CO})_3^-$  ( $\text{L} = \text{MeGapz}_3$ ,  $\text{MeGa}(3,5\text{-Me}_2\text{pz})_3$ ) as their sodium, tetraethylammonium, and triphenylarsonium salts, and presents spectroscopic evidence for the interaction of the  $\text{LMo}(\text{CO})_3^-$  anion with the  $\text{Na}^+$  cation in THF. The reactivity of the  $\text{MeGapz}_3\text{Mo}(\text{CO})_3^-$  anion toward alkyl halides, benzoyl chloride, protonating species and halogens is also explored in this Chapter.

The reactivity of the  $\text{LMo}(\text{CO})_3^-$  anions ( $\text{L} = \text{HBpz}_3$ ,  $\text{MeGapz}_3$ ,  $[\text{Me}_2\text{Gapz}(\text{OCH}_2\text{CH}_2\text{NMe}_2)]$ ) toward Wilkinson's catalyst  $\text{RhCl}(\text{PPh}_3)_3$ , and also the reactivity of the  $\text{MeGapz}_3\text{Mo}(\text{CO})_3^-$  anion toward a variety of transition metal halide species are detailed in Chapter III. Complexes containing direct transition metal-transition metal bonds isolated from the reactions are discussed, and X-ray structural data are presented for two of the complexes  $[\text{MeGapz}_3]\text{Mo}(\text{CO})_3\text{Rh}(\text{PPh}_3)_2$  and  $[\text{MeGapz}_3]\text{Mo}(\text{CO})_3\text{Cu}(\text{PPh}_3)$ .

Chapter IV explores the reactivity of the  $\text{MeGapz}_3\text{Mo}(\text{CO})_3^-$  anion toward Group 14 (Si, Ge, Sn) alkyl or aryl halide species. Complexes featuring direct transition metal-group 14 element bonds are discussed and X-ray crystallographic analysis of the compound  $[\text{MeGapz}_3]\text{Mo}(\text{CO})_3\text{SnPh}_3$  is presented. Compounds isolated from the direct reaction of  $[\text{MeGapz}_3]^-$  and  $[\text{MeGa}(3,5\text{-Me}_2\text{pz})_3]^-$  ligands with organotin chlorides are also presented and discussed.

The synthesis, characterization and X-ray crystal structural determinations of the coordination compounds  $[\text{Me}_2\text{GaO}(\text{C}_5\text{H}_3\text{N})\text{CH}_2\text{NMe}_2]$ , and  $[\text{Me}_2\text{GaO}(\text{C}_9\text{H}_6\text{N})]_2$ , the syntheses of the two novel unsymmetric, tridentate pyrazolylgallate ligands,  $[\text{Me}_2\text{Gapz}\cdot\text{O}(\text{C}_5\text{H}_3\text{N})\text{CH}_2\text{NMe}_2]^-$ , ( $\text{L}_a^-$ ), and  $[\text{Me}_2\text{Gapz}\cdot\text{O}(\text{C}_9\text{H}_6\text{N})]^-$ , ( $\text{L}_q^-$ ), and the reactivity of the ligands towards a variety of transition metal halide species are the subject of Chapter V. In the same Chapter, the reactivity of  $\text{L}^*\text{Rh}(\text{CO})$  ( $\text{L}^* = \text{L}_a, \text{L}_q$ ) toward methyl iodide and molecular iodine is also discussed.

## 1.2 General Techniques

### 1.2.1 Handling of Reagents

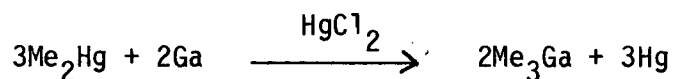
Since most of the materials were air-sensitive, all manipulations were carried out in a dry box (Vacuum/Atmospheres Corporation model DRI LAB HE-43-2), containing pre-purified nitrogen (Linde USP, Union Carbide Canada), and fitted with a Dritrain (model HE 493), or on a high vacuum line equipped with a duo-seal pump (Welch Scientific Company). Reactions

were carried out under an inert atmosphere in the dry box or in a nitrogen-blanketed atmosphere unless otherwise stated.

All reaction solvents were routinely dried by refluxing under  $N_2$ , followed by distillation according to literature methods [45,46]. The most frequently used solvents were dried as follows; THF over Na/benzophenone, and benzene over potassium by continuous refluxing in 2 liter still pots, collected prior to use or stored in the dry box under  $N_2$ . In the case of THF, the characteristic blue coloration of the benzophenone ketyl radical was taken as an indication of complete dryness. The less frequently used solvents  $CH_2Cl_2$ , hexane and acetonitrile were dried by refluxing over  $CaH_2$ ,  $CaSO_4$  and  $P_2O_5$ , respectively, followed by distillation.

### 1.2.2 Starting Materials

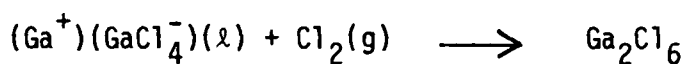
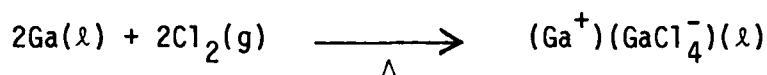
#### i) Preparation of Trimethylgallium, $Me_3Ga$ [47]



Trimethylgallium was prepared by the gallium metal-mercury alkyl exchange method. Typically, dimethylmercury (25 g, 108 mmol) was added to gallium metal (7.2 g, 103 mmol) and a catalytic amount of mercuric chloride placed in a Carius tube. The tube and its contents were then frozen to liquid nitrogen temperatures ( $\sim -196^\circ C$ ). The tube was then evacuated, flame-sealed at the constriction, and slowly warmed to room temperature. The tube was then stored for about one week at  $\sim 120^\circ C$  in a metal bomb apparatus. At this stage, the product  $Me_3Ga$ , which is a

colorless liquid, had separated from the mercury and excess gallium metal deposited at the bottom of the tube. The  $\text{Me}_3\text{Ga}$  was then carefully isolated and condensed into ampoules on the vacuum line. Its purity was checked by  $^1\text{H}$  nmr measurements. It was then used in subsequent reactions without further purification.

ii) Preparation of Gallium Trichloride,  $\text{GaCl}_3$  [48]



Gallium trichloride was prepared by direct reaction of the elements. Pure chlorine gas (Matheson) was dried by passing through concentrated sulfuric acid in a gas bubbler, after which the gas was passed into the glass apparatus shown in Figure 9. The gallium metal, about 22 grams was placed in A. The apparatus was flushed with chlorine gas, and the gallium metal slowly warmed to melting (m.p.  $29.78^\circ\text{C}$ ) using a bunsen flame. The molten gallium reacted with the chlorine, first giving a colorless liquid, gallium tetrachlorogallate,  $\text{Ga}_2\text{Cl}_4$  (m.p.  $170.5^\circ\text{C}$ ). The liquid  $\text{Ga}_2\text{Cl}_4$  disappeared upon addition of more chlorine, and finally gave a volatile white solid, gallium trichloride,  $\text{GaCl}_3$  (m.p.  $79^\circ\text{C}$ ).

The rate of flow of the chlorine gas and the rate of heating the molten gallium were adjusted so that most of the volatile  $\text{GaCl}_3$  was deposited in the cooled receiver boat C. After all the gallium had reacted (essentially 100%), any sublimate in A was driven into C by warming and flame-sealing the constriction at B. The apparatus was then

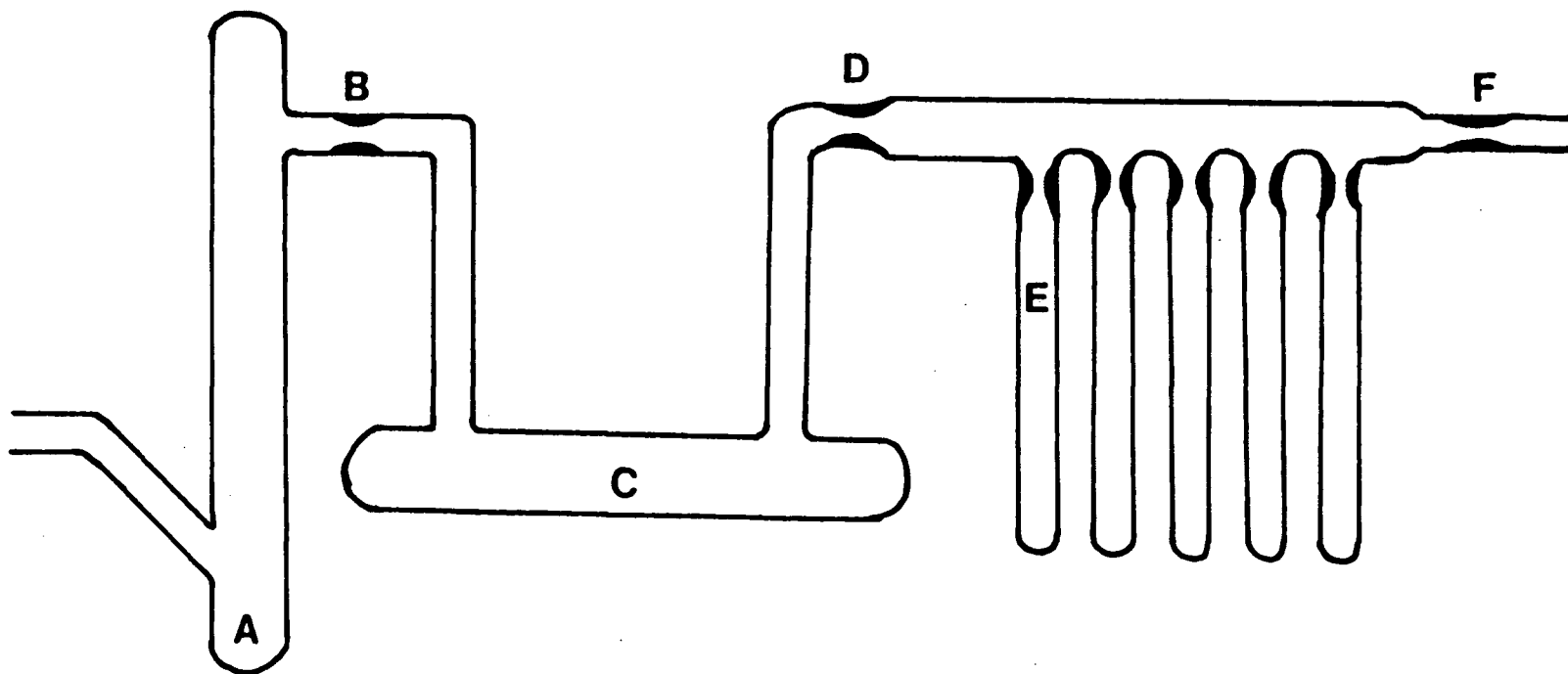
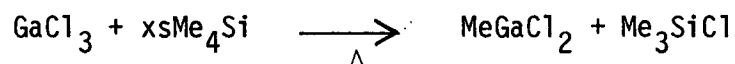


Figure 9. Apparatus for the preparation of GaCl<sub>3</sub>.

evacuated and flame-sealed at F. The crude halide was then re-sublimed into the ampoules E, and each sealed at their respective constrictions. Assuming a 100% yield (55 grams), the weight of gallium trichloride in each ampoule was then estimated. The gallium trichloride was found to remain stable indefinitely when stored in this manner.

iii) Preparation of methylchlorogallane, MeGaCl<sub>2</sub> [49]



An ampoule containing a known quantity of GaCl<sub>3</sub> was cracked open in the glove box and loaded into the left side-arm of the apparatus shown in Figure 10. This side-arm was capped and a tap adapter fitted onto the B24 joint. The apparatus was then evacuated via the tap adapter on the vacuum line, and bulb E was then frozen in liquid nitrogen. The constriction at A was flame-sealed and the GaCl<sub>3</sub> was melted by warming with a bunsen flame. The melted GaCl<sub>3</sub> was allowed to run down into bulb E, excess spectrograde tetramethylsilane was condensed into bulb E, and the apparatus flame-sealed at constrictions B and C. The apparatus and its contents were slowly warmed to room temperature, followed by placing in a hot water bath for several days. On cooling, white crystals of MeGaCl<sub>2</sub> were deposited at the bottom of the flask. The unreacted tetramethylsilane and the trimethylchlorosilane by-product were removed by rupturing the break-seal at D and condensing them into a liquid nitrogen solvent trap. The white crystals of MeGaCl<sub>2</sub> isolated (~95% yield) were divided

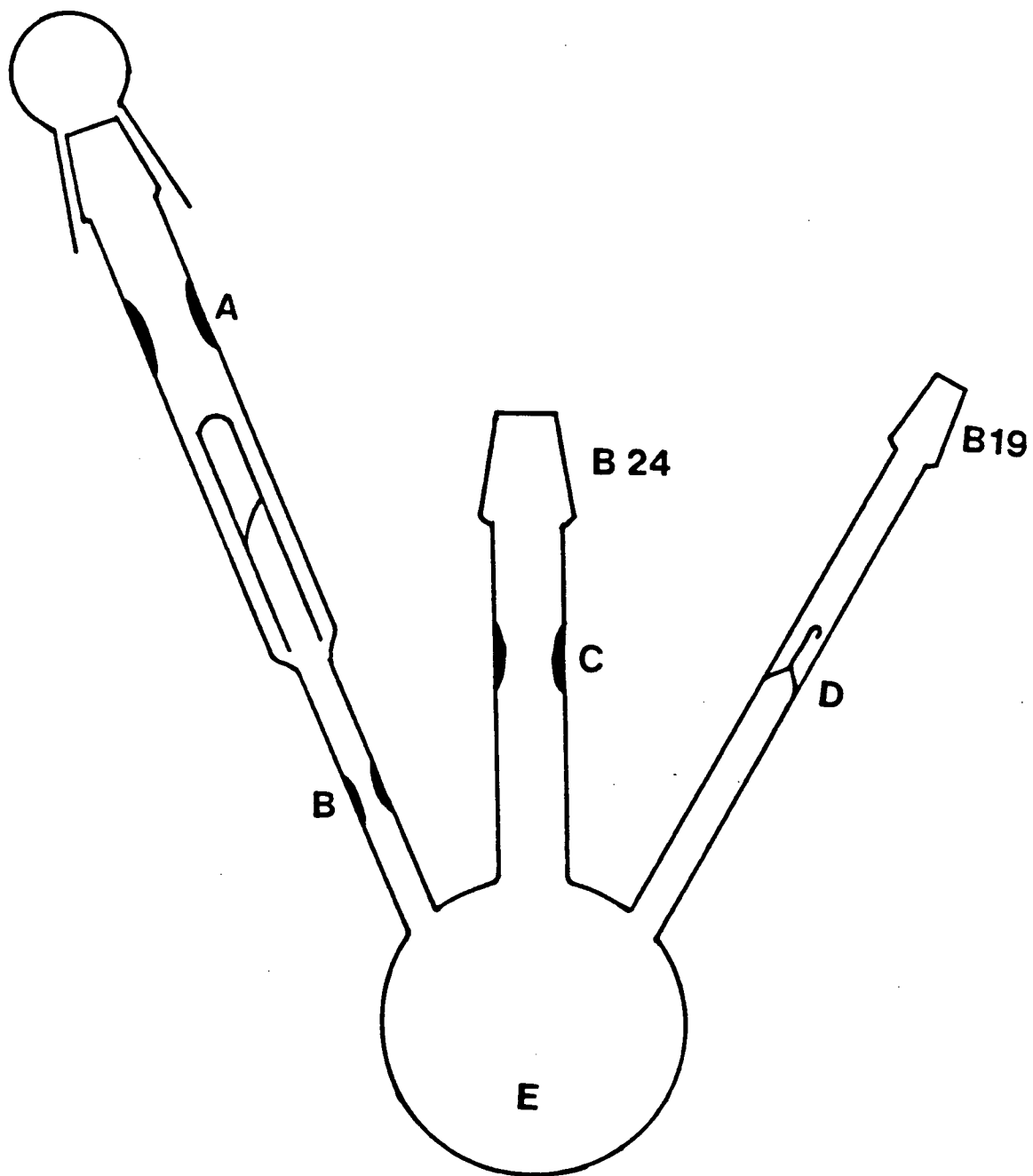
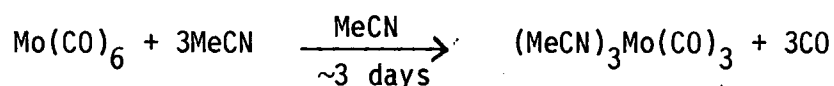


Figure 10. Apparatus for the preparation of  $\text{MeGaCl}_2$ .

into smaller fractions and stored as THF solutions in sealed ampoules. The ampoules were cracked open and used for subsequent reactions when needed.

iv) Preparation of the tricarbonyltris(acetonitrile)-molybdenum(0)  $(\text{MeCN})_3\text{Mo}(\text{CO})_3$  [50]



In a typical preparation, excess acetonitrile (~60 mL) was added to ~1 g  $\text{Mo}(\text{CO})_6$  in a 250 mL round-bottom flask. The reaction mixture was then refluxed for ~3 days. The resulting yellow-green solution was cooled to room temperature and the solvent stripped off in vacuo. Yellow-green, air-sensitive crystals of  $(\text{MeCN})_3\text{Mo}(\text{CO})_3$  ( $\nu_{\text{CO}}$ : 1918(s), 1781(s)  $\text{cm}^{-1}$ , Nujol; 1912(s), 1773(s)  $\text{cm}^{-1}$ , THF) were recovered in almost quantitative yield. The compound was then used in subsequent reactions no more than a few days after preparation since it is unstable even under inert conditions. It is recommended that the compound  $(\text{MeCN})_3\text{Mo}(\text{CO})_3$  be prepared in small quantities at a time, since from our experience, several attempts at the preparation of larger quantities in a single preparation always resulted in a mixture of compounds.

The compound  $(\text{MeCN})_3\text{Mo}(\text{CO})_3$  is preferred as the starting material in most of the reactions discussed in this thesis primarily because acetonitrile is a ligand which has very little  $p\pi-d\pi$  bonding ability [51]; therefore the molybdenum-acetonitrile bond in the  $(\text{MeCN})_3\text{Mo}(\text{CO})_3$  complex is weak, and the acetonitrile ligand is easily replaced from the complex [52].

### 1.3 Physical Measurements

$^1\text{H}$  nmr spectra were recorded on a Bruker WP-80 instrument using Fourier Transform techniques. A Bruker WH-400 or a Nicolet-Oxford H-270 spectrometer was employed whenever a more detailed or enhanced resolution spectrum was desired. Samples were prepared by condensing the appropriate amount of deuterated solvent ( $\text{C}_6\text{D}_6$ ,  $\text{CDCl}_3$  or  $d_6$ -acetone, Merck Frost Canada Inc.; and  $d_8$ -toluene, Merck Sharp and Dohme Canada Ltd.) onto the solid material contained in an nmr tube. The nmr tube was subsequently flame-sealed under vacuum. Chemical shifts were measured relative to the residual protons of the internal standard where  $\tau_{\text{C}_6\text{H}_6} = 2.84$  ppm,  $\tau_{\text{CHCl}_3} = 2.73$  ppm,  $\tau_{(\text{CH}_3)_2\text{CO}} = 7.89$  ppm, and  $\tau_{\text{Toluene-Me}} = 7.91$  ppm.

Infrared spectra were recorded on a Perkin Elmer 598 double beam spectrometer. Samples were prepared as solutions, usually in dichloromethane, cyclohexane or THF (KBr and CsI solution cells), or as Nujol mulls (KBr plates). The spectra were calibrated with the  $1601\text{ cm}^{-1}$  band of polystyrene.

Mass spectra were recorded on a Kratos AES MS 50 spectrometer equipped with a direct insertion probe and interfaced to a computer for higher molecular weight ( $>500$  amu) compounds or a VARIAN MAT CH4 spectrometer for low molecular weight ( $<500$ ) compounds. In general, interpretation of fragmentation patterns was simplified by direct comparison of the observed intensity patterns to the theoretical intensity patterns generated by computer simulation from the natural isotopic abundances of the elements.

Crystallographic determinations were conducted on single crystals using graphite monochromated Mo-K<sub>α</sub> radiation on an Enraf-Nonius CAD4-F diffractometer. This work was performed by Dr. S. Rettig of the U.B.C. Crystallography Laboratory. Stereodiagrams and related bond distances and angles are collected in Appendix I.

Elemental analyses were performed by Mr. P. Borda of the U.B.C. Microanalytical Laboratory.

## Chapter II

THE MOLYBDENUM TRICARBONYL ANION  $[\text{MeGapz}_3]\text{Mo}(\text{CO})_3^-$ ;  
 SYNTHESIS AND CHARACTERIZATION OF THE  $\text{Na}^+$ ,  $\text{Et}_4\text{N}^+$  AND  $\text{HAsPh}_3^+$  SALTS,  
 AND INVESTIGATION OF THE REACTIVITY TOWARDS ALKYL HALIDES,  
 PROTONATING SPECIES AND HALOGENS.

2.1 INTRODUCTION

The uninegative, tridentate, six-electron donor ligands  $\text{RBpz}_3^-$  ( $\text{R} = \text{H}$ , alkyl, aryl, pyrazolyl,  $\text{N}_2\text{C}_3\text{H}_3$ ), and  $\text{MeGapz}_3^-$  show many similarities to the analogous cyclopentadienyl ( $\text{Cp}^-$ ) ligand. For example the  $\text{RBpz}_3^-$  and  $\text{MeGapz}_3^-$  ligands react with molybdenum hexacarbonyl or tris(acetonitrile)-molybdenum tricarbonyl yielding anions of the type  $\text{LMo}(\text{CO})_3^-$  ( $\text{L} = \text{RBpz}_3$ ,  $\text{RB}(3,5\text{-Me}_2\text{pz})_3$ ,  $\text{MeGapz}_3$ ) analogous to the  $\text{CpMo}(\text{CO})_3^-$  anion, and isolable as the tetraethylammonium salts [53,54]. Differences in behaviour are sometimes observed. The reaction of  $\text{LMo}(\text{CO})_3^-$  [ $\text{L} = \text{RBpz}_3$  ( $\text{R} = \text{H}$ , pyrazolyl,  $\text{N}_2\text{C}_3\text{H}_3$ ) [53],  $\text{MeGapz}_3$  [34], and  $\text{PhBpz}_3$  [54]] anions with allyl halides gives directly the  $\pi$ -allyl derivatives with loss of CO. In contrast, the  $\text{CpMo}(\text{CO})_3^-$  anion reacts with allyl halides to give the  $\sigma$ -allyl complex  $\text{CpMo}(\text{CO})_3(\sigma\text{-allyl})$ , which decarbonylates only upon UV irradiation to give the  $\pi$ -allyl derivative  $\text{CpMo}(\text{CO})_2(\pi\text{-allyl})$  [55,56]. There is, however, another notable difference in behaviour: in contrast to the numerous

seven-coordinate cyclopentadienyl complexes generally denoted as  $\text{CpML}_4$  [57], relatively few of such derivatives are known for the poly(1-pyrazolyl)borate complexes. The reported examples of seven-coordinate poly(1-pyrazolyl)borate complexes are  $[\text{HBpz}_3]\text{Mo}(\text{CO})_3\text{R}$  ( $\text{R} = \text{H, Me, Et}$ ) [53],  $[\text{HBpz}_3]\text{W}(\text{CO})_2(\text{CS})\text{I}$  [58],  $[\text{RBpz}_3]\text{TaMe}_3\text{Cl}$  ( $\text{R} = \text{H}$  or  $\text{pz}$ ) [59], and most recently  $[\text{HBpz}_3]\text{Mo}(\text{CO})_3\text{X}$  ( $\text{X} = \text{H, Br, I}$ ) [60]. The electronic nature of the  $\text{HBpz}_3^-$  ligand has been shown to be considerably different from that of the  $\text{Cp}^-$  ligand in that the former hybridizes the metal orbitals into an octahedral disposition much more effectively than does the  $\text{Cp}^-$  ligand [36,60]. The propensity of the molybdenum tricarbonyl complexes incorporating the  $\text{RBpz}_3^-$  ligand to remain preferentially six-coordinate is manifested in the stability of the radical species  $[\text{HBpz}_3]\text{Mo}(\text{CO})_3^\bullet$  [38], in contrast, to the analogous  $\text{CpMo}(\text{CO})_3^\bullet$  [61], and  $(\eta\text{-C}_5\text{Me}_5)\text{Mo}(\text{CO})_3^\bullet$  [62] radical species which are unstable with respect to their  $[\text{CpMo}(\text{CO})_3]_2$  and  $[(\eta\text{-C}_5\text{Me}_5)\text{Mo}(\text{CO})_3]_2$  dimer precursor. Comparison of the chemistry of compounds incorporating the  $\text{RBpz}_3^-$ ,  $\text{MeGapz}_3^-$  and  $\text{Cp}^-$  ligand systems was therefore considered to be instructive especially where the coordination number about the central metal atom is greater than six. The 3:4 or "four-legged piano stool" structure is the paradigm for seven-coordinate  $\text{CpML}_4$  complexes of group 5 and 6 transition metals [63].

At the inception of this work, only one type of molybdenum  $\eta^2$ -acyl complex incorporating the tridentate poly(1-pyrazolyl)borate ligand,  $[\text{HB}(3,5\text{-Me}_2\text{pz})_3]\text{Mo}(\text{CO})_2(\eta^2\text{-COR})$  ( $\text{R} = \text{Ph, C}_6\text{H}_4\text{NMe}_2\text{-p, C}_6\text{H}_4\text{CF}_3\text{-p, C}_6\text{H}_4\text{Me-p}$ ,

$C_6H_{11}$ ) [32] was known. The other examples are  $[HBpz_3]Mo(CO)_2(\eta^2-COR)$  ( $R = Me, Ph$ ) [64,65] and their phosphine adducts reported during the course of this work. In the latter examples, the authors concluded that the combination of the relief of steric congestion and orbital hybridization favored the transformation of  $[HBpz_3]Mo(CO)_3R$  to the  $\eta^2$ -acyl complex  $[HBpz_3]Mo(CO)_2(\eta^2-COR)$  [65]. We reasoned that the combination of both effects (relief of steric congestion and orbital hybridization) could potentially stabilize the isoelectronic, isostructural  $[MeGapz_3]Mo(CO)_2(\eta^2-COR)$  ( $R = Me, Ph$ ) complexes in a manner similar to the boron system.

The  $LMo(CO)_3^-$  ( $L = MeGapz_3, MeGa(3,5-Me_2pz)_3$ ) anions have been isolated as their  $Na^+$ ,  $Et_4N^+$  and  $HAsPh_3^+$  salts. The  $LMo(CO)_3^-$  anions interact with the  $Na^+$  cation in THF, and ir spectroscopic evidence for this anion-cation interaction in THF is presented and discussed. Thus, this result constitutes the first reported observation of the involvement of the  $LMo(CO)_3^-$  ( $L = RBpz_3$  or  $MeGapz_3$ ) anion in ion-pairing with cations in basic and polar solvents such as THF. The general reactivity of the  $[MeGapz_3]Mo(CO)_3^-$  anion toward alkyl halides, benzoyl chloride, protonating species and halogens has been investigated. The compounds  $[MeGapz_3]Mo(CO)_3R$  ( $R = H, Et$ ) have been prepared and the hydride has been shown to exhibit dissociative phenomena in THF. The compound  $[MeGapz_3]Mo(CO)_2(\eta^2-COMe)$ , a product of facile alkyl to CO migration reaction, is presented and discussed. An X-ray crystal structural determination of the

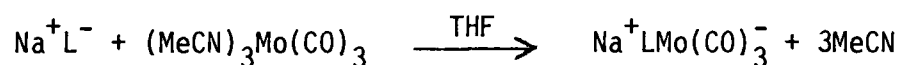
$[\text{HAsPh}_3]^+[\text{MeGa}(3,5\text{-Me}_2\text{pz})_3\text{Mo}(\text{CO})_3]^-$  salt is currently in progress. Parts of this chapter have been submitted for publication [66].

## 2.2 EXPERIMENTAL

### 2.2.1 Starting Materials

Triphenylarsonium chloride (Strem Chemicals), tetraethylammonium chloride (Eastman Organic Chemicals), ethyl bromide (Allied Chemicals),  $\text{HCl}(\text{g})$  (Matheson),  $\text{DBr}(\text{g})$  (Merck Sharpe and Dohme), methanol and benzoyl chloride (Fisher Scientific) were used as supplied. The sodium salts of the methyltris(1-pyrazolyl)gallate  $\text{Na}^+\text{MeGapz}_3^-$  [34], and methyltris(3,5-dimethyl-1-pyrazolyl)gallate  $\text{Na}^+[\text{MeGa}(3\text{-}5\text{-Me}_2\text{pz})_3]^-$  [35] were prepared as described previously. Methyl iodide (Fisher Scientific) was dried by distillation over  $\text{P}_2\text{O}_5$  and stored over mercury droplets before use. Glacial acetic acid (Allied Chemicals) was dried according to literature methods [45].

### 2.2.2 Preparation of $\text{Na}^+\text{LMo}(\text{CO})_3^-$ (L = $\text{MeGapz}_3$ , $\text{MeGa}(3,5\text{-Me}_2\text{pz})_3$ )



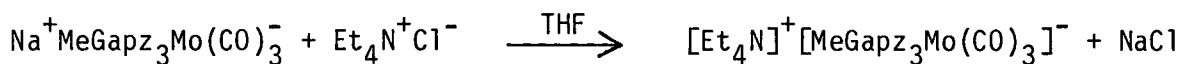
A 30 ml aliquot of  $\text{Na}^+\text{MeGapz}_3^-$  (~0.51 mol) ligand solution in THF was added to a stirred solution of  $(\text{MeCN})_3\text{Mo}(\text{CO})_3$  (0.154 g, 0.510 mmol) in the same solvent. The reaction mixture was stirred until the  $\nu_{\text{CO}}$  bands characteristic of the  $(\text{MeCN})_3\text{Mo}(\text{CO})_3$  starting material had disappeared.

The solvents were then allowed to evaporate from the mixture to give an amber colored solid product of the desired salt,  $\text{Na}^+[\text{MeGapz}_3\text{Mo}(\text{CO})_3]^-$ . The salt  $\text{Na}^+[\text{MeGa}(3,5\text{-Me}_2\text{pz})_3\text{Mo}(\text{CO})_3]^-$  was prepared by a similar method. Both salts were very air-sensitive. The pronounced instability of these  $\text{Na}^+$  salts precluded satisfactory analyses, however they were characterized by their solution ir and  $^1\text{H}$  nmr spectra.

For  $\text{Na}^+[\text{MeGapz}_3\text{Mo}(\text{CO})_3]^-$ : IR(THF)  $\nu_{\text{CO}}$ : 1895(s), 1775(s), 1720(s)  $\text{cm}^{-1}$ ; IR( $\text{CH}_2\text{Cl}_2$ )  $\nu_{\text{CO}}$ : 1888(s), 1760(br)  $\text{cm}^{-1}$ .  $^1\text{H}$  NMR ( $d_6$ -acetone, 80 MHz):  $\tau(\text{CH}_3)_2\text{CO} = 7.89$  ppm, 9.58s (Ga-Me); 3.83t (pz-H<sup>4</sup>); 2.35d (pz-H<sup>5</sup>); 2.00d (pz-H<sup>3</sup>). ( $J_{\text{HCCH}} = \sim 2$  Hz for pz protons.)

For  $\text{Na}^+[\text{MeGa}(3,5\text{-Me}_2\text{pz})_3\text{Mo}(\text{CO})_3]^-$ : IR(THF)  $\nu_{\text{CO}}$ : 1890(s), 1765(s), 1710(s)  $\text{cm}^{-1}$ ; IR( $\text{CH}_2\text{Cl}_2$ )  $\nu_{\text{CO}}$ : 1885(s), 1745(br)  $\text{cm}^{-1}$ .  $^1\text{H}$  NMR ( $d_6$ -acetone, 80 MHz):  $\tau(\text{CH}_3)_2\text{CO} = 7.89$  ppm, 9.54s (Ga-Me); 7.78s (pz-Me<sup>5</sup>); 7.19s (pz-Me<sup>3</sup>); 4.38s (pz-H<sup>4</sup>).

### 2.2.3 Preparation of $[\text{Et}_4\text{N}]^+[\text{MeGapz}_3\text{Mo}(\text{CO})_3]^-$

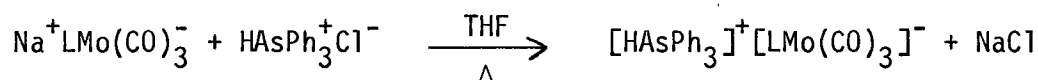
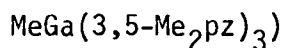


To a stirred THF solution of  $(\text{MeCN})_3\text{Mo}(\text{CO})_3$  (0.309 g, 1.02 mmol) was added a 60 ml aliquot of the  $\text{Na}^+\text{MeGapz}_3^-$  ( $\sim 1.20$  mmol) ligand solution in THF. The reaction mixture was stirred at room temperature overnight at which time the solution ir spectrum of the mixture indicated complete

formation of the  $\text{Na}^+\text{MeGapz}_3\text{Mo}(\text{CO})_3^-$  ( $\nu_{\text{CO}}$  1895, 1775, 1720  $\text{cm}^{-1}$ , THF) salt. An equimolar amount of  $\text{Et}_4\text{N}^+\text{Cl}^-$  (0.169 g, 1.02 mmol) dissolved in ~5 ml MeOH was added to the carbonyl salt solution. The resulting cloudy yellow solution was stirred for another hour. The yellow precipitate was collected by filtration and dried in vacuo to give the desired product  $[\text{Et}_4\text{N}]^+[\text{MeGapz}_3\text{Mo}(\text{CO})_3]^-$  in ~40% yield. This salt is unstable in air and solutions deteriorate with time.

IR( $\text{CH}_2\text{Cl}_2$ )  $\nu_{\text{CO}}$ : 1890(s), 1760(br)  $\text{cm}^{-1}$ ; IR(Nujol)  $\nu_{\text{CO}}$ : 1885(s), 1752(s), 1730(s)  $\text{cm}^{-1}$ .  $^1\text{H}$  NMR ( $d_6$ -acetone, 270 MHz):  $\tau(\text{CH}_3)_2\text{CO}$  = 7.89 ppm, 9.57s (Ga-Me); 3.81t (pz-H<sup>4</sup>); 2.27d (pz-H<sup>5</sup>); 1.92d (pz-H<sup>3</sup>); 8.57br (N-CH<sub>2</sub>-CH<sub>3</sub>); 6.41br (N-CH<sub>2</sub>-CH<sub>3</sub>) ( $J_{\text{HCCH}}$  = ~2 Hz for pz protons.)

#### 2.2.4 Preparation of $[\text{HAsPh}_3]^+[\text{LMo}(\text{CO})_3]^-$ (L = MeGapz<sub>3</sub>,



To the stirred THF solution of  $\text{Na}^+\text{MeGapz}_3\text{Mo}(\text{CO})_3^-$  (~0.85 mmol) salt was added solid  $\text{HAsPh}_3^+\text{Cl}^-$  (0.29 g 0.85 mmol). The resulting mixture was heated under nitrogen at reflux temperatures overnight after which the solution was cooled and the solvent removed in vacuo. The resulting yellow residue was extracted with benzene and filtered. Upon evaporation of the benzene solvent containing the extracts, a yellow solid was obtained. Recrystallization from  $\text{CH}_2\text{Cl}_2$ /hexane (1:1) mixed solvents afforded golden yellow needles of the desired  $[\text{HAsPh}_3]^+[\text{MeGapz}_3\text{Mo}(\text{CO})_3]^-$

salt in ~90% yield. The salt  $[\text{HAsPh}_3]^+[\text{MeGa}(3,5\text{-Me}_2\text{pz})_3\text{Mo}(\text{CO})_3]^-$  was prepared via a similar procedure except that the residue was extracted with  $\text{CH}_2\text{Cl}_2$  and hexane was added to the  $\text{CH}_2\text{Cl}_2$  filtrate. This enabled the isolation of the product without benzene solvation. Both of the above salts are considerably more stable either as solids or in solution than the corresponding  $\text{Na}^+$  or  $\text{Et}_4\text{N}^+$  salts respectively.

Anal. Calcd. For  $[\text{HAsPh}_3]^+[\text{MeGapz}_3\text{Mo}(\text{CO})_3]^- \cdot 0.75 \text{C}_6\text{H}_6$ : C, 51.26; H, 3.91; N, 10.11. Found: C, 51.41; H, 3.54; N, 9.94. IR( $\text{CH}_2\text{Cl}_2$ )  $\nu_{\text{CO}}$ : 1890(s), 1750(br)  $\text{cm}^{-1}$ ; IR(THF)  $\nu_{\text{CO}}$ : 1890(s), 1755(br)  $\text{cm}^{-1}$ ; IR(Nujol)  $\nu_{\text{CO}}$ : 1885(s), 1760(s), 1735(s)  $\text{cm}^{-1}$ .  $^1\text{H}$  NMR ( $d_6$ -acetone, 80 MHz):  $\tau(\text{CH}_3)_2\text{CO} = 7.89$  ppm, 9.56s (Ga-Me); 3.83t (pz-H<sup>4</sup>); 2.35d (pz-H<sup>5</sup>); 1.98d (pz-H<sup>3</sup>); 2.05s (As-Ph); 2.58s (As-H). ( $J_{\text{HCCH}} = \sim 2$  Hz for pz protons.)

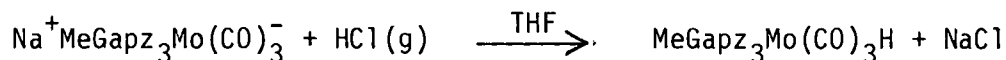
Anal. Calcd. For  $[\text{HAsPh}_3]^+[\text{MeGa}(3,5\text{-Me}_2\text{pz})_3\text{Mo}(\text{CO})_3]^-$ : C, 51.83; H, 4.67; N, 9.81. Found: C, 52.43; H, 4.80; N, 9.22. IR( $\text{CH}_2\text{Cl}_2$ )  $\nu_{\text{CO}}$ : 1885(s), 1740(br)  $\text{cm}^{-1}$ ; IR(THF)  $\nu_{\text{CO}}$ : 1885(s), 1750(br)  $\text{cm}^{-1}$ .  $^1\text{H}$  NMR ( $d_6$ -acetone, 80 MHz):  $\tau(\text{CH}_3)_2\text{CO} = 7.89$  ppm, 9.55s (Ga-Me); 7.80s (pz-Me<sup>5</sup>); 7.21s (pz-Me<sup>3</sup>); 4.38s (pz-H<sup>4</sup>); 2.09s (As-Ph); 2.61s (As-H).

### 2.2.5 Attempted Preparation of $[\text{MeGapz}_3]\text{Mo}(\text{CO})_3\text{H}$ using Acetic Acid

A THF solution of the  $\text{Na}^+ \text{MeGapz}_3\text{Mo}(\text{CO})_3^-$  salt was acidified with glacial acetic acid. The reaction mixture was stirred overnight, and the solvent removed under vacuum. The resulting residue was extracted with benzene and filtered. Orange-yellow solids were recovered upon evaporation of the benzene solvent containing the extracts. Both the ir

and  $^1\text{H}$  nmr data for this product indicated the presence of perhaps two compounds. IR(THF): 1960, 1930, 1910, 1810, 1895, 1775, 1725  $\text{cm}^{-1}$ . IR( $\text{C}_6\text{H}_{12}$ ): 1950, 1935, 1912, 1810  $\text{cm}^{-1}$ .  $^1\text{H}$  NMR ( $d_6$ -acetone, 80 MHz):  $\tau(\text{CH}_3)_2\text{CO} = 7.89$  ppm, 10.14s, 9.63s (Ga-Me); 3.88t, 3.83t (pz-H<sup>4</sup>); 2.40d, 2.33d (pz-H<sup>5</sup>); 2.05d, 1.90d (pz-H<sup>3</sup>). ( $J_{\text{HCCH}} = \sim 2$  Hz for pz protons.) The ir  $\nu_{\text{CO}}$  bands at 1895, 1775, 1725  $\text{cm}^{-1}$  in THF, and one set of signals in the  $^1\text{H}$  nmr spectrum, compared quite well with those obtained for the  $\text{Na}^+\text{MeGapz}_3\text{Mo}(\text{CO})_3^-$  salt starting material (see section 2.2.2). This is suggestive of incomplete protonation of the  $\text{MeGapz}_3\text{Mo}(\text{CO})_3^-$  anion by acetic acid; hence a stronger protonating species may be necessary to fully protonate the anion. The reaction was then repeated using the strong acid HCl, as the protonating species.

#### 2.2.6 Preparation of $[\text{MeGapz}_3]\text{Mo}(\text{CO})_3\text{H}$ using HCl



An equimolar amount of HCl(g) ( $\sim 0.5$  mmol) was condensed into a THF solution containing the  $\text{Na}^+\text{MeGapz}_3\text{Mo}(\text{CO})_3^-$  ( $\sim 0.51$  mmol) salt under vacuum. The reaction mixture was warmed up to room temperature and the resulting orange solution was stirred for  $\sim 2$  h. The solvent was then removed in vacuo, and the resulting residue extracted with hexane. Upon evaporation of the hexane filtrate containing the extracts, air-sensitive orange solids of the desired hydride species were obtained in  $\sim 60\%$  yield. Slow decomposition of this compound occurs in the basic and weakly polar

solvent, THF. For example, the ir spectrum of the hydride species in THF showed the presence of the  $\text{MeGapz}_3\text{Mo}(\text{CO})_3^-$  anion presumably emanating from the acid-base dissociation of the Mo-H bond in the  $\text{MeGapz}_3\text{Mo}(\text{CO})_3\text{H}$  complex.

Anal. Calcd. for  $\text{MeGapz}_3\text{Mo}(\text{CO})_3\text{H} \cdot 0.5 \text{C}_6\text{H}_{14}$ : C, 37.67; H, 3.92; N, 16.48. Found: C, 37.21; H, 3.62; N, 16.41. IR( $\text{C}_6\text{H}_{14}$ ): 1952(w), 1928(s), 1908(s), 1808(s)  $\text{cm}^{-1}$ .  $^1\text{H}$  NMR ( $d_6$ -acetone, 300 MHz):  $\tau(\text{CH}_3)_2\text{CO} = 7.89$  ppm, 9.90s (Ga-Me); 3.60t (pz-H<sup>4</sup>); 2.50d (pz-H<sup>5</sup>); 2.16d (pz-H<sup>3</sup>) 18.50s (Mo-H). ( $J_{\text{HCCH}} = \sim 2$  Hz for pz protons.)

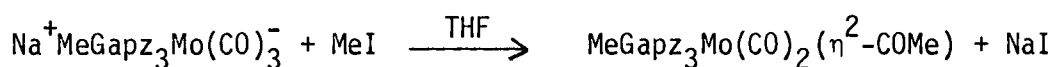
### 2.2.7 Preparation of $[\text{MeGapz}_3]\text{Mo}(\text{CO})_3\text{D}$



A slight excess of DBr(g) was condensed into a MeCN solution containing the  $\text{MeGapz}_3\text{Mo}(\text{CO})_3^-$  anion as its  $\text{HAsPh}_3^+$  salt (0.50 g, 0.66 mmol) under vacuum. The reaction mixture was warmed to room temperature and then stirred for  $\sim 2$  h. Work-up of the dark orange reaction mixture resulted in an orange sticky solid. This product is very air-sensitive and solutions deteriorate in a matter of minutes. The solution ir spectrum of this product in  $\text{C}_6\text{H}_6$  indicated the formation of the expected  $\text{MeGapz}_3\text{Mo}(\text{CO})_3\text{D}$  deuteride. However, in THF solution, the ir spectrum of the product displayed  $\nu_{\text{CO}}$  bands characteristic of the  $\text{MeGapz}_3\text{Mo}(\text{CO})_3^-$  anion, in addition to those of the deuteride species. Evidently, acid-base dissociation of the Mo-D bond in the  $\text{MeGapz}_3\text{Mo}(\text{CO})_3\text{D}$  complex similar to that observed in the hydride species (Section 2.2.6) is

operative in THF solution. IR(C<sub>6</sub>H<sub>6</sub>): 1935(s), 1910(s), 1845(w), 1380(w) cm<sup>-1</sup>. IR(CH<sub>2</sub>Cl<sub>2</sub>): 1940(s), 1905(m), 1838(w) cm<sup>-1</sup>. IR(THF): 1940(s), 1905(s), 1830(m), 1380(w); 1885(s), 1770(br) cm<sup>-1</sup>. Persistent attempts at the crystallization of this product were unsuccessful; hence no further characterization was performed.

### 2.2.8 Preparation of [MeGapz<sub>3</sub>]Mo(CO)<sub>2</sub>(η<sup>2</sup>-COMe)

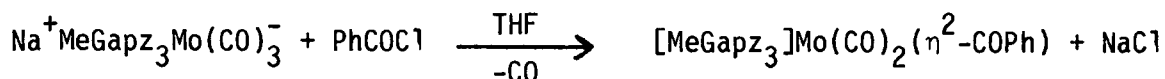


To a THF solution containing the MeGapz<sub>3</sub>Mo(CO)<sub>3</sub><sup>-</sup> (1.28 mmol) anion as its Na<sup>+</sup> salt was added excess MeI in the same solvent. The resulting dark orange-red reaction mixture was then stirred for about 2 days at which stage the ir spectrum of the mixture showed new bands in the ν<sub>CO</sub> region of the spectrum at ~1970, 1920 and 1855 cm<sup>-1</sup>, in addition to the ν<sub>CO</sub> bands characteristic of the MeGapz<sub>3</sub>Mo(CO)<sub>3</sub><sup>-</sup> anion in THF. After stirring the mixture for another 2 days, a new weak absorption band appeared at ~1570 cm<sup>-1</sup>. The ν<sub>CO</sub> bands observed at 1970, 1920 and 1955 cm<sup>-1</sup> presumably emanated from the presence of a transient σ-methyl intermediate 'MeGapz<sub>3</sub>-Mo(CO)<sub>3</sub>Me' in solution. However, the presence of the ν<sub>CO</sub> bands due to the MeGapz<sub>3</sub>Mo(CO)<sub>3</sub><sup>-</sup> anion in solution, even after stirring for ~4 days, is probably indicative of a low yield of this reaction in THF. The solvent and the unreacted MeI were then removed under vacuum. The resulting dark-red residue was extracted with CH<sub>2</sub>Cl<sub>2</sub> and filtered. An equal amount of hexane was added to the CH<sub>2</sub>Cl<sub>2</sub> filtrate. Upon evaporation of the mixed

$\text{CH}_2\text{Cl}_2$ /hexane solvents, air-sensitive brick-red crystals of the product were obtained in ~30% yield.

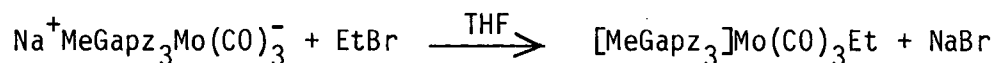
Anal. Calcd. For  $[\text{MeGapz}_3]\text{Mo}(\text{CO})_2(\eta^2\text{-COMe})$ : C, 34.95; H, 3.12; N, 17.48. Found: C, 35.10, H, 3.16 N, 17.15. IR( $\text{CH}_2\text{Cl}_2$ ): 1980(s), 1855(s), 1570(w)  $\text{cm}^{-1}$ .  $^1\text{H}$  NMR ( $d_6$ -acetone, 80 MHz):  $\tau(\text{CH}_3)_2\text{CO} = 7.89$  ppm, 9.30s (Ga-Me); 3.63t, 3.53t (pz-H<sup>4</sup>); 2.46d, 2.24d (pz-H<sup>5</sup>); 2.06d, 1.95d (pz-H<sup>3</sup>); 6.60s (-COMe). ( $J_{\text{HCCH}} = \sim 2$  Hz for pz protons.) Pyrazolyl ring protons appeared in a 2:1 ratio. MS:  $\text{P}^+$ ,  $\text{P-Me}^+$ ,  $\text{P-CO}^+$ ,  $\text{P-CO-Me}^+$ ,  $\text{P-2CO}^+$ ,  $\text{P-3CO}^+$ , and  $\text{P-3CO-Me}^+$  (P = parent) ion signals were displayed.

#### 2.2.9 Attempted Preparation of $[\text{MeGapz}_3]\text{Mo}(\text{CO})_2(\eta^2\text{-COPh})$



Excess benzoyl chloride in THF was added portion-wise to a THF solution of the  $\text{Na}^+\text{MeGapz}_3\text{Mo}(\text{CO})_3^-$  (~0.35 mmol) salt. The reaction mixture was heated for ~2 h at which stage the ir spectrum of the dark solution indicated the complete consumption of the  $\text{MeGapz}_3\text{Mo}(\text{CO})_3^-$  anion. The solvent was then removed under vacuum. Hexane was added to the resulting dark oil and slowly poured off. The dark solid residue left behind in the flask was extracted with  $\text{CH}_2\text{Cl}_2$  and filtered. Work-up of the  $\text{CH}_2\text{Cl}_2$  filtrate containing the extracts afforded dark blue crystals of the product in very low yield. The very low yield (<5%) of this product discouraged repetition of this experiment. However the yield was sufficient for obtaining an ir spectrum. IR( $\text{CH}_2\text{Cl}_2$ ): 1965(s), 1820(s), 1535(w)  $\text{cm}^{-1}$ .

### 2.2.10 Preparation of $[\text{MeGapz}_3]\text{Mo}(\text{CO})_3\text{Et}$



A 50-fold excess of EtBr in THF was added dropwise to a solution of the  $\text{Na}^+\text{MeGapz}_3\text{Mo}(\text{CO})_3^-$  (~0.68 mmol) salt in the same solvent. The mixture was stirred for ~1 day at room temperature followed by another day of stirring at reflux temperatures, after which the solvent was removed in vacuo. The resulting residue was extracted with benzene. Evaporation of the benzene solvent from the extracts resulted in a dark-brown sticky solid. Recrystallization out of  $\text{CH}_2\text{Cl}_2$ /hexane mixed-solvents afforded reddish-brown solids of the product in low yields. The compound is unstable even under inert conditions either as a solid or in solution.

Anal. Calcd. For  $[\text{MeGapz}_3]\text{Mo}(\text{CO})_3\text{Et}$ : C, 36.39; H, 3.44; N, 16.98. Found: C, 36.55, H, 3.28, N, 16.33. IR( $\text{CH}_2\text{Cl}_2$ ): 1970(s), 1930(s), 1820(s)  $\text{cm}^{-1}$ ; 1890(s), 1755(br)  $\text{cm}^{-1}$ .  $^1\text{H}$  NMR ( $d_6$ -acetone, 270 MHz):  $(\text{CH}_3)_2\text{CO} = 7.89$  ppm; 9.53s (Ga-Me); 3.81 (pz-H<sup>4</sup>); 2.36 (pz-H<sup>5</sup>); 1.97 (pz-H<sup>3</sup>) 8.15br (Mo-Et-CH<sub>3</sub>); 6.32br (Mo-Et-CH<sub>2</sub>). ( $J_{\text{HCCH}}$  - unresolved for pz protons.) Excessive fragmentation indicative of thermal decomposition was observed in the mass spectrum of this compound. However, weak signals corresponding to the  $\text{P-3CO-Et}^+$  ion were observed.

### 2.2.11 Attempted Preparation of $[\text{MeGapz}_3]\text{Mo}(\text{CO})_3\text{X}$ ( $\text{X} = \text{Br}, \text{I}$ )

Bromine (0.14 g, 1.7 mmol) in THF was reacted with  $\text{Na}^+\text{MeGapz}_3\text{Mo}(\text{CO})_3^-$  (0.85 mmol) salt in THF. The reaction mixture was stirred overnight and the solution ir spectrum of the mixture at this stage showed three new  $\nu_{\text{CO}}$  bands at 2010, 1975, 1930  $\text{cm}^{-1}$  as expected for the product. Solvent removal in vacuo, extraction of the residue with  $\text{CH}_2\text{Cl}_2$  and recrystallization from  $\text{CH}_2\text{Cl}_2$ /hexane mixed solvents gave a yellow solid. The ir spectrum of the yellow solid showed three bands (2010, 1980, 1900  $\text{cm}^{-1}$ ,  $\text{CH}_2\text{Cl}_2$ ; 2010, 1975, 1930  $\text{cm}^{-1}$ , THF) in the  $\nu_{\text{CO}}$  region of the spectrum. The  $^1\text{H}$  nmr spectrum of this yellow solid product in both  $\text{CDCl}_3$  and  $d_6$ -acetone indicated decomposition of the expected  $[\text{MeGapz}_3]\text{Mo}(\text{CO})_3\text{Br}$  compound. Repeated attempts at obtaining analytically pure samples of the product were unsuccessful.

Similarly, reaction of iodine (0.108 g, 0.85 mmol) dissolved in MeCN with an equimolar amount of  $\text{Na}^+\text{MeGapz}_3\text{Mo}(\text{CO})_3^-$  salt in THF gave a dark red solid. The ir spectrum of the solid product showed three  $\nu_{\text{CO}}$  bands as expected for the product but repeated recrystallization out of  $\text{CH}_2\text{Cl}_2$ /hexane solvent mixtures did not yield an analytically pure compound. IR(THF): 2015, 1972, 1928  $\text{cm}^{-1}$ ; IR( $\text{CH}_2\text{Cl}_2$ ): 2015, 1978, 1925  $\text{cm}^{-1}$ .  $^1\text{H}$  NMR ( $d_6$ -acetone, 80 MHz):  $\tau(\text{CH}_3)_2\text{CO} = 7.89$  ppm, 9.59s (Ga-Me); 3.87br (pz-H<sup>4</sup>); 2.38br (pz-H<sup>5</sup>); 2.03br (pz-H<sup>3</sup>).

## 2.3 Results and Discussion

### 2.3.1 $M^+LMo(CO)_3^-$ (L = MeGapz<sub>3</sub>, MeGa(3,5-Me<sub>2</sub>pz)<sub>3</sub>; $M^+$ = Na<sup>+</sup>, Et<sub>4</sub>N<sup>+</sup>, HAsPh<sub>3</sub><sup>+</sup>) salts

The physical phenomenon of ion-pair interactions of group 1 and 2 cations with the carbonyl oxygen of transition metal carbonylates has been well-documented. For example, the crystal structures of  $[CpMo(CO)_3]_2Mg^{2+}(C_5H_5N)_4$  [67], and  $[(Co(salen))_2Na^+Co(CO)_4^-THF]$  [68] have indicated interactions of the transition metal carbonylates with the  $Mg^{2+}$  and  $Na^+$  cations in the above complexes. A very common mode of preparation of transition metal carbonyl anions for further synthetic purposes is by metal amalgam, or direct metal reductions of the metal carbonyl precursors in basic, low polarity, donor solvents, typically THF. Transition metal carbonylate anion/alkali or alkaline earth cation interactions occur quite extensively in these systems. The first ir spectroscopic evidence for ion-pairing between alkali-metal cations and metal carbonyl anions in solvents of moderate polarity was reported sometime ago by Edgell et al. [69]. Since that original report and subsequent work on the  $Na^+Co(CO)_4^-$  [70] salt, analyses of THF-solution  $\nu_{CO}$  ir spectra have been employed quite successfully to unravel alkali-metal cation interactions with  $CpFe(CO)_2^-$  [71,72], and  $CpMo(CO)_3^-$  (M = Cr, Mo, W) [73] anions. Infrared spectroscopy in the  $\nu_{CO}$  region is particularly valuable in the study of

interactions involving direct contact of anion(s) and cation(s) especially where the geometry of the free carbonylate anion is perturbed by the cation.

The  $\text{LMo}(\text{CO})_3^-$  ( $\text{L} = \text{MeGapz}_3, \text{MeGa}(3,5\text{-Me}_2\text{pz})_3$ ) anions have been prepared and isolated as their sodium  $\text{Na}^+$ , tetraethylammonium  $\text{Et}_4\text{N}^+$ , and triphenylarsonium  $\text{HAsPh}_3^+$  salts. The ir spectra of the salts in  $\text{CH}_2\text{Cl}_2$  solution displayed two strong bands in the  $\nu_{\text{CO}}$  region, consistent with a symmetrical  $\text{C}_{3v}$  structure (A + E modes) as expected for the free anions. However, in THF solution, three strong bands were observed for the  $\text{Na}^+$  salts. As an illustrative example, the solution ir spectra of the  $\text{M}^+[\text{MeGapz}_3\text{Mo}(\text{CO})_3]^-$  ( $\text{M}^+ = \text{Na}^+, \text{Et}_4\text{N}^+, \text{HAsPh}_3^+$ ) salts in the  $\nu_{\text{CO}}$  region are shown in figure 11. The presence of three  $\nu_{\text{CO}}$  bands in THF is suggestive of  $\text{C}_s$  symmetry for the anion of the  $\text{Na}^+\text{MeGapz}_3\text{Mo}(\text{CO})_3^-$  salt in THF. Since for  $\text{C}_s$  symmetry ( $2\text{A}' + \text{A}''$  modes), three bands are expected in the  $\nu_{\text{CO}}$  region of the spectrum, evidently the initial  $\text{C}_{3v}$  symmetry of the free  $\text{MeGapz}_3\text{Mo}(\text{CO})_3^-$  anion has been reduced to  $\text{C}_s$  symmetry upon perturbation by the  $\text{Na}^+$  cation in THF. A comparison of the  $\nu_{\text{CO}}$  values for the  $\text{M}^+\text{LMo}(\text{CO})_3^-$  salts (Table 1) shows the presence of a low frequency band for the  $\text{Na}^+\text{LMo}(\text{CO})_3^-$  salts in THF.

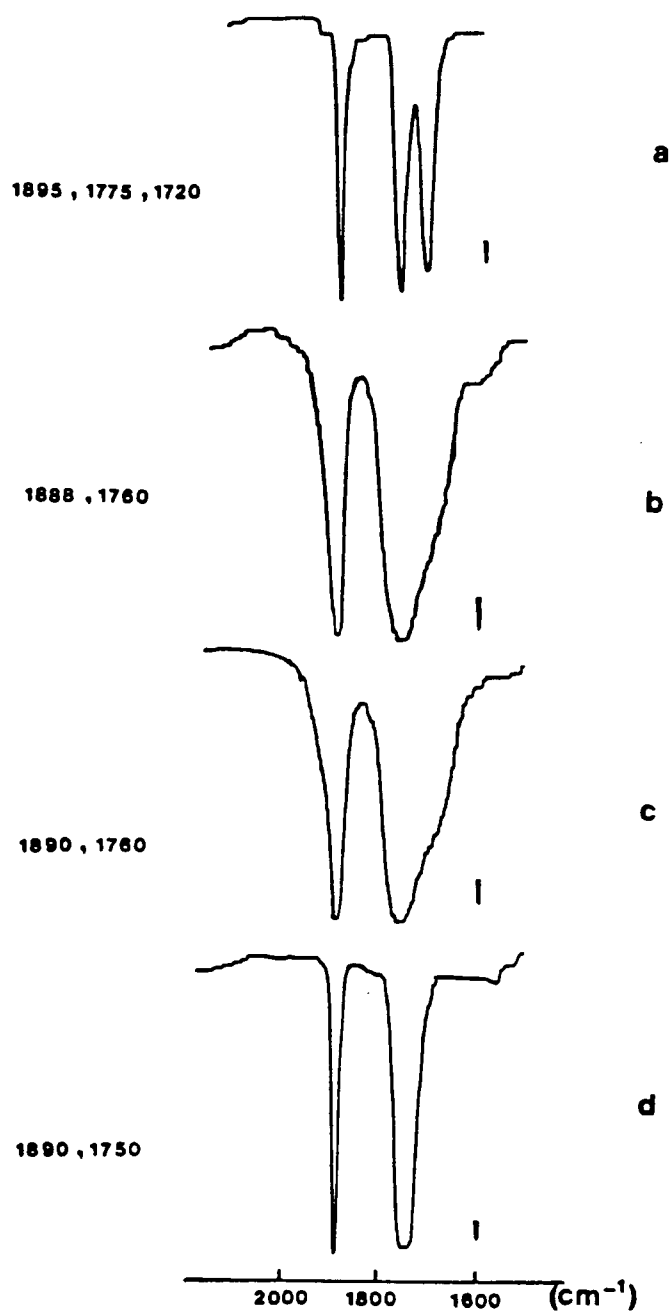


Figure 11. Ir spectrum of  $M^+MeGapz_3Mo(CO)_3^-$  salts in the  $\nu CO$  region.  
 a.  $M^+ = Na^+$  in THF. b.  $M^+ = Na^+$  in  $CH_2Cl_2$ . c.  $M^+ = Et_4N^+$  in  $CH_2Cl_2$ . d.  $M^+ = HAsPh_3^+$  in  $CH_2Cl_2$ .

Table I.  $\nu_{\text{CO}}$  ( $\text{cm}^{-1}$ ) Infrared Data for  $\text{M}^+\text{L}(\text{CO})_3^-$  ( $\text{L} = \text{MeGapz}_3, \text{MeGa}(3,5\text{-Me}_2\text{pz})_3$   
 $\text{M}^+ = \text{Na}^+, \text{Et}_4\text{N}^+, \text{HAsPh}_3^+$  salts).

COMPOUND	SOLVENT	A'	A <sub>1</sub>	A''	E	A'(CO...M <sup>+</sup> )
$\text{Na}^+\text{MeGapz}_3\text{Mo}(\text{CO})_3^-$	THF	1895		1775		1720
	$\text{CH}_2\text{Cl}_2$		1888		1760	
$\text{Na}^+\text{MeGa}(3,5\text{-Me}_2\text{pz})_3\text{Mo}(\text{CO})_3^-$	THF	1890		1765		1710
	$\text{CH}_2\text{Cl}_2$		1885		1745	
$\text{Et}_4\text{N}^+\text{MeGapz}_3\text{Mo}(\text{CO})_3^-$	THF		1890		1765	
	$\text{CH}_2\text{Cl}_2$		1890		1760	
$\text{HAsPh}_3^+\text{MeGapz}_3\text{Mo}(\text{CO})_3^-$	THF		1890		1755	
	$\text{CH}_2\text{Cl}_2$		1890		1750	
$\text{HAsPh}_3^+\text{MeGa}(3,5\text{-Me}_2\text{pz})_3\text{Mo}(\text{CO})_3^-$	THF		1885		1750	
	$\text{CH}_2\text{Cl}_2$		1885		1740	

The low frequency band observed in THF is indicative of a carbonyl oxygen perturbed by the  $\text{Na}^+$  cation in an interaction of the type  $\text{Mo-CO}\cdots\text{Na}^+$ . Such an interaction would lead to a collapse of the 'E' vibration of the  $C_{3v}$  symmetry of the unperturbed anion (figure 12a) to give the 'A"' and A' contact modes of the  $C_s$  symmetry of the perturbed anion as shown in figure 12b.

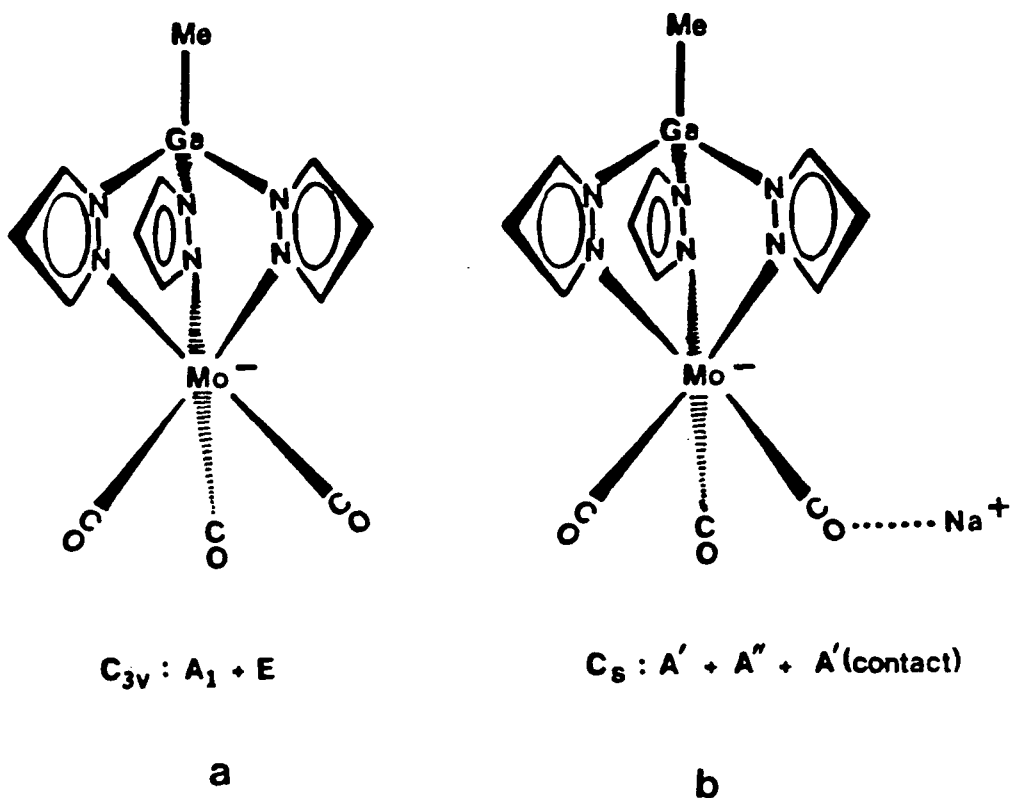


Figure 12. Proposed structures for the interactions of  $\text{MeGaapz}_3\text{Mo}(\text{CO})_3^-$  anion with  $\text{Na}^+$  cation in THF solution. a. Unperturbed anion. b. Perturbed anion.

In this type of ion-pairing external to the carbonylate coordination sphere, substantial  $\pi$ -electron density is expected to reside in the region

of the lone pairs on the oxygen involved in the interaction [74]. A molecular orbital description of the CO electron density in this interaction is shown in figure 13a. In the picture, the  $\text{Na}^+$  cation is positioned for maximum interaction with the electron density in both the  $\sigma$  and  $\pi$  orbitals. In any case, whether the arrangement is of a linear type (figure 13b), or non-linear (figure 13c), this interaction would, of course, tend to increase the CO bond order in the non-interacting Mo-CO groups with concomitant decrease in the CO bond order in the  $\text{Mo-CO}\cdots\text{Na}^+$  group. This polarization of electrons (electronic-drift) in the  $\pi$ -bonding molecular orbital, region towards the  $\text{Mo-CO}\cdots\text{Na}^+$  interaction site, would reinforce the  $d\pi(\text{Mo}) \rightarrow \pi^* (-\text{CO}\cdots\text{Na}^+)$  backbonding component. The result would be a decrease in the  $\nu_{\text{CO}}$  value for the CO group involved in the cation-anion contact ion-pairing. Alternatively, the  $\nu_{\text{CO}}$  values for the CO groups not involved in the interaction with the  $\text{Na}^+$  cation would be increased due to decreased competitive backbonding ability by the CO groups for the Mo metal d electrons.

The ir data for the  $\text{Na}^+\text{LMo}(\text{CO})_3^-$  salts in THF (Table I) are in accord with this observation. The solution ir spectrum of the  $[\text{Et}_4\text{N}]^+[\text{MeGapz}_3\text{Mo}(\text{CO})_3]^-$  salt in THF is rather interesting since it displayed one strong band at  $\sim 1890\text{ cm}^{-1}$ , and a second continuous broad band with two or more maxima centered at  $\sim 1765\text{ cm}^{-1}$ . This observation may be suggestive of some perturbation of the  $\text{MeGapz}_3\text{Mo}(\text{CO})_3^-$  anion  $\text{C}_{3v}$  symmetry, emanating from some contact of the anion with the  $\text{Et}_4\text{N}^+$  cation in THF solvent. It is not clear whether the  $\text{Et}_4\text{N}^+$  cation interacts with one or more carbonyl oxygens in this case. However, an X-ray crystal structure study of the related

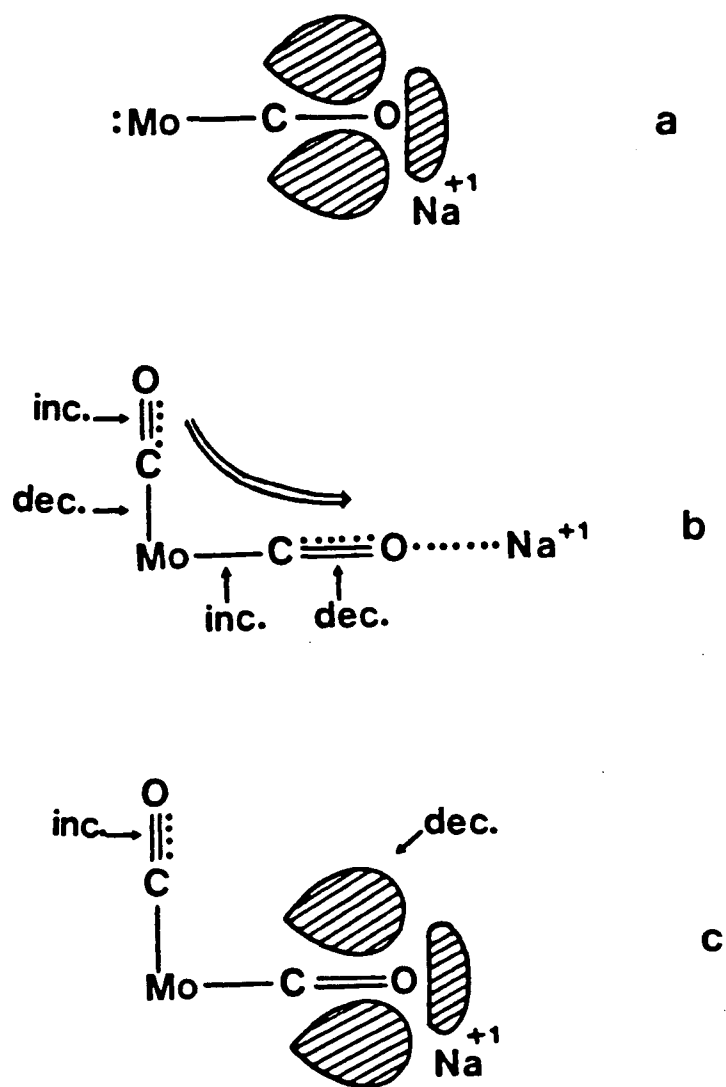


Figure 13. Proposed cation ( $\text{Na}^+$ ) interaction with  $\text{MeGapz}_3\text{Mo}(\text{CO})_3^-$  anion, external to the Mo coordination sphere in THF. a. M.O. description of CO electron density. b. Linear interaction. c. Non-linear interaction.

$[\text{Me}_4\text{N}]^+[\text{CpCr}(\text{CO})_3]^-$  complex [75] has revealed some electrostatic interaction between the  $\text{Me}_4\text{N}^+$  cation and the  $\text{CpCr}(\text{CO})_3^-$  anion in the above salt. The  $\nu_{\text{CO}}$  values for  $\text{Na}^+\text{MeGapz}_3\text{Mo}(\text{CO})_3^-$  (1895, 1775, 1720  $\text{cm}^{-1}$ , THF)

compare nicely with the  $\nu_{\text{CO}}$  values reported independently for the  $\text{Na}^+\text{CpMo}(\text{CO})_3^-$  salt ( $\nu_{\text{CO}}$  1893, 1775, 1749  $\text{cm}^{-1}$ , pyridine) [67], and ( $\nu_{\text{CO}}$  1899, 1796, 1743  $\text{cm}^{-1}$ , THF) [73] respectively. Ion-pairing of transition metal carbonylates with cations in low polarity solvents has been discussed in recent review articles [76,77].

The  $^1\text{H}$  nmr spectrum of the  $[\text{HAsPh}_3]^+[\text{MeGapz}_3\text{Mo}(\text{CO})_3]^-$  salt in  $d_6$ -acetone solution (figure 14) shows all the three pyrazolyl groups to be equivalent, displaying one signal for each of the pyrazolyl ring proton resonances. This is indicative of a symmetrical  $\text{C}_{3v}$  structure for the anion in solution. Similar  $^1\text{H}$  nmr spectra were obtained for all the salts studied in solution. Detection of the asymmetry indicated by ir measurement of the perturbed anion (figure 12) in THF would be rather unlikely on the NMR time scale. Oxygen-17 and carbon-13 nmr spectral studies have indicated, however, that the lifetime of any one of the equally probable  $\text{CpMo}(\text{CO})_2\text{CO}^- \cdots \text{Na}^+$  interactions in the  $\text{Na}^+\text{CpMo}(\text{CO})_3^-$  salt solution is shorter than the time scale of an observable event using nmr techniques (ca.  $10^{-2}$  s) [77]. The lower limit of the lifetime of a particular ion site may be taken as the mean lifetime of a collision pair, and is on the order of  $10^{-11}$  s [78], obviously detectable by ir spectroscopy since the excited state lifetime of an ir experiment is  $\sim 10^{-11}$  s [79].

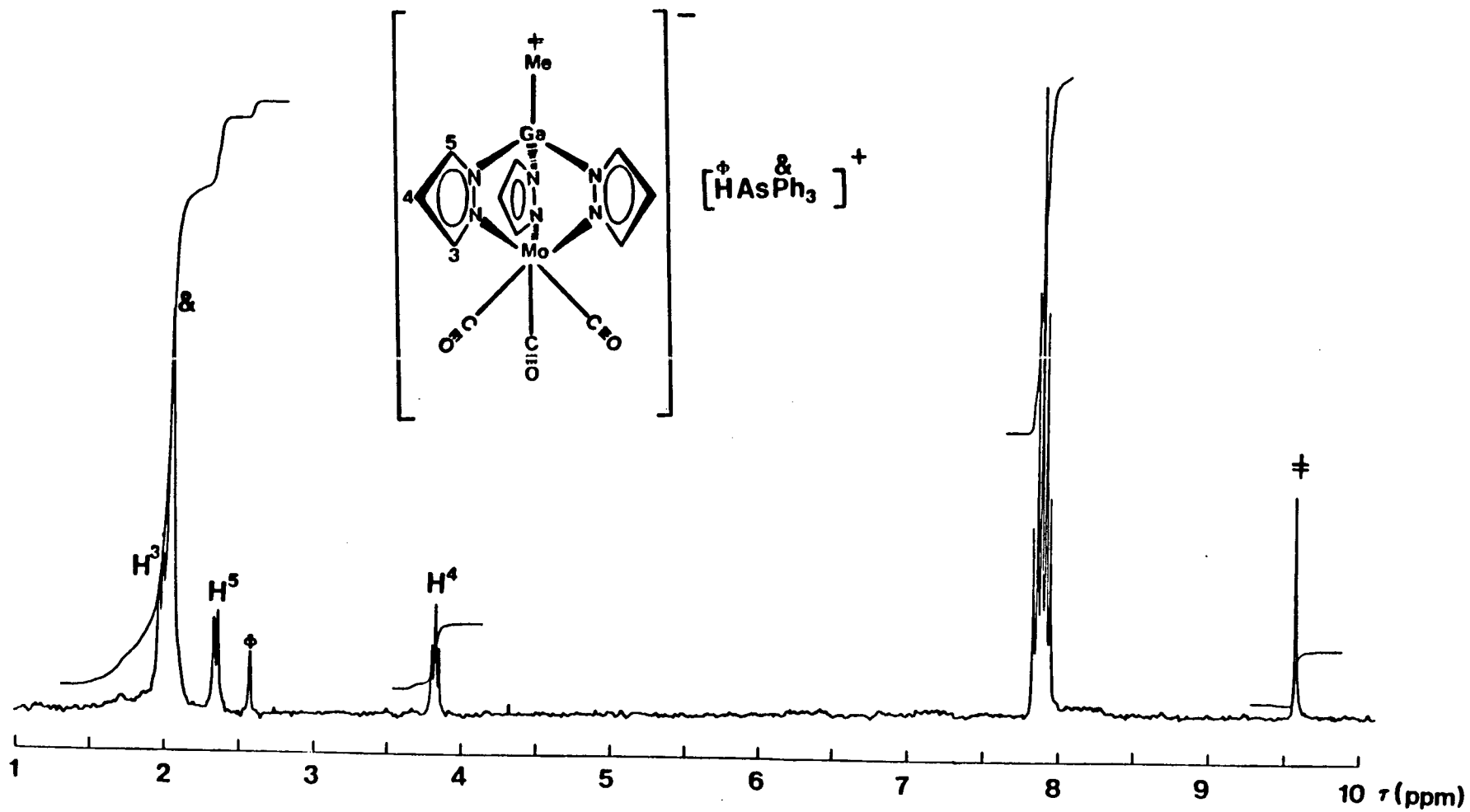


Figure 14. 80 MHz  $^1H$  nmr spectrum of  $[HAsPh_3]^+[MeGapz_3Mo(CO)_3]^-$  in  $d_6$ -acetone.

### 2.3.2 $[\text{MeGapz}_3]\text{Mo}(\text{CO})_3\text{H}$

It was reported originally that acidification of  $[\text{RBpz}_3]\text{Mo}(\text{CO})_3^-$  (R = H, or pyrazolyl,  $\text{N}_2\text{C}_3\text{H}_3$ ) anions with acetic acid yielded the corresponding  $[\text{RBpz}_3]\text{Mo}(\text{CO})_3\text{H}$  [53] acids. Similarly, the weak acid  $\text{CpMo}(\text{CO})_3\text{H}$  is readily obtained by protonation of the corresponding base  $\text{CpMo}(\text{CO})_3^-$  anion with acetic acid [55]. The preparation of  $[\text{MeGapz}_3]\text{Mo}(\text{CO})_3\text{H}$  was attempted initially by acidification of the  $\text{Na}^+\text{MeGapz}_3\text{Mo}(\text{CO})_3^-$  salt solution with glacial acetic acid. Both the solution ir and  $^1\text{H}$  nmr spectra of the yellow powdery solid isolated from the reaction indicated the presence of two compounds in solution in ~2:1 ratio (two Ga-Me signals were observed in the  $^1\text{H}$  nmr spectrum in a 2:1 ratio). An incomplete protonation of the  $\text{MeGapz}_3\text{Mo}(\text{CO})_3^-$  anion was therefore suspected. A comparison of the ir and  $^1\text{H}$  nmr data for the mixture, with those obtained for the  $\text{Na}^+\text{MeGapz}_3\text{Mo}(\text{CO})_3^-$  salt (section 2.2.2), confirmed that the species responsible for the weaker set of signals emanated from the unreacted  $\text{Na}^+\text{MeGapz}_3\text{Mo}(\text{CO})_3^-$  salt. The stronger set of signals was suspected to have arisen from the expected  $[\text{MeGapz}_3]\text{Mo}(\text{CO})_3\text{H}$  hydride species. If true, then the suggestion would be that the  $\text{MeGapz}_3\text{Mo}(\text{CO})_3^-$  anion is perhaps a weaker base than the analogous  $\text{CpMo}(\text{CO})_3^-$  anion, the implication being that under conditions where acetic acid suffices to protonate the  $\text{CpMo}(\text{CO})_3^-$  anion, a stronger acid would be required to fully protonate the  $\text{MeGapz}_3\text{Mo}(\text{CO})_3^-$  anion.

To test this hypothesis, the reaction was repeated using the stronger acid,  $\text{HCl}(\text{g})$ , for acidification. An orange-yellow air-sensitive solid of

the desired complex,  $[\text{MeGapz}_3]\text{Mo}(\text{CO})_3\text{H}$ , was obtained in good yields. This compound displayed three strong bands and one weak band (1952, 1928, 1908, 1808  $\text{cm}^{-1}$ , hexane), in the  $\nu_{\text{CO}}$ /hydride region of the ir spectrum. These bands were close to those observed for one of the species suspected to be the hydride in the product mixture from the acetic acid reaction (1950, 1935, 1912, 1810  $\text{cm}^{-1}$ ,  $\text{C}_6\text{H}_{12}$ ; section 2.2.5). For a 7-coordinate compound such as  $[\text{MeGapz}_3]\text{Mo}(\text{CO})_3\text{H}$ , three  $\nu_{\text{CO}}$  bands are expected in the ir as befits a complex possessing  $\text{C}_s$  symmetry ( $2\text{A}' + \text{A}''$ ), consistent with a 3:4 or 'four-legged piano stool' structure. The closely related  $\text{CpMo}(\text{CO})_3\text{H}$  (2030, 1949, 1913  $\text{cm}^{-1}$ ,  $\text{CS}_2$ ) [55], and  $[\text{HBpz}_3]\text{Mo}(\text{CO})_3\text{H}$  (2000, 1905, 1880  $\text{cm}^{-1}$ , Nujol) [53] compounds have been shown to display three  $\nu_{\text{CO}}$  bands in their ir spectra, without accompanying  $\nu_{\text{Mo-H}}$  bands in each case. Thus, one of the four bands observed for the  $[\text{MeGapz}_3]\text{Mo}(\text{CO})_3\text{H}$  complex must be due to the Mo-H stretching vibration in the molecule.

The replacement of hydrogen by deuterium is a well-known technique for studying vibrations involving hydrogen. For a pure (where 'pure' implies that virtually all the potential energy involved in the corresponding normal mode is associated with the M-H bond stretching) stretching mode, substitution of deuterium for hydrogen attached to a metal results in a shift in frequency by a factor of  $\sqrt{2}$  or 1.414 (i.e.,  $\nu(\text{M-H})/\nu(\text{M-D}) \sim \sqrt{2}$  Harmonic oscillator approximation) [80]. To establish which of the four bands observed for the  $[\text{MeGapz}_3]\text{Mo}(\text{CO})_3\text{H}$  is due to the Mo-H stretching vibration, the deuteride species  $[\text{MeGapz}_3]\text{Mo}(\text{CO})_3\text{D}$  was prepared and its solution ir obtained. The solution ir spectrum of the

molybdenum deuteride showed three bands (1935, 1910, 1845  $\text{cm}^{-1}$ ,  $\text{C}_6\text{H}_6$ ) in the  $\nu_{\text{CO}}$  region, and a weak band at  $\sim 1380 \text{ cm}^{-1}$ . Evidently, the band at  $\sim 1952 \text{ cm}^{-1}$  in the  $[\text{MeGapz}_3]\text{Mo}(\text{CO})_3\text{H}$  compound had shifted to lower wavenumbers by a factor of  $\sim 2$  just by substitution of deuterium for hydrogen in the molybdenum hydride complex. Based on this observation, the bands at  $1952 \text{ cm}^{-1}$  in the hydride complex, and  $1380 \text{ cm}^{-1}$  in the deuteride compound were assigned to Mo-H and Mo-D stretching vibrations respectively.

The ir spectrum of the  $[\text{MeGapz}_3]\text{Mo}(\text{CO})_3\text{H}$  or  $[\text{MeGapz}_3]\text{Mo}(\text{CO})_3\text{D}$  in THF solution is interesting in that the  $\nu_{\text{CO}}$  bands of the  $[\text{MeGapz}_3\text{Mo}(\text{CO})_3]^-$  anion are also displayed. This is thought to arise from the acid-base dissociation of the Mo-H or Mo-D bond in the polar and weakly basic THF solvent. This latter observation, in conjunction with the requirement of a strong acid to fully protonate the  $[\text{MeGapz}_3\text{Mo}(\text{CO})_3]^-$  anion, suggests that  $[\text{MeGapz}_3]\text{Mo}(\text{CO})_3\text{H}$  is more protonic and less hydridic than the analogous  $\text{CpMo}(\text{CO})_3\text{H}$ . This conclusion is at odds with the trend established earlier, i.e., that  $[\text{MeGapz}_3]^-$  and  $[\text{HBpz}_3]^-$  ligands are better electron-donors than the  $\text{Cp}^-$  ligand as judged from the higher  $\nu_{\text{CO}}$  values for  $[\text{CpMo}(\text{CO})_3]^-$  anion compared to either  $[\text{HBpz}_3\text{Mo}(\text{CO})_3]^-$  [53] or  $[\text{MeGapz}_3\text{Mo}(\text{CO})_3]^-$  [34] anions respectively. If this argument holds, then the only logical conclusion is that the six-coordinate  $[\text{MeGapz}_3\text{Mo}(\text{CO})_3]^-$  anion is more stable with respect to its seven-coordinate hydride than is the case in the analogous cyclopentadienyl system. Similar observations on the  $[\text{HBpz}_3]\text{Mo}(\text{CO})_3\text{H}$  [60] compound were reported during the course of this work.

The  $^1\text{H}$  nmr spectrum of the  $[\text{MeGapz}_3]\text{Mo}(\text{CO})_3\text{H}$  in  $d_6$ -acetone solution displayed one set of signals for the pyrazolyl ring protons, indicating equivalent pyrazolyl rings in the above complex, and a Mo-H resonance at 18.5  $\tau$ . It is evident, however, that the pz groups are inequivalent in the above complex (ir showed three  $\nu_{\text{CO}}$  bands, consistent with a  $\text{C}_s$  symmetry for the complex). Since seven-coordinate complexes of this type are known for their fluxional behaviour in solution, it is probable that the present compound is stereochemically non-rigid in solution. Thus, interconversion of the CO ligands and the H ligand in the basal plane of the 3:4 structure of  $[\text{MeGapz}_3]\text{Mo}(\text{CO})_3\text{H}$ , similar to that observed for  $[\text{HBpz}_3]\text{Mo}(\text{CO})_3\text{X}$  ( $\text{X} = \text{H}, \text{Br}, \text{I}$ ) [60] must be operative in solution. Such interconversion of ligands in the basal plane of the 3:4 structure would at some stage place the H ligand along the Ga...Mo axis, giving a symmetrical 3:3:1 or 'capped-octahedral' structure, leading to the equalization of the environments of the pz rings; hence, one sees in the  $^1\text{H}$  nmr experiment a dynamic  $\text{C}_{3v}$  structure in solution. Alternatively, and perhaps less likely, is a rapid rotation of the 'MeGapz<sub>3</sub>' moiety about the Ga...Mo axis, resulting in the equalization of the chemical environments of the pz groups. The Mo-H resonance for  $[\text{MeGapz}_3]\text{Mo}(\text{CO})_3\text{H}$  appeared at 18.5  $\tau$ , a considerably higher field position than those reported for  $\text{CpMo}(\text{CO})_3\text{H}$  (Mo-H  $\sim 12.8$   $\tau$ ) [55] and  $[\text{HBpz}_3]\text{Mo}(\text{CO})_3\text{H}$  (Mo-H  $\sim 13.3$   $\tau$  [53]; 13.02  $\tau$  [60]), respectively. It is difficult to rationalize the large Mo-H chemical shift difference between the  $[\text{MeGapz}_3]\text{Mo}(\text{CO})_3\text{H}$  and the analogous  $\text{CpMo}(\text{CO})_3\text{H}$  and  $[\text{HBpz}_3]\text{Mo}(\text{CO})_3\text{H}$  hydride species. It is reasonable to speculate however, that since the MeGapz<sub>3</sub><sup>-</sup> ligand is a better electron-donor than the HBpz<sub>3</sub><sup>-</sup> ligand [34], the proton in the present

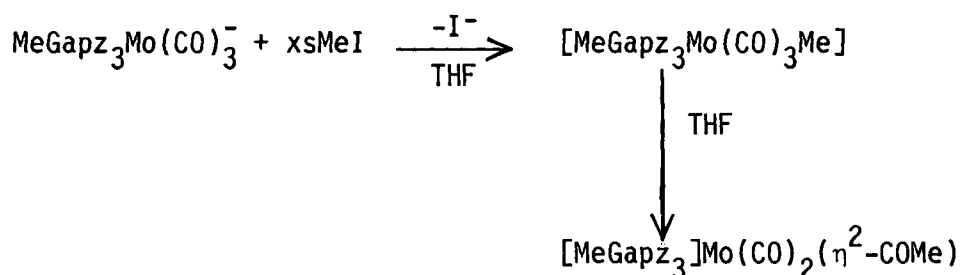
[MeGapz<sub>3</sub>]Mo(CO)<sub>3</sub>H compound most likely experiences greater shielding effect from the electron-rich Mo center in the complex.

It is noteworthy that the crystal structure of the analogous ( $\eta$ -C<sub>5</sub>Me<sub>5</sub>)Mo(CO)<sub>3</sub>H [81] compound has recently been reported by Leoni et al. According to the authors, even though the H atom was not located, its position was inferred from the geometry of the remainder of the molecule. The authors concluded that the geometrical facts obtained for the molecule were characteristic of a 'four-legged piano stool' geometry, and the 'hole' in the Mo atom coordination sphere at a basal vertex of the square pyramid was interpreted to be the result of the 'missing' H atom.

### 2.2.3 [MeGapz<sub>3</sub>]Mo(CO)<sub>2</sub>( $\eta$ <sup>2</sup>-COR) (R = Me, Ph)

In an earlier report, it was stated that the reaction of the HBpz<sub>3</sub>Mo(CO)<sub>3</sub><sup>-</sup> anion with MeI gave the  $\sigma$ -methyl complex, HBpz<sub>3</sub>Mo(CO)<sub>3</sub>Me [53]. Recently, Curtis et al. communicated that the product of the above reaction was in fact an  $\eta$ <sup>2</sup>-acyl complex [HBpz<sub>3</sub>]Mo(CO)<sub>2</sub>( $\eta$ <sup>2</sup>-COMe), no detectable quantities of the  $\sigma$ -methyl complex being observed in solution. The ir and <sup>1</sup>H nmr for the complex were corroborated definitively by an X-ray structure determination showing the presence of an  $\eta$ <sup>2</sup>-acyl geometry in the solid state [64]. In an attempt to clarify the above observations [53,64], the reaction of the isoelectronic, isostructural MeGapz<sub>3</sub>Mo(CO)<sub>3</sub><sup>-</sup> anion with MeI was investigated. Of particular interest to us was the actual pathway of such a reaction. Is the  $\sigma$ -methyl complex '[MeGapz<sub>3</sub>]Mo(CO)<sub>3</sub>Me' formed at some stage, and rearranged to give the  $\eta$ <sup>2</sup>-acyl complex [MeGapz<sub>3</sub>]Mo(CO)<sub>2</sub>( $\eta$ <sup>2</sup>-COMe)? In order to observe this

$\sigma$ -methyl intermediate, if formed at all, the reaction was carried out in THF and monitored at room temperature by solution ir spectroscopy. The results obtained indicate that the  $\sigma$ -methyl complex is formed but rearranges to give the  $\eta^2$ -acyl complex as the final product according to the equations below:-



Thus, after stirring the reaction mixture at room temperature for ~2 days, the ir spectrum of the solution showed three new  $\nu_{\text{CO}}$  bands at 1970, 1920 and 1855  $\text{cm}^{-1}$ . The three bands intensified after stirring the reaction mixture for another 2 days, after which additional stirring produced no change in the ir spectrum. The presence of the  $\nu_{\text{CO}}$  bands characteristic of the unreacted  $\text{MeGapz}_3\text{Mo}(\text{CO})_3^-$  anion, even after stirring the reaction mixture for 4 days, is indicative of the low yield of this reaction in THF at room temperature. The ir spectrum of the brick-red crystals isolated from this reaction showed two strong bands at 1980, 1855  $\text{cm}^{-1}$ , and a weak band at 1570  $\text{cm}^{-1}$ . The  $\nu_{\text{CO}}$  bands at 1970, 1920 and 1855  $\text{cm}^{-1}$  observed during the reaction are thought to have emanated from the presence of a transient  $\sigma$ -methyl 'MeGapz<sub>3</sub>Mo(CO)<sub>3</sub>Me' intermediate in solution. This pattern is characteristic of C<sub>s</sub> symmetry M(CO)<sub>3</sub>X groups

which typically show three  $\nu_{\text{CO}}$  bands in their ir consistent with the three (2A' + A'') modes expected. These  $\nu_{\text{CO}}$  values for 'MeGapz<sub>3</sub>Mo(CO)<sub>3</sub>Me' are compared with  $\nu_{\text{CO}}$  bands reported for related  $\sigma$ -methyl complexes in Table II below. The presence of only two bands instead of the expected three bands in the ( $\eta$ -C<sub>5</sub>H<sub>5</sub>)Mo(CO)<sub>3</sub>Me compound was interpreted as being due to the coincidence of two bands [55].

Table II. Ir carbonyl stretching frequencies of some LMo(CO)<sub>3</sub>Me complexes (L =  $\eta$ -C<sub>5</sub>H<sub>5</sub>,  $\eta$ -C<sub>5</sub>Me<sub>5</sub>,  $\pi$ -C<sub>9</sub>H<sub>7</sub>, HBpz<sub>3</sub>, MeGapz<sub>3</sub>).

<u>COMPOUND</u>	<u><math>\nu_{\text{CO}}</math> (cm<sup>-1</sup>)</u>	<u>Reference</u>
( $\eta$ -C <sub>5</sub> H <sub>5</sub> )Mo(CO) <sub>3</sub> Me	2020,1937 (CCl <sub>4</sub> )	55
( $\eta$ -C <sub>5</sub> Me <sub>5</sub> )Mo(CO) <sub>3</sub> Me	2014,1929 (C <sub>6</sub> H <sub>12</sub> )	82
( $\pi$ -C <sub>9</sub> H <sub>7</sub> )Mo(CO) <sub>3</sub> Me	2024,1945,1911	83
[HBpz <sub>3</sub> ]Mo(CO) <sub>3</sub> Me	1985,1970,1948	
	1848,1830,1800 (Nujol)	53
[MeGapz <sub>3</sub> ]Mo(CO) <sub>3</sub> Me	1970,1920,1855 (THF)	This work

The presence of two sharp  $\nu_{\text{CO}}$  bands at 1980 and 1855 cm<sup>-1</sup>, and a weak band at 1570 cm<sup>-1</sup> in the ir spectrum of the brick-red crystals isolated from the reaction of MeGapz<sub>3</sub>Mo(CO)<sub>3</sub><sup>-</sup> with MeI, suggested that the present compound is indeed the  $\eta^2$ -acyl compound with the formulation [MeGapz<sub>3</sub>]Mo-(CO)<sub>2</sub>( $\eta^2$ -COMe). Complexes are described as  $\eta^2$ -acyl compounds either from structural determination or from ir spectra [ $\nu_{\text{C=O}}$  ( $\eta^2$ -acyl) < 1600 cm<sup>-1</sup>] [84,85]. The metal-bonded  $\eta^1$ -acetyl groups ( $\eta^1$  M-C(O)R) usually absorbed at higher frequencies in the ir (>1600 cm<sup>-1</sup>) [85,86]. An X-ray structural

determination of the isoelectronic, isostructural  $[\text{HBpz}_3]\text{Mo}(\text{CO})_2(\eta^2\text{-COMe})$  has indeed revealed that this is an  $\eta^2$ -acyl complex [64]. The bands at 1983, 1856, 1570  $\text{cm}^{-1}$  observed for this complex are in close agreement with those observed for the present  $[\text{MeGapz}_3]\text{Mo}(\text{CO})_2(\eta^2\text{-COMe})$  (1980, 1855, 1570  $\text{cm}^{-1}$ ,  $\text{CH}_2\text{Cl}_2$ ) complex. A plausible reaction sequence for the formation of the present  $\eta^2$ -acyl complex is shown in figure 15. In this reaction sequence, CO migration with subsequent insertion into the Mo-Me bond of the  $\sigma$ -methyl intermediate ' $\text{MeGapz}_3\text{Mo}(\text{CO})_3\text{Me}$ ' would give the final  $\eta^2$ -acyl complex  $[\text{MeGapz}_3]\text{Mo}(\text{CO})_2(\eta^2\text{-COMe})$ . Methyl migration onto the coordinated CO ligand is equally viable. It is difficult to discuss which of the above routes is operative solely on the results obtained from this experiment. Mechanistic studies on the classic carbonylation of alkyl-(pentacarbonyl)manganese by Calderazzo [85], have shown, that it is actually the alkyl group that migrates and subsequently bonds to the carbon of a coordinated CO group. It is clear, however, that a decarbonylation step was involved in the reaction of the  $\text{HBpz}_3\text{Mo}(\text{CO})_3^-$  anion with  $\text{PhCOBr}$ . By use of  $^{13}\text{C}$ -labelled  $\text{PhC}^*\text{OBr}$  as the starting halide species in their preparation of the  $\eta^2$ -benzoyl  $[\text{HBpz}_3]\text{Mo}(\text{CO})_2(\eta^2\text{-COPh})$  compound, Curtis et al. [65] clearly established that the CO initially on the metal is lost in a decarbonylation process. In this same paper, using the Extended Hückel Molecular Orbital (EHMO) treatment, the authors showed that there is substantial double-bond character in the  $\text{Mo}=\text{C}(\text{acyl})$  bond but a very weak Mo-O bond; hence they suggested that the compounds  $[\text{HBpz}_3]\text{Mo}(\text{CO})_2(\eta^2\text{-COR})$  ( $\text{R} = \text{Me}, \text{Ph}$ ) could be regarded as stabilized 16-electron Mo complexes.

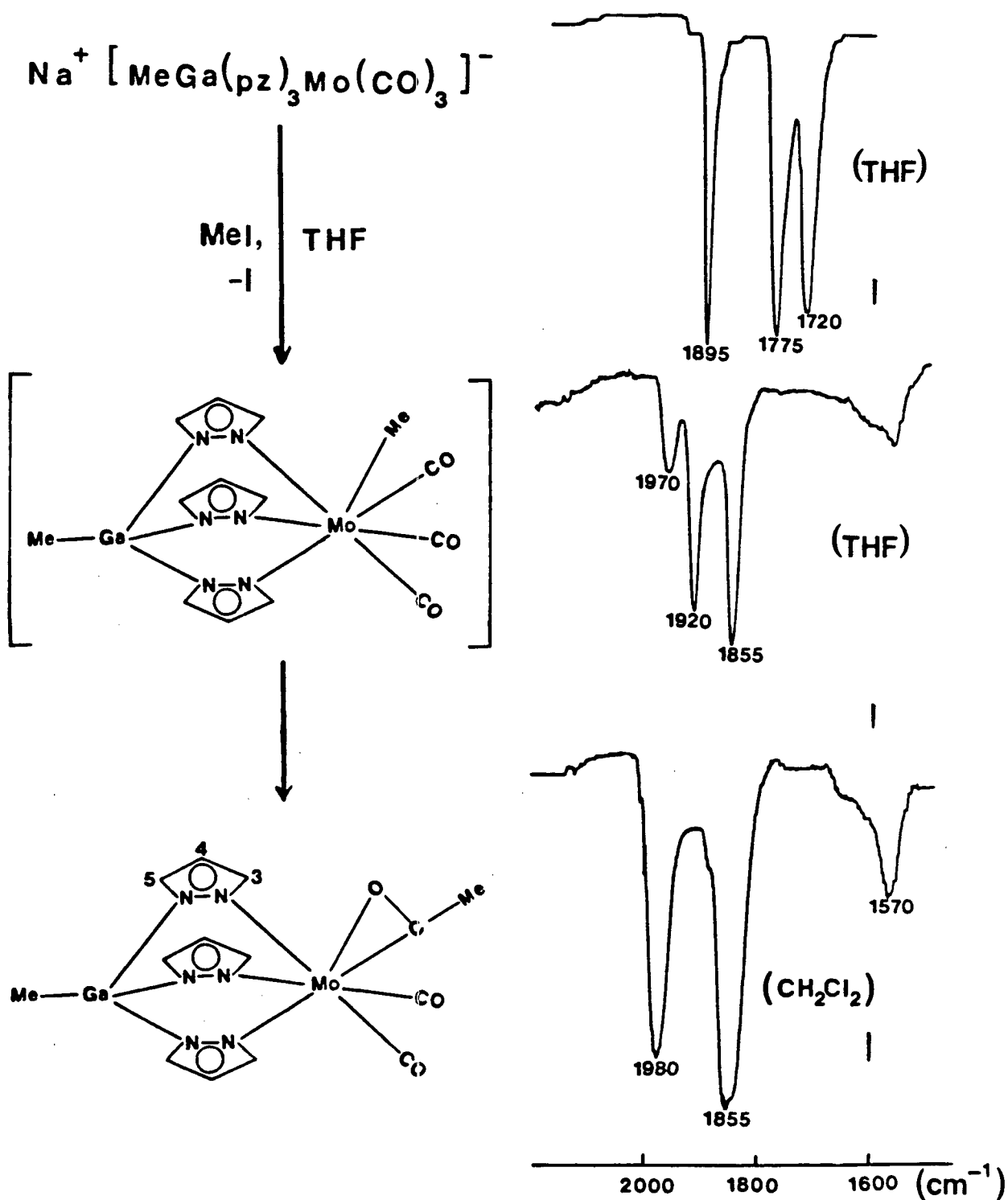


Figure 15. Ir spectra of the carbonyl stretching frequency region observed during the reaction of  $\text{MeGa}(\text{pz})_3\text{Mo}(\text{CO})_3$  with MeI.

The  $^1\text{H}$  nmr spectrum of the present  $[\text{MeGapz}_3]\text{Mo}(\text{CO})_2(\eta^2\text{-COMe})$  compound in  $\text{d}_6$ -acetone solution (figure 16) is consistent with the formulation as an  $\eta^2$ -acyl complex. The pyrazolyl protons of the ligand appear in a 2:1 pattern indicating that two of the pyrazolyl groups are equivalent with one pyrazolyl ring being different. This is suggestive of a stereochemically rigid structure in solution. The acetyl COMe signal is also displayed at 6.60  $\tau$ .

Much current interest has been directed towards the preparation and chemical reactivity of the  $\eta^2$ -acyl metal complexes partly due to the possible role of these species in the metal-catalyzed hydrogenation of carbon monoxide [87,88,89]. The facile alkyl to CO migration observed in the formation of the present  $[\text{MeGapz}_3]\text{Mo}(\text{CO})_2(\eta^2\text{-COMe})$  compound and the analogous  $[\text{HBpz}_3]\text{Mo}(\text{CO})_2(\eta^2\text{-COMe})$  [64] complex are unprecedented in either  $\text{CpMo}(\text{CO})_3\text{R}$  or  $\text{CpMo}(\text{CO})_3(\sigma\text{-COR})$  chemistry. In fact to our knowledge, the hypothetical  $\text{CpMo}(\text{CO})_2(\eta^2\text{-COR})$  ( $\text{R} = \text{Me}, \text{Ph}$ ) complexes have never been reported. However, a related tungsten complex,  $\text{CpW}(\text{CO})(\text{HCCH})(\eta^2\text{-COMe})$  [90] has been reported but no definitive structural data are available.

Mass spectral data for the present  $[\text{MeGapz}_3]\text{Mo}(\text{CO})_2(\eta^2\text{-COMe})$  complex displayed signals attributable to the  $\text{P}^+$ ,  $\text{P-Me}^+$ ,  $\text{P-CO}^+$ ,  $\text{P-COMe}^+$ ,  $\text{P-2CO}^+$ ,  $\text{P-CO-COMe}^+$ ,  $\text{P-3CO}^+$  and  $\text{P-2CO-COMe}^+$  ( $\text{P} = \text{parent}$ ) ions respectively. Interestingly, the above mass spectral data are in perfect agreement with those reported for the isostructural  $[\text{HBpz}_3]\text{Mo}(\text{CO})_2(\eta^2\text{-COMe})$  compound [65].

Similarly, reaction of the  $[\text{MeGapz}_3\text{Mo}(\text{CO})_3]^-$  anion with  $\text{PhCOCl}$  gave a

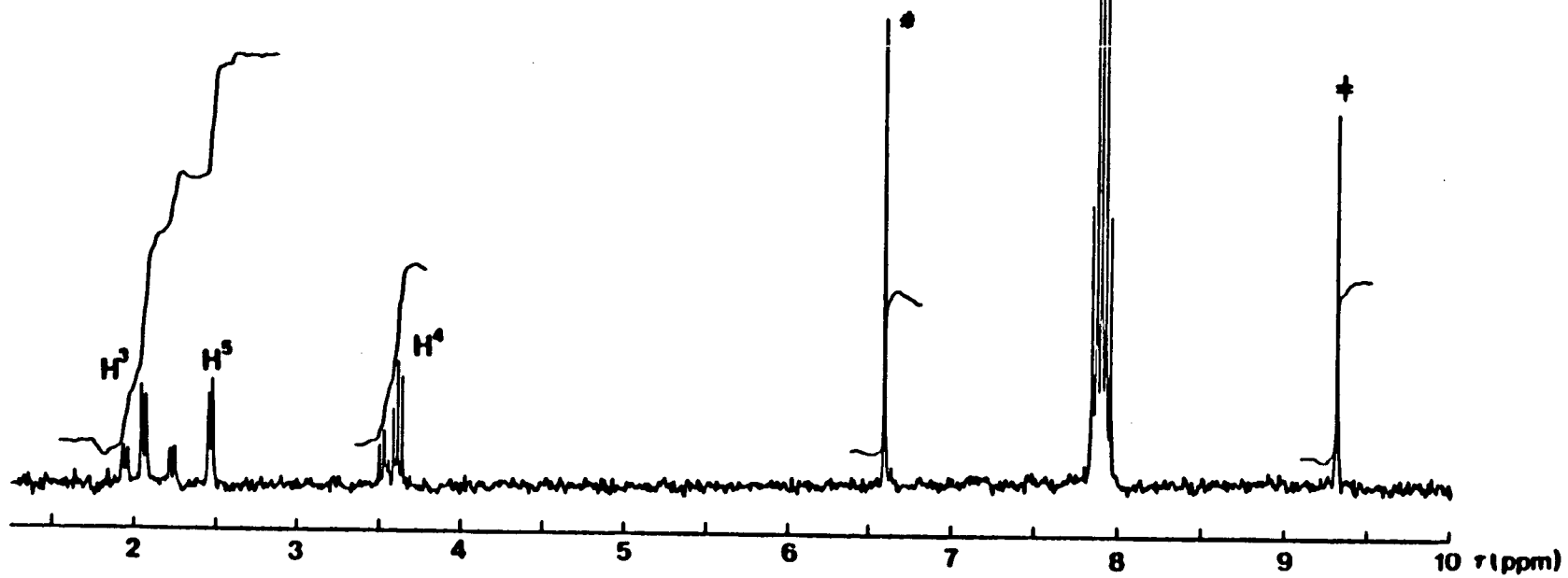
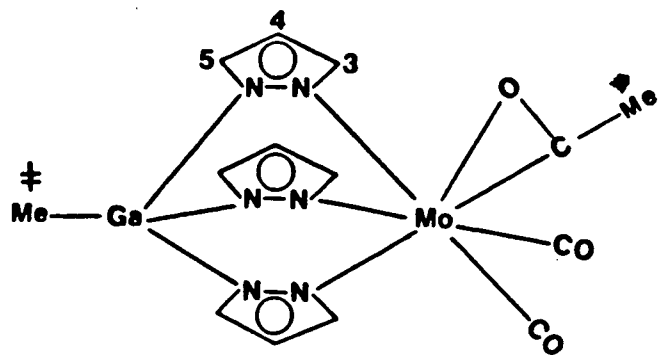


Figure 16. 80 MHz <sup>1</sup>H nmr spectrum of [MeGapz<sub>3</sub>]Mo(CO)<sub>2</sub>(η<sup>2</sup>-COMe) in d<sub>6</sub>-acetone solution.

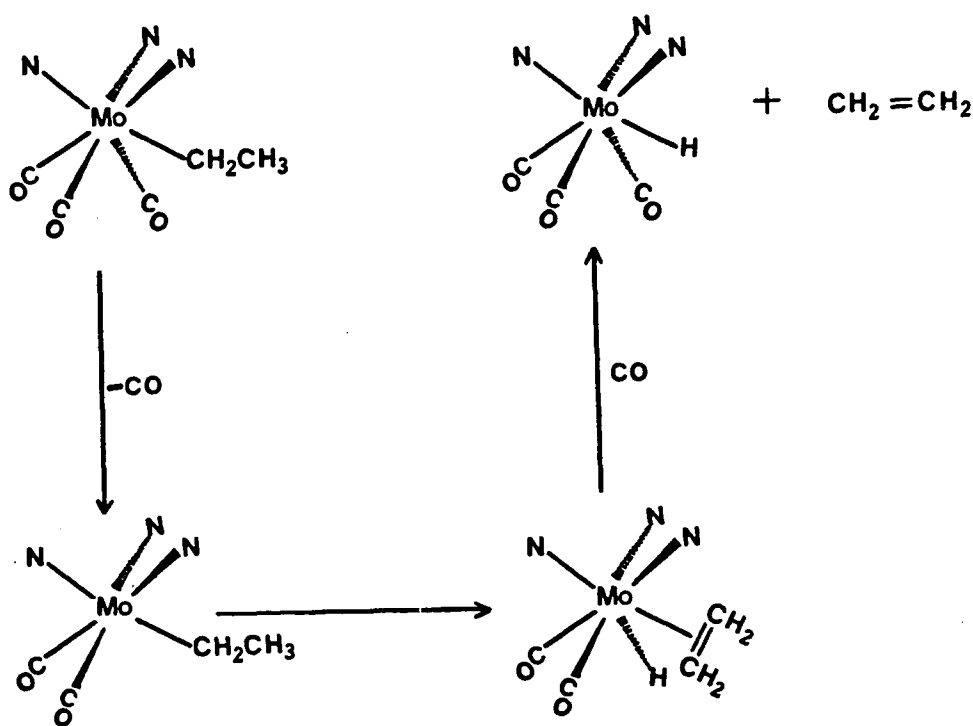
dark blue product, albeit in very low yield, and characterized solely by its ir spectrum (1965, 1820 and 1535  $\text{cm}^{-1}$ ,  $\text{CH}_2\text{Cl}_2$ ) as the  $\eta^2$ -benzoyl product,  $[\text{MeGapz}_3]\text{Mo}(\text{CO})_2(\eta^2\text{-COPh})$ . The ir data for this compound compare well with that obtained for the complex structurally characterized as  $[\text{HBpz}_3]\text{Mo}(\text{CO})_2(\eta^2\text{-COPh})$  (1965, 1852, 1490  $\text{cm}^{-1}$ ,  $\text{CH}_2\text{Cl}_2$ ) [65].

Thus, it appears that the tendency of the  $\sigma$ -donor electrons localized at the nitrogen donor sites of the ligands  $\text{MeGapz}_3^-$  and  $\text{HBpz}_3^-$ , to promote octahedral coordination about the metal center and the steric bulk of the ligands favor the transformation of the seven-coordinate 3:4 structure of the  $\text{LMo}(\text{CO})_3\text{R}$  ( $\text{L} = \text{MeGapz}_3, \text{HBpz}_3$ ) species to the quasi-six-coordinate  $\text{LMo}(\text{CO})_2(\eta^2\text{-COR})$  arrangement. In fact the  $\text{HBpz}_3^-$  ligand has been shown to promote six-coordination over seven-coordination in the successful isolation of the paramagnetic radical species,  $\text{HBpz}_3\text{Mo}(\text{CO})_3\cdot$  [38], and also in the  $\text{HBpz}_3\text{Mo}(\text{CO})_3\text{Br}$  compound, where the four "legs" of the piano stool structure of the latter compound were found to be compressed together [60]. Similar reasoning was invoked by Curtis et al. [65] in rationalizing the transformation of  $[\text{HBpz}_3]\text{Mo}(\text{CO})_3\text{R}$  to  $[\text{HBpz}_3]\text{Mo}(\text{CO})_2(\eta^2\text{-COR})$  ( $\text{R} = \text{Me}, \text{Ph}$ ) complexes.

#### 2.3.4 $[\text{MeGapz}_3]\text{Mo}(\text{CO})_3\text{Et}$

The reaction of the  $\text{MeGapz}_3\text{Mo}(\text{CO})_3^-$  anion with ethyl bromide afforded the metal-alkyl bonded  $[\text{MeGapz}_3]\text{Mo}(\text{CO})_3\text{Et}$  derivative. The red-brown compound is unstable and decomposes on storage after a few days even under inert conditions. However, the decomposition is much more rapid in solution, the ir spectrum of solutions of this ethyl derivative clearly

showing the presence of the anion  $\text{MeGapz}_3\text{Mo}(\text{CO})_3^-$ . The solution ir spectrum of the ethyl compound in  $\text{CH}_2\text{Cl}_2$  shows  $\nu_{\text{CO}}$  bands at 1970, 1930, 1820  $\text{cm}^{-1}$ , in addition to two  $\nu_{\text{CO}}$  bands at 1890 and 1755  $\text{cm}^{-1}$  respectively. The latter two bands are characteristic of the  $\text{MeGapz}_3\text{Mo}(\text{CO})_3^-$  anion, presumably due to slow decomposition of the  $[\text{MeGapz}_3]\text{Mo}(\text{CO})_3\text{Et}$  compound in solution probably by  $\beta$ -elimination (see scheme below).



In the scheme, the decomposition of the Mo-Et bond involves a facile  $\beta$ -hydride migration to form the hydride  $[\text{MeGapz}_3]\text{Mo}(\text{CO})_3\text{H}$  species with expulsion of ethylene. Dissociation of the Mo-H bond in the above hydride species (similar to that discussed in section 2.3.2, p 45) would then explain the presence of the  $\text{MeGapz}_3\text{Mo}(\text{CO})_3^-$  anion in the solution ir spectrum of the present  $[\text{MeGapz}_3]\text{Mo}(\text{CO})_3\text{Et}$  compound.

It is interesting that the ir spectrum of the closely related  $[\text{HBpz}_3]\text{Mo}(\text{CO})_3\text{Et}$  complex, reported earlier by Trofimenko, displayed five  $\nu_{\text{CO}}$  bands (1980, 1960, 1850, 1835, 1816  $\text{cm}^{-1}$ , Nujol) [53], perhaps indicating a similar tendency to decomposition for the boron compound. The ir spectra of related cyclopentadienyl analogues are interesting in that they display only two strong  $\nu_{\text{CO}}$  bands. For example, two  $\nu_{\text{CO}}$  bands were observed for the  $\text{CpMo}(\text{CO})_3\text{Et}$  (2016, 1932  $\text{cm}^{-1}$ ,  $\text{CCl}_4$ ) [55] and  $\text{CpCr}(\text{CO})_3\text{Et}$  (2012, 1933  $\text{cm}^{-1}$ , pentane) [91] complexes respectively. The appearance of only two  $\nu_{\text{CO}}$  bands for the above cyclopentadienyl ethyl derivatives may result from the coincidence of two bands with similar energies. The three bands observed in the  $\nu_{\text{CO}}$  region of the ir spectrum for the present  $[\text{MeGapz}_3]\text{Mo}(\text{CO})_3\text{Et}$  compound are consistent with a  $\text{C}_s$  symmetry ( $2\text{A}' + \text{A}''$ ), and again suggestive of a 3:4 or 'four-legged piano stool' structure for the complex.

The room temperature  $^1\text{H}$  nmr spectrum of  $[\text{MeGapz}_3]\text{Mo}(\text{CO})_3\text{Et}$  in  $\text{d}_6$ -acetone solution (figure 17), displayed one set of signals for the pz protons, indicating equivalent pz rings in the complex. The methyl and methylene protons of the ethyl group appeared as unresolved broad resonances centered at 8.15  $\tau$  and 6.32  $\tau$  respectively. The nmr spectrum of the present complex is different from that reported for the analogous

[HBpz<sub>3</sub>]Mo(CO)<sub>3</sub>Et [53] complex. Although the methyl and methylene peaks of the latter complex appeared at 8.60  $\tau$  and 6.38  $\tau$ , respectively, the pz protons of the ligand appeared in a 2:1 pattern. This observation was interpreted by the author as indicative of a stereochemically rigid structure with the ethyl group probably equidistant from two of the pz groups.

There are perhaps three possible interpretations of the <sup>1</sup>H nmr results for the [MeGapz<sub>3</sub>]Mo(CO)<sub>3</sub>Et complex. Firstly, a rigid 3:3:1 or "capped octahedral" structure with the Et group lying along the principal axis of the molecule. Such a symmetrical C<sub>3v</sub> structure would give equivalent pz groups hence one set of signals are displayed for the pz protons. Secondly, a rigid 3:4 or 'four-legged piano stool' structure in which case rapid rotation of the 'MeGapz<sub>3</sub>' moiety about the Ga...Mo axis would lead to equivalent set of signals for the pz proton resonances. Thirdly, interconversions between the various isomers of the 3:4 structure of the [MeGapz<sub>3</sub>]Mo(CO)<sub>3</sub>Et complex as shown in figure 18, with an average 3:3:1 or C<sub>3v</sub> structure predominating due to a fluxional process in solution. The first possibility can be disregarded based on the ir data (three  $\nu_{CO}$  bands were observed in the ir; a rigid 3:3:1 structure in solution would show only two bands). It is difficult, however, to discount either the second or the third possibility since both are equally probable. However, from our experience with the related compound [MeGapz<sub>3</sub>]Mo(CO)<sub>3</sub>SnMe<sub>2</sub>Cl [92], a complex which showed a transition from a 3:4 to a 3:3:1 arrangement in solution, the second possibility most likely accounts for the observed <sup>1</sup>H nmr results in the present Mo-Et complex. In

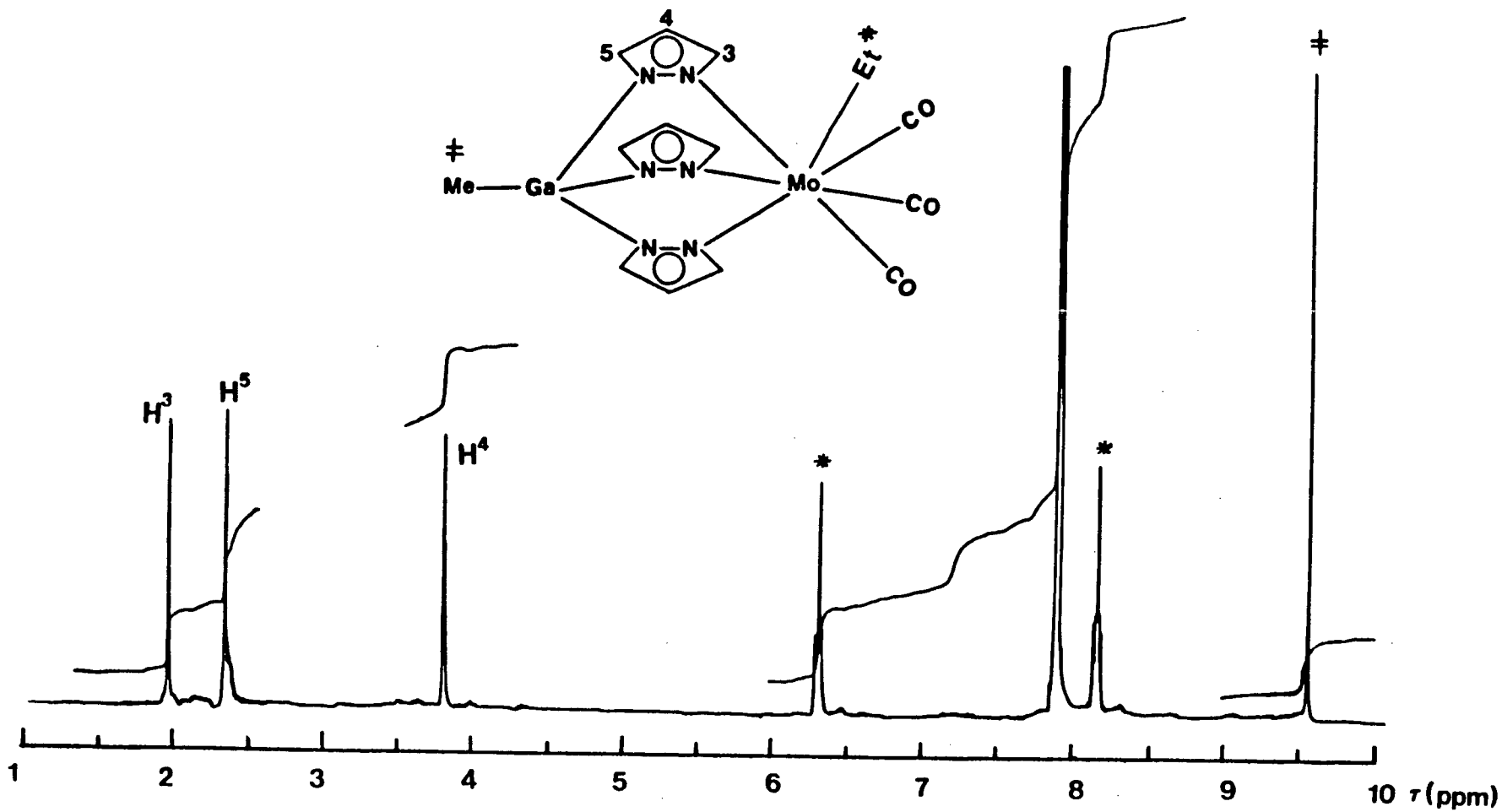


Figure 17. 270 MHz  $^1\text{H}$  nmr spectrum of  $[\text{MeGapz}_3]\text{Mo}(\text{CO})_3\text{Et}$  in  $\text{d}_6$ -acetone solution.

the Mo-Sn complex, the observed equivalence of the pz groups in the 3:3:1 arrangement was rationalized by a rotation of the 'MeGapz<sub>3</sub>' moiety about the Ga...Mo axis. It is worthy of mention that Curtis and Shiu reported one set of equivalent pz rings and one set of equivalent CO groups in the <sup>1</sup>H and <sup>13</sup>C nmr spectra for the [HBpz<sub>3</sub>]Mo(CO)<sub>3</sub>X (X = H, Br, I) complexes in solution from room temperature to -80°C [60]. This observation was interpreted by the authors as being indicative of dynamic C<sub>3v</sub> symmetry for the complexes in solution. A 3:4 structure for the boron complexes in the solid state has been confirmed by a single crystal X-ray structural determination of the [HBpz<sub>3</sub>]Mo(CO)<sub>3</sub>Br compound by the same authors [60].

It is noteworthy that in the CpMo(CO)<sub>3</sub>Et compound the methyl and methylene group signals were unresolved, appearing at 6.0 τ [55], but in the valence isoelectronic CpCr(CO)<sub>3</sub>Et complex [91], the methyl and methylene group signals were resolved, appearing at 8.89 τ and 6.39 τ respectively. The crystal structure of the CpMo(CO)<sub>3</sub>Et complex has been determined, and is in accord with a 3:4 structure for this complex in the solid state [93].

The mass spectrum of [MeGapz<sub>3</sub>]Mo(CO)<sub>3</sub>Et was characterized by excessive fragmentation, indicative of thermal instability of the compound under the mass spectrometric conditions. The highest mass observed corresponded to trace signals attributable to the P-3CO-Et<sup>+</sup> ion. A recent thermodynamic study of the CO-insertion into the Mo-R bond in the CpMo(CO)<sub>3</sub>R (R = H, Me, Et) compounds [94], has concluded that the Mo-Et bond is weaker than the Mo-Me bond (CO insertion into the Mo-Et bond is ~3

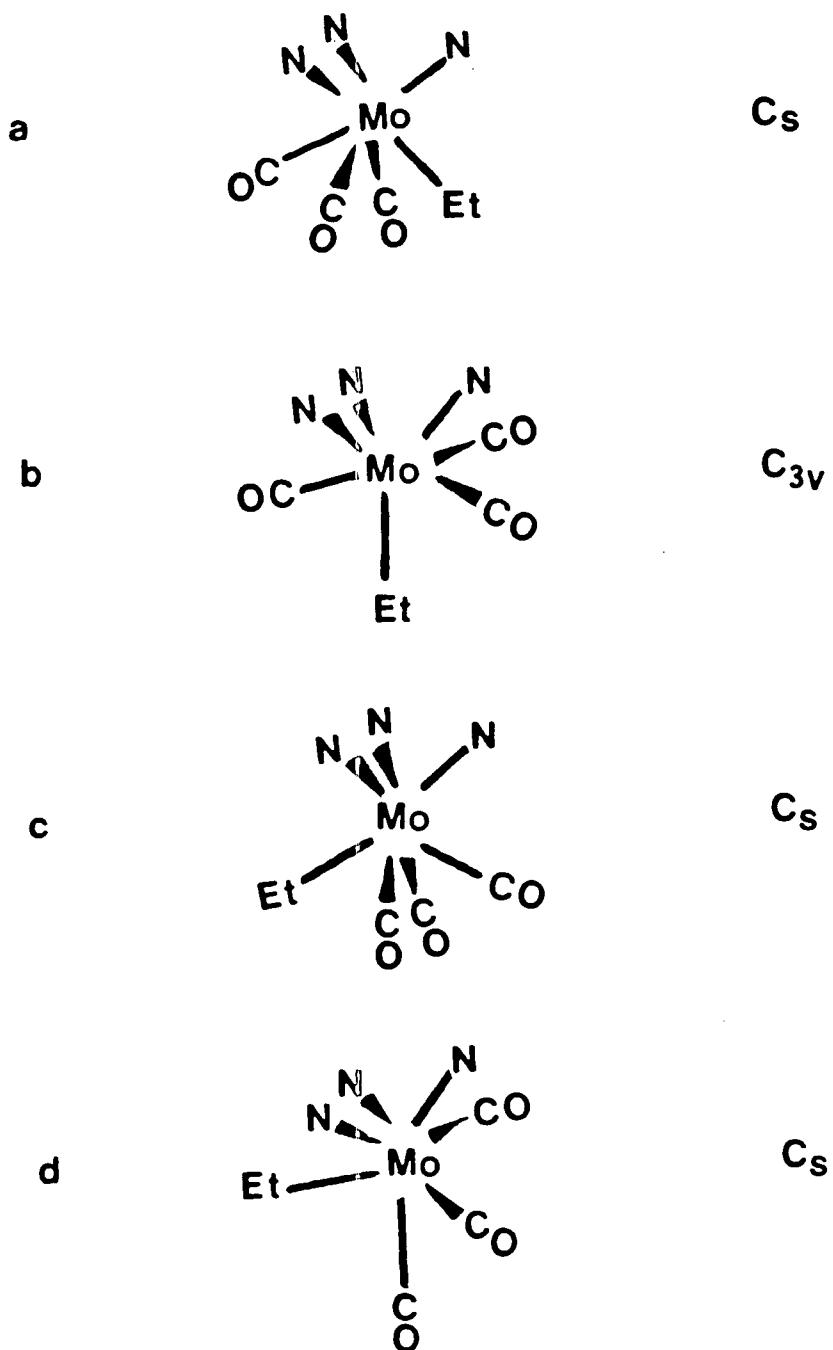
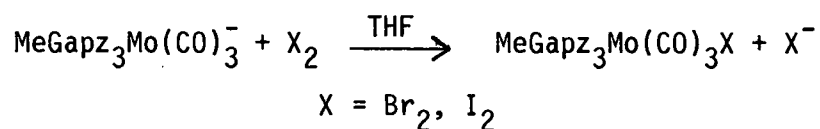


Figure 18. Various isomers of the seven-coordinate  $[MeGapz_3]Mo(CO)_3Et$ .

kcal/mol more favourable than into the Mo-Me bond). However, methyl transition-metal derivatives which lack  $\beta$ -hydrogen atoms are kinetically more stable than the ethyl compounds having  $\beta$ -hydrogen atoms. The combination of these factors is probably responsible for the inability to form the  $\eta^2$ -COEt derivative as well as the excessive fragmentation pattern observed for the present  $[\text{MeGapz}_3]\text{Mo}(\text{CO})_3\text{Et}$  compound in the mass spectrometer under electron impact conditions.

### 2.3.5 The $[\text{MeGapz}_3]\text{Mo}(\text{CO})_3\text{X}$ (X = Br, I) complexes

The reaction of the molybdenum tricarbonyl anion with halogens, as shown below,



was used in an attempt to prepare the  $[\text{MeGapz}_3]\text{Mo}(\text{CO})_3\text{X}$  (X = Br, I) complexes. Yellow (X = Br) and dark red (X = I) solids, sparingly soluble in most organic solvents, were isolated from these reactions. However, persistent attempts at obtaining analytically pure products were consistently unsuccessful. This was very discouraging since both the <sup>1</sup>H nmr and ir spectra of the reaction products indicated the presence of the expected halide species. In contrast, the isoelectronic, isostructural  $[\text{HBpz}_3]\text{Mo}(\text{CO})_3\text{X}$  (X = Br, I) compounds have been prepared and one of them (X = Br) structurally characterized [60].

### 2.4 Summary

The  $\text{LMo}(\text{CO})_3^-$  (L = MeGapz<sub>3</sub>, MeGa(3,5-Me<sub>2</sub>pz)<sub>3</sub>) anions have been isolated and characterized as their Na<sup>+</sup>, Et<sub>4</sub>N<sup>+</sup> and HAsPh<sub>3</sub><sup>+</sup> salts. Anion-

cation interaction of the  $\text{MeGapz}_3\text{Mo}(\text{CO})_3^-$  anion and the  $\text{Na}^+$  cation in THF has been described and supported by ir spectroscopic evidence. This study represents the first isolation of the  $\text{M}^+\text{MeGapz}_3\text{Mo}(\text{CO})_3^-$  salts and, most importantly, the first reported evidence for the involvement of the  $\text{LMo}(\text{CO})_3^-$  anions in ion-pair interactions with the  $\text{Na}^+$  cation in polar but weakly basic solvents such as THF.

The hydride complex  $[\text{MeGapz}_3]\text{Mo}(\text{CO})_3\text{H}$  has been prepared and characterized. It was found that a strong acid such as HCl is required to protonate fully the  $\text{MeGapz}_3\text{Mo}(\text{CO})_3^-$  anion under conditions where acetic acid suffices to fully protonate the analogous  $\text{CpMo}(\text{CO})_3^-$  anion. The Mo-H bond of the hydride species  $[\text{MeGapz}_3]\text{Mo}(\text{CO})_3\text{H}$  dissociates in the polar but weakly basic solvent, THF. These results taken together indicate the seven-coordinate  $[\text{MeGapz}_3]\text{Mo}(\text{CO})_3\text{H}$  compound is more destabilized with respect to its six-coordinated anion  $\text{MeGapz}_3\text{Mo}(\text{CO})_3^-$ , than is the case in the analogous cyclopentadienyl system.

The reaction of  $\text{MeGapz}_3\text{Mo}(\text{CO})_3^-$  anion with MeI was found to proceed via a  $\sigma$ -methyl ' $\text{MeGapz}_3\text{Mo}(\text{CO})_3\text{Me}$ ' intermediate to give the  $\eta^2$ -acyl compound  $[\text{MeGapz}_3]\text{Mo}(\text{CO})_2(\eta^2\text{-COMe})$  as the final product. The use of the poorly-coordinating solvent, THF as the reaction medium may have retarded the rate of the migratory CO insertion step in the above reaction, thereby allowing spectroscopic detection of the  $\sigma$ -methyl intermediate. Migratory CO insertion reactions have been shown to be 'solvent-catalyzed' by Wax and Bergman [95]. The use of the polar, highly coordinating, acetonitrile, the reaction medium used by Curtis et al., may have catalyzed the

transformation of the 'HBpz<sub>3</sub>Mo(CO)<sub>3</sub>Me'  $\sigma$ -methyl intermediate to [HBpz<sub>3</sub>]Mo(CO)<sub>2</sub>( $\eta^2$ -COMe) [17] preventing direct observation of this intermediate.

The transformation of the  $\sigma$ -methyl 'MeGapz<sub>3</sub>Mo(CO)<sub>3</sub>Me' intermediate to the  $\eta^2$ -acyl derivative [MeGapz<sub>3</sub>]Mo(CO)<sub>2</sub>( $\eta^2$ -COMe) is believed to be favoured by a combination of the relief of steric congestion and the ability of the  $\sigma$ -donor electrons localized on the nitrogens of the MeGapz<sub>3</sub><sup>-</sup> ligand to promote octahedral coordination.

The reaction of the MeGapz<sub>3</sub>Mo(CO)<sub>3</sub><sup>-</sup> anion with EtBr yielded the seven-coordinate [MeGapz<sub>3</sub>]Mo(CO)<sub>3</sub>Et  $\sigma$ -ethyl compound. No evidence for the migratory CO insertion into the Mo-Et to form an  $\eta^2$ -COEt product was observed in this reaction. It is not clear at this stage why an acyl complex was obtained with MeI but not with EtBr. The difference in reactivity between both of these alkyl halides is probably related to the Mo-R and Mo-CO bond strengths in the [MeGapz<sub>3</sub>]Mo(CO)<sub>3</sub>R (R = Me, Et) compounds. The rate of alkyl to acyl formation reaction is known to be dependent on the strengths of the M-C (alkyl) and M-CO bonds in the starting alkyl complex [96]. It is worthy of mention, however, that the CpMo(CO)<sub>3</sub>R (R = Me, Et) compounds have been shown to react with phosphines and phosphites to afford the stable crystalline acyl complexes CpMo(CO)<sub>2</sub>(L)COR (L = phosphines, phosphites) via CO insertion reactions [97].

The preparation of the compounds [MeGapz<sub>3</sub>]Mo(CO)<sub>3</sub>X (X = Br, I) was attempted and spectroscopic evidence was gathered to support their formation. However, all attempts at obtaining analytically pure products were unsuccessful.

## CHAPTER III

## TRANSITION METAL - TRANSITION METAL BONDED COMPLEXES

## INCORPORATING PYRAZOLYL GALLATE/BORATE LIGANDS

3.1. Introduction

The uninegative, tridentate, chelating  $\text{RB}(\text{pz})_3^-$  ( $\text{R} = \text{H}$ , alkyl, aryl, pyrazolyl),  $\text{MeGapz}_3^-$  and  $[\text{Me}_2\text{Gapz}(\text{OCH}_2\text{CH}_2\text{NR}_2)]^-$  ( $\text{R} = \text{H}$ , Me) ligand systems, being six-electron donors, are formally analogous to the cyclopentadienyl ion ( $\text{Cp}^-$ ). The reactivity of the  $\text{LMo}(\text{CO})_3^-$  anions of the above ligand systems toward a number of three electron donor ligands has been well documented [34,98-100]. Differences are sometimes observed between these ligand systems. While the compounds  $[\text{MeGapz}_3]_2\text{Rh}_2(\mu\text{-CO})_3$  [101],  $[\text{HBpz}_3]_2\text{Rh}_2(\text{CO})_3$  [102], and  $(\eta\text{-C}_5\text{H}_5)_2\text{Rh}_2(\mu\text{-CO})(\text{CO})_2$  [103] have similar formulation, they display markedly different geometry.

One obvious difference between the cyclopentadienyl and tris(1-pyrazolyl)borate/gallate ligands is that while the former is found in an extensive array of heterobimetallic complexes (compounds having metal-metal bonds between two dissimilar metals), no such complexes are known for the tridentate polypyrazolylborate/gallate ligands.

Much current research has been directed towards heterobimetallic complexes with transition metal-transition metal bonds, partly since it is reasoned that cooperative effects between the different metal centers may influence the reactivity of such complexes [104-113]. For example, incorporation of both early and late transition metals into the same

dinuclear compound might lead to systems capable of activating and polarizing substrates such as CO [114-118]. It is also argued that studies of simple binuclear species may well provide useful clues in the design and synthesis of larger heterometallic cluster species with potential catalytic applications [107,119,120].

The present study was undertaken with the primary objective of isolating heteronuclear (or mixed-metal) compounds incorporating the  $\text{HBpz}_3^-$ ,  $\text{MeGapz}_3^-$ , and  $[\text{Me}_2\text{Gapz}(\text{OCH}_2\text{CH}_2\text{NMe}_2)]^-$  ligand systems in which direct transition metal-transition metal bonds are featured. The evidence for the presence of a metal-metal bond between the different metals is based on the generally accepted criteria for such bonds. That is, a metal-metal distance close to the sum of the van der Waals radii of the two metals as revealed by X-ray studies, spectroscopic evidence and/or the necessity of a metal-metal bond to provide each metal with a reasonable number of valence electrons (generally 16 or 18) [114].

A number of transition metal-transition metal bonded complexes has been prepared by the reaction of  $\text{LMo}(\text{CO})_3^-$  ( $\text{L} = \text{HBpz}_3, \text{MeGapz}_3, \text{Me}_2\text{Gapz}(\text{OCH}_2\text{CH}_2\text{NMe}_2)]^-$ ) anions with a variety of transition metal halide species. Results of the analyses confirm the presence of direct metal-metal bonds in these compounds in addition to carbonyl groups in a number of different bonding environments [76,121-123]. Thus, these compounds constitute the first examples of heterobimetallic transition metal-transition metal bonded complexes incorporating the tridentate pyrazolylborate/gallate ligands. The Mo-Cu bonded complex provides a rare example of a 3:3:1 or 'capped octahedral' structure.

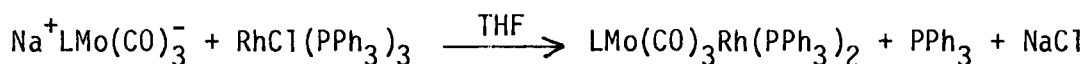
The  $[\text{MeGapz}_3]\text{Mo}(\text{CO})_3\text{Rh}(\text{PPh}_3)_2$  complex prepared and discussed in this chapter, was tested as a potential reagent for the desulfurization of  $\text{H}_2\text{S}$  at ambient temperatures, but no noticeable activity was observed. Parts of this chapter have been published elsewhere [124].

## 3.2 Experimental

### 3.2.1 Starting Materials

The ligand  $\text{Na}^+[\text{Me}_2\text{Gapz}(\text{OCH}_2\text{CH}_2\text{NMe}_2)]^-$  was prepared as a THF solution as described elsewhere [41].  $\text{K}^+\text{HBpz}_3^-$  [125],  $[\text{CuCl}(\text{PPh}_3)]_4$  [126],  $\text{PtCl}(\text{Me})(\text{COD})$  [127],  $\text{Co}(\text{NO})_2\text{I}$  [128], and  $\text{Mn}(\text{CO})_5\text{Br}$  [129] were prepared by literature methods.  $\text{RhCl}(\text{PPh}_3)_3$  (Strem chemicals),  $\text{CuCl}$ ,  $\text{HgCl}_2$  (M&B Chemicals),  $\text{CO}$  (Linde Union Carbide),  $\text{ZrCl}_4$ ,  $\text{HfCl}_4$  (Merck-Schuchardt) and  $\text{H}_2\text{S}$  (Matheson), were used as supplied.

### 3.2.2 Preparation of $\text{LMo}(\text{CO})_3\text{Rh}(\text{PPh}_3)_2$ (where $\text{L} = [\text{MeGapz}_3]$ , $[\text{HBpz}_3]$ or $[\text{Me}_2\text{Gapz}(\text{OCH}_2\text{CH}_2\text{NMe}_2)]$ )

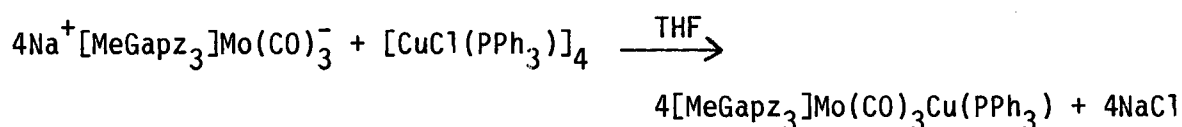


The  $\text{Na}^+\text{L}^-$  ligand solution ( $\sim 0.40$  mmol in 100 ml THF) was added to a stirred solution of an equimolar amount of  $(\text{MeCN})_3\text{Mo}(\text{CO})_3$  ( $\sim 0.10$  g, 0.40 mmol) in the same solvent. The initial yellow coloration of the molybdenum complex in THF changed to an amber color on addition of the ligand solution. The reaction mixture was stirred for  $\sim 2$  days during which time the amber color intensified. The resulting solution of  $\text{Na}^+\text{LMo}(\text{CO})_3^-$  was reacted directly with  $\text{RhCl}(\text{PPh}_3)_3$  (0.37 g, 0.40 mmol),

added as a slurry in ~100 ml THF. The dark red reaction mixture was stirred for a further 2 days and then the solvent was removed in vacuo to afford a dark red-black residue. The residue was extracted with benzene and the solution filtered. Evaporation of the solvent from the filtrate gave an oily red-black material which was recrystallized from CH<sub>2</sub>Cl<sub>2</sub>/hexane to give air-stable dark-red crystals of the desired product in approximately 60% yield. Physical data for these complexes are collected in Table III. The mass spectrum of the complex [MeGapz<sub>3</sub>]Mo(CO)<sub>3</sub>-Rh(PPh<sub>3</sub>)<sub>2</sub> displayed signals due to the P-PPh<sub>3</sub><sup>+</sup> ion (P<sup>+</sup> = parent ion) at ~890 (based on <sup>69</sup>Ga and <sup>98</sup>Mo).

In the preparation of the complexes LMo(CO)<sub>3</sub>Rh(PPh<sub>3</sub>)<sub>2</sub> (where L = [HBpz<sub>3</sub>] or [MeGapz<sub>3</sub>]), yellow crystalline samples of the complex RhCl(CO)(PPh<sub>3</sub>)<sub>2</sub> (Calcd.: C, 64.31; H, 4.34. Found: C, 63.73; H, 4.27; ν<sub>CO</sub>: 1980 cm<sup>-1</sup> (CH<sub>2</sub>Cl<sub>2</sub>)) were also isolated in ~5% yield.

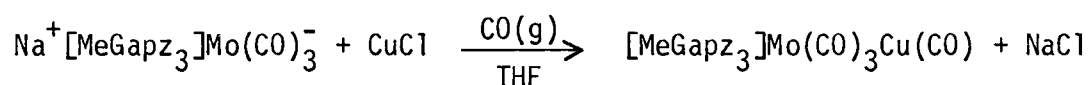
### 3.2.3 Preparation of [MeGapz<sub>3</sub>]Mo(CO)<sub>3</sub>Cu(PPh<sub>3</sub>)



A solution of the Na<sup>+</sup>[MeGapz<sub>3</sub>]Mo(CO)<sub>3</sub><sup>-</sup> salt (1.7 mmol) in THF was prepared as described above (section 3.2.2). A one-quarter molar amount of [CuCl(PPh<sub>3</sub>)<sub>4</sub>] (0.61 g, 0.43 mmol) was added to the reaction mixture and produced an immediate rusty-orange color. This reaction mixture was stirred for approximately one day before the removal of solvent under vacuum. The resulting orange residue was extracted with CH<sub>2</sub>Cl<sub>2</sub> and the

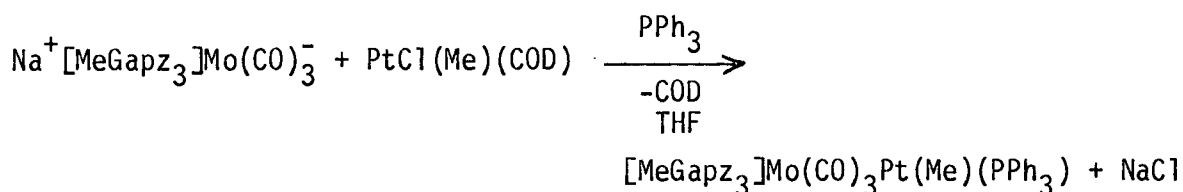
mixture filtered. Hexane was added to the filtrate and the mixed solvents allowed to evaporate slowly. Golden-yellow air-stable crystals of the product,  $[\text{MeGapz}_3]\text{Mo}(\text{CO})_3\text{Cu}(\text{PPh}_3)$ , were produced from the concentrated solutions in approximately 60% yield. Pertinent physical data are included in Table III for the complex.

#### 3.2.4 Preparation of $[\text{MeGapz}_3]\text{Mo}(\text{CO})_3\text{Cu}(\text{CO})$



A suspension of CuCl (0.08 g, 0.85 mmol) in THF was added to a solution of  $\text{Na}^+[\text{MeGapz}_3]\text{Mo}(\text{CO})_3^-$  salt (0.85 mmol) in THF and produced an immediate rusty-brown color. The reaction mixture was stirred for ~4 h. CO(g) was bubbled through the mixture for another 2 h at which stage the brown color had intensified. The solvent was then removed under vacuum and the residue extracted with benzene. Slow evaporation of the benzene filtrate, afforded the product,  $[\text{MeGapz}_3]\text{Mo}(\text{CO})_3\text{Cu}(\text{CO})$ , as a yellow air-stable solid in low yields (~20%). Solutions of this compound deteriorate slowly with time. Physical data for the complex are given in Table III.

#### 3.2.5 Preparation of $[\text{MeGapz}_3]\text{Mo}(\text{CO})_3\text{Pt}(\text{Me})(\text{PPh}_3)$



To a stirred solution of  $\text{Na}^+[\text{MeGapz}_3]\text{Mo}(\text{CO})_3^-$  salt (0.350 mmol) in THF, was added  $\text{PtCl}(\text{Me})(\text{COD})$  (0.123 g, 0.350 mmol) dissolved in THF. The reaction mixture was stirred for  $\sim 1$  h, after which the stabilizing ligand  $\text{PPh}_3$  (0.091 g, 0.350 mmol) dissolved in THF was added slowly to the mixture. The solution was then stirred for  $\sim 4$  days. At this stage, the solution ir spectrum of the mixture indicated completion of the reaction. The solvent was then removed in vacuo and the resulting brown residue extracted with  $\text{CH}_2\text{Cl}_2$ . Hexane was added to the  $\text{CH}_2\text{Cl}_2$  filtrate (1:1), and evaporation of the  $\text{CH}_2\text{Cl}_2$ /hexane mixed solvents afforded dark brown crystals of the product in  $\sim 50\%$  yield. Elemental analysis and  $^1\text{H}$  nmr data indicated a methylene chloride solvated complex as the product. The complex is stable as a solid but unstable in solution.

Anal. Calcd. For  $[\text{MeGapz}_3]\text{Mo}(\text{CO})_3\text{Pt}(\text{Me})(\text{PPh}_3)\cdot\text{CH}_2\text{Cl}_2$ : C, 38.72; H, 3.13; N, 8.21. Found: C, 38.05; H, 2.90; N, 8.57. IR( $\text{CH}_2\text{Cl}_2$ )  $\nu_{\text{CO}}$ : 1900s, 1815s, 1785s  $\text{cm}^{-1}$ .  $^1\text{H}$  NMR ( $d_6$ -acetone, 80 MHz):  $\tau(\text{CH}_3)_2\text{CO} = 7.89$  ppm, 9.50s (Ga-Me); 4.18t (pz-H<sup>4</sup>); 2.35d (pz-H<sup>5</sup>); pz-H<sup>3</sup> obscured by  $\text{PPh}_3$ ; 9.45s (Pt-Me,  $J_{195\text{Pt-Me}} \approx 72$  Hz); 2.13m, 2.50m ( $\text{PPh}_3$ ).

### 3.2.6 Preparation of $[\text{MeGapz}_3]\text{Mo}(\text{CO})_3\text{M}'\text{Cl}_3$ ( $\text{M}' = \text{Zr}$ or $\text{Hf}$ )



An equimolar amount of  $\text{M}'\text{Cl}_4$  dissolved in THF was added to a stirred solution of  $\text{Na}^+[\text{MeGapz}_3]\text{Mo}(\text{CO})_3^-$  in the same solvent. The resulting cloudy

Table III. Physical Data for the Complexes  $\text{LMo}(\text{CO})_3\text{MY}$ .

L	M	Y	ANALYSIS CALCD/FOUND			$\nu_{\text{CO}}$ ( $\text{cm}^{-1}$ ) $\text{CH}_2\text{Cl}_2$ (Nujol)	1 a H nmr					
			C	H	N		GaMe	pz-H <sup>3</sup>	pz-H <sup>4</sup>	pz-H <sup>5</sup>	PPh <sub>3</sub>	Other
MeGapz <sub>3</sub>	Rh	(PPh <sub>3</sub> ) <sub>2</sub>	53.82 54.04	3.88 4.07	7.67 7.58	1873,1772,1758 (1897,1763,1744)	<sup>b</sup> 10.00s	2.70d	4.06t	2.89d	2.05m 3.04m	- -
<sup>c</sup> HBPz <sub>3</sub>	Rh 1.0 $\text{CH}_2\text{Cl}_2$	(PPh <sub>3</sub> ) <sub>2</sub>	53.23 53.49	3.80 3.83	7.60 7.73	1871,1772,1757 (1863,1772,1766)	<sup>b</sup> -	2.71d	4.24t	2.96d	2.09m 3.04m	5.71s $\text{CH}_2\text{Cl}_2$ solvate
Me <sub>2</sub> Gapz(OCH <sub>2</sub> - CH <sub>2</sub> NMe <sub>2</sub> )	Rh	(PPh <sub>3</sub> ) <sub>2</sub>	54.26 54.52	4.65 4.72	3.96 3.83	1852,1762,1737	<sup>e</sup> 10.42s 10.29s	2.32d	3.69t	obscured by PPh <sub>3</sub> signals	2.60m	8.07s 7.09s NMe <sub>2</sub>
MeGapz <sub>3</sub>	Cu	PPh <sub>3</sub>	46.96 46.91	3.41 3.43	10.61 10.54	1898,1798 (1890,1805,1780)	<sup>e</sup> 9.42s	2.02d	3.69t	2.19d	2.45m	
MeGapz <sub>3</sub>	Cu	CO	30.15 30.78	2.15 2.85	15.08 15.45	2010,1955,1810 (1898,1880, 1772,1745sh)	<sup>e</sup> 9.45s	1.71d	3.66t	2.20d		
MeGapz <sub>3</sub>	Zr	Cl <sub>3</sub>	29.64 29.00	2.34 2.87		2015,1920,1895	<sup>b</sup> 10.10s	2.19d	4.18t	3.08d		
MeGapz <sub>3</sub>	Hf 1,5 $\text{C}_6\text{H}_{14}$	Cl <sub>3</sub>	30.01 29.80	3.75 3.65	9.55 9.51	2015,1915,1895	<sup>b</sup> 10.07s	2.15d	4.18t	3.09d		

a s=singlet, d=doublet, m=multiplet, sh=shoulder and t=triplet. b  $\text{C}_6\text{D}_6$  solution,  $\tau_{\text{C}_6\text{H}_6}$  = 2.84 ppm,  $J_{\text{HCCH}}$  = 2Hz for pz protons.  
 c  $\nu_{\text{BH}} = 2483 \text{ cm}^{-1}$ . e  $(\text{CD}_3)_2\text{CO}$  solution,  $\tau(\text{CH}_3)_2\text{CO} = 7.89 \text{ ppm}$ ,  $J_{\text{HCCH}}$  = 2Hz for pz protons.

reaction mixture was stirred for ~ 1 day after which the solvent was removed under vacuum. The residue was extracted with benzene ( $M' = \text{Zr}$ ),  $\text{CH}_2\text{Cl}_2$  ( $M' = \text{Hf}$ ) and the solution filtered. Hexane was added to the  $\text{CH}_2\text{Cl}_2$  filtrate. Evaporation of the solvents afforded yellow solids of the products in ~60% yield. The complexes are unstable as solids and solutions deteriorate with time even under inert conditions, turning visibly from bright yellow to dark green. The complexes were isolated as benzene ( $M' = \text{Zr}$ ), and hexane ( $M' = \text{Hf}$ ) solvates respectively. Physical data for the complexes are compiled in Table III. Satisfactory analysis for C and H were obtained for the Mo-Zr complex but the N analyses were inconsistent each time the sample was analyzed.

### 3.2.7 Attempted Preparation of $[\text{MeGapz}_3]\text{Mo}(\text{CO})_3\text{Co}(\text{NO})_2$

Equimolar amounts of  $\text{Na}^+[\text{MeGapz}_3]\text{Mo}(\text{CO})_3^-$  salt solution and  $\text{Co}(\text{NO})_2\text{I}$  were reacted in THF. After stirring the reaction mixture overnight, the solvent was removed under vacuum. Work-up of the resulting residue yielded orange crystals (~60% yield). Analytical, ir and  $^1\text{H}$  nmr data for this product were in perfect agreement with that of the compound  $[\text{MeGapz}_3]\text{Mo}(\text{CO})_2\text{NO}$  reported previously [34].

Anal. Calcd. For  $[\text{MeGapz}_3]\text{Mo}(\text{CO})_2\text{NO}$ : C, 30.79; H, 2.57; N, 20.96.  
 Found: C, 30.74; H, 2.65; N, 20.85. IR( $\text{CH}_2\text{Cl}_2$ )  $\nu_{\text{CO}}$ : 2020s, 1930s  $\text{cm}^{-1}$ ;  
 $\nu_{\text{NO}}$ : 1665s  $\text{cm}^{-1}$ .  $^1\text{H}$  NMR ( $\text{C}_6\text{D}_6$ , 80 MHz):  $\tau_{\text{C}_6\text{H}_6} = 2.84$  ppm, 10.03s  
 (Ga-Me); 4.28t, 4.10t (pz-H<sup>4</sup>); 3.10d, 2.95d (pz-H<sup>5</sup>); 2.63d, 2.23d (pz-H<sup>3</sup>).  
 ( $J_{\text{HCCH}} = \sim 2.0$  Hz for pz protons.) (The pyrazolyl protons appeared in a 2:1 ratio.)

The mass spectrum of this compound displayed signals corresponding to the parent ( $P^+$ ) ion at ~469, in addition to  $P-CO^+$ ,  $P-2CO^+$ ,  $P-2CO-NO^+$  ion signals at 441, 413, and 383 mass units (based on  $^{69}\text{Ga}$  and  $^{98}\text{Mo}$ ), respectively.

In order to obtain additional evidence as to the identity of this product, the reaction was repeated, this time employing the  $\text{Na}^+[\text{MeGa}(3,5\text{-Me}_2\text{pz})_3]\text{Mo}(\text{CO})_3^-$  salt as the starting material. Again, orange crystals were isolated as the product of the reaction. Both the ir and  $^1\text{H}$  nmr data for this compound were consistent with the formulation  $[\text{MeGa}(3,5\text{-Me}_2\text{pz})_3]\text{Mo}(\text{CO})_2\text{NO}$ . IR( $\text{CH}_2\text{Cl}_2$ )  $\nu_{\text{CO}}$ : 2020s, 1920s;  $\nu_{\text{NO}}$ : 1650  $\text{cm}^{-1}$ .  $^1\text{H}$  NMR ( $\text{C}_6\text{D}_6$ , 80 MHz):  $\tau_{\text{C}_6\text{H}_6}$  = 2.84 ppm, 9.75s (Ga-Me); 8.20s, 7.60s (pz-Me<sup>5</sup>); 8.09s, 7.35s (pz-H<sup>3</sup>); 4.58s, 4.40s (pz-H<sup>4</sup>). (The pz proton and methyl resonances appeared in a 2:1 ratio.)

Thus, it appears that the  $\text{Co}(\text{NO})_2\text{I}$  reagent is acting primarily as a nitrosylating agent in these reactions.

### 3.2.8 Preparation of $[\text{MeGapz}_3\text{Mo}(\text{CO})_3]_2\text{Hg}$



One-half molar amount of  $\text{HgCl}_2$  (0.115 g, 0.425 mmol) was added to a THF solution of the  $\text{Na}^+[\text{MeGapz}_3]\text{Mo}(\text{CO})_3^-$  salt. An almost immediate cloudiness resulted indicating precipitation of  $\text{NaCl}$ . The yellow brown cloudy solution was stirred overnight and the solvent then removed in vacuo. The residue was extracted with benzene. The benzene filtrate was

concentrated and supernatant liquid slowly poured off, leaving behind air-sensitive off-yellow crystals of the desired product in ~80% yield.

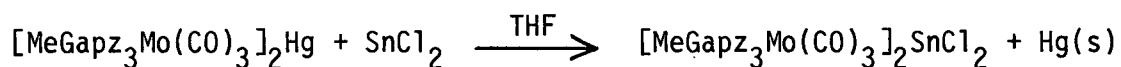
Anal. Calcd. For  $[\text{MeGapz}_3\text{Mo}(\text{CO})_3]_2\text{Hg}$ : C, 27.56; H, 2.12; N, 14.84.

Found: C, 28.05; H, 2.33; N, 14.99. IR( $\text{CH}_2\text{Cl}_2$ )  $\nu_{\text{CO}}$ : 2020m, 1985m,

1952m, 1890s  $\text{cm}^{-1}$ . The  $^1\text{H}$  nmr spectrum of the compound showed the

presence of the Ga-Me signal but signals due to the pz protons were not observed in either  $\text{C}_6\text{D}_6$  or  $d_6$ -acetone solution.

### 3.2.9 Attempted Reaction of $[\text{MeGapz}_3\text{Mo}(\text{CO})_3]_2\text{Hg}$ with $\text{SnCl}_2$

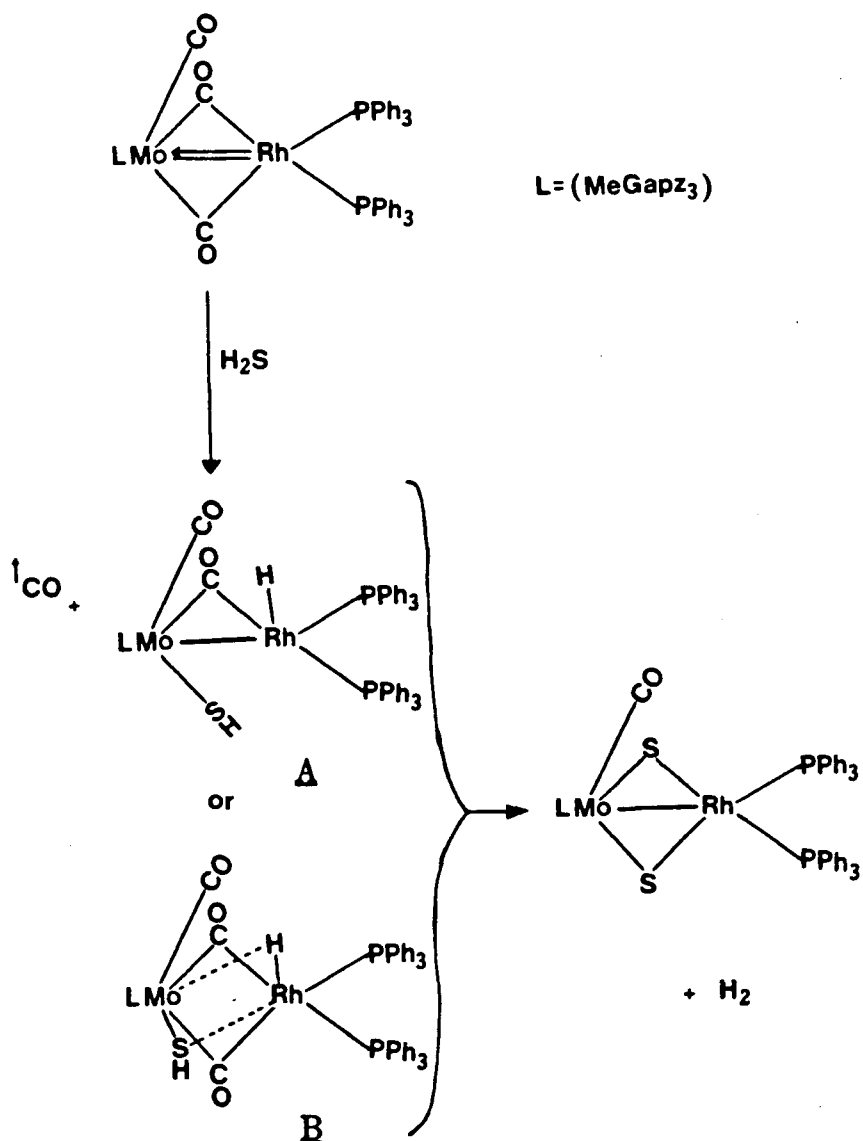


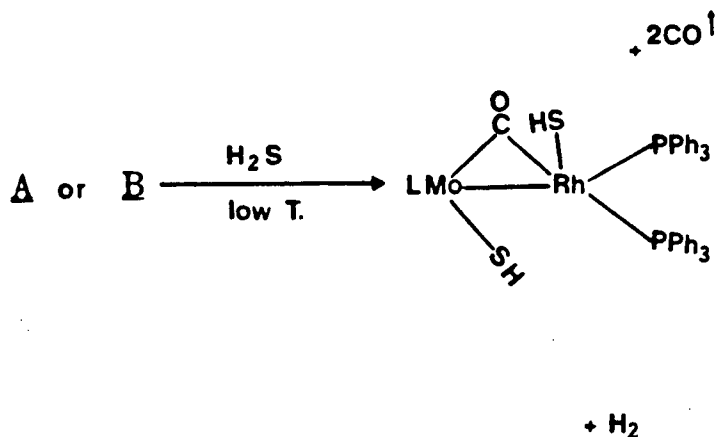
Reaction of  $[\text{MeGapz}_3\text{Mo}(\text{CO})_3]_2\text{Hg}$  (0.602 g, 0.530 mmol) with an equimolar amount of  $\text{SnCl}_2$  in THF did not result in the expected replacement reaction product  $[\text{MeGapz}_3\text{Mo}(\text{CO})_3]_2\text{SnCl}_2$ . The solution ir spectrum of the dark orange brown solid obtained from this reaction was devoid of absorption bands in the  $\nu_{\text{CO}}$  region of the spectrum. Repeated recrystallization attempts with a variety of solvents failed to give the pure product, hence no further characterization was attempted.

Although  $\text{SnCl}_2$  is known to insert into the M-M bonds in the dimers  $[\text{CpFe}(\text{CO})_2]_2$  and  $[\text{CpMo}(\text{CO})_3]_2$  [130], and the fact that both Hg and Sn form strong covalent bonds with transition metals [131], the Mo-Hg-Mo bond in the present compound  $[\text{MeGapz}_3](\text{CO})_3\text{Mo-Hg-Mo}(\text{CO})_3[\text{pz}_3\text{GaMe}]$  may be too strong, thereby preventing the replacement of Hg with  $\text{SnCl}_2$  in the complex.

### 3.2.10 Attempted desulfurization of $\text{H}_2\text{S}$ by $[\text{MeGapz}_3]\text{Mo}(\text{CO})_3\text{Rh}(\text{PPh}_3)_2$

During the course of this work, the first quantitative formation of molecular hydrogen  $\text{H}_2$  via abstraction of sulfur from  $\text{H}_2\text{S}$  by the dimer  $[\text{Pd}_2\text{X}_2(\mu\text{-dppm})_2]$  ( $\text{X} = \text{Cl}, \text{Br}, \text{I}$ ; dppm = bis(diphenylphosphino)methane) [132] was communicated in preliminary form. It was therefore of interest to us to see if the heterobimetallic complex  $[\text{MeGapz}_3]\text{Mo}(\text{CO})_3\text{Rh}(\text{PPh}_3)_2$  would effect a similar transformation of  $\text{H}_2\text{S}$  into molecular hydrogen  $\text{H}_2$  according to the scheme shown below.





However, the reaction of the Mo-Rh complex with  $\text{H}_2\text{S}$  in  $\text{CH}_2\text{Cl}_2$  at ambient temperatures resulted in a black solid. The solution ir spectrum of the black solid indicated a non-carbonyl containing compound as the product, while the  $^1\text{H}$  nmr spectrum in  $\text{C}_6\text{D}_6$  or  $d_6$ -acetone displayed a sharp Ga-Me signal in the gallium alkyl region but there was no evidence of the pyrazolyl ring proton resonances in the spectrum. Attempts at the purification of this product were unsuccessful.

### 3.2.11 Attempted Preparation of $[\text{MeGapz}_3]\text{Mo}(\text{CO})_3\text{Mn}(\text{CO})_5$

The  $\text{MeGapz}_3\text{Mo}(\text{CO})_3^-$  (0.51 mmol) anion was reacted with  $\text{Mn}(\text{CO})_5\text{Br}$  (0.154 g, 0.510 mmol) in THF. The reaction mixture was stirred for ~2 days, after which the solvent was removed under vacuum and the resulting residue extracted with benzene. Evaporation of the benzene filtrate containing the extracts gave a dark sticky solid. This dark solid was

washed with hexane and the hexane-washings discarded leaving behind a dark solid product.

IR(C<sub>6</sub>H<sub>12</sub>)  $\nu_{\text{CO}}$ : 2045, 2035, 2015, 2000, 1980, 1930, 1900, 1875 cm<sup>-1</sup>.  
<sup>1</sup>H nmr (C<sub>6</sub>D<sub>6</sub>, 80 MHz):  $\tau_{\text{C}_6\text{H}_6}$  = 2.84 ppm, 10.03 (Ga-Me); 4.05br (pz-H<sup>4</sup>);  
 2.14br (pz-H<sup>3</sup>). The pz-H<sup>5</sup> resonance was obscured by the solvent peak.  
 Analytically pure samples of the product could not be obtained.

### 3.3 Results and Discussion

#### 3.3.1 LMo(CO)<sub>3</sub>Rh(PPh<sub>3</sub>)<sub>2</sub> (where L = [MeGapz<sub>3</sub>], [HBpz<sub>3</sub>], or [Me<sub>2</sub>Gapz(OCH<sub>2</sub>CH<sub>2</sub>NMe<sub>2</sub>)])

The reactions of the anionic ligands [MeGapz<sub>3</sub>]Mo(CO)<sub>3</sub><sup>-</sup>, [HBpz<sub>3</sub>]Mo(CO)<sub>3</sub><sup>-</sup>, and [Me<sub>2</sub>Gapz(OCH<sub>2</sub>CH<sub>2</sub>NMe<sub>2</sub>)]Mo(CO)<sub>3</sub><sup>-</sup> with Wilkinson's catalyst, RhCl(PPh<sub>3</sub>)<sub>3</sub>, in THF resulted in the displacement of the chloro ligand, the formation of molybdenum-rhodium bonds, and the loss of triphenylphosphine from the rhodium coordination sphere. The crystalline products are air-stable but solutions of the complexes decompose on exposure to air. In the experiment (using either the [HBpz<sub>3</sub>]Mo(CO)<sub>3</sub><sup>-</sup> or [MeGapz<sub>3</sub>]Mo(CO)<sub>3</sub><sup>-</sup> anion) a small amount of the yellow crystalline material RhCl(CO)(PPh<sub>3</sub>)<sub>2</sub> was isolated, presumably being produced via displacement of a triphenylphosphine from RhCl(PPh<sub>3</sub>)<sub>3</sub> by a CO ligand of the molybdenum tricarbonyl anion starting material.

Physical data for the complexes are listed in Table III p. 72. The ir  $\nu_{\text{CO}}$  frequencies indicate the presence of both terminal and bridging

carbonyl groups in the compounds. The room temperature  $^1\text{H}$  nmr data for the complexes containing the 'MeGapz<sub>3</sub>' and 'HBpz<sub>3</sub>' ligands suggest equivalence of the three pyrazolyl rings since only one set of signals is observed for the ring protons (see figure 19). Low temperature spectra, although showing sharpening of these proton signals, did not distinguish clearly any difference between the three pyrazolyl rings. The room temperature  $^1\text{H}$  nmr spectrum of the  $[\text{Me}_2\text{Gapz}(\text{OCH}_2\text{CH}_2\text{NMe}_2)]\text{Mo}(\text{CO})_3\text{Rh}(\text{PPh}_3)_2$  complex is consistent with a facial coordination of the unsymmetric gallate ligand about the molybdenum center, with two Ga-Me and two N-Me signals being recorded. A complicated spectral pattern was observed for the  $-\text{CH}_2\text{CH}_2-$  group, lending further support for a facial organogallate ligand in this complex. A meridional coordination of the unsymmetric ligand would give an  $\text{A}_2\text{X}_2$  pattern (two triplets) for the  $-\text{CH}_2\text{CH}_2-$  group.

The crystal structure of the  $[\text{MeGapz}_3]\text{Mo}(\text{CO})_3\text{Rh}(\text{PPh}_3)_2$  complex is shown in figure 20, and consists of discrete molecules separated by normal van der Waals distances.

The structure clearly shows the presence of a terminal Mo-C(1)-O(1) unit, which, although significantly non-linear ( $173.9(5)^\circ$ ), is too far removed from the Rh center ( $\text{Rh}\cdots\text{C}(1)$ ,  $2.845(5)\text{\AA}$ ) to suggest any bridging interaction. This CO ligand presumably accounts for the highest  $\nu_{\text{CO}}$  value recorded at  $1879\text{ cm}^{-1}$  (Nujol). The two remaining Mo-CO units, although different, are both clearly in bridging range of the Rh center with Mo-C-O angles of  $167.4(4)$  and  $153.2(4)^\circ$  and  $\text{Rh}\cdots\text{C}$  distances of  $2.334(5)$  and  $2.079(5)\text{\AA}$  respectively ( $\nu_{\text{CO}}$  values  $1758$ ,  $1772\text{ cm}^{-1}$ ). The  $\text{Ga}\cdots\text{Mo}-\text{Rh}$  unit is significantly non-linear in this structure with an angle of  $161.59(3)^\circ$  at Mo.

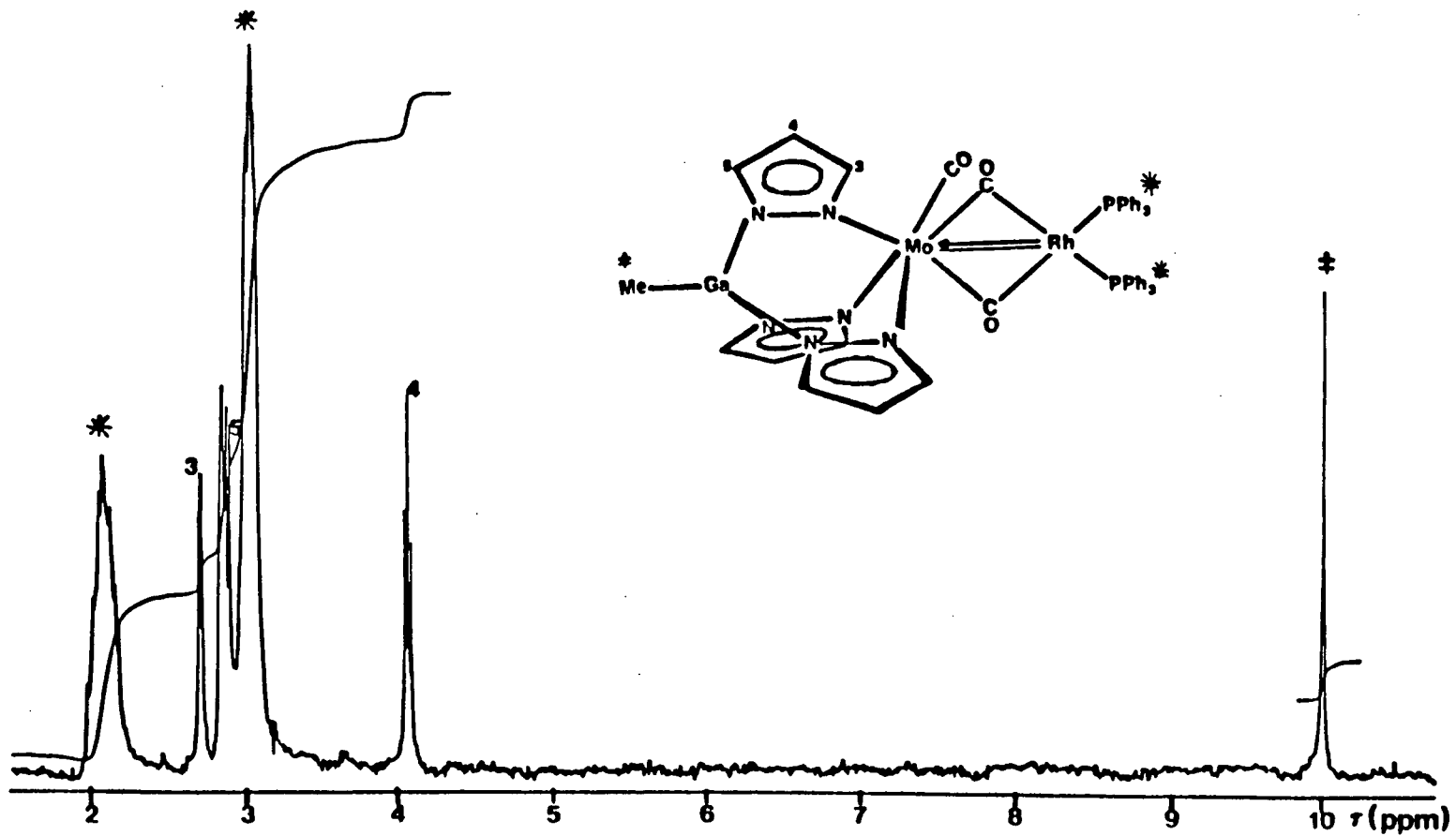


Figure 19. Room temperature 100 MHz  $^1\text{H}$  nmr spectrum of  $[\text{MeGaz}_3]\text{Mo}(\text{CO})_3\text{Rh}(\text{PPh}_3)_2$  in  $\text{C}_6\text{D}_6$  solution.

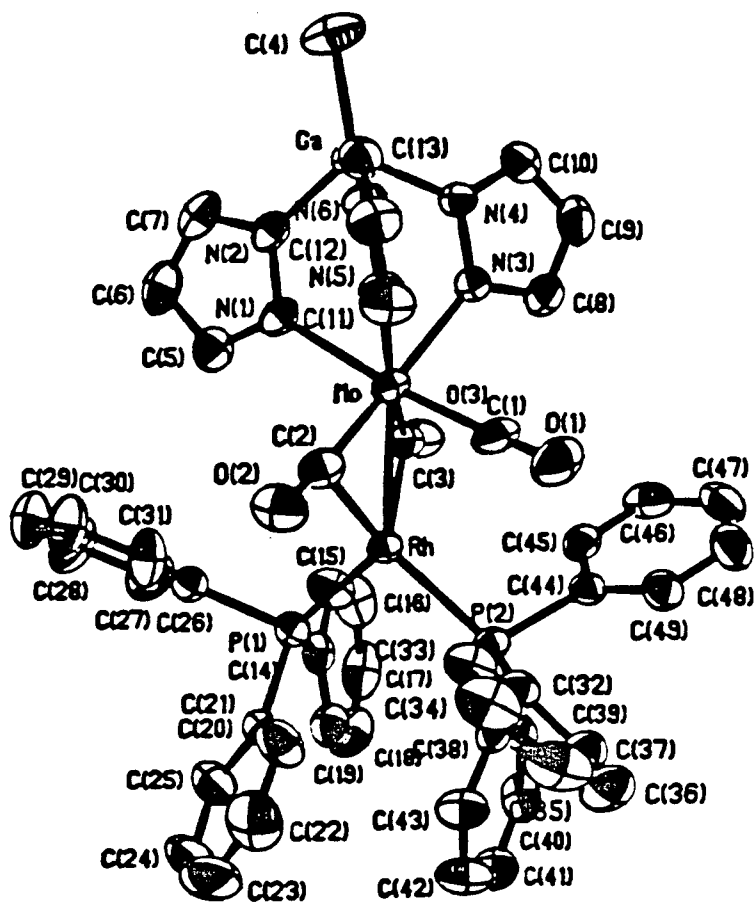


Figure 20. Molecular structure of  $[\text{MeGapz}_3]\text{Mo}(\text{CO})_3\text{Rh}(\text{PPh}_3)_2$

It is also evident that the pyrazolyl rings are non-equivalent in the solid state and to explain the solution  $^1\text{H}$  nmr data it is necessary to postulate that a rapid fluxional process is taking place in solution. Two such processes may be envisaged, one in which there is a rapid rotation of the 'MeGapz<sub>3</sub>' ligand about the Ga...Mo axis, and another, perhaps more likely, in which there is rapid interchange of the different roles of the three CO ligands, with concomitant equalization of the environments of the three pyrazolyl rings.

The rhodium complex reported here is very similar to the one reported earlier by Carlton et al. [104]. These authors reported the structure of the compound  $(\eta\text{-C}_5\text{H}_5)\text{Mo}(\text{CO})_3\text{Rh}(\text{PPh}_3)_2$ , in which a ' $\eta\text{-C}_5\text{H}_5$ ' ligand substitutes the ' $\text{MeGapz}_3$ ' ligand of the present complex. The similarity of the two complexes illustrates once more the interchangeability of the ' $\eta\text{-C}_5\text{H}_5$ ' and ' $\text{MeGapz}_3$ ' ligand systems [34]. The Mo-Rh bond distance of 2.6066(5)Å (cf. 2.588(1)Å in the  $\eta\text{-C}_5\text{H}_5$  complex) in the present compound is well below the estimated single bond distance of 2.8-3.0Å and suggests some multiple bond character between the two transition metals.

A bonding scheme similar to that proposed by Carlton et al. would give an 18-electron count to the Mo atom and a 16-electron count to the Rh center. In this picture (figure 21), in addition to two bridging CO

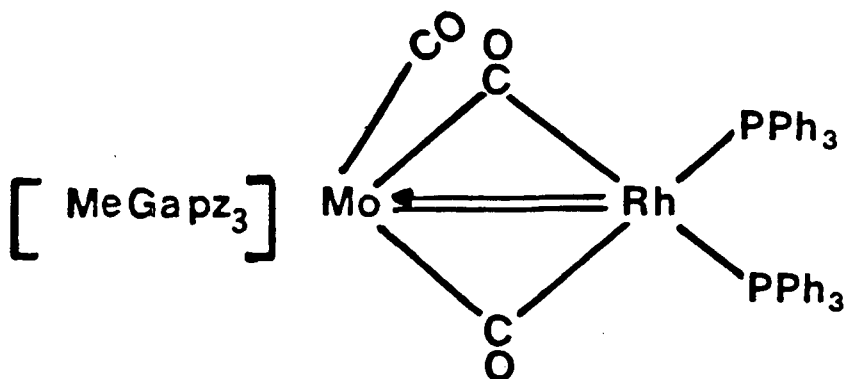


Figure 21. Proposed bonding scheme for  $[\text{MeGapz}_3]\text{Mo}(\text{CO})_3\text{Rh}(\text{PPh}_3)_2$ .

groups, a double bond between the two transition metals, with one component being a Rh→Mo dative link, constitutes an integral part of the overall molecular framework, and is consistent with the observed Mo-Rh bond length in the present complex.

Such dative interactions between metals have been proposed for a number of heterobimetallic complexes [107,133,134]. In keeping with the different roles of the carbonyl ligands, the C-O bond lengths involving the 'bridging' ligands (1.190(5) and 1.175(6)Å) are significantly longer than that of the unique terminal CO ligand (1.154(6)Å). The Rh(μ-CO)<sub>2</sub>Mo framework possesses a butterfly arrangement as seen in the analogous η-C<sub>5</sub>H<sub>5</sub> complex [104] with the Rh-C-Mo dihedral angle of 156° compared with 161° in the η-C<sub>5</sub>H<sub>5</sub> compound.

### 3.3.2 [MeGapz<sub>3</sub>]Mo(CO)<sub>3</sub>Cu(PPh<sub>3</sub>)

The reaction of the [MeGapz<sub>3</sub>]Mo(CO)<sub>3</sub><sup>-</sup> anion with the tetramer [CuCl(PPh<sub>3</sub>)<sub>4</sub>] in THF led to the isolation of a yellow crystalline product which resulted from the displacement of the chloro ligand by the molybdenum tricarbonyl anion. The solid material is air-stable but solutions of the complex decompose rapidly on air-exposure. The physical data for the complex are compiled in Table III p. 72.

The solution ir spectrum for this complex shows two ν<sub>CO</sub> bands suggestive of a symmetrical C<sub>3v</sub> (A + E modes) structure for the complex. The positions of these ν<sub>CO</sub> bands (1898 and 1798 cm<sup>-1</sup>, CH<sub>2</sub>Cl<sub>2</sub> solution) are slightly higher than those observed for the uncomplexed anion [MeGapz<sub>3</sub>]Mo(CO)<sub>3</sub><sup>-</sup> (Et<sub>4</sub>N<sup>+</sup> salt) (1890 and 1760 cm<sup>-1</sup>, CH<sub>2</sub>Cl<sub>2</sub> solution) and [MeGapz<sub>3</sub>]Mo(CO)<sub>3</sub><sup>-</sup>(HAsPh<sub>3</sub><sup>+</sup> salt) (1890 and 1750 cm<sup>-1</sup>, CH<sub>2</sub>Cl<sub>2</sub> solution). These results are close in value to the ν<sub>CO</sub> vibrations, recorded some time earlier by

Trofimenko [53], for the corresponding  $[\text{HBpz}_3]\text{Mo}(\text{CO})_3^-$  anion ( $\text{Et}_4\text{N}^+$  salt) ( $1897$  and  $1761\text{ cm}^{-1}$ , MeCN solution). In the solid state the Cu complex displays three bands in the  $\nu_{\text{CO}}$  region of the spectrum ( $1890$ ,  $1805$  and  $1780\text{ cm}^{-1}$ , Nujol). These could arise either from a splitting of the 'E' mode observed in the solution spectrum, or from slightly different packing environments for the two independent molecules. From the crystal structure data discussed below, one of the carbonyl groups of the unprimed molecule is involved in a possible  $\text{C-H}\cdots\text{O}$  interaction. The solid state ir spectrum of the uncomplexed carbonyl anion in the salt  $[\text{Et}_4\text{N}]^+[\text{MeGapz}_3\text{Mo}(\text{CO})_3]^-$  displayed two  $\nu_{\text{CO}}$  bands ( $1885$  and  $1730\text{ cm}^{-1}$ , Nujol) as expected from its  $\text{C}_{3v}$  symmetry. These values again compare closely with those reported for the analogous boron species in the salt  $[\text{Et}_4\text{N}]^+[\text{HBpz}_3\text{Mo}(\text{CO})_3]^-$  ( $1890$  and  $1750\text{ cm}^{-1}$ , KBr disc) [60]. A structure consistent with the ir data of the Mo-Cu complex is shown below.

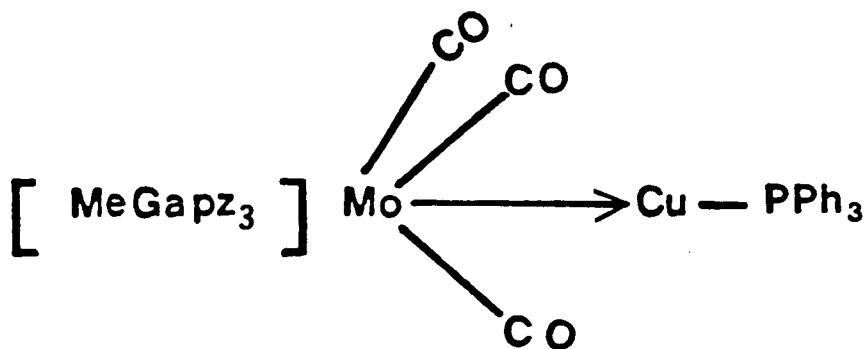


Figure 22. Possible structure of the  $[\text{MeGapz}_3]\text{Mo}(\text{CO})_3\text{Cu}(\text{PPh}_3)$  complex as suggested by the ir data.

In the scheme, the Mo center retains an 18-electron count if it is assumed that the CO groups of the molybdenum tricarbonyl anion retain their terminal character to the molybdenum atom. The single donor bond, Mo→Cu, between the two transition metals gives the Cu of the  $\text{Cu}^{\text{I}}(\text{PPh}_3)^+$  moiety a 14-electron count.

The  $^1\text{H}$  nmr data of  $[\text{MeGapz}_3]\text{Mo}(\text{CO})_3\text{Cu}(\text{PPh}_3)$  in  $\text{C}_6\text{D}_6$  solution at room temperature are consistent with a symmetrical structure for the complex in solution, being similar to the  $^1\text{H}$  nmr spectrum obtained for the uncomplexed anion  $[\text{MeGapz}_3]\text{Mo}(\text{CO})_3^-$  ( $\text{HAsPh}_3^+$  salt) (figure 14, section 2.3.1 p. 44) except for the presence of the  $\text{PPh}_3$  ligand. Only one set of signals is displayed for the pyrazolyl protons, indicating equivalent pyrazolyl groups in the complex. The chemical shift data from the  $^1\text{H}$  nmr results compare quite well with those measured for the uncomplexed anion  $[\text{MeGapz}_3]\text{Mo}(\text{CO})_3^-$  ( $\text{HAsPh}_3^+$  salt) (see section 2.2.4 p. 29).

The crystal structure of the  $[\text{MeGapz}_3]\text{Mo}(\text{CO})_3\text{Cu}(\text{PPh}_3)$  complex is shown in figure 23 and again consists of discrete molecules separated by normal van der Waals distances.

The only intermolecular contact of any possible significance is a C-H...O interaction associating pairs of unprimed molecules about the inversion center at (0,0,1/2) [ $\text{C}(30)\text{-H}(30)\cdots\text{O}(2)$  ( $-\underline{x}$ ,  $-\underline{y}$ ,  $\underline{z}$ ), C...O = 3.424(9), H...O = 2.55Å, C-H...O = 151°]. Apart from several small but statistically significant differences between the corresponding bond lengths and angles (Appendix I), the most notable difference between the two crystallographic independent molecules of  $[\text{MeGapz}_3]\text{Mo}(\text{CO})_3\text{Cu}(\text{PPh}_3)$  is

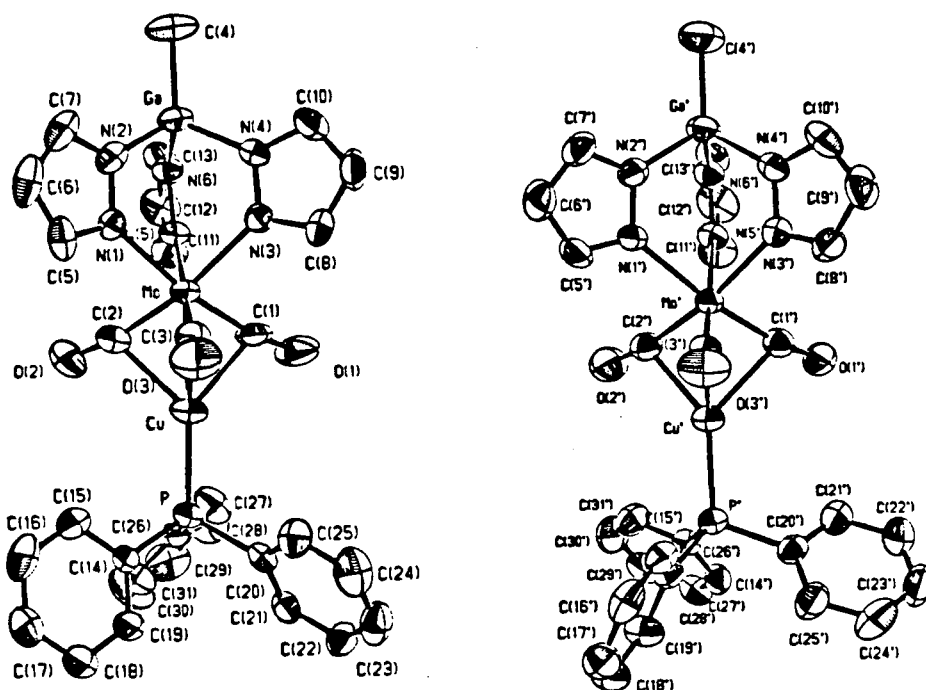


Figure 23. Molecular structures of  $[\text{MeGapz}_3]\text{Mo}(\text{CO})_3\text{Cu}(\text{PPh}_3)$ .

in the orientation of the  $\text{PPh}_3$  ligand. The conformation about the  $\text{Cu-P}$  in the molecule denoted by unprimed atom labels is about  $4^\circ$  from staggered compared with a value of  $26^\circ$  in the second molecule. The complex  $[\text{MeGapz}_3]\text{Mo}(\text{CO})_3\text{Cu}(\text{PPh}_3)$  is valence isoelectronic with the Rh compound,  $[\text{MeGapz}_3]\text{Mo}(\text{CO})_3\text{Rh}(\text{PPh}_3)_2$  discussed in section 3.3.1. However, the Cu complex is of much higher symmetry, possessing an approximate 3-fold axis along the near-linear  $\text{C}(4)\text{-Ga}\cdots\text{Mo-Cu-P}$  atomic arrangement (mean angles:  $\text{C-Ga}\cdots\text{Mo} = 178.0(3)$ ,  $\text{Ga}\cdots\text{Mo-Cu} = 175.2(6)$ , and  $\text{Mo-Cu-P} = 176.1(9)^\circ$ ). In this solid state structure the three pyrazolyl rings are equivalent, this being consistent with the  $^1\text{H}$  nmr results already discussed above.

The three CO ligands are essentially symmetrically placed with mean bond angles  $\text{Mo-C-O}$  of  $170.1(5)$ ,  $170.7(1)$ , and  $172.1(6)^\circ$ ,  $\text{Cu-C-O}$  of

117.0(1), 117.5(3) and 118.5(1)°, and mean bond lengths Mo-C of 1.973(7), 1.964(6) and 1.966(6)Å, Cu...C of 2.247(13), 2.298(23) and 2.415(5)Å. These X-ray data, however, do suggest some interaction between the Cu center and the carbonyl groups, although the exact nature of this interaction is not clear. Obviously the interaction is of a semi-bridging type since the Mo-C-O angles are not far removed from linear.

Numerous recent publications have documented and discussed different types of bridging CO interactions in heterobimetallic transition metal complexes [76,121-123,135 and references therein]. The present Cu compound does not appear to fit into the category of a distal electron-rich metal center (the Cu center has a 14-electron count) donating excessive charge into the CO  $\pi^*$  orbitals [123]. Although, if  $d\pi-d\pi$  bonding occurs between the Cu and the Mo centers, then an interaction with the CO groups similar to that postulated for the complex  $(\eta-C_5H_5)_2Mo_2(CO)_4$  [76,136] may be possible. Such an interaction between a Mo-Cu  $\pi$ -bond and the  $\pi^*$  orbital of a CO ligand is shown schematically in figure 24 (p. 88).

This type of interaction would, of course, tend to lengthen the C-O bond, and, with a mean C-O bond distance of 1.164Å, the carbonyl ligands do display slightly longer bonds than usually found for terminal CO ligands. The present structure does not meet the requirements for  $\Pi$ -CO type bonding (figure 25 p. 89). These requirements were recently reviewed by Horwitz and Shriver [76].

Thus, the Cu-O distances (2.945(5) - 3.143(5)Å) are much longer than the Cu-C distances (2.234(6)-2.419(6)Å), leading to  $\Omega$  values of approximately 2.14 - 2.16 (where  $\Omega = \exp[D(Cu-C)/D(Cu-O)]$ , D = distance).

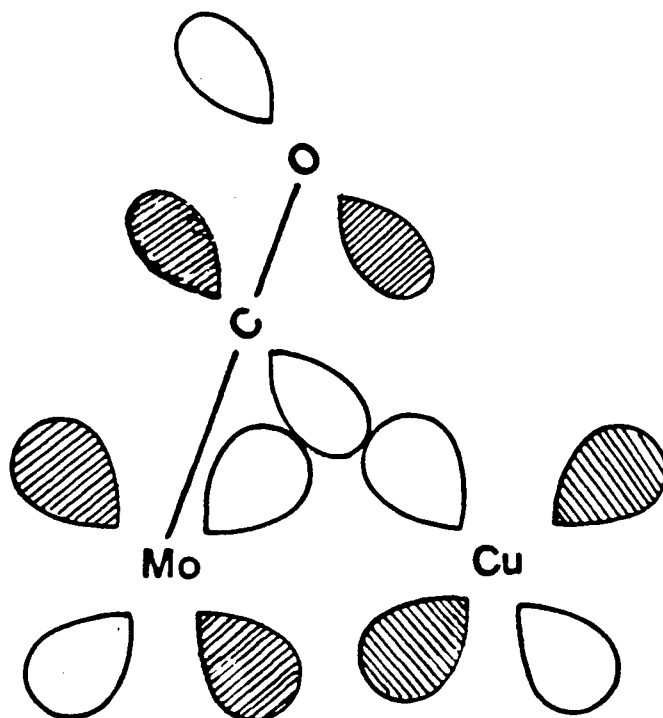
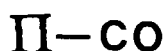
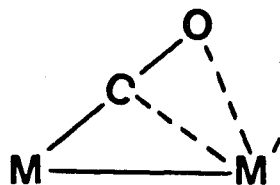


Figure 24. Possible interaction between the Mo-Cu  $\pi$  bond and the  $\pi^*$  orbital of the CO ligand in the complex  $[\text{MeGapz}_3]\text{Mo}(\text{CO})_3\text{Cu}(\text{PPh}_3)$ .

These  $\Omega$  values provide a measure of the extent of interaction of Cu with the C and O ends of the CO ligands, but are much lower than expected for a strong  $\Pi$ -CO type interaction [76]. In addition, the  $\nu_{\text{CO}}$  frequencies observed for the complex are all much higher than the expected value of  $\sim 1650 \text{ cm}^{-1}$  for a  $\Pi$ -CO group.



$$\Omega = 2.2 - 3.3$$

$$\Omega = \exp[D(M'-C)/D(M'-O)]$$

(where D = distance)

Figure 25. The structure of a linear semi-bridging CO type bonding.

Perhaps the bonding in the present complex is more subtle. In this regard recent M.O. calculations [105] on the complex  $(\eta\text{-C}_6\text{H}_6)(\text{CO})\text{Cr}-(\mu\text{-CO})_2\text{Rh}(\text{CO})(\eta\text{-C}_5\text{H}_5)$ , a complex originally postulated to contain a Cr→Rh donor bond in addition to semi-bridging CO interactions [107], suggest a strong interaction between the distal Rh center and the bridging CO ligands (Cr-CO (bridge), 1.902(7)Å, Rh-CO (bridge), 2.200(7)Å), with a net bond order close to zero between the metal atoms (Rh···Cr, 2.757(2)Å). Similar calculations on the present system may well be invaluable in determining the major bonding interactions responsible for the short Mo-Cu separation.

It is again interesting to compare similar complexes in this area. Carlton et al. [104] have provided structural data on two different forms of the complex  $(\eta\text{-C}_5\text{H}_5)\text{W}(\text{CO})_3\text{Cu}(\text{PPh}_3)_2$ , and suggest some semi-bridging interactions involving the two metals and two of the CO ligands. Three important differences occur with the  $[\text{MeGapz}_3]\text{Mo}(\text{CO})_3\text{Cu}(\text{PPh}_3)$  complex. First, only one  $\text{PPh}_3$  ligand is attached to the Cu center, making the molecule valence isoelectronic with the  $[\text{MeGapz}_3]\text{Mo}(\text{CO})_3\text{Rh}(\text{PPh}_3)_2$  compound (see section 3.3.1). Second, the present structure has three roughly equivalent CO groups, whereas in Carlton's tungsten compounds one of the three CO groups is clearly terminal to tungsten. Third, the mean Mo-Cu distance of 2.513(9)Å is considerably shorter than either of the W-Cu distances of 2.771(1) and 2.721(1)Å reported by Carlton et al. Given that the radii for Mo and W are very similar at ~1.61Å (the M-M distances in  $(\eta\text{-C}_5\text{H}_5)(\text{CO})_3\text{M}-\text{M}(\text{CO})_3(\eta\text{-C}_5\text{H}_5)$  are 3.222(5)Å for M = Mo [137] and 3.24(1)Å for M = W [138]), these differences in bond lengths suggest a much stronger Mo-Cu interaction in the present complex. Indeed, the observed Mo-Cu distance is significantly shorter than the estimated single Mo-Cu bond length of ~2.7 — 2.8Å. Another noticeable difference occurs in the Cu-P distances in the two complexes. Thus the compound reported here displays a mean Cu-P distance of 2.196(3)Å, somewhat shorter than the corresponding mean distance of 2.299(12)Å reported for the two crystalline forms of  $(\eta\text{-C}_5\text{H}_5)\text{W}(\text{CO})_3\text{Cu}(\text{PPh}_3)_2$ . Recently, structural data were provided for the  $(\eta\text{-C}_5\text{H}_5)\text{Mo}(\text{CO})_3\text{Cu}(\text{tmed})$  (tmed = N, N, N', N'-tetramethylethylenediamine,  $\text{Me}_2\text{NCH}_2\text{CH}_2\text{NMe}_2$ ) compound by Doyle et al. [139]. Even though

different metals were involved and the ligands on the Cu were quite dissimilar both sterically and electronically, the overall geometry of the latter molecule is surprisingly similar to that of one of the  $(\eta\text{-C}_5\text{H}_5)\text{W}(\text{CO})_3\text{Cu}(\text{PPh}_3)_2$  isomers reported by Carlton. Both the Mo complex reported by Doyle and the W complexes reported by Carlton have 'four-legged piano stool' configurations about the Mo or W atoms in addition to a Cu-M (M = Mo or W) bond with a single terminal and two semi-bridging CO groups respectively. The Mo-Cu distance in the present  $[\text{MeGapz}_3]\text{Mo}(\text{CO})_3\text{Cu}(\text{PPh}_3)$  complex is comparable (2.513(9) Å vs. 2.592 Å) to that of the  $(\eta\text{-C}_5\text{H}_5)\text{Mo}(\text{CO})_3\text{Cu}(\text{tmed})$  compound.

The structures of the  $(\eta\text{-C}_5\text{H}_5)\text{W}(\text{CO})_3\text{Au}(\text{PPh}_3)$  [140] and  $[\text{HBpz}_3]\text{Mo}(\text{CO})_3\text{Br}$  [60] complexes are worthy of comparison with the  $[\text{MeGapz}_3]\text{Mo}(\text{CO})_3\text{Cu}(\text{PPh}_3)$  structure. The W-Au compound displays an arrangement very different from that found for Mo-Cu complex. Thus, instead of a symmetrical structure analogous to that depicted in figure 23, with the ' $\eta\text{-C}_5\text{H}_5$ ' ligand replacing the ' $\text{MeGapz}_3$ ' ligand and the Au atom replacing the Cu atom the arrangement adopted is that of a 'four-legged piano stool', or a distorted square-pyramid with the  $(\eta\text{-C}_5\text{H}_5)\text{W}$  unit at the apex and the three CO ligands and the  $\text{Au}(\text{PPh}_3)$  grouping occupying the basal positions. A similar structure, described as a 3:4 piano stool, has been reported recently by Curtis and Shiu for  $[\text{HBpz}_3]\text{Mo}(\text{CO})_3\text{Br}$ . These authors [60] mentioned that one of the interesting aspects which prompted their study, was the possibility of observing a capped octahedral (3:3:1) structure, since calculations by Kubacek et al. [141] had shown that this arrangement represents a minimum in the potential energy surface for

analogous  $(\eta\text{-C}_5\text{H}_5)\text{ML}_4$  complexes whose global minimum (ground state) is always the 'four-legged piano stool', or 3:4 structure. It appears that the present copper complex  $[\text{MeGapz}_3]\text{Mo}(\text{CO})_3\text{Cu}(\text{PPh}_3)$  closely approaches this 3:3:1 capped octahedral arrangement.

Finally, the structure of the complex,  $(\eta\text{-C}_3\text{H}_5)\text{Fe}(\text{CO})_3\text{Au}(\text{PPh}_3)$  [142] has many features similar to those of the Mo-Cu complex presented here. It has been proposed that the bonding in this iron complex results from the Lewis base  $(\eta\text{-C}_3\text{H}_5)\text{Fe}(\text{CO})_3^-$  donating a pair of electrons to the Lewis acid  $\text{Au}(\text{PPh}_3)^+$ , and does not necessarily involve any direct interaction between the Au atom and the CO ligand, the geometry of the complex being dictated by transition metal basicity. If this reasoning is correct then the Au center attains a 14-electron count and the Fe-Au separation of 2.519(1)Å results entirely from the Fe→Au dative bond.

### 3.3.3 $[\text{MeGapz}_3]\text{Mo}(\text{CO})_3\text{Cu}(\text{CO})$

The introduction of the  $\text{HBpz}_3^-$  ligand in place of the  $\text{C}_5\text{H}_5^-$  ligand is often known to have a stabilizing effect on the resulting complex. For example, while the compound  $(\eta\text{-C}_5\text{H}_5)\text{CuCO}$  [23] decomposes rapidly at room temperature even under inert conditions, the analogous  $[\text{HBpz}_3]\text{CuCO}$  [143] is a white, crystalline air- and heat-stable solid. Even though previous attempts at the isolation of the analogous  $[\text{MeGa}(3,5\text{-Me}_2\text{pz})_3]\text{CuCO}$  were unsuccessful [144], it was open to speculation as to whether the ' $\text{MeGapz}_3^-$ ' ligand would stabilize the compound  $[\text{MeGapz}_3]\text{Mo}(\text{CO})_3\text{Cu}(\text{CO})$ , especially with the  $\pi$ -acceptor CO ligand attached to the already electron-deficient Cu metal center (assuming the Cu has a 14-electron count similar to that in the ' $\text{PPh}_3$ ' derivative discussed in section 3.3.2).

Reaction of the  $[\text{MeGapz}_3]\text{Mo}(\text{CO})_3^-$  anion with  $\text{CuCl}$  in the presence of  $\text{CO}$  resulted in the yellow  $[\text{MeGapz}_3]\text{Mo}(\text{CO})_3\text{Cu}(\text{CO})$  compound as expected. Analytical, ir and  $^1\text{H}$  nmr data for this compound are collected in Table III p. 72. The solution ir spectrum of this compound showed three bands in the  $\nu_{\text{CO}}$  region of the spectrum (2020, 1955, 1810  $\text{cm}^{-1}$ ,  $\text{CH}_2\text{Cl}_2$ ). Since the  $\text{Cu}$  metal would not be expected to donate electron density efficiently to the  $\pi^*$  system of its  $\text{CO}$  ligand, the backbonding present in the  $\text{Cu}-\text{CO}$  link is relatively weak and consequently this  $\text{CO}$  ligand probably accounts for the highest  $\nu_{\text{CO}}$  value at 2010  $\text{cm}^{-1}$ . The two other bands at 1955 and 1810  $\text{cm}^{-1}$  must be due to the three symmetrically placed  $\text{CO}$  ligands on the  $\text{Mo}$  atom (assuming a complex isostructural to  $[\text{MeGapz}_3]\text{Mo}(\text{CO})_3\text{Cu}(\text{PPh}_3)$  which is discussed in section 3.3.2). The slightly higher  $\nu_{\text{CO}}$  values obtained for the present complex compared to those recorded for  $[\text{MeGapz}_3]\text{Mo}(\text{CO})_3\text{Cu}(\text{PPh}_3)$  (1898 and 1798  $\text{cm}^{-1}$ ,  $\text{CH}_2\text{Cl}_2$ ), are presumably due to greater withdrawal of electron density from the  $\text{Mo}$  atom to the  $\text{Cu}$  atom in the  $[\text{MeGapz}_3]\text{Mo}(\text{CO})_3\text{Cu}(\text{CO})$  complex.

The  $^1\text{H}$  nmr data for this  $\text{Cu}-\text{CO}$  complex are consistent with a symmetrical  $\text{C}_{3v}$  structure in solution, and display one set of resonances for the pyrazolyl protons, being indicative of equivalent pyrazolyl groups. These  $^1\text{H}$  nmr data compare quite well with those recorded for the  $[\text{MeGapz}_3]\text{Mo}(\text{CO})_3\text{Cu}(\text{PPh}_3)$  compound, and suggest this complex may indeed be isostructural to the ' $\text{Cu}(\text{CO})$ ' derivative. Supportive evidence comes from the facile replacement of the  $\text{CO}$  ligand of the complex  $[\text{MeGapz}_3]\text{Mo}(\text{CO})_3\text{Cu}(\text{CO})$  by  $\text{PPh}_3$  ligand to give the  $[\text{MeGapz}_3]\text{Mo}(\text{CO})_3\text{Cu}(\text{PPh}_3)$  compound.

### 3.3.4 $[\text{MeGapz}_3]\text{Mo}(\text{CO})_3\text{Pt}(\text{Me})(\text{PPh}_3)$

The  $\text{PtCl}(\text{Me})(\text{COD})$  ( $\text{COD} = 1,5\text{-cyclo-octadiene}, \pi\text{-}1,5\text{-C}_8\text{H}_{12}$ ) complex, previously reported as unreactive toward  $\text{RBpz}_3^-$  ligand unless the very tightly-bonded COD ligand is first activated by a strong oxidant such as  $\text{AgPF}_6$  via halogen abstraction [24,145], was recently shown to be reactive toward  $\text{Me}_2\text{Gapz}_2^-$  ligand in the absence of a strong oxidant [146].

Similarly the  $[\text{MeGapz}_3]\text{Mo}(\text{CO})_3^-$  anion reacted with  $\text{PtCl}(\text{Me})(\text{COD})$  without the  $\text{AgPF}_6$ , but in the presence of the stabilizing  $\text{PPh}_3$  ligand, to form the complex  $[\text{MeGapz}_3]\text{Mo}(\text{CO})_3\text{Pt}(\text{Me})(\text{PPh}_3)$  with the elimination of the chloro and COD ligands. Analytical, ir and  $^1\text{H}$  nmr data for this complex are listed in section 3.2.5 (p. 71).

The ir spectrum of the  $[\text{MeGapz}_3]\text{Mo}(\text{CO})_3\text{Pt}(\text{Me})(\text{PPh}_3)$  compound showed three strong bands ( $1900, 1815, 1785\text{ cm}^{-1}$ ,  $\text{CH}_2\text{Cl}_2$ ) in the  $\nu_{\text{CO}}$  region. If one terminal and two bridging CO groups are assumed to be present in this compound as suggested by the ir data, then a bonding scheme between the Mo atom and the Pt metal center can be proposed. Such a bonding scheme is shown in figure 26. In this bonding scheme, the Mo atom is provided with an 18-electron environment with the Pt having a 16-electron count if a double  $\text{Mo}=\text{Pt}$  bond exists in the complex. This is not unusual, since 18-electron environments are common for Mo in low oxidation states, and similarly 16-electron states are not exceptional for Pt(II) complexes. The  $\nu_{\text{CO}}$  values recorded for the present Mo-Pt complex are in good agreement with those reported for the closely related compound structurally characterized as  $(\eta\text{-C}_5\text{H}_5)\text{Mo}(\text{CO})_3\text{Pt}(\text{H})(\text{PPh}_3)_2$  ( $\nu_{\text{CO}}$ :  $1916, 1828, 1797\text{ cm}^{-1}$ , KBr disc) [112]. According to the X-ray structural

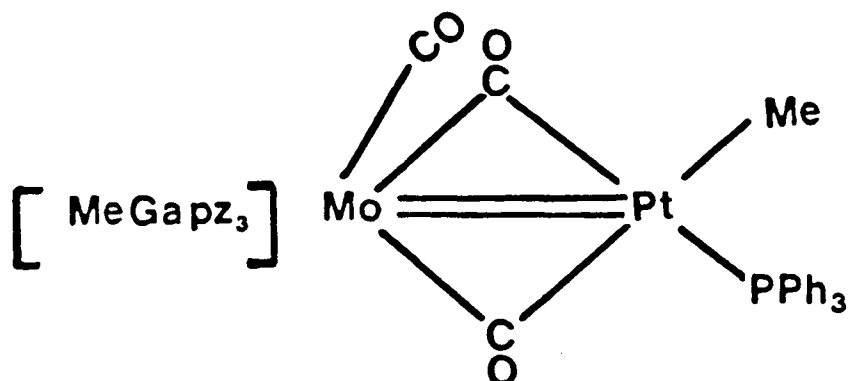


Figure 26. Proposed bonding scheme for  $[\text{MeGapz}_3]\text{Mo}(\text{CO})_3\text{Pt}(\text{Me})(\text{PPh}_3)$ .

analysis, the usual square-planar environment found for Pt(II) compounds is strongly distorted in the latter complex. This arrangement was rationalized by the authors as being due to minimization of steric repulsions between the bulky phosphine groups in the complex.

The room temperature  $^1\text{H}$  nmr spectrum of the  $[\text{MeGapz}_3]\text{Mo}(\text{CO})_3\text{Pt}(\text{Me})(\text{PPh}_3)$  complex in  $d_6$ -acetone solution indicated equivalent pz groups in the compound. A rapid rotation of the 'MeGapz<sub>3</sub>' moiety about the Ga...Mo axis might explain the observed equivalence of the pz groups in solution. The Pt-Me signal was also displayed in the spectrum at  $\sim 9.45\tau$  with the accompanying  $^{195}\text{Pt}$ -satellites ( $J_{^{195}\text{Pt}-\text{Me}} \approx 72$  Hz).

Unfortunately, the actual structure of the present Mo-Pt complex could not be confirmed since attempts to obtain crystals suitable for X-ray structural studies were unsuccessful.

### 3.3.5 $[\text{MeGapz}_3]\text{Mo}(\text{CO})_3\text{M}'\text{Cl}_3$ ( $\text{M}' = \text{Zr}$ or $\text{Hf}$ )

The reaction of  $[\text{MeGapz}_3]\text{Mo}(\text{CO})_3^-$  anion and  $\text{M}'\text{Cl}_4$  resulted in the mixed transition metal  $[\text{MeGapz}_3]\text{Mo}(\text{CO})_3\text{M}'\text{Cl}_3$  complexes. The compounds have been characterized by the usual physical methods (Table III p. 72) and are reasonably stable as solids under inert conditions, but decompose quite readily in solution. For example, a  $\text{C}_6\text{D}_6$  yellow solution of the Mo-Zr complex in a flame-sealed nmr tube turned dark green in 3 days.

The room temperature  $^1\text{H}$  nmr spectra of the complexes indicated the presence of equivalent pz groups in solution. The  $^1\text{H}$  nmr spectrum for the Mo-Zr complex in  $\text{C}_6\text{D}_6$  solution is shown in figure 27. Interestingly, the Mo-Hf complex had a  $^1\text{H}$  nmr spectrum almost superimposable to that of the Mo-Zr compound, suggesting identical structures for both complexes. A rigid symmetrical 3:3:1 structure (figure 28a) for the complexes in solution would be consistent with the observed equivalence of the pz groups indicated by the  $^1\text{H}$  nmr spectrum.

Alternatively, the  $^1\text{H}$  nmr results can also be explained by a 3:4 structure (figure 28b) in which a rapid rotation of the 'MeGapz<sub>3</sub>' moiety about the Ga...Mo axis might equalize the environments of the pz rings in the complexes.

As in the  $^1\text{H}$  nmr results discussed above, the ir spectra of both the Mo-Zr and Mo-Hf compounds were almost identical, providing additional evidence for the similarity in the structures of both compounds. The ir

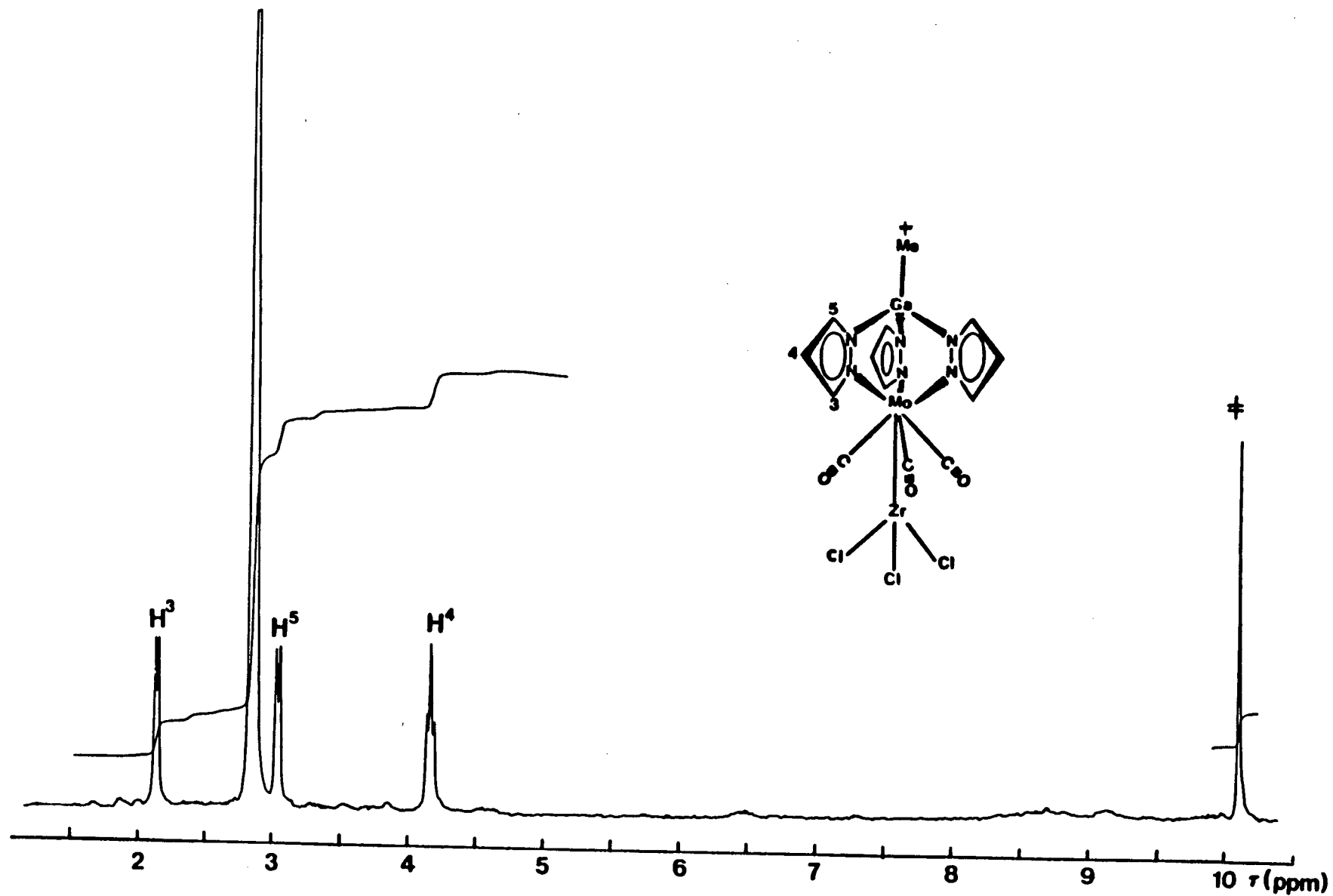


Figure 27. 80 MHz  $^1\text{H}$  nmr spectrum of  $[\text{MeGaz}_3]\text{Mo}(\text{CO})_3\text{ZrCl}_3$  in  $\text{C}_6\text{D}_6$  solution.

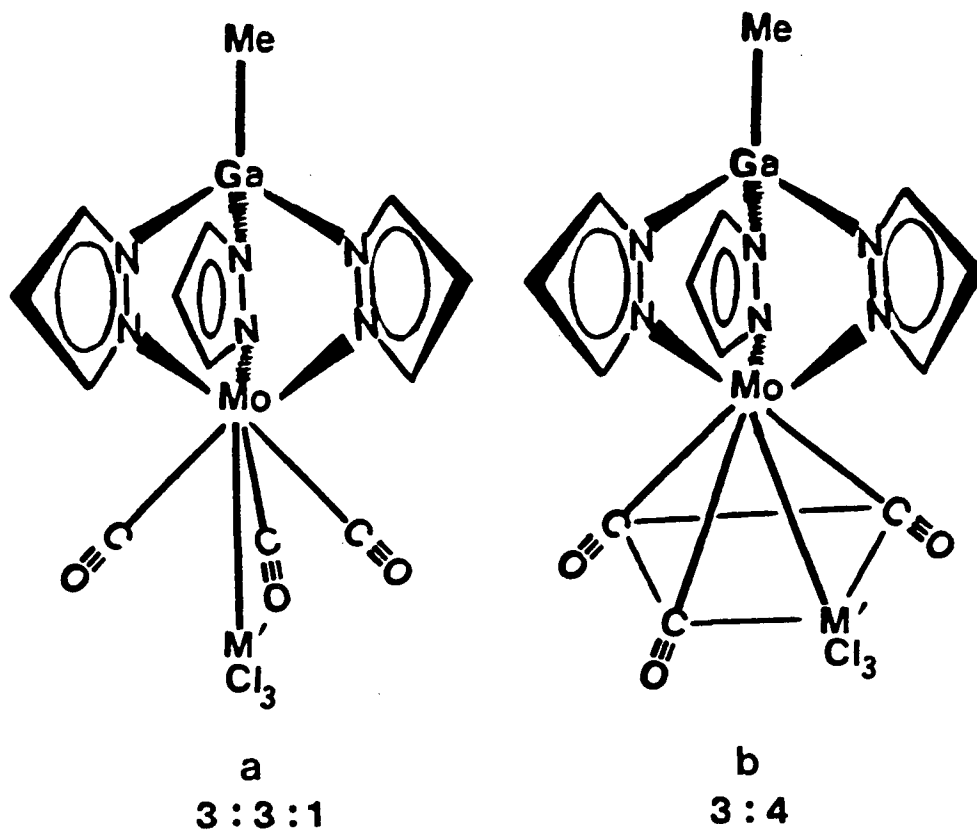


Figure 28. Possible molecular arrangements for the  $[\text{MeGapz}_3]\text{Mo}(\text{CO})_3\text{M}'\text{Cl}_3$  ( $\text{M}' = \text{Zr}$  or  $\text{Hf}$ ) complexes.

spectra of the  $[\text{MeGapz}_3]\text{Mo}(\text{CO})_3\text{M}'\text{Cl}_3$  ( $\text{M}' = \text{Zr}$  or  $\text{Hf}$ ) complexes displayed three strong bands in the  $\nu_{\text{CO}}$  region. This is suggestive of  $C_3$  symmetry for the complexes in solution. A typical ir spectrum for the  $[\text{MeGapz}_3]\text{Mo}(\text{CO})_3\text{HfCl}_3$  complex is shown in figure 29.

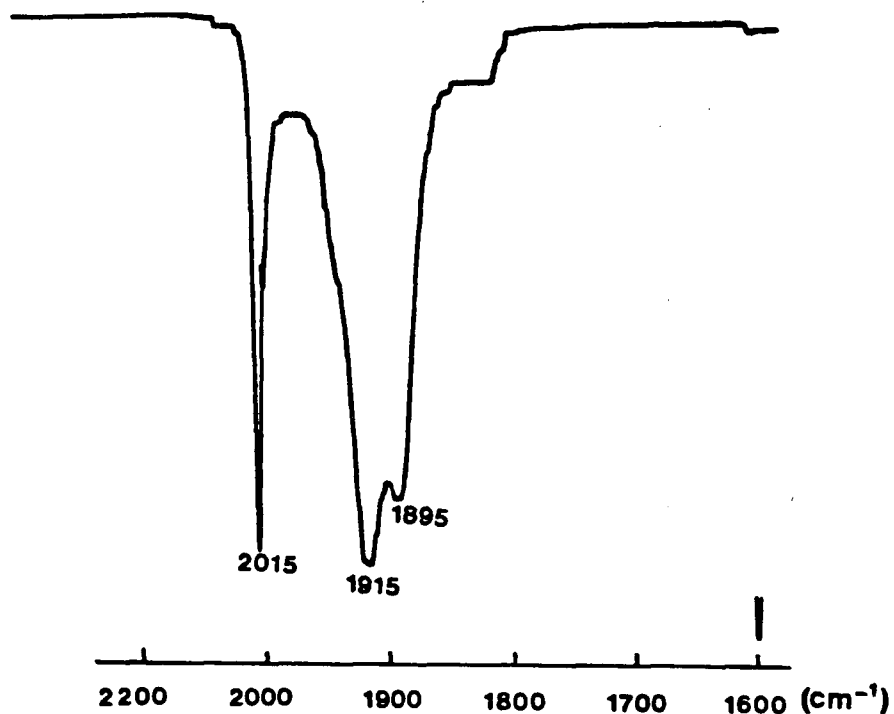


Figure 29. Ir spectrum of  $[\text{MeGapz}_3]\text{Mo}(\text{CO})_3\text{HfCl}_3$  in  $\text{CH}_2\text{Cl}_2$  solution.

The presence of only terminal  $\nu_{\text{CO}}$  bands in the ir spectra of the complexes is indicative of direct Mo-M' (M' = Zr or Hf) interactions with no accompanying bridging CO ligands. However, all attempts at isolating crystals suitable for X-ray crystal structure analyses were unsuccessful. This was rather discouraging especially since relatively few derivatives of the titanium group metals with M-M' (M = Cr, Mo or W; M' = Ti, Zr or Hf) bonds have been reported in the literature [114].

### 3.3.6 $[\text{MeGapz}_3\text{Mo}(\text{CO})_3]_2\text{Hg}$

An extensive array of metal-metal bonded dimers and clusters are known in cyclopentadienyl chemistry. In contrast, only one such dimer,  $[\text{HBpz}_3\text{Mo}(\text{CO})_2]_2$  [38] is known with the tridentate poly(1-pyrazolyl)borate

ligand coordinated on more than one metal. Even more interesting is the fact that X-ray structural analysis of this complex showed the presence of a Mo≡Mo triple bond, rather than the expected Mo-Mo single bond in the elusive  $[\text{HBpz}_3\text{Mo}(\text{CO})_3]_2$  compound.

Metathetical reaction of the  $\text{Na}^+\text{MeGapz}_3\text{Mo}(\text{CO})_3^-$  salt with  $\text{HgCl}_2$  in THF resulted in the off-yellow, air-sensitive compound  $[\text{MeGapz}_3\text{Mo}(\text{CO})_3]_2\text{Hg}$  in good yield. The solution ir spectrum of this product showed four bands (2020, 1985, 1952, 1890  $\text{cm}^{-1}$ ,  $\text{CH}_2\text{Cl}_2$ ) in the terminal  $\nu_{\text{CO}}$  region. The above ir data are in good agreement to those reported for the  $[(\eta\text{-C}_5\text{H}_5)\text{Mo}(\text{CO})_3]_2\text{Hg}$  compound by the two independent groups of Fischer and Noack [147], and by Burlitch and Ferrari [148]. These authors interpreted their spectra in terms of a single isomer with a skew configuration of the  $\text{Mo}(\text{CO})_3(\eta\text{-C}_5\text{H}_5)$  groups about the Mo-Hg-Mo system in the  $[(\eta\text{-C}_5\text{H}_5)\text{Mo}(\text{CO})_3]_2\text{Hg}$  complex. The ir result for the present  $[\text{MeGapz}_3\text{Mo}(\text{CO})_3]_2\text{Hg}$  complex is perhaps suggestive of the adoption of a 3:3:1 array for the  $\text{MeGapz}_3\text{Mo}(\text{CO})_3$  groups about a linear Mo-Hg-Mo backbone in the compound as shown below (figure 30).

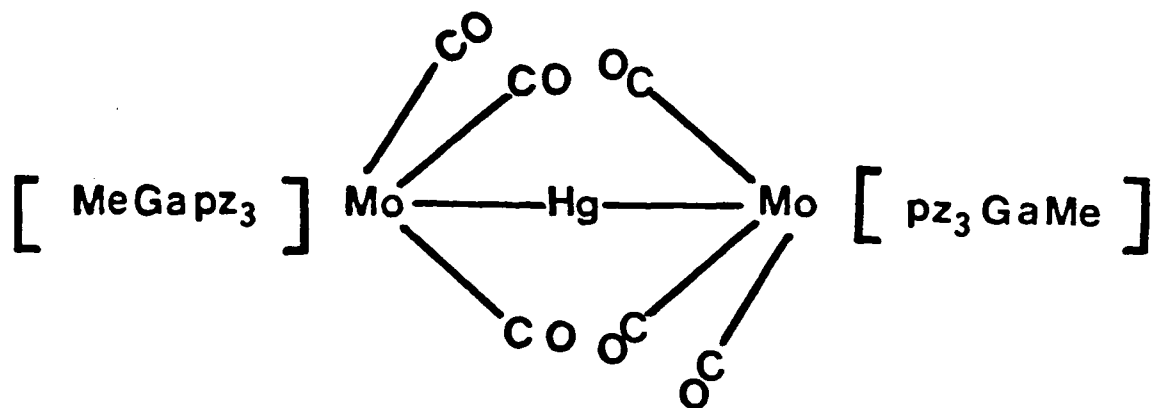


Figure 30. Possible molecular arrangement for the complex  $[\text{MeGapz}_3\text{Mo}(\text{CO})_3]_2\text{Hg}$ .

The mass spectrum of the compound  $[\text{MeGapz}_3\text{Mo}(\text{CO})_3]_2\text{Hg}$  was characterized by extensive low fragment ions, usually indicative of thermal decomposition of the sample under electron impact (E.I) conditions. However, the monomeric  $\text{MeGapz}_3\text{Mo}(\text{CO})_3^+$  ion fragment was observed at ~467, in addition to  $\text{MeGapz}_3\text{Mo}(\text{CO})_2^+$ ,  $\text{MeGapz}_3\text{Mo}(\text{CO})^+$ , and  $\text{MeGapz}_3\text{Mo}^+$  fragment ions at 439, 411 and 383 mass units (based on  $^{69}\text{Ga}$ ,  $^{98}\text{Mo}$ ), respectively. The most intense signals in the spectrum were those attributable to the  $\text{MeGapz}_3\text{Mo}(\text{CO})_3^+$  fragment ion at ~565. Interestingly, a similar fragmentation pattern has been observed in the mass spectrum of the compound  $[(\eta\text{-C}_5\text{H}_5)\text{Mo}(\text{CO})_3]_2$  by King [149].

The  $^1\text{H}$  nmr spectrum of the  $[\text{MeGapz}_3\text{Mo}(\text{CO})_3]_2\text{Hg}$  complex is rather strange, in that a sharp Ga-Me signal was displayed in the gallium alkyl region but the pz proton resonances were not observed in either  $d_8$ -toluene,  $\text{C}_6\text{D}_6$  or  $d_6$ -acetone solution. Attempts to obtain suitable crystals for X-ray crystal structure analyses were unsuccessful.

### 3.3.7 The ' $[\text{MeGapz}_3]\text{Mo}(\text{CO})_3\text{Mn}(\text{CO})_5$ ' Complex

The preparation of the compound  $[\text{MeGapz}_3]\text{Mo}(\text{CO})_3\text{Mn}(\text{CO})_5$  was attempted by the reaction of the  $\text{MeGapz}_3\text{Mo}(\text{CO})_3^-$  anion with  $\text{Mn}(\text{CO})_5\text{Br}$ . Spectral data obtained on the black solid isolated from the reaction indicated the desired compound to be present in the product mixture. The solution ir spectrum of the black solid in cyclohexane showed  $\nu_{\text{CO}}$  bands at 2045, 2035, 2015, 2000, 1980, 1930, 1900 and  $1875\text{ cm}^{-1}$ , indicative of terminally bound CO groups. This  $\nu_{\text{CO}}$  pattern observed compares quite well to the bands reported for the analogous  $(\eta\text{-C}_5\text{H}_5)\text{Mo}(\text{CO})_3\text{Mn}(\text{CO})_5$  complex [150,151].

Unfortunately all attempts to isolate an analytically pure sample of  $[\text{MeGapz}_3]\text{Mo}(\text{CO})_3\text{Mn}(\text{CO})_5$  were unsuccessful and further investigations were not undertaken. It is probable that the compound  $[\text{MeGapz}_3]\text{Mo}(\text{CO})_3\text{Mn}(\text{CO})_5$  would adopt a capped octahedral arrangement, since severe steric interactions between the pz rings and the CO groups attached to the Mn atom would most likely preclude the adoption of a 'four-legged piano stool' geometry of the  $(\eta\text{-C}_5\text{H}_5)\text{Mo}(\text{CO})_3\text{Mn}(\text{CO})_5$  complex [152].

### 3.4 Summary

The mixed transition metal complexes  $\text{LMo}(\text{CO})_3\text{Rh}(\text{PPh}_3)_2$  ( $\text{L} = [\text{MeGapz}_3], [\text{HBpz}_3],$  or  $[\text{Me}_2\text{Gapz}(\text{OCH}_2\text{CH}_2\text{NMe}_2)]$ ) have been prepared and characterized. One of the above formally unsaturated bimetallic complexes,  $[\text{MeGapz}_3]\text{Mo}(\text{CO})_3\text{Rh}(\text{PPh}_3)_2$ , has been structurally characterized, and displays one terminal and two bridging CO ligands. Double bonding between the Rh and Mo is proposed with one of the bonds being a dative link ( $\text{Rh} \rightleftharpoons \text{Mo}$ ).

The heterobimetallic complexes  $[\text{MeGapz}_3]\text{Mo}(\text{CO})_3\text{CuY}$  (where  $\text{Y} = \text{PPh}_3$  or CO) featuring Mo-Cu bonds have also been prepared. The structure of the compound  $[\text{MeGapz}_3]\text{Mo}(\text{CO})_3\text{Cu}(\text{PPh}_3)$  has been determined by X-ray crystal structure analysis. The three CO ligands are essentially terminally bound to Mo, with the possibility of some weak semi-bridging interactions with the Cu center. This Mo-Cu complex provides a rare example of a 3:3:1, or capped octahedral structure.

The  $\text{MeGapz}_3\text{Mo}(\text{CO})_3^-$  anion reacted with  $\text{PtCl}(\text{Me})(\text{COD})$  in the presence of the stabilizing  $\text{PPh}_3$  ligand, eliminating the chloro and COD ligands to

give the heterobimetallic compound  $[\text{MeGapz}_3]\text{Mo}(\text{CO})_3\text{Pt}(\text{Me})(\text{PPh}_3)$ , in which Mo-Pt bonding is featured. Unfortunately the actual structure of this complex could not be confirmed due to the lack of success in obtaining suitable crystals for X-ray structural analysis.

The complexes  $[\text{MeGapz}_3]\text{Mo}(\text{CO})_3\text{M}'\text{Cl}_3$  ( $\text{M}' = \text{Zr}$  or  $\text{Hf}$ ) have been prepared from the reaction of the  $[\text{MeGapz}_3\text{Mo}(\text{CO})_3]^-$  anion and the  $\text{M}'\text{Cl}_4$  starting halide species. The presence of only terminally-bonded CO ligands is indicative of direct Mo-M' ( $\text{M}' = \text{Zr}$  or  $\text{Hf}$ ) interactions in the complexes without accompanying bridging CO ligands.

## CHAPTER IV

TRANSITION METAL-GROUP 14 ELEMENT BONDED COMPLEXES  
INCORPORATING POLY(1-PYRAZOLYL)GALLATE LIGANDS4.1 Introduction

The reactivity of the tricarbonyl anions  $\text{LMo(CO)}_3^-$  ( $\text{L} = [\text{MeGapz}_3]$ ,  $[\text{HBpz}_3]$ , or  $[\text{Me}_2\text{Gapz(OCH}_2\text{CH}_2\text{NMe}_2)]$ ) toward a variety of transition metal halide species to produce novel transition metal-transition metal bonded compounds was explored in Chapter III. As part of an on-going investigation into the similarity of the  $\text{MeGapz}_3\text{Mo(CO)}_3^-$  anion and the analogous  $\text{CpMo(CO)}_3^-$  anion, the behaviour of the  $\text{MeGapz}_3\text{Mo(CO)}_3^-$  anion toward a number of group 14 (Si, Ge, Sn) element organo halides has been studied; and the results from the study will be discussed in the present Chapter. Complexes containing direct transition metal-group 14 element single bonds have been isolated, and confirmed structurally for the complex  $[\text{MeGapz}_3]\text{Mo(CO)}_3\text{SnPh}_3$  by means of a crystal structure determination in the solid state. The complex  $[\text{MeGapz}_3]\text{Mo(CO)}_3\text{SnMe}_2\text{Cl}$  was shown to be non-rigid in solution by a variable temperature  $^1\text{H}$  nmr experiment. The 3:3:1 or capped octahedral arrangement has been demonstrated for the compound structurally characterized as  $[\text{MeGapz}_3]\text{Mo(CO)}_3\text{SnPh}_3$  in the solid state. Thus, the above compound constitutes the first reported structure for complexes of the type  $\text{LM(CO)}_3\text{M}'\text{R}_3$  (where  $\text{L} = (\eta\text{-C}_5\text{H}_5)$ ,  $[\text{HBpz}_3]$ , or  $[\text{MeGapz}_3]$ ;  $\text{M} = \text{Cr, Mo, or W}$ ;  $\text{M}' = \text{Si, Ge, or Sn}$ ;  $\text{R} = \text{alkyl or aryl}$ ).

The preparation and characterization of the six-coordinate triorganotin complexes  $\text{LSnMe}_3$  ( $\text{L} = [\text{MeGapz}_3]$ ,  $[\text{MeGa}(3,5\text{-Me}_2\text{pz})_3]$ ), and the  $[\text{MeGapz}_3]\text{SnMe}_2\text{Cl}$  compound are also described in this chapter. Parts of this chapter have been published elsewhere [92].

## 4.2 Experimental

### 4.2.1 Starting materials

$\text{Me}_3\text{SiCl}$ ,  $\text{Me}_3\text{GeCl}$ ,  $\text{Ph}_3\text{GeCl}$  (Strem Chemicals),  $\text{Me}_3\text{SnCl}$  (Aldrich Chemicals),  $\text{Ph}_3\text{SnCl}$  (Alpha Chemicals) and  $\text{Me}_2\text{SnCl}_2$  (PCA Chemicals) were used as supplied.

### 4.2.2 Preparation of $[\text{MeGapz}_3]\text{Mo}(\text{CO})_3\text{SiMe}_3$



To the molybdenum tricarbonyl anion  $\text{MeGapz}_3\text{Mo}(\text{CO})_3^-$  (0.35 mmol) in THF was added  $\text{Me}_3\text{SiCl}$  (0.038 g, 0.350 mmol) in the same solvent. The resulting reaction mixture was stirred overnight after which the solvent was removed in vacuo. The residue was extracted with benzene and filtered. Evaporation of the benzene solvent from the filtrate containing the extract afforded yellow solids of the desired product in moderate yield. This compound is unstable as a solid and in solution even under inert conditions if left for a few days. Pertinent physical data for this compound are listed in Table IV.

#### 4.2.3 Preparation of $[\text{MeGapz}_3]\text{Mo}(\text{CO})_3\text{GeR}_3$ (R = Me, Ph)



$\text{Me}_3\text{GeCl}$  (0.13 g, 0.85 mmol) was added to a stirred solution of the  $\text{Na}^+\text{MeGapz}_3\text{Mo}(\text{CO})_3^-$  (0.85 mmol) salt in THF. The reaction mixture was stirred overnight after which the solvent was removed under vacuum. The resulting orange residue was extracted with benzene and filtered. The benzene solution containing the extracts was then concentrated to give orange needles of the desired product  $[\text{MeGapz}_3]\text{Mo}(\text{CO})_3\text{GeMe}_3$  in moderate yield.

The compound  $[\text{MeGapz}_3]\text{Mo}(\text{CO})_3\text{GePh}_3$  was prepared similarly using  $\text{Ph}_3\text{GeCl}$  as the starting material. Orange crystals of this product were isolated in approximately the same yield. Both of the above Mo-Ge complexes are air-sensitive solids and deterioration of the compounds occurs slowly in solution. Physical data for the complexes are collected in Table IV.

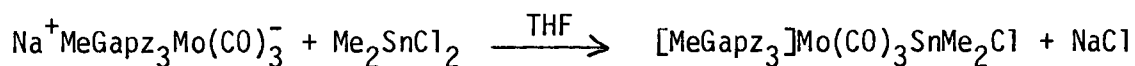
#### 4.2.4 Preparation of $[\text{MeGapz}_3]\text{Mo}(\text{CO})_3\text{SnMe}_3$



The  $\text{Na}^+\text{MeGapz}_3\text{Mo}(\text{CO})_3^-$  (0.353 mmol) salt solution in THF was reacted with an equimolar amount of  $\text{Me}_3\text{SnCl}$  (0.070 g, 0.353 mmol) in the same solvent. The cloudy, dark orange, reaction mixture produced was stirred for ~2 days after which the solvent was removed in vacuo to afford a dark

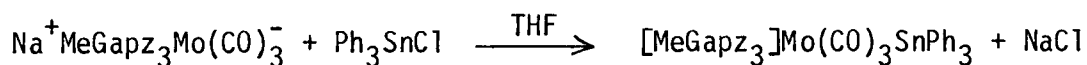
orange-brown oily residue. This residue was extracted with n-hexane and filtered. Upon slow evaporation of the solvent from the filtrate, dark orange crystals of the desired product were recovered in ~70% yield. The compound is stable under nitrogen but decomposes slowly on exposure to air. Analytical, ir and  $^1\text{H}$  nmr data for the complex are compiled in Table IV.

#### 4.2.5 Preparation of $[\text{MeGapz}_3]\text{Mo}(\text{CO})_3\text{SnMe}_2\text{Cl}$



An equimolar amount of  $\text{Me}_2\text{SnCl}_2$  (0.193 g, 0.880 mmol) dissolved in THF, was slowly added to a THF solution of the  $\text{Na}^+\text{MeGapz}_3\text{Mo}(\text{CO})_3^-$  (0.880 mmol) salt. The initial amber-yellow color of the starting molybdenum tricarbonyl anion darkened slightly during the reaction. The reaction mixture was stirred overnight after which the solvent was removed in vacuo. The resulting orange residue was extracted with benzene and filtered. Slow evaporation of the solvent from the filtrate yielded yellow crystals of the desired product from concentrated solution in ~50% yield. Pertinent physical data for this complex are included in Table IV.

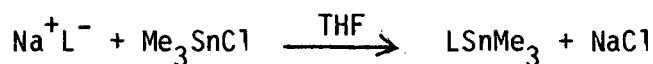
#### 4.2.6 Preparation of $[\text{MeGapz}_3]\text{Mo}(\text{CO})_3\text{SnPh}_3$



To a stirred THF solution of the  $\text{Na}^+\text{MeGapz}_3\text{Mo}(\text{CO})_3^-$  (0.353 mmol) salt was added an equimolar amount of  $\text{Ph}_3\text{SnCl}$  (0.136 g, 0.353 mmol) dissolved

in the same solvent. The resulting cloudy reaction mixture was stirred for 2 days after which the solvent was removed in vacuo. The dark yellow residue remaining was extracted with  $\text{CH}_2\text{Cl}_2$  and filtered. An equal amount of hexane was added to the filtrate and the mixed solvents were allowed to evaporate slowly. A chocolate-brown sticky solid with some visible tinge of yellow was left behind. This mixture was washed with  $\text{CH}_2\text{Cl}_2$  and the liquid decanted off slowly to leave behind bright-yellow air-stable crystals of the desired product  $[\text{MeGapz}_3]\text{Mo}(\text{CO})_3\text{SnPh}_3$  in approximately 40% yield. Pertinent physical data for this complex are presented in Table IV.

#### 4.2.7 Preparation of $\text{LSnMe}_3$ ( $\text{L} = [\text{MeGapz}_3]$ or $[\text{MeGa}(3,5\text{-Me}_2\text{pz})_3]$ )



$\text{Na}^+\text{MeGapz}_3^-$  (0.88 mmol) was reacted with  $\text{Me}_3\text{SnCl}$  (0.18 g, 0.90 mmol) in THF. The resulting cloudy solution was stirred overnight after which the solvent was removed under vacuum. The residue was then extracted with benzene and filtered. Slow evaporation of the benzene solvent containing the extracts afforded colorless, air-sensitive crystals of the desired  $[\text{MeGapz}_3]\text{SnMe}_3$  compound in ~50% yield.

The compound  $[\text{MeGa}(3,5\text{-Me}_2\text{pz})_3]\text{SnMe}_3$  was prepared in similar yield by an identical procedure starting with the  $[\text{MeGa}(3,5\text{-Me}_2\text{pz})_3]^-$  ligand. Solutions of the above complexes are unstable especially in chlorinated solvents ( $\text{CH}_2\text{Cl}_2$ ,  $\text{CHCl}_3$ ) and also in acetone.

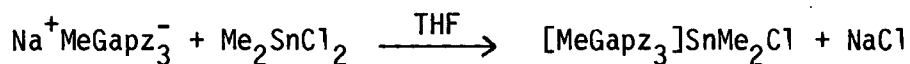
Anal. Calcd. For  $[\text{MeGapz}_3]\text{SnMe}_3$ : C, 34.71; H, 4.67. Found: C,

34.93; H, 4.19.  $^1\text{H}$  NMR ( $\text{C}_6\text{D}_6$ , 270 MHz):  $\tau_{\text{C}_6\text{H}_6} = 2.84$  ppm, 10.45s (Ga-Me); 9.81s (Sn-Me<sub>3</sub>); 4.00t (pz-H<sup>4</sup>); 3.29d (pz-H<sup>5</sup>); pz-H<sup>3</sup> obscured by solvent peak. ( $J_{\text{HCCH}} \approx 2$  Hz for pz protons.) ( $J_{119\text{Sn-Me}}$ ,  $J_{117\text{Sn-Me}} \approx 50$  Hz.)

Anal. Calcd. For  $[\text{MeGa}(3,5\text{-Me}_2\text{pz})_3]\text{SnMe}_3 \cdot 0.5 \text{C}_6\text{H}_6$ : C, 46.12; H, 6.29. Found: C, 46.34; H, 6.35.  $^1\text{H}$  NMR ( $\text{C}_6\text{D}_6$ , 80 MHz):  $\tau_{\text{C}_6\text{H}_6} = 2.84$  ppm, 10.41s (Ga-Me); 9.83s (Sn-Me<sub>3</sub>); 7.93s (pz-Me<sup>3</sup>); 7.71s (pz-Me<sup>5</sup>); 4.38s (pz-H<sup>4</sup>). ( $J_{119\text{Sn-Me}}$ ,  $J_{117\text{Sn-Me}} \approx 50$  Hz.)

Satisfactory analysis was obtained for C and H in both complexes but the N analyses were inconsistent each time the compounds were analyzed.

#### 4.2.8 Preparation of $[\text{MeGapz}_3]\text{SnMe}_2\text{Cl}$



To  $\text{Me}_2\text{SnCl}_2$  (0.193 g, 0.880 mmol) dissolved in THF, was added a 50 ml aliquot of the  $\text{Na}^+\text{MeGapz}_3^-$  (0.88 mmol) salt solution in the same solvent. The resulting reaction mixture turned cloudy as NaCl precipitated. To ensure complete precipitation, the reaction mixture was stirred overnight after which the solvent was removed under vacuum and the residue extracted with  $\text{CH}_2\text{Cl}_2$ . Slow evaporation of the  $\text{CH}_2\text{Cl}_2$  solvent containing the extracts, gave colorless flaky crystals of the desired  $[\text{MeGapz}_3]\text{SnMe}_2\text{Cl}$  compound in ~50% yield. This compound is unstable in air and slowly decomposes in solution.

Anal. Calcd. For  $[\text{MeGapz}_3]\text{SnMe}_2\text{Cl}\cdot 0.5 \text{CH}_2\text{Cl}_2$ : C, 29.27; H, 3.71; N, 16.39. Found: C, 29.51; H, 3.97; N, 15.87.  $^1\text{H}$  NMR ( $\text{C}_6\text{D}_6$ , 80 MHz):  $\tau\text{C}_6\text{H}_6 = 2.84$  ppm. 9.95s (Ga-Me); 9.15s (Sn-Me<sub>2</sub>); 3.98t (pz-H<sup>4</sup>); 3.08d (pz-H<sup>5</sup>); 2.43d (pz-H<sup>3</sup>). ( $J_{\text{HCCH}} \approx 2$  Hz for pz protons.) ( $J_{119\text{Sn-Me}}$ ,  $J_{117\text{Sn-Me}} \approx 50$  Hz.)

### 4.3 Results and Discussion

Continued interest in the chemistry of compounds featuring group 14-transition metal bonds stems partly from the hope of finding useful catalytic systems and also from interest in the structural, spectroscopic and bonding properties of this class of compounds [153,154]. The chemistry of the cyclopentadienyl compounds of group 14 elements has been studied quite extensively. In contrast, the use of poly(1-pyrazolyl)borate/gallate ligands in group 14 chemistry is virtually unexplored. Recently, the compound  $[\text{HBpz}_3]\text{SnMe}_3$  was reported by Nicholson as the first structurally characterized six-coordinate trialkyltin complex [37]. The present work was therefore designed to extend the chemistry of the  $\text{MeGapz}_3^-$  ligand to include group 14 elements and furthermore to explore the reactivity of the  $\text{MeGapz}_3\text{Mo}(\text{CO})_3^-$  anion toward a variety of group 14 element halide species with the hope of isolating complexes featuring direct transition metal-group 14 element covalent bonds. The basis for this expectation is two-fold: firstly, the valence orbitals of group 14 elements are known to be energetically compatible with the  $d^2sp^3$ ,  $dsp^3$  and  $dsp^2$  orbitals of transition metals and hence stable  $\sigma$ -bonds are readily

formed between these elements and transition metal species [155]; and secondly the proposition that metals capable of forming  $\sigma$ -bonded organometallic compounds would also be capable of forming covalent bonds to other metals [156,157]. Thus, 1:1 reactions of  $\text{MeGapz}_3\text{Mo}(\text{CO})_3^-$  anion with a variety of group 14 element organo halide species have yielded yellow-orange crystalline products in which direct molybdenum-group 14 element covalent bonds are featured. The complexes are moderately air-stable solids, except for the Mo-Si and Mo-Ge derivatives which are unstable to air. Solutions of all the complexes deteriorate slowly with time. The presence of a direct single covalent bond between the molybdenum atom and the appropriate group 14 element (Si, Ge, or Sn) in question has been demonstrated unequivocally by the crystal structure determination of one of the complexes,  $[\text{MeGapz}_3]\text{Mo}(\text{CO})_3\text{SnPh}_3$ . This latter compound represents the first structurally characterized complex of the type  $\text{LM}(\text{CO})_3\text{M}'\text{R}_3$  (where  $\text{L} = (\eta\text{-C}_5\text{H}_5)$ ,  $[\text{HBpz}_3]$ , or  $[\text{MeGapz}_3]$ ;  $\text{M} = \text{Cr}, \text{Mo},$  or  $\text{W}$ ;  $\text{M}' = \text{Si}, \text{Ge},$  or  $\text{Sn}$ ;  $\text{R} = \text{Me}$  or  $\text{Ph}$ ), and also provides a rare example of a 3:3:1, or capped octahedral structure.

#### 4.3.1 $[\text{MeGapz}_3]\text{Mo}(\text{CO})_3\text{SiMe}_3$

The  $(\eta\text{-C}_5\text{H}_5)(\text{Mo}(\text{CO})_3\text{SiR}_3)$  ( $\text{R} = \text{alkyl}$  or  $\text{aryl}$ ) complexes have been reported as being obtainable via salt elimination reaction of the  $(\eta\text{-C}_5\text{H}_5)\text{Mo}(\text{CO})_3^-$  anion with the alkyl or aryl silyl halide only in non-basic solvents such as cyclohexane [154]. An earlier attempt at obtaining these Mo-silyl derivatives by the same salt elimination route in basic solvents such as THF, proved unsuccessful [157]. However, these derivatives were obtained via an amine elimination reaction between

$(\eta\text{-C}_5\text{H}_5)\text{Mo}(\text{CO})_3\text{H}$  and  $\text{Me}_3\text{Si-NMe}_2$  in THF under CO pressure [158], and also from the reaction of  $\text{K}^+(\eta\text{-C}_5\text{H}_5)\text{Mo}(\text{CO})_3^-$  and  $\text{H}_3\text{SiBr}$  in the absence of solvent [159]. The latter report attributed the unsuccessful metathetical reaction of  $(\eta\text{-C}_5\text{H}_5)\text{Mo}(\text{CO})_3^-$  anion and  $\text{R}_3\text{SiCl}$  in THF to competition between the nucleophilic halide ion and the molybdenum tricarbonyl anion in this solvent. Judicious selection of solvents has been emphasized in the preparation of molybdenum-silicon compounds since polar solvents have the tendency to cleave the Mo-Si bond in the complexes [160,161,162]. The reaction of the  $\text{MeGapz}_3\text{Mo}(\text{CO})_3^-$  anion with  $\text{Me}_3\text{SiCl}$  in THF has yielded the yellow, air-sensitive  $[\text{MeGapz}_3]\text{Mo}(\text{CO})_3\text{SiMe}_3$  complex. Analytical, ir and  $^1\text{H}$  nmr data for this compound are collected in Table IV, p. 114.

The ir spectrum of the  $[\text{MeGapz}_3]\text{Mo}(\text{CO})_3\text{SiMe}_3$  in  $\text{CH}_2\text{Cl}_2$  solution (figure 31), shows the presence of three strong terminal  $\nu_{\text{CO}}$  bands, suggesting a  $\text{C}_s$  symmetry ( $2\text{A}' + \text{A}''$  modes) for the complex in solution. In this regard, the present complex resembles the halogen derivatives  $(\eta\text{-C}_5\text{H}_5)\text{Mo}(\text{CO})_3\text{X}$  ( $\text{X} = \text{Cl}, \text{Br}$  or  $\text{I}$ ) [55], and  $[\text{HBpz}_3]\text{Mo}(\text{CO})_3\text{X}$  ( $\text{X} = \text{Br}$  or  $\text{I}$ ) [60], but differs from the methyl and ethyl derivatives  $(\eta\text{-C}_5\text{H}_5)\text{Mo}(\text{CO})_3\text{R}$  ( $\text{R} = \text{Me}, \text{Et}$ ) [55], which show only two bands. The  $\nu_{\text{CO}}$  bands observed for the present  $[\text{MeGapz}_3]\text{Mo}(\text{CO})_3\text{SiMe}_3$  ( $2015, 1920, 1895 \text{ cm}^{-1}$ ,  $\text{CH}_2\text{Cl}_2$ ) complex are in good agreement with those reported for the analogous  $(\eta\text{-C}_5\text{H}_5)\text{Mo}(\text{CO})_3\text{SiMe}_3$  ( $1974, 1955, 1890 \text{ cm}^{-1}$ , Nujol) [158] compound. The terminally bonded CO groups suggested by the ir data of the complex are indicative of the presence of a direct single covalent bond between the Mo and Si atoms in the present  $[\text{MeGapz}_3]\text{Mo}(\text{CO})_3\text{SiMe}_3$  compound.

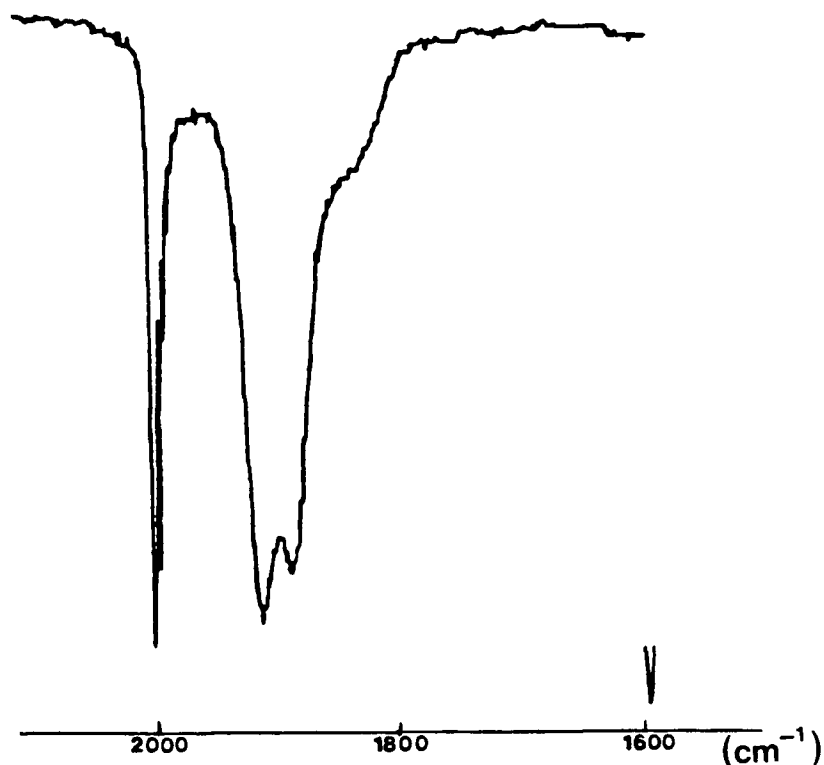


Figure 31. The  $\nu_{\text{CO}}$  region of the ir spectrum of  $[\text{MeGapz}_3]\text{Mo}(\text{CO})_3\text{SiMe}_3$  in  $\text{CH}_2\text{Cl}_2$  solution.

The  $^1\text{H}$  nmr spectrum of the present Mo-Si complex indicated equivalent pyrazolyl groups and hence is suggestive of a 3:3:1 symmetrical structure for the complex in solution, contrary to the  $\text{C}_5$  symmetry indicated by the ir results. There are two possible explanations for the  $^1\text{H}$  nmr results: firstly, a symmetrical 3:3:1 arrangement in solution would give equivalent environments for the pz groups. Secondly, a 3:4 structure in which there is rapid rotation of the 'MeGapz<sub>3</sub>' grouping about the Ga...Mo axis would also be consistent with the observed equivalent environments for the pz groups in solution. The latter possibility is further supported by the ir results discussed above.

Table IV. Physical Data for  $[\text{MeGapz}_3]\text{Mo}(\text{CO})_3\text{M}'\text{Y}$  ( $\text{M}' = \text{Si}, \text{Ge}, \text{Sn}$ ).

M'	Y	ANALYSIS CALCD/FOUND			$\nu_{\text{CO}} (\text{cm}^{-1})$ $\text{CH}_2\text{Cl}_2$ (NuJo1)	$^1\text{H}$ nmr						
		C	H	N		GaMe	M'Me	pz-H <sup>4</sup>	pz-H <sup>5</sup>	pz-H <sup>3</sup>	Ph <sub>3</sub>	
Si	$\text{Me}_3 \cdot 0.17 \text{C}_6\text{H}_6$	36.97 37.15	3.99 4.00	15.22 14.80	2015,1920,1895	<sup>b</sup> 9.95	10.08s	4.15t	3.05d	2.14d		
Ge	$\text{Me}_3 \cdot 1.0 \text{C}_6\text{H}_6$	39.92 39.78	4.08 3.84		2015,1920,1892	<sup>b</sup> 9.88s	9.43s	4.19t	3.08d	2.14d		
Ge	$\text{Ph}_3 \cdot 2.0 \text{C}_6\text{H}_6$	55.76 55.07	4.22 4.28	9.08 9.63	2015,1922,1898	<sup>b</sup> 10.10s		4.15t	3.04d	2.13d	2.38m 2.93m	
Sn	$\text{Me}_3$	30.51 31.13	3.34 3.45	13.35 13.65	2020,1970,1870	<sup>a</sup> 9.86s	9.01s	4.09t	2.91d	2.36d		
Sn	$\text{Me}_2\text{Cl}$	27.70	2.77	12.93	2018,1912,1890	<sup>A</sup> 9.93s	8.73s	4.12t	2.95d	2.40d		
		27.72	2.74	13.00	(1989,1905,1880)	<sup>J</sup> <sub>119</sub> Sn-Me = 52 Hz, <sup>J</sup> <sub>117</sub> Sn-Me = 50 Hz	B10.00s	8.96s 9.11s	4.19t	3.07d	2.17d	
Sn	$\text{Ph}_3$	45.62 44.98	3.31 3.32	10.50 10.42	(1990,1900,1875)	<sup>b</sup> 9.98s		4.14t	2.73d	2.12d	1.86d 2.65m 2.93m	

a In  $d_8$ -toluene ( $\tau_{\text{Me}} = 7.91$  ppm)

b In  $\text{C}_6\text{D}_6$  solution ( $\tau_{\text{C}_6\text{H}_6} = 2.84$  ppm)

A 3:3:1 structure. B 3:4 structure (Fig. 36)

$J_{\text{HCCH}} = 2.0$  Hz for pz protons.

s = singlet, d = doublet, t = triplet, m = multiplet

#### 4.3.2 $[\text{MeGapz}_3]\text{Mo}(\text{CO})_3\text{GeR}_3$ (R = Me, Ph)

The reaction of the anion  $[\text{MeGapz}_3\text{Mo}(\text{CO})_3]^-$  with  $\text{R}_3\text{GeCl}$  (R = Me, Ph) halide species afforded the  $[\text{MeGapz}_3]\text{Mo}(\text{CO})_3\text{GeR}_3$  complexes as yellow-orange, air-sensitive solids. Analytical and spectroscopic data for the complexes are given in Table IV, p. 114. The solution ir spectra of the complexes displayed three strong  $\nu_{\text{CO}}$  bands suggestive of  $\text{C}_s$  symmetry ( $2\text{A}' + \text{A}''$ ) for the complexes in solution. The  $\nu_{\text{CO}}$  bands observed for the present  $[\text{MeGapz}_3]\text{Mo}(\text{CO})_3\text{GeMe}_3$  (2015, 1920, 1892  $\text{cm}^{-1}$ ,  $\text{CH}_2\text{Cl}_2$ ) and  $[\text{MeGapz}_3]\text{Mo}(\text{CO})_3\text{GePh}_3$  (2015, 1922, 1898  $\text{cm}^{-1}$ ,  $\text{CH}_2\text{Cl}_2$ ) complexes are in good agreement with those reported for the analogous  $(\eta\text{-C}_5\text{H}_5)\text{Mo}(\text{CO})_3\text{GeMe}_3$  (1999, 1929, 1905  $\text{cm}^{-1}$ ,  $\text{C}_6\text{H}_6$ ) [163] and  $(\eta\text{-C}_5\text{H}_5)\text{Mo}(\text{CO})_3\text{GePh}_3$  (2008, 1925, 1918  $\text{cm}^{-1}$ ,  $\text{CCl}_4$ ) [157] compounds, respectively. For all of the above cyclopentadienyl Mo-Ge derivatives, the authors concluded that there is a direct covalent bond between the Mo and Ge centers with no interactions of the CO ligands with the Ge atom. It appears, likely that a similar bonding arrangement is operative in the present  $[\text{MeGapz}_3]\text{Mo}(\text{CO})_3\text{GeR}_3$  complexes based on the ir data obtained for the compounds.

The room temperature  $^1\text{H}$  nmr spectrum of the  $[\text{MeGapz}_3]\text{Mo}(\text{CO})_3\text{GePh}_3$  in  $\text{C}_6\text{D}_6$  solution is shown in figure 32. Again, one set of signals was displayed for the pyrazolyl protons suggesting equivalent environments for the pz rings. Evidently, similar rotation of the 'MeGapz<sub>3</sub>' moiety about the Ga...Mo axis (see Section 4.3.1) might afford a rationale for the observed  $^1\text{H}$  nmr results. A similar  $^1\text{H}$  nmr spectrum was obtained for the  $[\text{MeGapz}_3]\text{Mo}(\text{CO})_3\text{GeMe}_3$  complex. These compounds  $[\text{MeGapz}_3]\text{Mo}(\text{CO})_3\text{GeR}_3$  (R = Me or Ph) persist in solution for only a few days. For example, the room

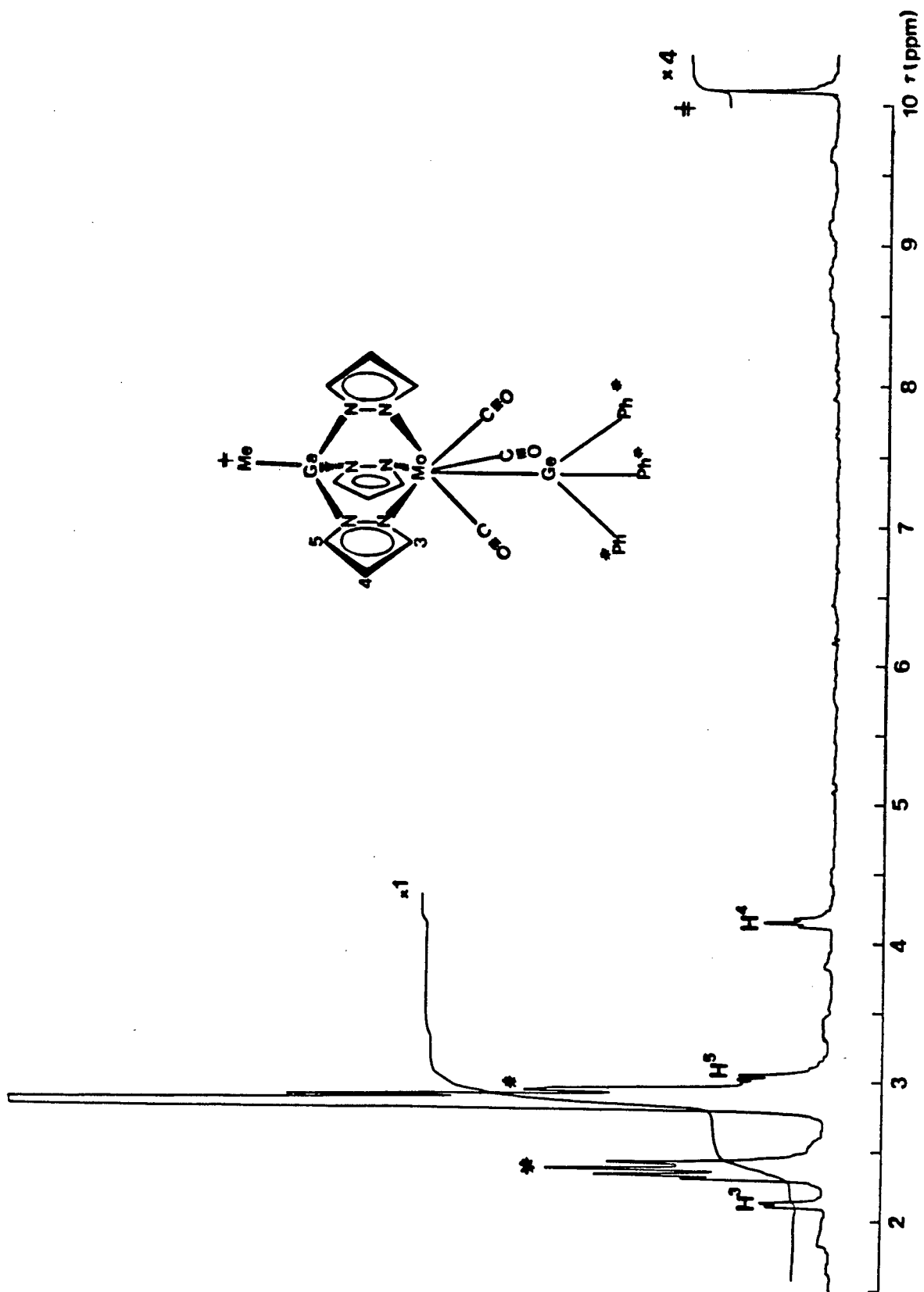


Figure 32. 270 MHz  $^1\text{H}$  nmr spectrum of  $[\text{MeGa}(\text{pz})_3]\text{Mo}(\text{CO})_3\text{GePh}_3$  in  $\text{C}_6\text{D}_6$  solution.

temperature  $^1\text{H}$  nmr spectrum of the same  $[\text{MeGapz}_3]\text{Mo}(\text{CO})_3\text{GePh}_3$  compound in  $\text{C}_6\text{D}_6$  solution, in a flame sealed nmr tube, showed new signals different from those displayed in the initial spectrum after 5 days. These new signals are presumably due to peaks arising from the decomposition of the sample in solution. Attempts to obtain crystals suitable for X-ray crystal structure determinations were unsuccessful.

#### 4.3.3. $[\text{MeGapz}_3]\text{Mo}(\text{CO})_3\text{SnR}_3$ (R = Me, Ph)

The reaction of the  $\text{MeGapz}_3\text{Mo}(\text{CO})_3^-$  anion with  $\text{Me}_3\text{SnCl}$  and  $\text{Ph}_3\text{SnCl}$  yielded yellow-orange crystalline products of the Mo-Sn bonded species  $[\text{MeGapz}_3]\text{Mo}(\text{CO})_3\text{SnR}_3$ . The complexes are moderately air-stable in the solid state but solutions deteriorate on exposure to air. Analytical and spectroscopic data for these complexes are presented in Table IV p. 114. It is interesting to compare the compounds with those reported by Patil and Graham in which the  $\text{MeGapz}_3^-$  ligand is replaced by the  $\text{Cp}^-$  group [157]. In both series of compounds only terminal  $\nu_{\text{CO}}$  bands are displayed in the ir spectra, indicative of direct Mo-Sn interaction without accompanying bridging CO ligands. In the case of the cyclopentadienyl complexes, three strong terminal CO bands were observed in each case whereas the two compounds reported here show different patterns. Thus, the 'SnPh<sub>3</sub>' complex gives one weak and two strong  $\nu_{\text{CO}}$  vibrations, whereas the 'SnMe<sub>3</sub>' complex displays one strong and two weak  $\nu_{\text{CO}}$  bands.

The  $^1\text{H}$  nmr data for the 'SnPh<sub>3</sub>' and 'SnMe<sub>3</sub>' complexes show all three pyrazolyl groupings to be equivalent in solution, displaying only one set of signals for the pyrazolyl rings protons, and are hence indicative of a symmetrical structure for the complexes. The room temperature  $^1\text{H}$  nmr

spectrum of the  $[\text{MeGapz}_3]\text{Mo}(\text{CO})_3\text{SnMe}_3$  complex in  $d_8$ -toluene solution is shown in figure 33.

The mass spectrum of the  $[\text{MeGapz}_3]\text{Mo}(\text{CO})_3\text{SnMe}_3$  compound displayed signals due to the  $\text{P-3CO}^+$  ion at  $m/e \sim 544$ , but signals due to the parent ion  $\text{P}^+$  were not observed. In contrast, the mass spectrum of the  $[\text{MeGapz}_3]\text{Mo}(\text{CO})_3\text{SnPh}_3$  complex displayed the parent ion signal,  $\text{P}^+$ , at  $m/e \sim 816$ , together with prominent signals due to the ions  $\text{P-CO}^+$ ,  $\text{P-2CO}^+$ ,  $\text{P-3CO}^+$ , and  $\text{P-3CO-Me}^+$ . Perhaps these variations reflect the greater thermal stability of the 'SnPh<sub>3</sub>' compound over the 'SnMe<sub>3</sub>' derivative under electron impact conditions.

The chemistry of M-M' bonded derivatives (where M' = Ge or Sn; M = Mo or W) has been studied quite extensively but, rather surprisingly, no X-ray structural data have been reported for complexes of the type  $(\eta\text{-C}_5\text{H}_5)\text{M}(\text{CO})_3\text{M}'\text{R}_3$  (where R = alkyl or aryl), the molecular arrangements proposed for these species being based primarily on ir and  $^1\text{H}$  nmr data [154]. The X-ray crystal structure of the complex  $[\text{MeGapz}_3]\text{Mo}(\text{CO})_3\text{SnPh}_3$  presented here represents what we believe to be the first reported structure of this type, in which the  $[\text{MeGapz}_3]$  moiety replaces the  $\eta\text{-C}_5\text{H}_5$  ligand in the general formulation given above. The X-ray structure analysis confirms the 3:3:1 arrangement predicted on the basis of the  $^1\text{H}$  nmr data. The molecule, which has approximate  $\text{C}_3$  symmetry, is shown in figure 34.

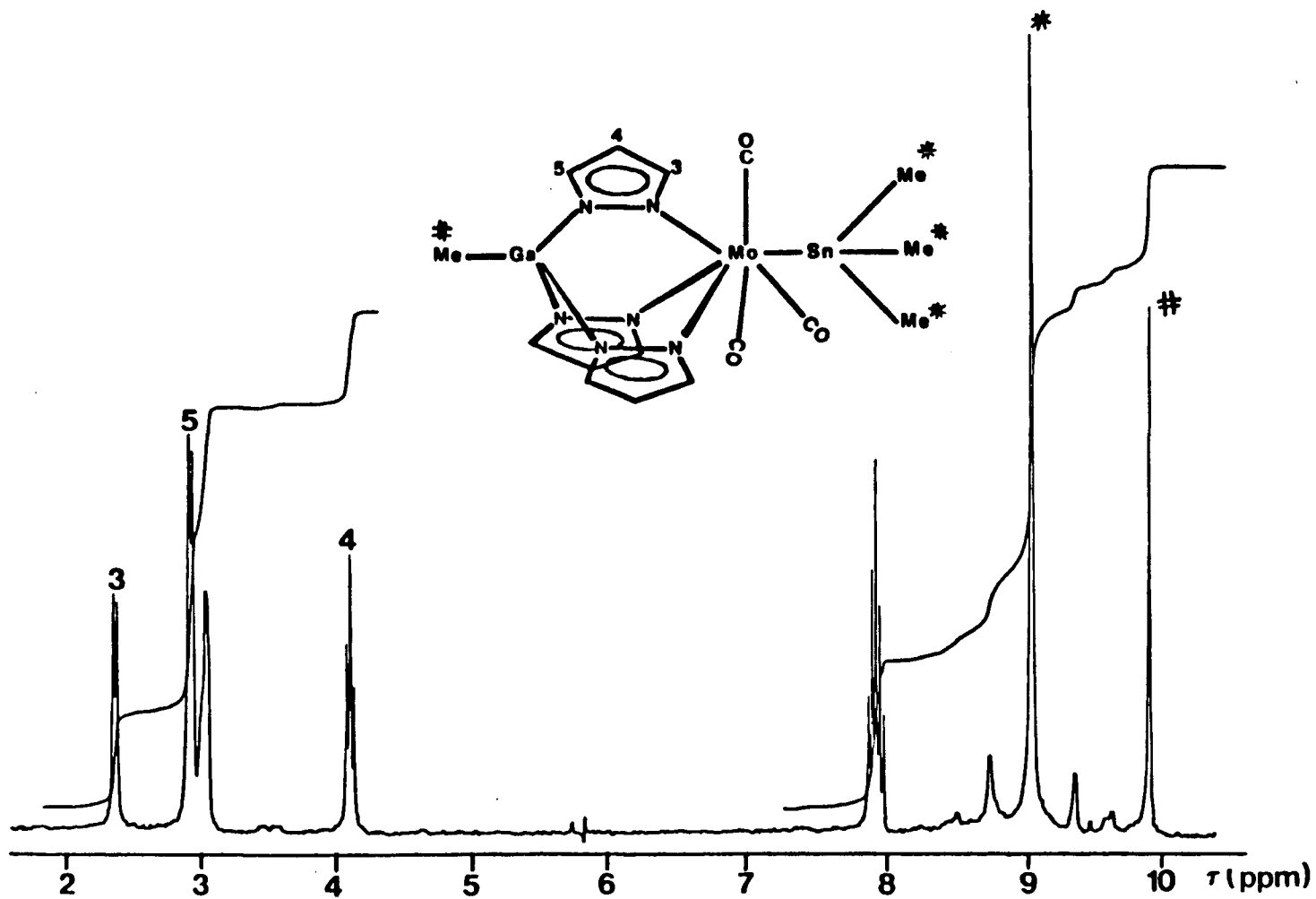


Figure 33. Room temperature 80 MHz  $^1\text{H}$  nmr spectrum of  $[\text{MeGapz}_3]\text{Mo}(\text{CO})_3\text{SnMe}_3$  in  $d_8$ -toluene.

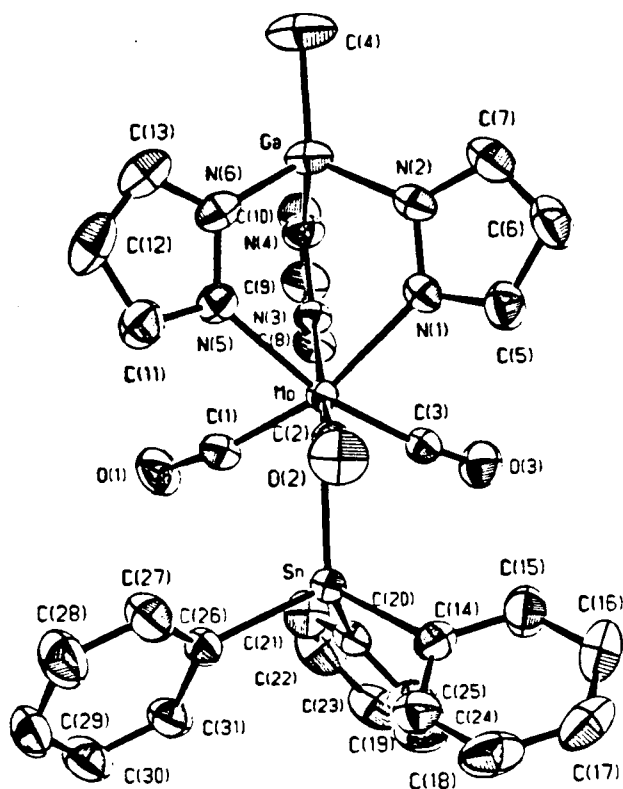


Figure 34. Molecular structure of  $[\text{MeGapz}_3]\text{Mo}(\text{CO})_3\text{SnPh}_3$ .

The structure is similar to that recently reported for the compound  $[\text{MeGapz}_3]\text{Mo}(\text{CO})_3\text{Cu}(\text{PPh}_3)$  [124] (see also section 3.3.2 p. 86) but is different from the 3:4 or 'four-legged piano stool' structures of the related molecules  $(n\text{-C}_5\text{H}_5)\text{Mo}(\text{CO})_3\text{Sn}(\text{Cl})[(n\text{-C}_5\text{H}_5)\text{Fe}(\text{CO})_2]_2$  [164],  $[\text{HBpz}_3]\text{Mo}(\text{CO})_3\text{Br}$  [60], and  $(n\text{-C}_5\text{H}_5)\text{Mo}(\text{CO})_3\text{Et}$  [93]. The multi-metal species with the  $n\text{-C}_5\text{H}_5$  replacing  $\text{MeGapz}_3$  on Mo, and the  $[(n\text{-C}_5\text{H}_5)\text{Fe}(\text{CO})_2]$  groupings replacing the Me groups on Sn, may well be incapable of adopting a 3:3:1 structure due to the bulky Fe-containing substituents.

The structure of the  $[\text{MeGapz}_3]\text{Mo}(\text{CO})_3\text{SnPh}_3$  complex clearly shows the presence of three terminal carbonyl groups with bond angles of  $169.7(3)$ ,  $172.1(3)$ , and  $172.7(3)^\circ$  for the Mo-C-O units, the slight deviations from

linearity being directed away from the Sn center and probably caused by the proximity of the phenyl groups on the Sn atom. The C-O bond distances of 1.154(4), 1.139(3), and 1.141(3)Å are also in the range expected for terminal carbonyl groups and the Mo-C distances of 1.967(3), 2.000(3), and 1.994(3)Å are consistent with a terminal CO bonding arrangement. The above parameters show that one of the carbonyl groups differs significantly from the other two. This represents the most significant departure from overall  $C_3$  molecular symmetry and can be ascribed to a weak C-H...O hydrogen bond [C(10)-H(10)...O(1) ( $\underline{x}$ ,  $1/2-\underline{y}$ ,  $\underline{z}-1/2$ ), H...O = 2.39, C...O = 3.326(4)Å, C-H...O = 162°, C-O...H = 156°] linking molecules in infinite chains extending along the  $\underline{b}$  axis. All other intermolecular distances are greater than the sums of van der Waals radii.

The Ga...Mo-Sn unit with an angle of 178.49(1)° is essentially linear and as expected the planar pyrazolyl groups, whilst eclipsing the distant phenyl groups on Sn, are staggered with respect to the three CO ligands on the Mo center. The Mo-Sn distance of 2.8579(3)Å observed for the present complex is considerably shorter than the expected distance of 3.00Å based on the sum of the covalent radii (1.39 + 1.61Å) for the two atoms [93,137,165,166]. The distance is, however, comparable to the first Mo-Sn distance reported (2.891(5)Å) for the complex  $[(\eta-C_5H_5)Mo(CO)_3]Sn(Cl)-[(\eta-C_5H_5)Fe(CO)_2]_2$  [164]. As in the structure described herein, the Sn atom in this multi-metal complex is in a pseudotetrahedral environment. Cameron and Prout [167] have reported a Mo-Sn distance of 2.691(4)Å for the complex  $(\eta-C_5H_5)_2Mo(SnBr_3)Br$  in which the Sn atom is in a distorted trigonal bipyramidal environment with a fourth, long, Sn...Br interaction of 3.411Å. A similar environment for the Sn atom has been reported for

the complex  $(\text{bipy})(\text{Cl})\text{Mo}(\text{CO})_3(\text{SnMeCl}_2)$ , in which the Mo-Sn distance of 2.753(3)Å was interpreted as indicative of some multiple bond character [168]. The same authors reported the structure of the tungsten-tin complex  $(\text{MeS}(\text{CH}_2)_2\text{SMe})(\text{Cl})\text{W}(\text{CO})_3(\text{SnMeCl}_2)$  in which the W-Sn distance of 2.759(3) was argued to reflect the similarity of the W and Mo covalent radii [169]. In both of these structures there is a bridging Cl ligand between the metal centers, with a long Sn-Cl distance.

#### 4.3.4 $[\text{MeGapz}_3]\text{Mo}(\text{CO})_3\text{SnMe}_2\text{Cl}$

The 1:1 reaction of  $\text{MeGapz}_3\text{Mo}(\text{CO})_3^-$  anion and  $\text{Me}_2\text{SnCl}_2$  resulted in the yellow crystalline product  $[\text{MeGapz}_3]\text{Mo}(\text{CO})_3\text{SnMe}_2\text{Cl}$ . This complex is air-stable in the solid state but solutions deteriorate slowly with time. The solution ir spectrum of this compound displays one weak and two strong  $\nu_{\text{CO}}$  vibrations (2018, 1912, 1890  $\text{cm}^{-1}$ ,  $\text{CH}_2\text{Cl}_2$ ). These  $\nu_{\text{CO}}$  values compare quite well with those reported for the analogous  $(\eta\text{-C}_5\text{H}_5)\text{Mo}(\text{CO})_3\text{SnMe}_2\text{Cl}$  compound by Patil and Graham [157]. The presence of only terminal  $\nu_{\text{CO}}$  bands in the ir spectrum of the present  $[\text{MeGapz}_3]\text{Mo}(\text{CO})_3\text{SnMe}_2\text{Cl}$  compound is indicative of direct Mo-Sn interaction without accompanying bridging CO ligands. However, the presence of three  $\nu_{\text{CO}}$  bands in the ir spectrum of the present complex is suggestive of a  $C_s$  symmetry for the compound in solution.

The room temperature  $^1\text{H}$  nmr spectrum of  $[\text{MeGapz}_3]\text{Mo}(\text{CO})_3\text{SnMe}_2\text{Cl}$  is interesting since it changes with time and solvent. (Figure 35 shows the change, with time, in the spectrum of the complex in  $d_8$ -toluene. A similar effect was observed using  $C_6D_6$  or  $\text{CDCl}_3$  as solvents). Thus,

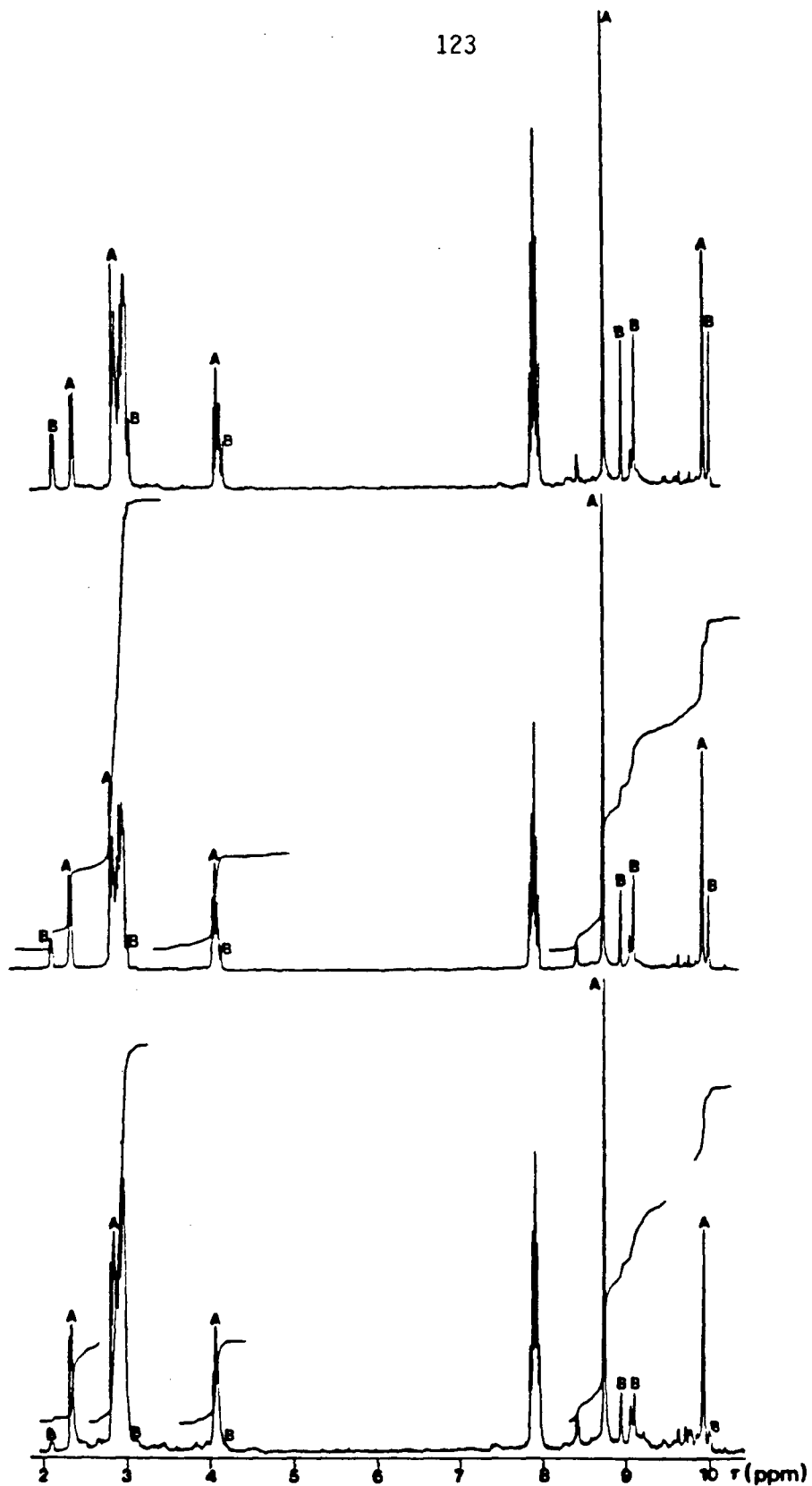


Figure 35. Room temperature 80 MHz  $^1\text{H}$  nmr spectra of  $[\text{MeGapz}_3]\text{Mo}(\text{CO})_3\text{SnMe}_2\text{Cl}$ , showing the change with time: initial spectrum (top), after 1 day (middle), and after 5 days (bottom). (A) 3:3:1 structure, (B) 3:4 structure.

initially the spectrum shows two 'sets' of signals. The most intense set of signals is consistent with a symmetrical 3:3:1 or capped-octahedral structure as shown in figure 36A, similar to that established for the 'SnPh<sub>3</sub>' derivative (see section 4.3.3, p. 117). In this arrangement free rotation about the Mo-Sn bond in solution would give the observed pattern of equivalent pyrazolyl signals and a singlet for the 'SnMe<sub>2</sub>' grouping. In the second 'set' of signals the two Sn-Me groups are non-equivalent and yet the pyrazolyl groups seemingly remain equivalent. This pattern is difficult to rationalize since even a static 3:4, or 'four-legged piano stool' arrangement (figure 36B) would be expected to give inequivalent pyrazolyl groups, as well as possibly distinguishing between the two Me groups on the Sn atom. A rotation of the MeGapz<sub>3</sub> moiety about the Ga...Mo axis might afford a rationale for the observed equivalence of the pyrazolyl groups in this second arrangement. A similar rotation of the HBpz<sub>3</sub> grouping in the complexes [HBpz<sub>3</sub>]Mo(CO)<sub>2</sub>(η<sup>3</sup>-C<sub>3</sub>H<sub>5</sub>) [170] and Cp<sub>2</sub>MoH<sub>2</sub>→Cu[HBpz<sub>3</sub>]<sub>2</sub> [171] has been invoked to explain the equivalence of the pyrazolyl groups in the room temperature <sup>1</sup>H nmr spectra of these compounds. In any event, with time, the species responsible for the weaker set of signals gradually disappears and there remains only one set of signals, explicable in terms of a 3:3:1 structure.

The proposed intramolecular rearrangement process is further supported by the temperature dependent 300 MHz <sup>1</sup>H nmr spectrum of the [MeGapz<sub>3</sub>]Mo(CO)<sub>3</sub>SnMe<sub>2</sub>Cl compound in d<sub>8</sub>-toluene shown in figure 37. In this spectrum, as the solution is warmed up to ~80°C, the set of signals consistent with the 3:3:1 structure predominates since the rate of the

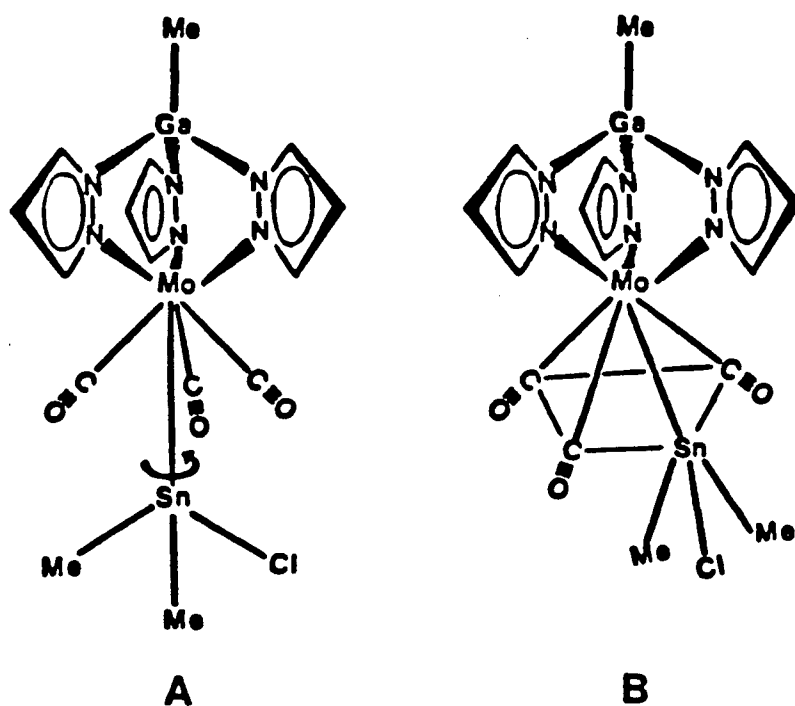


Figure 36. Possible molecular arrangements for the  $[\text{MeGa}\zeta_3]\text{Mo}(\text{CO})_3\text{SnMe}_2\text{Cl}$  complex in solution: (A) 3:3:1 structure, (B) 3:4 structure.

rearrangement process would be more rapid at high temperatures. As the solution is cooled down, the set of signals explicable in terms of the 3:3:1 structure decrease in intensity with concomitant increase in intensity for the signals attributable to the 3:4 structure, until at  $\sim -80^\circ\text{C}$ , the system shows only one set of signals consistent with the 3:4

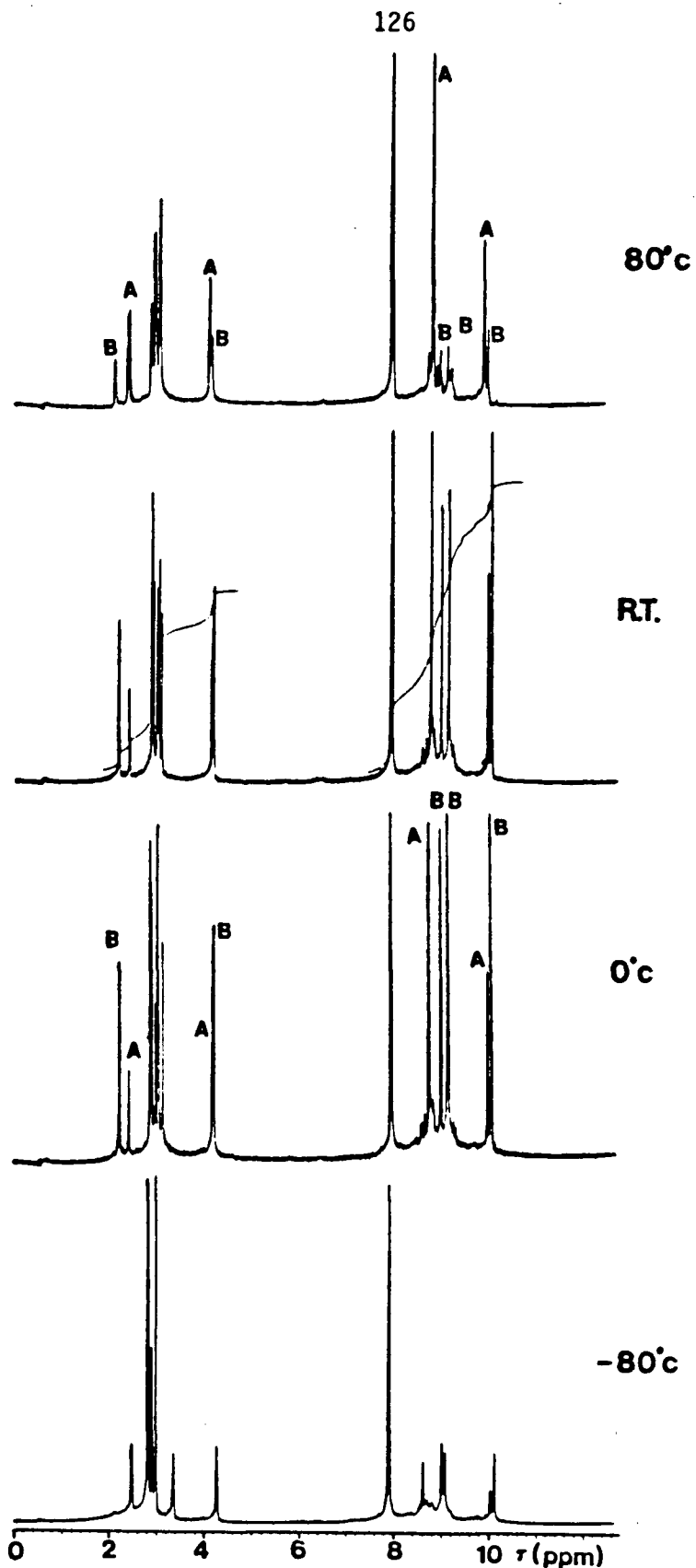


Figure 37. Temperature dependent 300 MHz  $^1\text{H}$  nmr spectrum of  $[\text{MeGapz}_3]\text{Mo}(\text{CO})_3\text{SnMe}_2\text{Cl}$  in  $d_8$ -toluene solution.

structure. The above behaviour is not surprising since the 3:4 or 'four-legged piano stool' structure has been shown to be the most stable point (ground state) in the potential energy surface for  $(\eta\text{-C}_5\text{H}_5)\text{ML}_4$  complexes [141]. Interestingly, Patil and Graham [157] report a singlet for the 'SnMe<sub>2</sub>' protons in their  $\text{CpMo}(\text{CO})_3\text{SnMe}_2\text{Cl}$  complex for which they speculate a 3:4 or piano stool structure, similar to that demonstrated for the complexes  $(\eta\text{-C}_5\text{H}_5)\text{Mo}(\text{CO})_3\text{Et}$  [93], and  $(\eta\text{-C}_5\text{H}_5)\text{Mo}(\text{CO})_3\text{Mn}(\text{CO})_5$  [152], respectively.

The mass spectrum of the present  $[\text{MeGaPz}_3]\text{Mo}(\text{CO})_3\text{SnMe}_2\text{Cl}$  complex displayed a strong parent ion,  $\text{P}^+$ , signal at  $m/e \sim 650$ . In addition signals due to the  $\text{P-CO}^+$ ,  $\text{P-2CO}^+$ ,  $\text{P-3CO-Me}^+$  and  $\text{P-3CO}^+$  ions were also observed, the latter being the strongest in the spectrum. The relative intensities of the lines in these signals agreed well with a computer-generated profile, taking into account the relative abundances of the naturally occurring isotopes of Mo, Ga, Sn, and Cl (see figure 38).

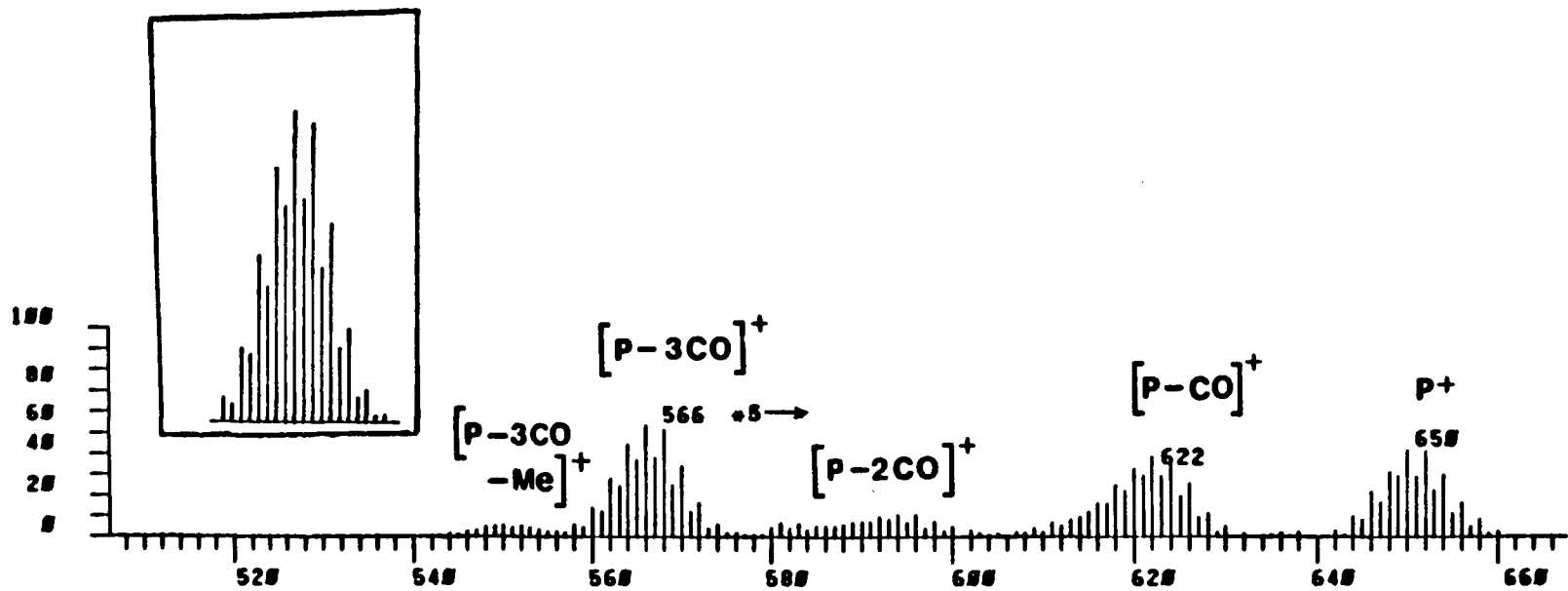
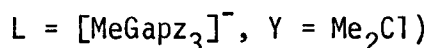
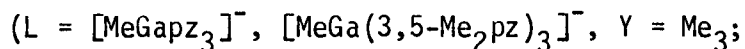


Figure 38. Partial mass spectrum of  $[MeGapz_3]Mo(CO)_3SnMe_2Cl$ . Inset: computer generated profile of signal for ions containing Ga, Mo, Sn, and Cl atoms.

#### 4.3.5 LSnY



The complexes LSnY were prepared by the reaction of the appropriate ligand with either  $\text{Me}_3\text{SnCl}$  or  $\text{Me}_2\text{SnCl}_2$  starting materials, respectively. The compounds were isolated as colorless, flaky, air-sensitive crystals. Solutions of the complexes were unstable even under inert conditions. The  $\text{LSnMe}_3$  ( $L = [\text{MeGapz}_3], [\text{MeGa}(3,5\text{-Me}_2\text{pz})_3]$ ) complexes consistently gave satisfactory analyses for C, and H; however, the N content was different each time. The reason for this discrepancy is not clear.

The  $^1\text{H}$  nmr spectra of the complexes showed all three of the pyrazolyl groups in each compound to be equivalent, suggesting tridentate coordination of the ligand to the Sn atom. The seemingly equivalent pyrazolyl groups indicated by the  $^1\text{H}$  nmr of the compound  $[\text{MeGapz}_3]\text{SnMe}_2\text{Cl}$  may be rationalized by a rapid rotation of the 'MeGapz<sub>3</sub>' moiety about the Ga...Sn axis in solution. However, attempts to isolate suitable crystals for X-ray structural determination proved unsuccessful. An X-ray structure determination of the analogous compound  $[\text{HBpz}_3]\text{SnMe}_3$  was reported recently by Nicholson [37], and confirms the presence of a six-coordinate tin bonded to three methyl groups and to three pyrazolyl groups.

#### 4.4 Summary

The reaction of the molybdenum tricarbonyl anion,  $[\text{MeGapz}_3]\text{Mo}(\text{CO})_3^-$  with a variety of group 14 (Si, Ge, Sn) organohalides has yielded a series of complexes in which direct Mo-M' (M' = Si, Ge, Sn) single covalent bonds are featured. The  $[\text{MeGapz}_3]\text{Mo}(\text{CO})_3\text{SnMe}_2\text{Cl}$  complex shows an interesting solution behaviour in which a transition from a 3:4, or piano stool structure, to a 3:3:1, or capped-octahedral arrangement, is thought to occur. The stereochemical non-rigidity of the above 'SnMe<sub>2</sub>Cl' derivative in solution was demonstrated by a variable temperature <sup>1</sup>H nmr experiment. The 3:3:1 structure has been demonstrated in the solid state for the  $[\text{MeGapz}_3]\text{Mo}(\text{CO})_3\text{SnPh}_3$  compound by means of a crystal structure determination.

The ligands  $[\text{MeGapz}_3]$  and  $[\text{MeGa}(3,5\text{-Me}_2\text{pz})_3]$  have been used in this study to form the elusive six-coordinate organotin complexes,  $\text{LSnMe}_3$  (L =  $[\text{MeGapz}_3]$  or  $[\text{MeGa}(3,5\text{-Me}_2\text{pz})_3]$ ) and  $[\text{MeGapz}_3]\text{SnMe}_2\text{Cl}$ .

## CHAPTER V

## TRANSITION METAL DERIVATIVES OF THE UNSYMMETRIC TRIDENTATE

PYRAZOLYL GALLATE LIGANDS  $[\text{Me}_2\text{Gapz}\cdot\text{O}(\text{C}_5\text{H}_3\text{N})\text{CH}_2\text{NMe}_2]^-$ AND  $[\text{Me}_2\text{Gapz}\cdot\text{O}(\text{C}_9\text{H}_6\text{N})]^-$ 5.1 Introduction

The first of a new class of unsymmetric tridentate chelating organogallate ligands was introduced sometime ago [41]. These ligand systems, containing a pyrazolyl group, together with a bifunctional donor moiety, both attached to a dimethylgallium unit, have been shown to coordinate facially in a variety of octahedral transition metal carbonyl compounds [172,173,174]. Meridional coordination of the above ligand systems to the metal center has been demonstrated for four-coordinate square-planar Rh(I) species [175,176], and the novel five-coordinate iron dinitrosyl complex  $[\text{Me}_2\text{Ga}(3,5\text{-Me}_2\text{pz})(\text{OCH}_2\text{CH}_2\text{NMe}_2)]\text{Fe}(\text{NO})_2$  [44]. Both the fac and mer isomers have been structurally characterized for the coordination compound  $[\text{Me}_2\text{Gapz}(\text{OCH}_2\text{CH}_2\text{NH}_2)]_2\text{Ni}$  [43]. Metal derivatives of multidentate ligand systems incorporating both the pyrazolyl and pyridyl functional groups have been the subject of recent publications [177,178]. It has been inferred that although pyrazole has stronger  $\sigma$ -donor properties than pyridine [177], the former has weaker  $\pi$ -acceptor capability [179]. The many novel aspects displayed by the compounds

incorporating this class of ligand prompted further investigation into the general area of unsymmetrical uninegative organogallate ligands to include an amino-pyridyl moiety as well as a fused quinolyyl 'aromatic' unit in the ligand system. This chapter describes the synthesis of the ligands  $L_a^-$ , and  $L_q^-$  derived from 2-(dimethylaminomethyl)-3-hydroxypyridine, and 8-hydroxyquinoline respectively, and details their reactivity toward a variety of transition metal halide species.

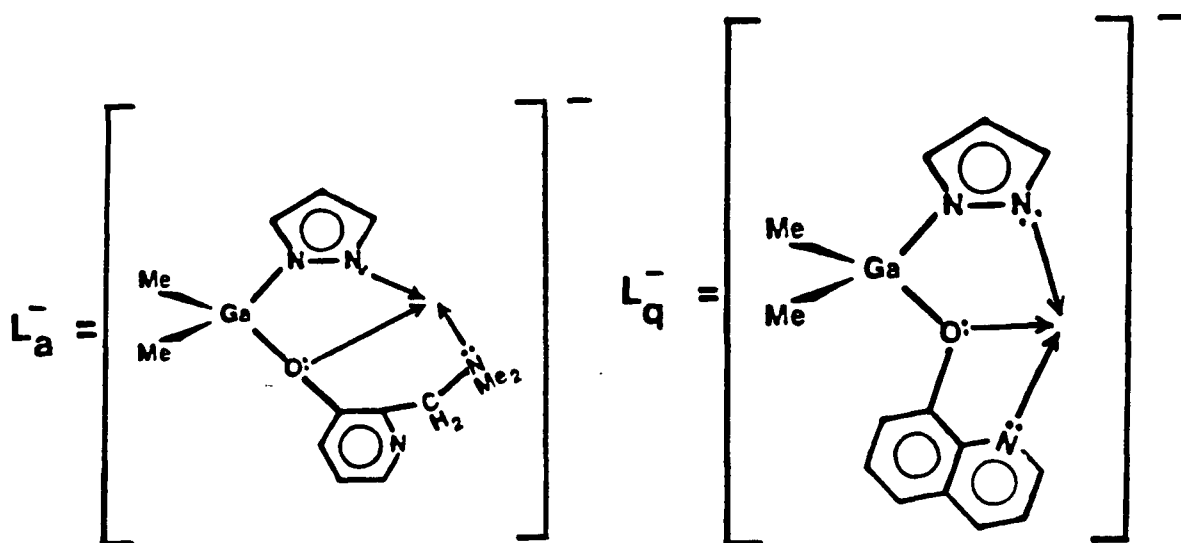


Figure 39. The unsymmetric organogallate ligands  $[Me_2Gapz \cdot O(C_5H_3N) - CH_2NMe_2]^-$  ( $L_a^-$ ), and  $[Me_2Gapz \cdot O(C_9H_6N)]^-$  ( $L_q^-$ ).

Thus, reactions of the new ligands  $L_a^-$ ,  $L_q^-$  with a variety of transition metal halide species yielded a diverse range of compounds which have been characterized by the usual physical methods. The reactivity of the

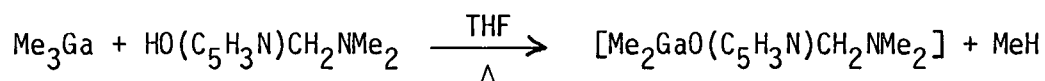
complexes  $L_aRh(CO)$ ,  $L_qRh(CO)$  toward methyl iodide and molecular iodine is also described and an X-ray crystal structural study of what is thought to be a methyl iodide oxidative addition product  $[Me_2Ga\mu z \cdot O(C_5H_3N)CH_2NMe_2]Rh(Me)(I)CO$  is in progress. The preparation, properties, crystal and molecular structures of the  $[Me_2Ga \cdot O(C_5H_3N)CH_2NMe_2]$ , and  $[Me_2Ga \cdot O(C_9H_6N)]_2$  coordination compounds are also presented. Parts of this work have been submitted for publication [180,181].

## 5.2 Experimental

### 5.2.1 Starting Materials

Sodium pyrazolide was prepared by reacting sodium hydride (Alfa) with pyrazole (K and K laboratories) in THF. Nickel nitrosyl iodide [128], manganese pentacarbonyl bromide [182], rhenium tetracarbonyl chloride dimer [183], and  $Mo(MeCN)_2(\eta^3-C_3H_5)(CO)_2Br$  [184] were prepared according to literature methods. Rhodium dicarbonyl chloride dimer, molybdenum hexacarbonyl (Strem Chemicals), iodine, 2-(dimethylaminomethyl)-3-hydroxypyridine (Aldrich), 8-hydroxyquinoline (Eastman Organic Chemicals) were used as supplied. Methyl iodide (Fisher Scientific) was dried by distillation from phosphorus pentoxide and stored over a few mercury droplets. Allyl bromide (Eastman Kodak Co.) was distilled before use.

### 5.2.2 Preparation of $[Me_2GaO(C_5H_3N)CH_2NMe_2]$

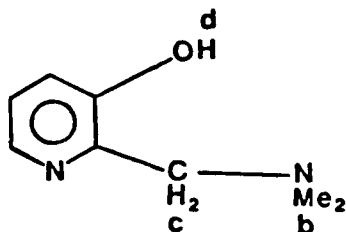


To a THF solution of 2-(dimethylaminomethyl)-3-hydroxypyridine (1.34 g, 8.8 mmol) was added trimethylgallium (1.01 g, 8.8 mmol) in the same solvent. The reaction mixture was refluxed under  $N_2$  until cessation of methane gas (~2 days). The solution was then cooled to room temperature and the solvent removed under vacuum. The resulting residue was extracted with benzene, and filtered. Slow evaporation of the benzene solvent containing the extracts afforded air- and moisture-sensitive pale yellow crystals of the desired product. Yield ~80%. Mp 62°C.

Anal. Calcd. for  $Me_2GaO(C_5H_3N)CH_2NMe_2$ : C, 47.85; H, 6.83; N, 11.16. Found: C, 48.05; H, 6.76; N, 10.96. The NMR data for this complex and the hydroxy starting material are compiled in Tables V and VI (see also figures 42 and 43; pp. 152 and 153), respectively.

Table V 400 MHz  $^1H$  NMR Data for  $HO(C_5H_3N)CH_2NMe_2$  in  $C_6D_6$  solution.

---

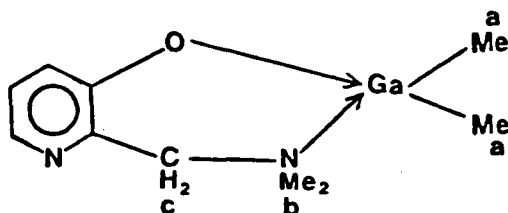


$\tau(\text{ppm})^*$	J(Hz)	$^\dagger$ Assignment
8.15(s)	-	H <sub>b</sub>
6.33(s)	-	H <sub>c</sub>
3.20(dd)	4.0(8.0)	
2.86(dd)	2.0(8.0)	
1.85(dd)	2.0(6.0)	
-1.45(s)	-	H <sub>d</sub>

\*  $\tau_{\text{C}_6\text{H}_6} = 2.84$  ppm; s = singlet; dd = doublet of doublets.

$^\dagger$  Ring protons are unassigned.

Table VI 400 MHz  $^1\text{H}$  NMR Data for  $\text{Me}_2\text{GaO}(\text{C}_5\text{H}_3\text{N})\text{CH}_2\text{NMe}_2$  in  $\text{C}_6\text{D}_6$  solution.

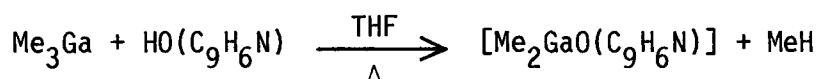


$\tau(\text{ppm})^*$	J(Hz)	$^\dagger$ Assignment
10.29(s)	-	H <sub>a</sub>
8.39(s)	-	H <sub>b</sub>
6.40(s)	-	H <sub>c</sub>
3.14(dd)	4.0(8.0)	
2.74(d)	8.0	
1.99(dd)	2.0(4.0)	

\*  $\tau_{\text{C}_6\text{H}_6} = 2.84$  ppm; s = singlet; d = doublet; dd = doublet of doublets

$^\dagger$  Ring protons are unassigned.

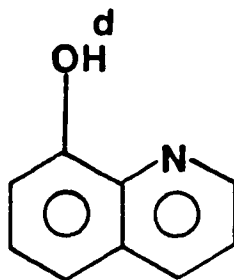
### 5.2.3 Preparation of $[\text{Me}_2\text{GaO}(\text{C}_9\text{H}_6\text{N})]_2$



The coordination compound  $[\text{Me}_2\text{GaO}(\text{C}_9\text{H}_6\text{N})]$  was prepared by the method described above (section 5.2.2), using 8-hydroxyquinoline as starting material. The air-sensitive lemon yellow product was isolated in ~85% yield. Mp 63°C.

Anal. Calcd. for  $[\text{Me}_2\text{GaO}(\text{C}_9\text{H}_6\text{N})]$ : C, 54.16; H, 4.92; N, 5.74.

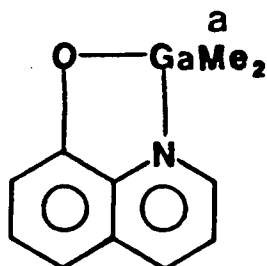
Found: C, 54.58; H, 4.61; N, 5.97. The NMR data for this compound and the hydroxy starting material are compiled in Tables VII and VIII (see also figures 44 and 45, pp. 155 and 156).

Table VII 400 MHz  $^1\text{H}$  NMR Data for  $\text{HO}(\text{C}_9\text{H}_6\text{N})$  in  $\text{C}_6\text{D}_6$  solution.

$\tau(\text{ppm})^*$	J(Hz)	$^\dagger$ Assignment
3.24(dd)	4.0(8.0)	-
3.00(dd)	2.0(8.0)	-
2.81(m)	8.0(32.0)	-
2.47(dd)	2.0(8.0)	-
1.60(dd)	2.0(4.0)	-
1.46(s)	-	$\text{H}_d$

\*  $\tau_{\text{C}_6\text{H}_6} = 2.84$  ppm; s = singlet, dd = doublet of doublets; m = multiplet.

$^\dagger$  Ring protons are unassigned.

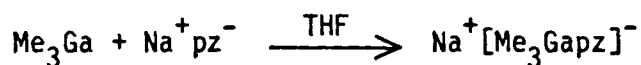
Table VIII 400 MHz  $^1\text{H}$  NMR Data for  $[\text{Me}_2\text{GaO}(\text{C}_9\text{H}_6\text{N})]_2$  in  $\text{C}_6\text{D}_6$  solution.

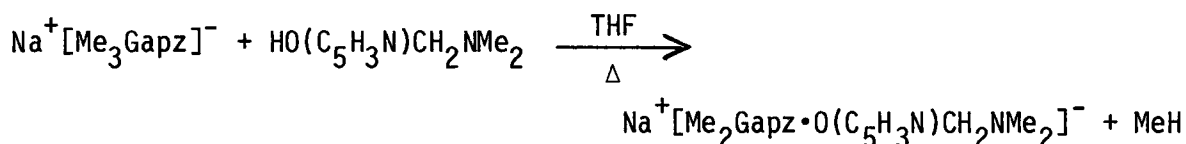
$\tau(\text{ppm})^*$	J(Hz)	$^\dagger$ Assignment
9.90(s)	-	$\text{H}_a$
3.58(dd)	4.0(8.0)	-
3.31(dd)	2.0(8.0)	-
2.71(m)	-	-
2.61(dd)	2.0(4.0)	-
2.57(dd)	2.0(8.0)	-

\*  $\tau_{\text{C}_6\text{H}_6} = 2.84$  ppm; s = singlet; dd = doublet of doublets; m = multiplet.

$^\dagger$  Ring protons are unassigned.

#### 5.2.4 Preparation of the ligand $\text{Na}^+[\text{Me}_2\text{Gapz}\cdot\text{O}(\text{C}_5\text{H}_3\text{N})\text{CH}_2\text{NMe}_2]^-$ ( $\text{Na}^+\text{L}_a^-$ )

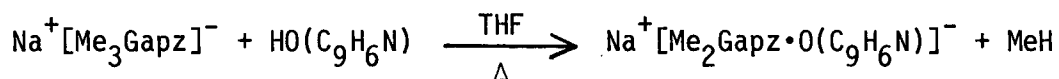




Trimethylgallium (6.20 g, 54.0 mmol) in ~50 ml THF was added to sodium pyrazolide (4.86 g, 54.0 mmol) dissolved in ~50 ml THF. The reaction mixture was stirred for ~4 h. The solution was then diluted with THF to 500 ml in a volumetric flask. An aliquot of this standard  $\text{Na}^+\text{Me}_3\text{Gapz}^-$  (12.96 mmol) ligand solution in THF was added to a stirred solution of 2-(dimethylaminomethyl)-3-hydroxypyridine (1.973 g, 12.96 mmol) in the same solvent. The reaction mixture was refluxed under  $\text{N}_2$  until the evolution of methane gas had ceased completely (~2 days). The cooled solution was then diluted with THF to 250 ml in a volumetric flask. Aliquots of this standard solution were used in subsequent reactions with transition metal halide species.

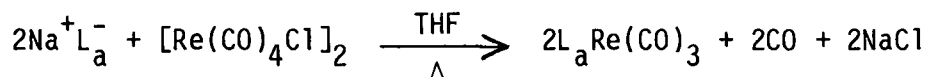
#### 5.2.5 Preparation of the ligand $\text{Na}^+[\text{Me}_2\text{Gapz} \cdot \text{O}(\text{C}_9\text{H}_6\text{N})]^-$ ( $\text{Na}^+\text{L}_q^-$ )

---



The ligand  $\text{Na}^+\text{L}_q^-$  was prepared by a method identical to that described in section 5.2.4, using 8-hydroxyquinoline as the starting material. Aliquots of the resulting yellow  $\text{Na}^+\text{L}_q^-$  standard solution were then used in subsequent reactions with metal halide species.

### 5.2.6 Preparation of $L_a\text{Re}(\text{CO})_3$



A 40.0 ml aliquot of the ligand solution  $\text{Na}^+\text{L}_a^-$  (0.64 mmol) was added slowly to  $[\text{Re}(\text{CO})_4\text{Cl}]_2$  (0.216 g, 0.324 mmol) dissolved in ~30 ml THF. The reaction mixture turned cloudy almost immediately. The reaction mixture was refluxed for ~24 h during which time the cloudiness increased and the yellow coloration intensified. The solution was cooled to room temperature, and the solvent removed under vacuum. The resulting residue was extracted with benzene and filtered. Evaporation of the benzene solvent containing the extracts afforded pale yellow crystalline needles of the desired rhenium tricarbonyl complex in ~80% yield. This compound is stable to oxidation but solutions deteriorate after prolonged periods even under an inert atmosphere. Physical data for this complex are given in Table XII, p. 161.

### 5.2.7 Preparation of $L_a\text{Mn}(\text{CO})_3$



To a stirred THF solution of  $\text{Mn}(\text{CO})_5\text{Br}$  (0.421 g, 1.53 mmol) was added a 30 ml aliquot of the  $\text{Na}^+\text{L}_a^-$  (1.53 mmol) ligand solution in the same solvent. The reaction mixture immediately turned a cloudy orange color. The mixture was refluxed overnight, after which the solvent was removed in vacuo, and the resulting orange residue extracted with benzene.

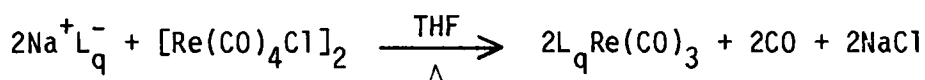
Evaporation of the benzene from the filtrate resulted in an orange oil. Trituration of the sticky orange oil eventually yielded an air-sensitive orange powder as the product in ~75% yield. Physical data for the complex are listed in Table XII, p. 161.

#### 5.2.8 Preparation of $L_aNi(NO)$



Ni(NO)I (0.33 g, 1.5 mmol) was dissolved in ~50 ml THF. A solution of  $Na^+L_a^-$  (1.5 mmol) in the same solvent was added to the stirred solution of the nitrosyl. The resulting dark blue solution was stirred overnight. The solvent was removed under vacuum, and the dark blue residue extracted with benzene. The benzene filtrate containing the extracts was concentrated and, upon evaporation of the solvent, flaky blue crystals of the product were recovered in ~60% yield. Analytical and spectroscopic data for this complex are collected in Table XII, p. 161.

#### 5.2.9 Preparation of $L_qRe(CO)_3$



Two molar equivalents of  $Na^+L_q^-$  were added to  $[Re(CO)_4Cl]_2$  (0.18 g, 0.27 mmol) dissolved in ~30 ml THF, and the resulting solution was refluxed overnight. The solvent was then removed from the reaction mixture under vacuum. The residue was extracted with benzene. Evaporation of solvent from the filtered extract resulted in a yellow cake.

Recrystallization of the yellow cake from  $\text{CH}_2\text{Cl}_2$ /hexane (1:1) afforded stable yellow crystals of the desired product in ~80% yield. Selected physical data for this complex are summarized in Table XVI, p. 174.

#### 5.2.10 Preparation of $\text{L}_q\text{Mn}(\text{CO})_3$



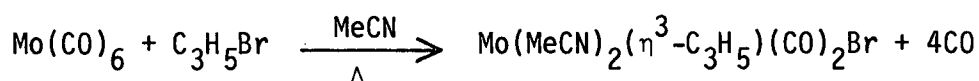
An equimolar amount of  $\text{Na}^+\text{L}_q^-$  ligand in THF, was added to  $\text{Mn}(\text{CO})_5\text{Br}$  (0.19 g, 0.68 mmol) dissolved in the same solvent. After refluxing the reaction mixture overnight, the solvent was removed from the cloudy orange solution in vacuo. Work-up of the resulting residue, using benzene as the extracting solvent, gave orange crystals of the product in ~80% yield. This complex is stable under inert conditions but darkens in color on exposure to air. Solutions of the complex (in acetone or benzene), deteriorate with time. Physical data for this compound are presented in Table XVI, p. 174.

#### 5.2.11 Attempted preparation of $\text{L}_q\text{Ni}(\text{NO})$

A 1:1 reaction of  $\text{Ni}(\text{NO})\text{I}$  and  $\text{Na}^+\text{L}_q^-$  ligand in THF was carried out both at room and reflux temperatures. In both reactions, the reaction mixture turned blue/green and after work-up, blue/green solids were obtained. The solution ir spectrum of either the reaction mixture or the final blue/green solid showed no noticeable evidence of absorption bands in the nitrosyl stretching frequency region of the spectrum. The  $^1\text{H}$  nmr and mass spectral data of the solid isolated were consistent with those expected for an octahedral Ni(II) complex formulated as  $[\text{Me}_2\text{GapzO}-(\text{C}_9\text{H}_6\text{N})]_2\text{Ni}$ . However, repeated attempts at obtaining analytically pure

samples, or isolating suitable crystals for X-ray structural determination, were unsuccessful.

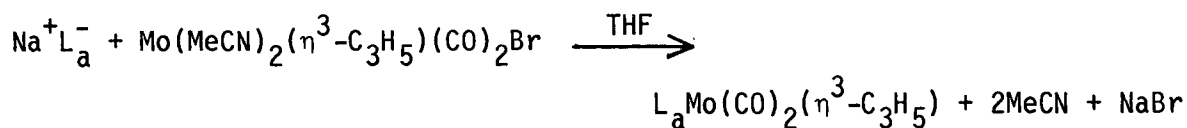
### 5.2.12 Preparation of $\text{Mo}(\text{MeCN})_2(\eta^3\text{-C}_3\text{H}_5)(\text{CO})_2\text{Br}$



Excess allyl bromide was refluxed with  $\text{Mo}(\text{CO})_6$  (2.04 g, 7.70 mmol) in ~60 ml acetonitrile for 2 days. The cooled yellow solution was left to stand in an inert atmosphere for another 2 days, at which stage a yellow crystalline precipitate had formed. The yellow solid was then collected and dried in vacuo to give air-sensitive yellow crystals of the product in ~80% yield. This compound exhibits two strong bands in the CO stretching frequency region of the ir spectrum ( $\nu_{\text{CO}}$ : 1945, 1860  $\text{cm}^{-1}$   $\text{CH}_2\text{Cl}_2$ ). [It is recommended that this compound be prepared immediately prior to further use since it decomposes readily on standing.]

Alternatively, the compound can be prepared via a two-step process-oxidative addition of allyl bromide to the labile  $(\text{MeCN})_3\text{Mo}(\text{CO})_3$  generated from  $\text{Mo}(\text{CO})_6$  as cited in the literature by Hayter [184].

### 5.2.13 Preparation of $\text{L}_a\text{Mo}(\text{CO})_2(\eta^3\text{-C}_3\text{H}_5)$



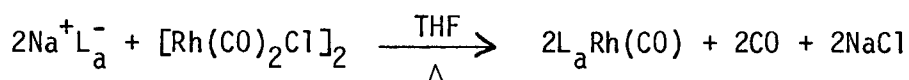
Equimolar amounts of the ligand  $\text{Na}^+\text{L}_a^-$  and  $\text{Mo}(\text{MeCN})_2(\eta^3\text{-C}_3\text{H}_5)(\text{CO})_2\text{Br}$

were reacted in THF. An immediate cloudiness was observed upon mixing the reagents, indicating precipitation of NaBr salt. The reaction mixture was stirred overnight followed by solvent removal under vacuum. The resulting residue was extracted with benzene and filtered. Evaporation of the benzene solvent from the solution containing the extracts afforded orange crystals of the desired product in ~70% yield. This compound is stable under inert conditions but solutions deteriorate with time. Pertinent physical data are collected in Table XII, p. 161.

#### 5.2.14 Preparation of $L_q Mo(CO)_2(\eta^3-C_3H_5)$

The compound  $L_q Mo(CO)_2(\eta^3-C_3H_5)$  was prepared by a procedure identical to that described in section 5.2.13. Work-up of the residue resulting from this reaction, using hexane as the extracting solvent, afforded shiny red-orange crystals of the product in ~70% yield. Analytical and spectroscopic data for the complex are listed in Table XVI, p. 174.

#### 5.2.15 Preparation of $L_a Rh(CO)$



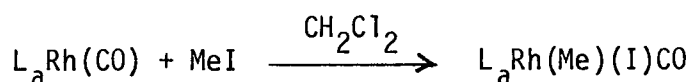
Two molar equivalents of the ligand  $Na^+L_a^-$  were added to  $[Rh(CO)_2Cl]_2$  (0.30 g, 0.77 mmol) dissolved in ~40 ml THF. The reaction mixture was refluxed under nitrogen until the disappearance of the  $[Rh(CO)_2Cl]_2$  dimer ( $\nu_{CO}$ : 2068, 1989  $cm^{-1}$  THF) was indicated by ir measurements. At this juncture, three new bands had appeared in the  $\nu_{CO}$  region of the spectrum at 2085, 2025 and 1970  $cm^{-1}$ , respectively. The reaction mixture was

cooled, and the solvent removed in vacuo. The residue was washed with hexane followed by extraction with benzene. Evaporation of the benzene solvent from the filtrate containing the extracts afforded orange crystals of the product in ~60% yield. The compound is moderately stable but solutions decompose with time. Physical data are summarized in Table XII, p. 161.

#### 5.2.16 Preparation of $L_qRh(CO)$

Preparation of the compound  $L_qRh(CO)$  was accomplished by a procedure similar to the one described in section 5.2.15. New  $\nu_{CO}$  bands at 2080, 2020, and  $1965\text{ cm}^{-1}$  in THF were indicated by ir sampling of the reaction mixture prior to solvent removal in vacuo. After work-up, yellow-orange crystals of the product were isolated in ~65% yield. Analytical, ir and  $^1H$  nmr data are collected in Table XVI, p. 174.

#### 5.2.17 Reaction of $L_aRh(CO)$ with MeI

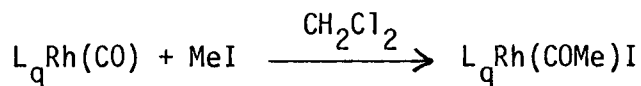


A slight excess of methyl iodide in  $CH_2Cl_2$  was added dropwise to a stirred solution of  $L_aRh(CO)$  (0.30 g, 0.70 mmol) in the same solvent. After stirring the reaction mixture at room temperature for about 18 h, the initial orange solution had turned deep red-orange. The ir spectrum of the solution at this stage revealed the presence of a new  $\nu_{CO}$  band at  $\sim 2060\text{ cm}^{-1}$  and the complete disappearance of the  $\nu_{CO}$  band at  $1970\text{ cm}^{-1}$ , attributable to the  $L_aRh(CO)$  starting material. Removal of the solvent in vacuo, extraction of the residue in benzene, followed by recrystallization

from  $\text{CH}_2\text{Cl}_2$ , afforded red crystals of the product in almost quantitative yield. This compound crystallized as a benzene solvate which remained after several days of pumping under vacuum.

Anal. Calcd. For  $[\text{Me}_2\text{Gapz}\cdot\text{O}(\text{C}_5\text{H}_3\text{N})\text{CH}_2\text{NMe}_2]\text{Rh}(\text{Me})(\text{I})\text{CO}\cdot 0.5 \text{C}_6\text{H}_6$ : C, 34.31; H, 4.13; N, 8.89. Found: C, 33.93; H, 4.06; N, 8.55. IR( $\text{CH}_2\text{Cl}_2$ )  $\nu_{\text{CO}}$ :  $2060 \text{ cm}^{-1}$ ; IR(Nujol)  $\nu_{\text{CO}}$ :  $2055 \text{ cm}^{-1}$ .  $^1\text{H}$  NMR (270 MHz,  $\text{CDCl}_3$ ):  $\tau\text{CHCl}_3 = 2.73 \text{ ppm}$ , 10.34s, 10.12s (-GaMe<sub>2</sub>); 8.85s, 7.63s (-NMe<sub>2</sub>); 6.15s (-CH<sub>2</sub>); 3.71t (pz-H<sup>4</sup>); 2.43d (pz-H<sup>3</sup>); 2.98d (pz-H<sup>5</sup>); 9.25s (Rh-Me). ( $J_{\text{HCCH}} = \sim 2\text{Hz}$  for pz protons.) Positive Ion Fast Atom Bombardment Mass Spectrometry (FABMS) in thioglycerol matrix:  $[\text{P}+\text{H}]^+$ ,  $[\text{P}-\text{H}]^+$ , and  $[\text{P}-\text{Me}]^+$  ( $\text{P}^+$  = parent ion) ion signals were observed at 591, 589 and 575 mass units, (based on  $^{69}\text{Ga}$ ) respectively.

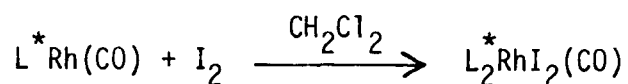
#### 5.2.18 Reaction of $\text{L}_q\text{Rh}(\text{CO})$ with MeI



To a solution of  $\text{L}_q\text{Rh}(\text{CO})$  (0.40 g, 0.91 mmol) in  $\sim 35 \text{ ml}$   $\text{CH}_2\text{Cl}_2$  was added one molar equivalent of MeI in the same solvent. The mixture was stirred for about 1-1/2 h, at which stage ir evidence indicated the presence of two new bands in the  $\nu_{\text{CO}}$  region of the spectrum at  $\sim 2070$  and  $1700 \text{ cm}^{-1}$ , respectively with no trace of the  $\nu_{\text{CO}}$  band due to the  $\text{L}_q\text{Rh}(\text{CO})$  starting material. The solvent was then allowed to evaporate from the solution. The dark orange solid obtained was washed in hexane followed by benzene to give small dark orange crystals in low yield ( $\sim 35\%$ ).

Anal. Calcd. for  $[\text{Me}_2\text{Gapz}\cdot\text{O}(\text{C}_9\text{H}_6\text{N})]\text{Rh}(\text{COMe})\text{I}$ : C, 32.90; H, 3.08; N, 7.20. Found: C, 33.00; H, 3.04; N, 6.90. IR( $\text{CH}_2\text{Cl}_2$ )  $\nu_{\text{CO}}$ : 2070, 1700  $\text{cm}^{-1}$ . IR(Nujol)  $\nu_{\text{CO}}$ : 1710  $\text{cm}^{-1}$ .  $^1\text{H}$  NMR (270 MHz,  $\text{CDCl}_3$ ):  $\tau$   $\text{CHCl}_3$  = 2.73 ppm, 10.08s, 9.89s ( $-\text{GaMe}_2$ ); 7.58s ( $-\text{COMe}$ ); 3.71t ( $\text{pz-H}^4$ ); 2.29d ( $\text{pz-H}^3$ );  $\text{pz-H}^5$  obscured by the quinolyl ring proton resonances. MS:  $\text{P}^+$ ,  $\text{P-Me}^+$ ,  $\text{P-Me-CO}^+$ ,  $\text{P-Me-I}^+$  and  $\text{P-2Me-I}^+$  ( $\text{P}^+$  = parent ion) ion signals were observed.

#### 5.2.19 Reaction of $\text{L}^*\text{Rh}(\text{CO})$ ( $\text{L}^* = \text{L}_a, \text{L}_q$ ) with $\text{I}_2$



To a  $\text{CH}_2\text{Cl}_2$  solution of  $\text{L}^*\text{Rh}(\text{CO})$  was added a slight excess of the dihalogen  $\text{I}_2$  in the same solvent. An immediate color change from orange to red was observed on mixing the reagents. After stirring the mixture for a few hours, an ir spectrum indicated complete disappearance of the  $\nu_{\text{CO}}$  band of the rhodium(I) monocarbonyl starting material, and the appearance of a new  $\nu_{\text{CO}}$  band at  $\sim 2090 \text{ cm}^{-1}$  ( $\text{L} = \text{L}_a$ ), and  $\sim 2085 \text{ cm}^{-1}$  ( $\text{L}^* = \text{L}_q$ ). The single  $\nu_{\text{CO}}$  band persisted in solution after stirring the reaction mixture overnight. Although the ir spectra of the reaction mixtures suggested the presence of six-coordinate Rh(III) monocarbonyl species in solution, analytically pure compounds of the expected diiodides,  $\text{L}^*\text{RhI}_2(\text{CO})$ , could not be isolated from the black solid material obtained after removal of solvent.

### 5.3 Results and Discussion

#### 5.3.1 $[\text{Me}_2\text{GaO}(\text{C}_5\text{H}_3\text{N})\text{CH}_2\text{NMe}_2]$

A general reaction of Group 13 (B, Al, Ga, In) alkyls toward active hydrogen-containing ligands is the elimination of alkanes. For example, a compound structurally characterized by X-ray crystallography as  $[\text{Me}_2\text{NCH}_2\text{CH}_2\text{OGaMe}_2]_2$  was isolated as the product of the reaction of trimethylgallium with N,N-dimethylethanolamine [185]. With the notable exception of  $\text{H}_2\text{NCH}_2\text{CH}_2\text{OGaMe}_2$ , the structure of which consists of monomeric molecules containing tetrahedrally coordinated gallium atoms [186], monomer units of similar dimethyl gallium systems have been shown by X-ray structural analyses to dimerize via four-membered  $[-\text{Ga}-\text{O}-]_2$  rings giving a distorted bipyramidal arrangement about each five-coordinate gallium atom [173,185].

The reaction of 2-(dimethylaminomethyl)-3-hydroxypyridine with trimethylgallium yielded the compound  $[\text{Me}_2\text{Ga}\cdot\text{O}(\text{C}_5\text{H}_3\text{N})\text{CH}_2\text{NMe}_2]$ , the crystal structure (figure 40) of which consists of discrete monomeric molecules which display the gallium atoms in distorted tetrahedral arrangements rather than a distorted trigonal bipyramidal geometry expected for a five-coordinate gallium dimeric species. It is interesting to compare the Ga-N bond length in this complex to those reported for similar dimethyl-gallium systems (figure 41, see also Table XI, p. 158). The Ga-N bond length of 2.135Å in the present  $[\text{Me}_2\text{Ga}\cdot\text{O}(\text{C}_5\text{H}_3\text{N})\text{CH}_2\text{NMe}_2]$  complex is considerably shorter than that of the dimer  $[\text{Me}_2\text{GaOCH}_2\text{CH}_2\text{NMe}_2]_2$  (Ga-N = 2.471Å) [185], but longer than 2.056Å and 2.072Å reported for the two independent molecules of the  $[\text{Me}_2\text{GaOCH}_2\text{CH}_2\text{NH}_2]$  monomeric species [186].

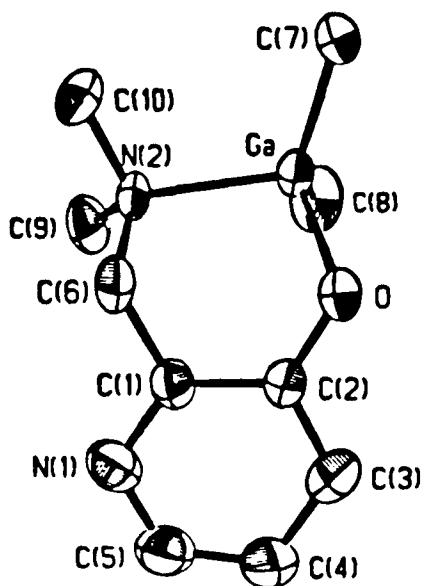


Figure 40. Molecular structure of  $[\text{Me}_2\text{Ga}\cdot\text{O}(\text{C}_5\text{H}_3\text{N})\text{CH}_2\text{NMe}_2]$

The shorter Ga-N bond length of 2.135Å in the present  $[\text{Me}_2\text{Ga}\cdot\text{O}(\text{C}_5\text{H}_3\text{N})\text{CH}_2\text{NMe}_2]$  complex compared with the 2.471Å above is suggestive of less steric interactions. In the  $[\text{Me}_2\text{GaOCH}_2\text{CH}_2\text{NMe}_2]$  complex, severe steric interactions led to bond lengthening. The monomeric nature of the present  $[\text{Me}_2\text{GaO}(\text{C}_5\text{H}_3\text{N})\text{CH}_2\text{NMe}_2]$  compound is probably related to the steric constraints imposed by the unsaturation of the pyridine ring. Since the pyridine substituent atoms O and C(6) are constrained to lie approximately in the plane of the pyridine ring, four atoms of the six-membered chelate must be roughly coplanar. In order to minimize angular strain, the chelate ring adopts a steep and slightly twisted boat conformation in which the  $\text{NMe}_2$  and  $\text{GaMe}_2$  groups are nearly eclipsed. The partial staggering about the Ga-N bond which would be required for dimerization most likely results in too high a degree of ring strain. It is noteworthy that in the related compound  $[\text{Me}_2\text{GaOCH}_2\text{CH}_2\text{NH}_2]$  [186], an extensive network of  $\text{N-H}\cdots\text{O}$  hydrogen bonding present in the compound prevented dimerization of the monomer units.

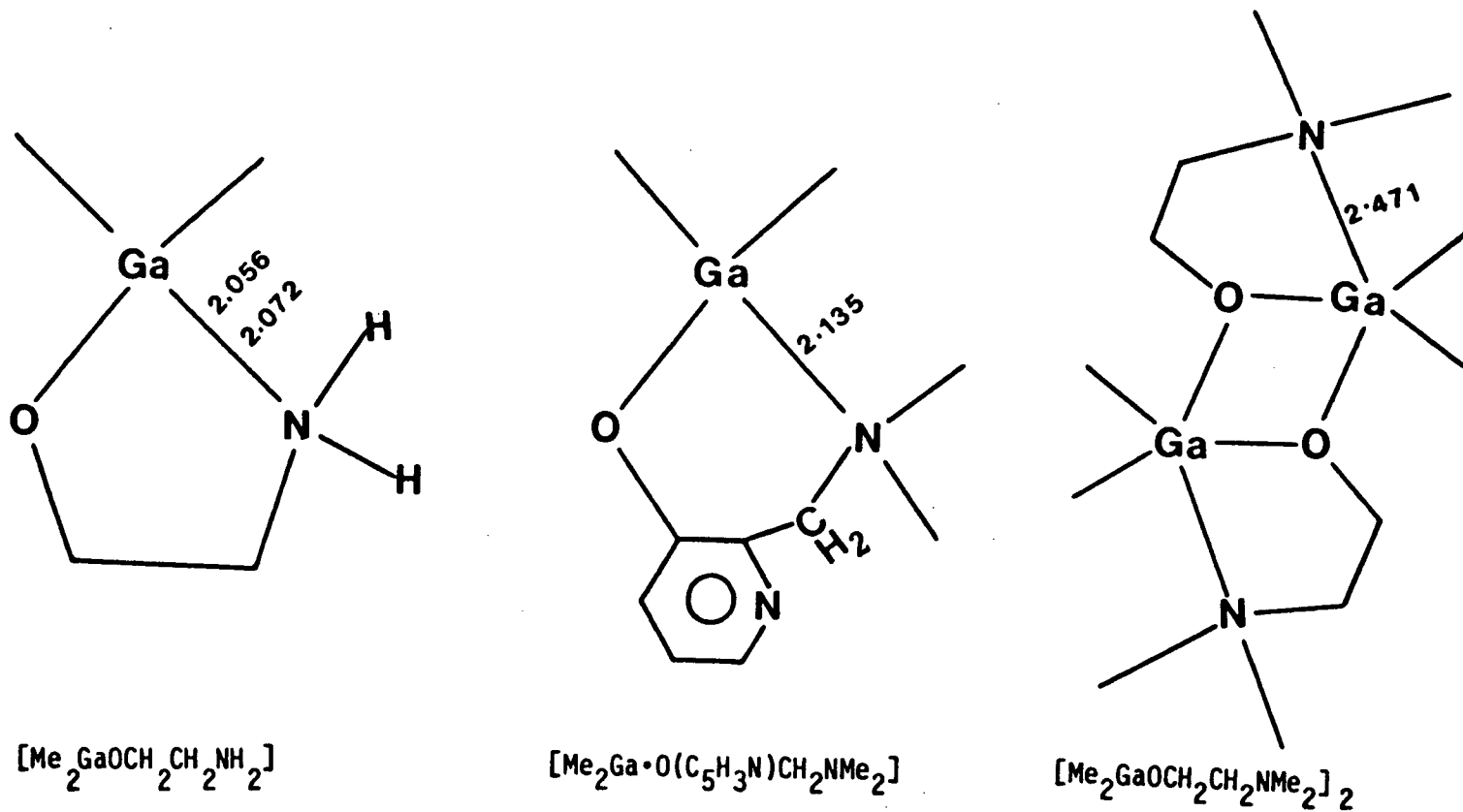


Figure 41. Comparison of the Ga-N bond lengths in the dimethylgallium compounds.

The mass spectrum of the compound  $[\text{Me}_2\text{GaO}(\text{C}_5\text{H}_3\text{N})\text{CH}_2\text{NMe}_2]$  displayed as its highest mass peaks, a moderately strong parent ion ( $\text{P}^+$ ) signal as well as a very strong  $\text{P-Me}^+$  signal, confirming the monomeric nature of the compound in the gas phase. The most intense signals were those corresponding to loss of the ' $\text{CH}_2\text{NMe}_2$ ' moiety from the monomer species. The mass spectral data for this compound are collected in Table IX below.

Table IX.  $^\dagger$  Mass Spectral Data of  $[\text{Me}_2\text{GaO}(\text{C}_5\text{H}_3\text{N})\text{CH}_2\text{NMe}_2]$

$^*\text{m/e}$	Assignment	Intensity
250	$[\text{Me}_2\text{Ga}\cdot\text{O}(\text{C}_5\text{H}_3\text{N})\text{CH}_2\text{NMe}_2]^+$	19.3
235	$[\text{MeGa}\cdot\text{O}(\text{C}_5\text{H}_3\text{N})\text{CH}_2\text{NMe}_2]^+$	85.3
192	$[\text{Me}_2\text{Ga}\cdot\text{O}(\text{C}_5\text{H}_3\text{N})]^+$	100.0
177	$[\text{MeGa}\cdot\text{O}(\text{C}_5\text{H}_3\text{N})]^+$	14.5
151	$[\text{O}(\text{C}_5\text{H}_3\text{N})\text{CH}_2\text{NMe}_2]^+$	5.0
109	$[\text{HO}(\text{C}_5\text{H}_3\text{N})\text{CH}_3]^+$	58.5
99	$[\text{Me}_2\text{Ga}]^+$	15.2
80	$\text{C}_5\text{H}_6\text{N}^+$	8.2
69	$\text{Ga}^+$	35.2
58	$[-\text{CH}_2\text{NMe}_2]^+$	43.2
44	$[\text{NMe}_2]^+$	18.6

$^\dagger$  At  $68^\circ\text{C}$ .

$^*$  Based on  $^{69}\text{Ga}$ .

The  $^1\text{H}$  nmr spectra of the hydroxy starting material,  $\text{HO}(\text{C}_5\text{H}_3\text{N})\text{CH}_2\text{NMe}_2$  in  $\text{C}_6\text{D}_6$  solution, and of the complex  $\text{Me}_2\text{GaO}(\text{C}_5\text{H}_3\text{N})\text{CH}_2\text{NMe}_2$  in  $\text{C}_6\text{D}_6$  solution, are shown in figures 42 and 43, respectively. The  $^1\text{H}$  nmr spectrum of  $\text{Me}_2\text{GaO}(\text{C}_5\text{H}_3\text{N})\text{CH}_2\text{NMe}_2$  complex is consistent with an overall planar structure for this species in solution, with the two methyl groups

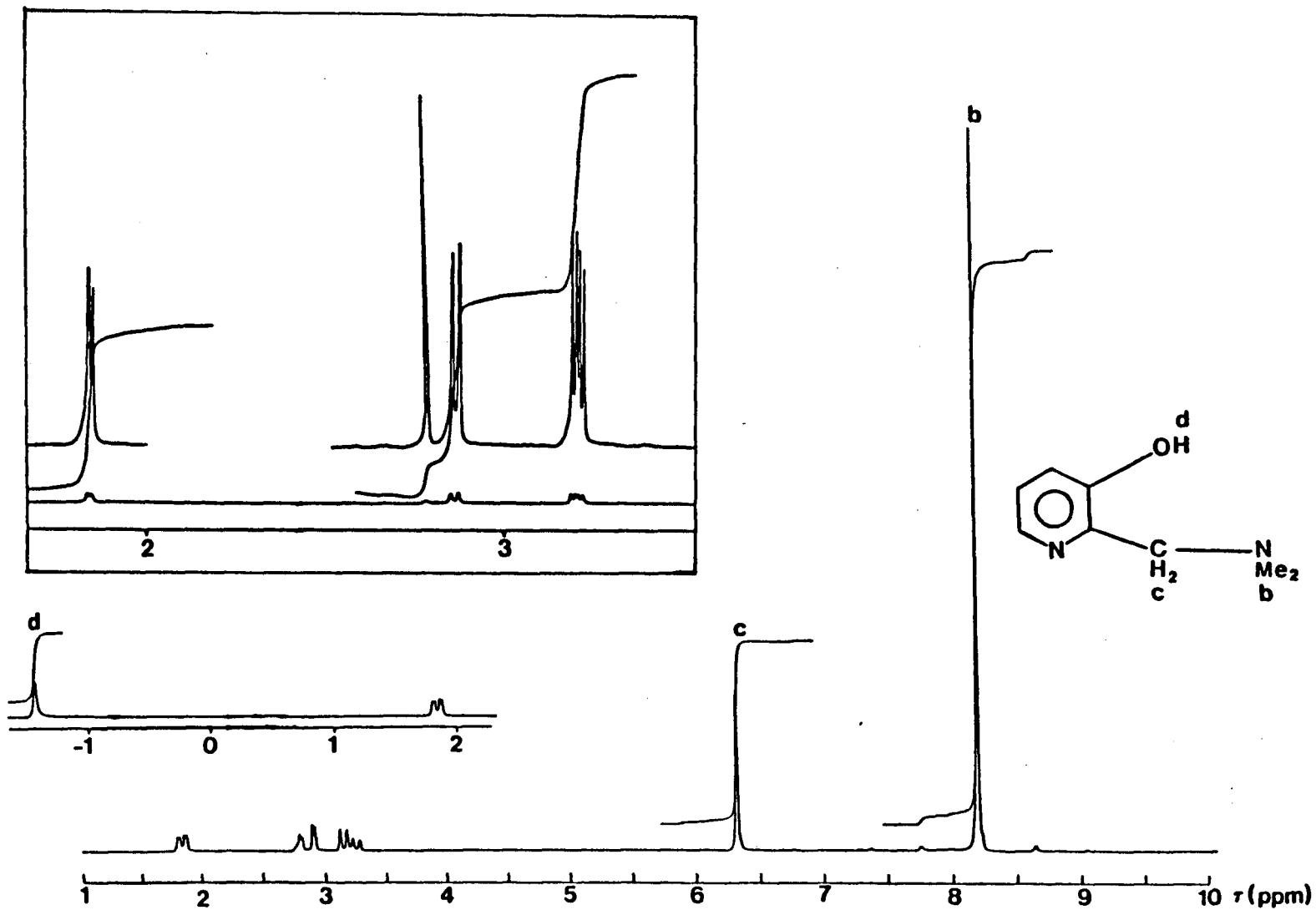


Figure 42. 80 MHz  $^1\text{H}$  nmr spectrum of  $\text{HO}(\text{C}_5\text{H}_3\text{N})\text{CH}_2\text{NMe}_2$  in  $\text{C}_6\text{D}_6$  solution. (400 MHz inset).

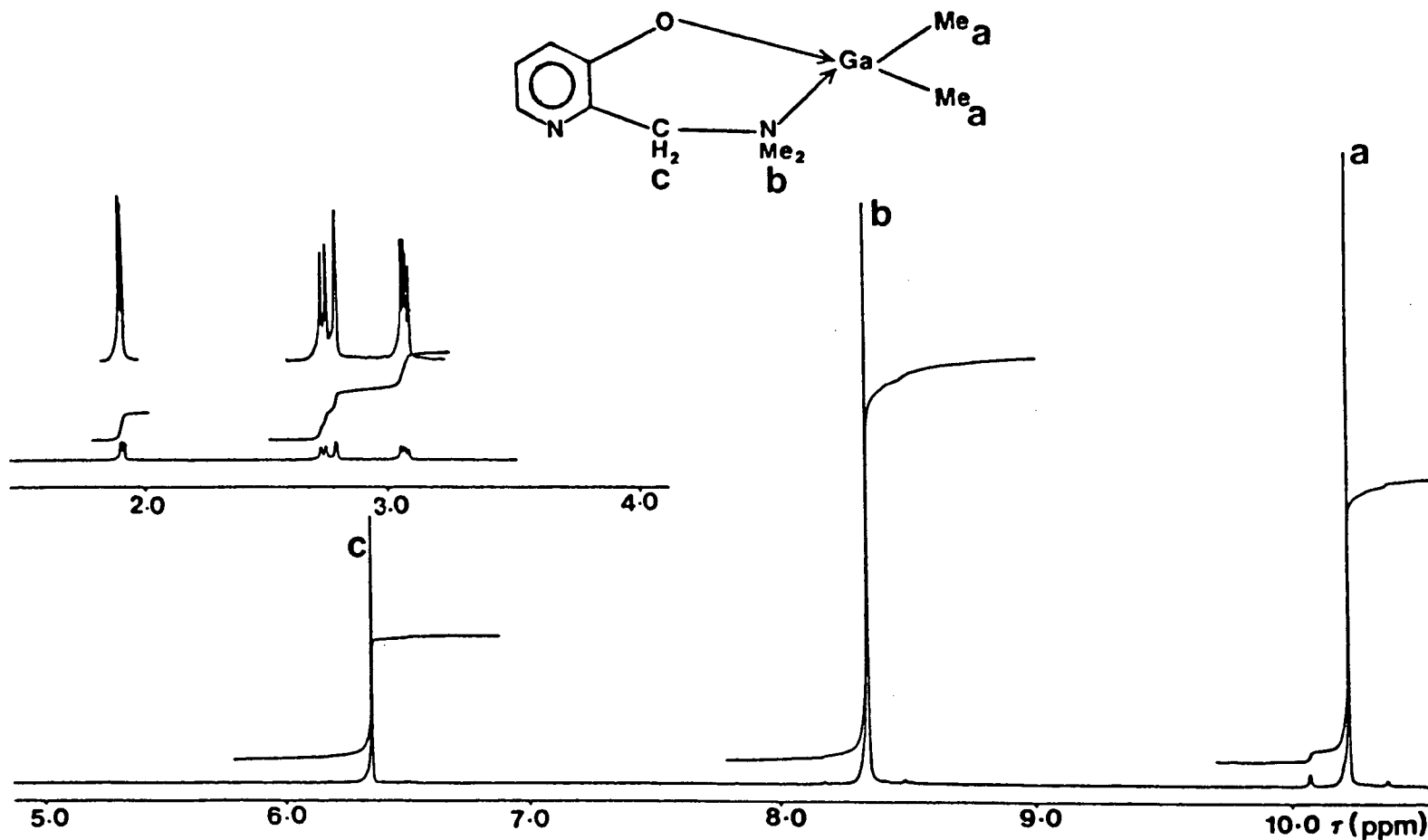


Figure 43. 400 MHz  $^1\text{H}$  spectrum of  $\text{Me}_2\text{GaO}(\text{C}_5\text{H}_3\text{N})\text{CH}_2\text{NMe}_2$  in  $\text{C}_6\text{D}_6$  solution.

on gallium, and the two methyl groups on nitrogen, as well as the two methylene protons lying above and below this plane; this leads to sharp singlets for the  $-\text{GaMe}_2$ ,  $-\text{NMe}_2$  and  $-\text{CH}_2-$  groupings.

### 5.3.2 $[\text{Me}_2\text{GaO}(\text{C}_9\text{H}_6\text{N})]_2$

The reaction of 8-hydroxyquinoline with trimethylgallium afforded the coordination compound  $[\text{Me}_2\text{GaO}(\text{C}_9\text{H}_6\text{N})]^+$  which has been shown to be monomeric in the gas phase. The mass spectrum of this compound displayed prominent signals due to the parent ion  $\text{P}^+$ ,  $\text{P-Me}^+$  and  $\text{P-2Me}^+$ , the latter being the most intense in the spectrum (see Table X below).

Table X.  $^\dagger$ Mass Spectral Data of  $[\text{Me}_2\text{GaO}(\text{C}_9\text{H}_6\text{N})]^+$

$^* \text{m/e}$	Assignment	Intensity
243	$[\text{Me}_2\text{GaO}(\text{C}_9\text{H}_6\text{N})]^+$	12.0
228	$[\text{MeGaO}(\text{C}_9\text{H}_6\text{N})]^+$	100.0
213	$[\text{GaO}(\text{C}_9\text{H}_6\text{N})]^+$	28.0
145	$[\text{HO}(\text{C}_9\text{H}_6\text{N})]^+$	5.9
115	$[\text{Me}_2\text{GaO}]^+$	6.2
99	$[\text{Me}_2\text{Ga}]^+$	2.3
84	$[\text{MeGa}]^+$	50.7
69	$\text{Ga}^+$	50.7

$^\dagger$  At  $180^\circ\text{C}$ .

$^*$  Based on  $^{69}\text{Ga}$ .

The  $^1\text{H}$  nmr spectra of the hydroxy starting material  $\text{HO}(\text{C}_9\text{H}_6\text{N})$ , and the quinolinolato complex  $\text{Me}_2\text{GaO}(\text{C}_9\text{H}_6\text{N})$  in  $\text{C}_6\text{D}_6$  solutions are shown in figures 44 and 45, respectively. The  $^1\text{H}$  nmr spectrum of the quinolinolato

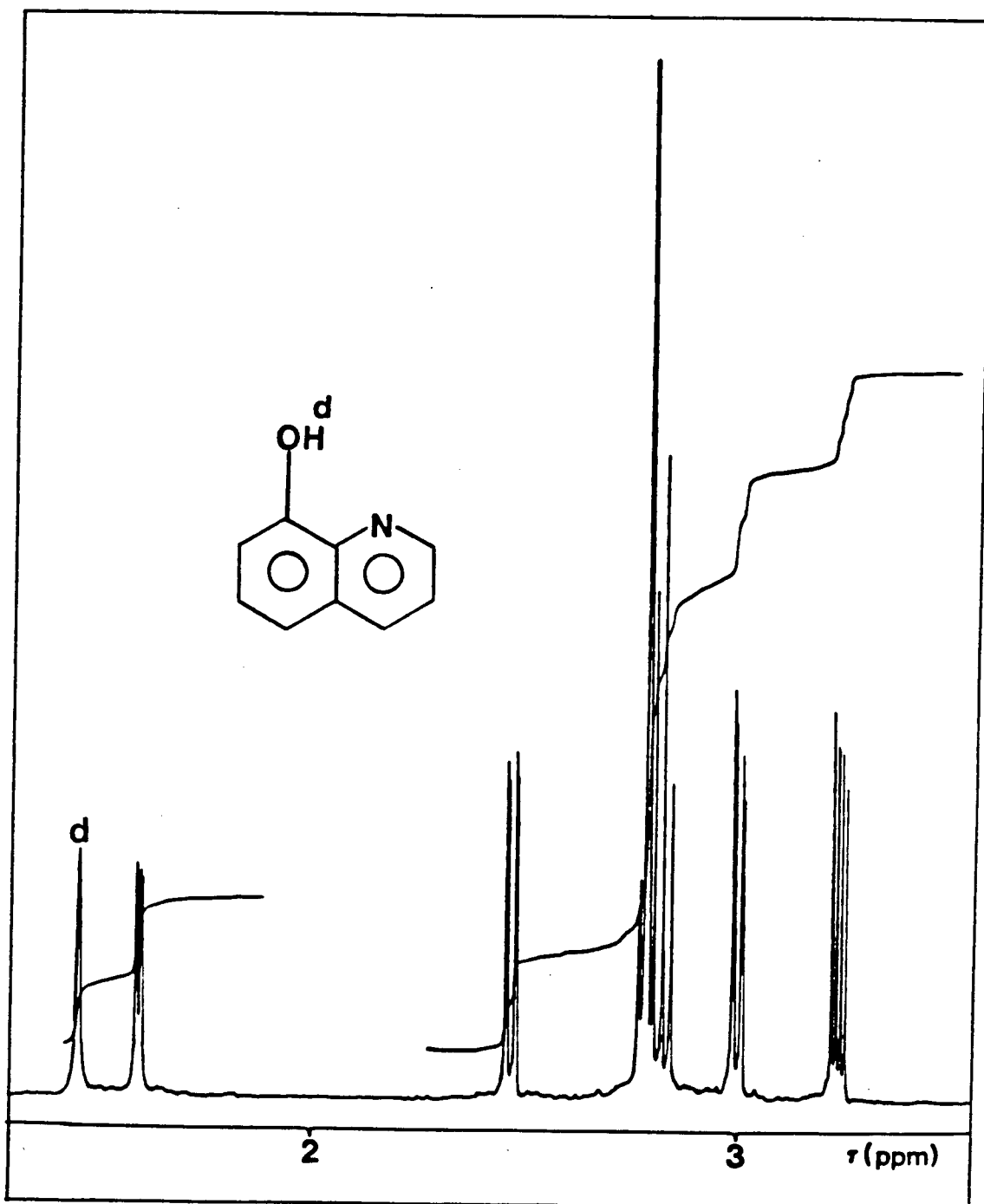


Figure 44. 400 MHz  $^1\text{H}$  nmr spectrum of  $\text{HO}(\text{C}_9\text{H}_6\text{N})$  in  $\text{C}_6\text{D}_6$  solution.

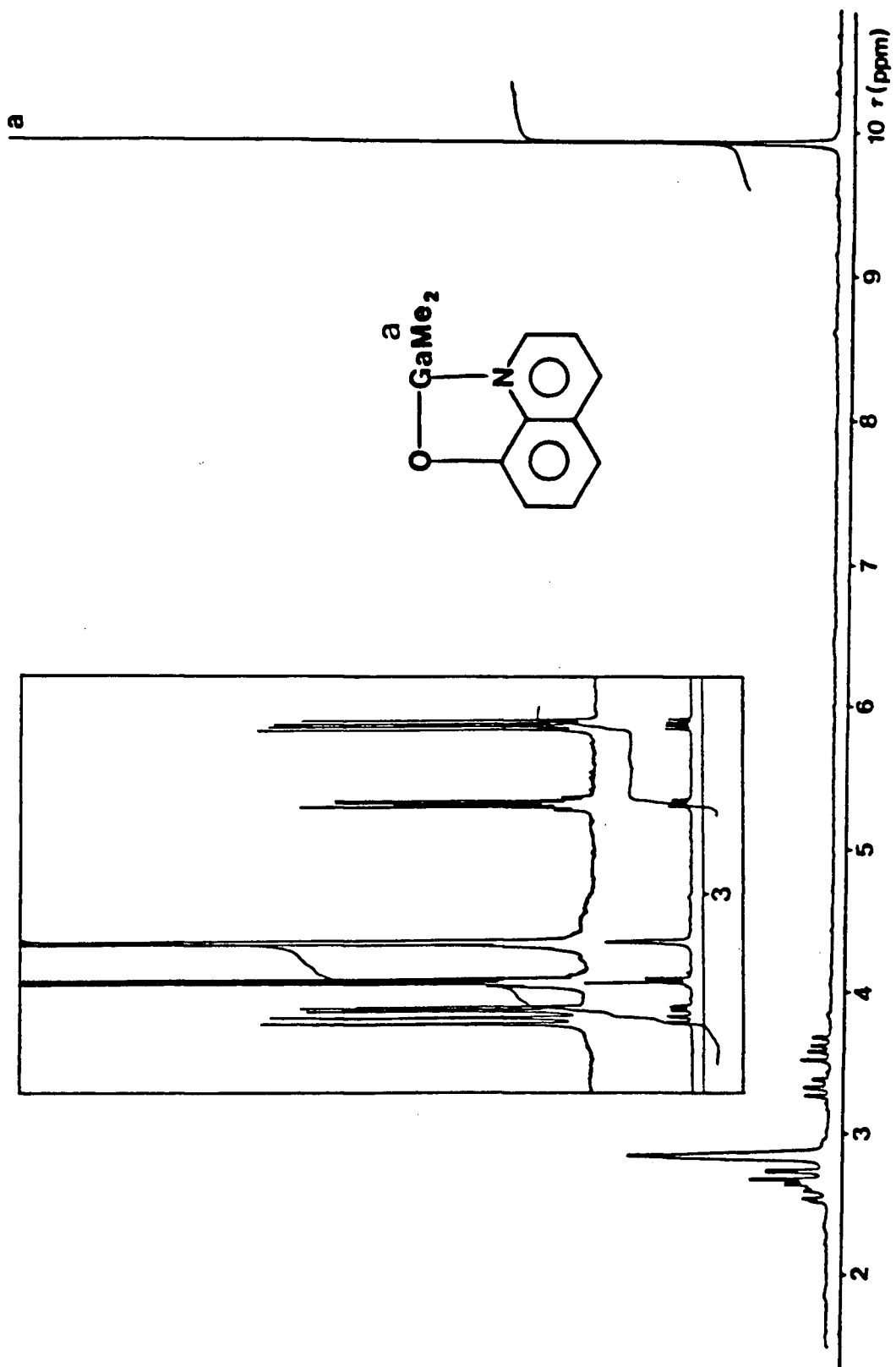


Figure 45. 80 MHz  $^1\text{H}$  nmr spectrum of  $\text{Me}_2\text{GaO}(\text{C}_9\text{H}_6\text{N})$  in  $\text{C}_6\text{D}_6$  solution. (400 MHz inset).

complex is in accord with an overall planar structure for the complex in solution. In this structure, the two methyl groups on gallium lie above and below the plane, hence a sharp singlet is observed for the 'GaMe<sub>2</sub>' protons.

The X-ray crystal structure of the [Me<sub>2</sub>GaO(C<sub>9</sub>H<sub>6</sub>N)]<sub>2</sub> complex is shown in figure 46. This structure revealed the dimerization of the monomer units via the formation of a four-membered [-Ga-O-]<sub>2</sub> ring to form a nearly planar (to within 0.053(5)Å) centrosymmetric molecule consisting of a system of seven fused rings. The coordination geometry about each gallium atom in the above ring system is distorted trigonal bipyramidal primarily due to the steric requirements imposed by the existence of the fused ring system. The Ga-N bond length of 2.211Å for the present quinolinolato complex is shorter than those reported for the related [Me<sub>2</sub>GaOCH<sub>2</sub>CH<sub>2</sub>NMe<sub>2</sub>]<sub>2</sub>

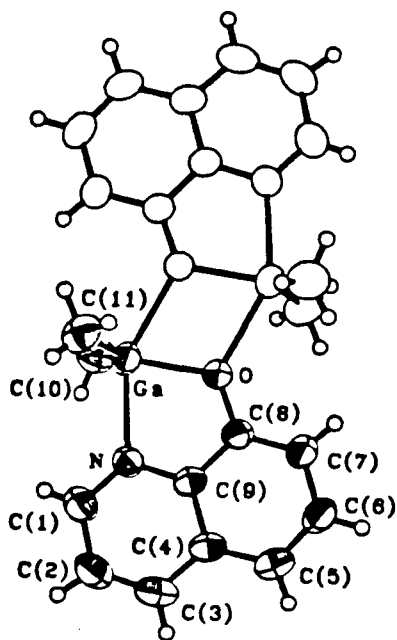


Figure 46. Molecular structure of [Me<sub>2</sub>GaO(C<sub>9</sub>H<sub>6</sub>N)]<sub>2</sub>.

(Ga-N = 2.471Å) [185], and  $[\text{Me}_2\text{GaO}(\text{C}_5\text{H}_4\text{N})]_2$  (Ga-N = 2.276Å) [173] dimers (see Table XI below). Thus steric interactions are likely less severe in the present  $[\text{Me}_2\text{GaO}(\text{C}_9\text{H}_6\text{N})]_2$  complex compared with the  $[\text{Me}_2\text{GaOCH}_2\text{CH}_2\text{NMe}_2]_2$  and  $[\text{Me}_2\text{Ga}\cdot\text{O}(\text{C}_5\text{H}_4\text{N})]_2$  complexes above. The Ga-N bond length of 2.211Å of the present quinolinolato compound is, however, longer than that reported for the first crystallographic example of a trigonal bipyramidal, five-coordinate gallium complex,  $\text{GaCl}[\text{OC}_{10}\text{H}_8\text{N}]_2$  (Ga-N = 2.109Å), 2.105Å) reported earlier by Dymock and Palenik [187].

Table XI. Comparison of Ga-N and Ga-O Bond Lengths in Four and Five Coordinate Gallium Compounds.

Compound	Gallium Coordination		Bond Distances (Å)		Reference
	Number	Ga-N	Ga-O		
$[\text{Me}_2\text{NCH}_2\text{CH}_2\text{OGaMe}_2]_2$	5	2.471	2.078, 1.913		185
$[\text{Me}_2\text{NCH}_2\text{CH}_2\text{OGaH}_2]_2$	5	2.279	2.053, 1.911		185
$[\text{Me}_2\text{Ga}\cdot\text{OCH}_2(\text{C}_5\text{H}_4\text{N})]_2$	5	2.276	1.939-2.086		173
$[\text{Me}_2\text{Ga}\cdot\text{O}(\text{C}_9\text{H}_6\text{N})]_2$	5	2.211	1.937		This work
$[\text{MeN}(\text{CH}_2\text{CH}_2\text{O})_2\text{GaH}]_2$	5	2.193	1.843-2.019		188
$\text{Me}_2\text{Ga}\cdot\text{O}(\text{C}_5\text{H}_3\text{N})\text{CH}_2\text{NMe}_2$	4	2.135	1.897		This work
$\text{Me}_2\text{GaOCH}_2\text{CH}_2\text{NH}_2$	4	2.056, 2.072	1.917		186

### 5.3.3 $L_a M(CO)_3$ (M = Mn, Re)

The first of this class of unsymmetric tridentate ligands,  $Me_2Gapz(O-CH_2CH_2NR_2)^-$  (R = H or Me), has been shown to be capable of either facial or meridional coordination in transition metal complexes [43]. However, in all octahedral transition metal tricarbonyl compounds studied thus far, coordination of the unsymmetrical pyrazolylgallate ligand has been found to be exclusively facial [173,174]. The present manganese and rhenium tricarbonyl compounds, incorporating the ligand  $Me_2GapzO(C_5H_3N)CH_2NMe_2^-$  ( $L_a^-$ ), therefore represent the first and the only examples of such complexes in which both fac and mer isomers co-exist in solution. Evidence for the presence of both isomers in solution is based solely on ir and  $^1H$  nmr data, since persistent attempts at isolating crystals suitable for X-ray crystal structure determination were unsuccessful.

Infrared measurements in cyclohexane showed six bands (four strong, two weak) in the  $\nu_{CO}$  region of the spectrum. A typical example of the spectra obtained for both complexes is shown in figure 47. Three strong bands were assigned to the fac isomer, while one strong and two weak bands were assigned to the mer isomer. Thus, for octahedral transition metal tricarbonyl complexes, a fac arrangement of the tridentate ligand would give three strong  $\nu_{CO}$  bands while for a mer arrangement one would expect to see one strong and two weak  $\nu_{CO}$  bands [51,80]. A comparison of the  $\nu_{CO}$  values obtained for both compounds (Table XII, p. 161), indicates that Re donates more electron density to the CO ligands than does Mn. This results in a lowering of the  $\nu_{CO}$  values due to increased M-CO backbonding, and hence implies a stronger 'M-CO' bond [189].

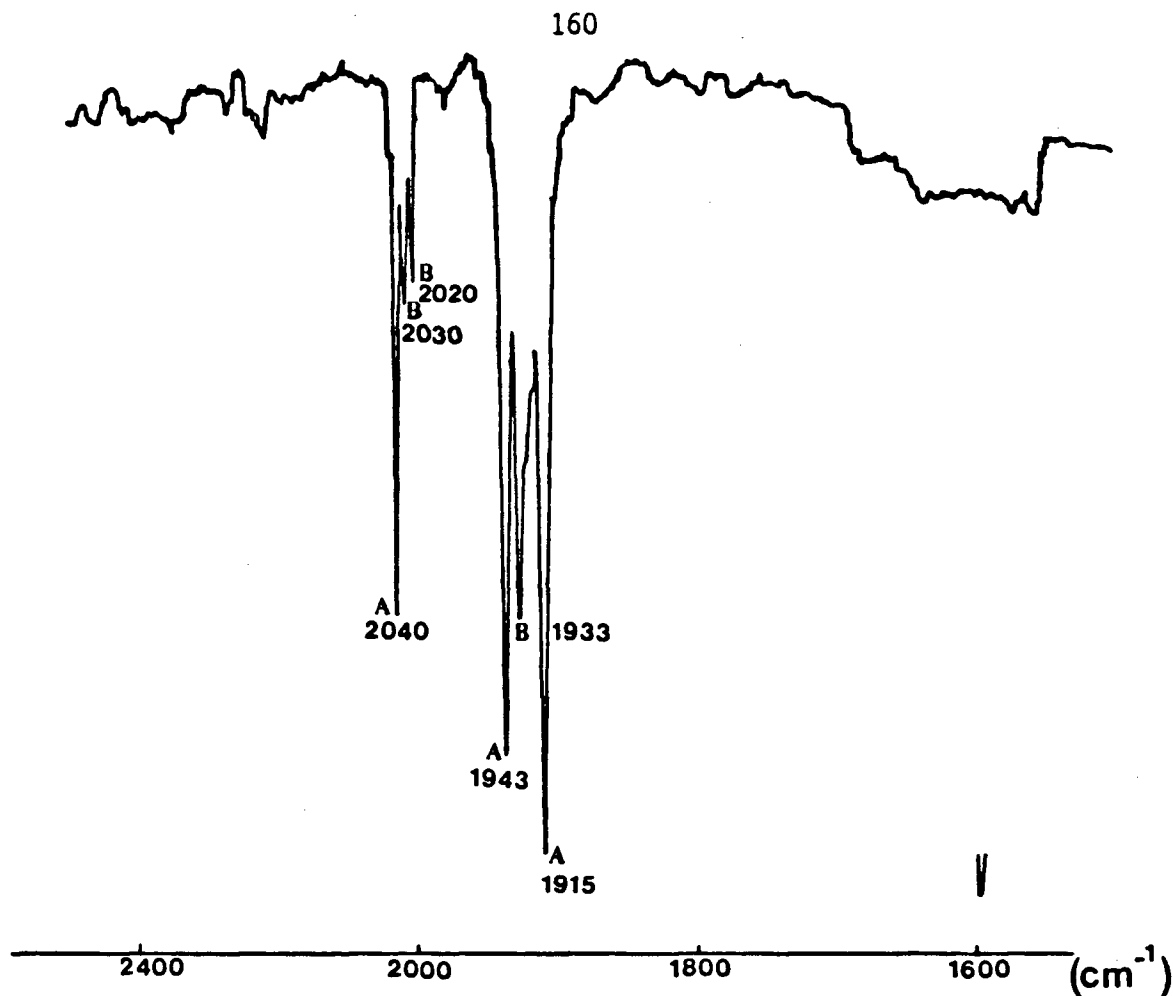


Figure 47. Ir spectrum in the  $\nu_{\text{CO}}$  region of  $[\text{Me}_2\text{Gapz}\cdot\text{O}(\text{C}_5\text{H}_3\text{N})\text{CH}_2\text{NMe}_2]\text{Mn}(\text{CO})_3$  in cyclohexane solution. A fac isomer; B mer isomer.

Further support for the proposed fac and mer isomers in solution is provided by the room temperature  $^1\text{H}$  nmr spectra of the complexes. As a representative example, the  $^1\text{H}$  nmr spectrum of the rhenium complex  $[\text{Me}_2\text{Gapz}\cdot\text{O}(\text{C}_5\text{H}_3\text{N})\text{CH}_2\text{NMe}_2]\text{Re}(\text{CO})_3$  in  $\text{C}_6\text{D}_6$  solution is shown in figure 48. In the spectrum two sets of signals were displayed. In one set the  $\text{GaMe}_2$ ,  $\text{NMe}_2$  and the  $\text{CH}_2$  methylene groups appeared as sharp singlets consistent with a mer structure (figure 49B, p. 163), and a second set consisting of

Table XII. Physical Data for the Complexes  $L_aMT$  (where  $L_a = Me_2Gapz \cdot O(C_5H_3N)CH_2NMe_2$ )

M	T	ANALYSIS CALCD/FOUND			$\nu_{CO}, \nu_{NO} (cm^{-1})$ $C_6H_{12}$ ( $CH_2Cl_2$ )	$^1H$ nmr						
		C	H	N		GaMe	NMe	$CH_2$	$H^A$	$H^5$	$H^3$	$\eta^3-C_3H_5$
Re	$(CO)_3$ $\cdot 0.17C_6H_6$	33.95	3.49	9.32	A 2035,1920,1900	<sup>b</sup> 10.53s	8.21s		4.19t	3.29d	2.41d	
		34.08	3.98	9.44	B 2022,2015,1910	9.83s	7.68s					
Mn	$(CO)_3$	42.05	4.41	12.26	A 2040,1943,1915	<sup>a</sup> 10.65s	7.58s	6.73br	3.54t	3.00d	2.51d	
		42.47	4.56	12.32	B 2030,2020,1933	10.05s	7.24s					
Mo	$(CO)_2$ $\eta^3-C_3H_5$	42.30	4.90		1950,1805	<sup>c</sup> 10.27s	7.43s	5.95s	3.56t	2.85d	2.30d	8.57d,8.67H <sub>A</sub>
		42.06	4.97		(1925,1825)	10.09s						(J = 9.0 Hz) 7.36 br H <sub>S</sub> 6.68 br H <sub>U</sub>
Ni	NO $\cdot 0.75C_6H_6$	45.17	5.27	15.06	1770 (THF)	<sup>c</sup> 10.39s	7.63s	6.16s	4.13t	3.35d	2.66d	
		44.86	5.79	14.51	(1775)	<sup>b</sup> 10.20s	8.35s	6.38s	3.98t	2.68d	2.33d	
Rh	CO $\cdot 0.33C_6H_{14}$	40.23	5.17	11.73		<sup>b</sup> 10.27s	8.40s	6.41s	4.01t	2.76d	2.38d	
		40.32	5.07	11.52	(1970)							

A = fac isomer; B = mer isomer

<sup>a</sup>  $(CD_3)_2CO$ ;  $\tau(CH_3)_2CO = 7.89$  ppm;  $J_{HCCH} = 2.0$  Hz for pz protons.  
<sup>b</sup>  $C_6D_6$ ;  $\tau C_6H_6 = 2.84$  ppm;  $J_{HCCH} = 2.0$  Hz for pz protons.  
<sup>c</sup>  $CDCl_3$ ;  $\tau CHCl_3 = 2.73$  ppm;  $J_{HCCH} = 2.0$  Hz for pz protons.

s = singlet

d = doublet

t = triplet

q = quartet

br = broad

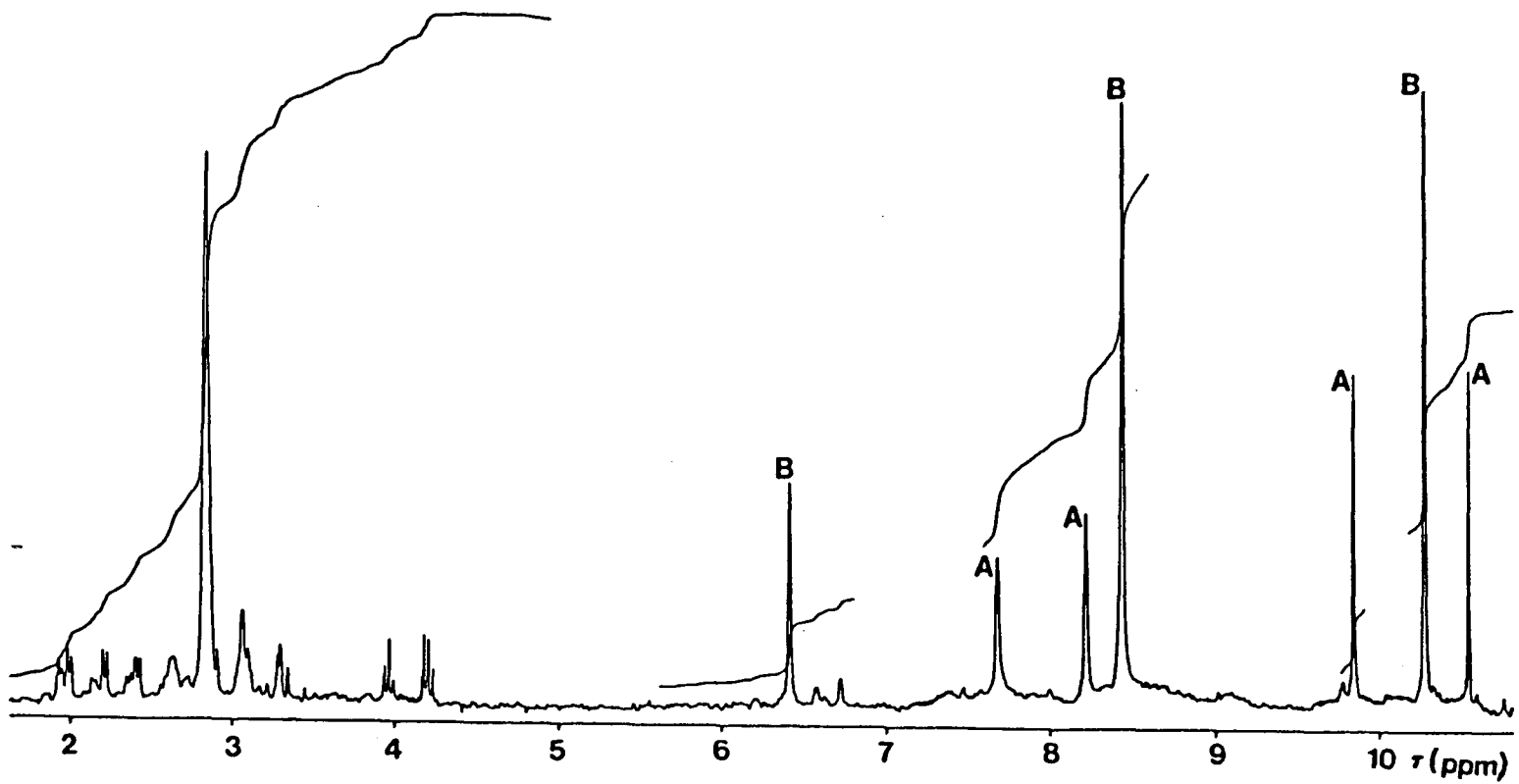
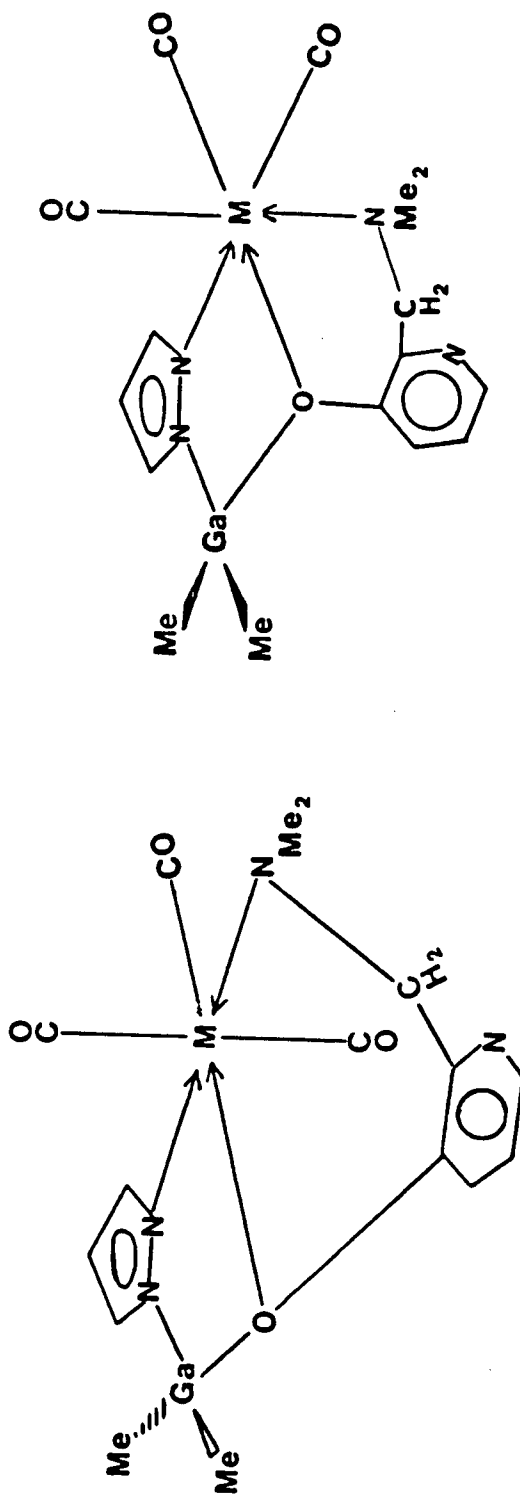


Figure 48. 80 MHz  $^1\text{H}$  nmr spectrum of  $[\text{Me}_2\text{GapzO}(\text{C}_5\text{H}_3\text{N})\text{CH}_2\text{NMe}_2]\text{Re}(\text{CO})_3$  in  $\text{C}_6\text{D}_6$  solution.  
 A fac isomer; B mer isomer.

A *fac.*B *mer.*Figure 49. Proposed conformation of  $[\text{Me}_2\text{Ga}(\text{C}_5\text{H}_3\text{N})\text{CH}_2\text{NMe}_2]\text{M}(\text{CO})_3$  (M = Mn or Re)

two singlets each of the 'GaMe<sub>2</sub>' and 'NMe<sub>2</sub>' moieties suggesting inequivalence of the methyl groups on gallium and nitrogen as expected for a facially coordinated ligand (figure 49A, p. 163). The absence of the clearly defined AB pattern expected for the methylene group of the fac isomer is somewhat puzzling however. The pz proton resonances appeared as two sets for each proton, adding further credence for the co-existence of both the fac and mer isomers of the complexes in solution. These results, the ir data discussed above, together with results from related complexes [173,174], strongly support the presence of both isomers in solution for the present [Me<sub>2</sub>GapzO(C<sub>5</sub>H<sub>3</sub>N)CH<sub>2</sub>NMe<sub>2</sub>]M(CO)<sub>3</sub> (M = Mn, Re) complexes.

Mass spectral data obtained for both the Mn and Re complexes (Tables XIII and XIV) revealed some interesting differences between the two compounds. For example, while the Re species displayed signals corresponding to the parent, P<sup>+</sup>, P-Me<sup>+</sup>, and P-2Me-2H<sup>+</sup> ions, the highest mass fragment observed for the Mn species was attributable to the P-3CO<sup>+</sup> ion. The reluctance to lose the CO ligands exhibited by the Re species is reflective of the comparatively stronger 'M-CO' bonds in this complex than in the valence isoelectronic Mn compound.

Table XIII. † Mass Spectral Data of  $[\text{Me}_2\text{GapzO}(\text{C}_5\text{H}_3\text{N})\text{CH}_2\text{NMe}_2]\text{Mn}(\text{CO})_3$ 

<u>* m/e</u>	<u>Assignment</u>	<u>Intensity</u>
372	$[\text{Me}_2\text{Gapz}\cdot\text{O}(\text{C}_5\text{H}_3\text{N})\text{CH}_2\text{NMe}_2\text{Mn}]^+$	12.7
342	$[\text{Gapz}\cdot\text{O}(\text{C}_5\text{H}_3\text{N})\text{CH}_2\text{NMe}_2\text{Mn}]^+$	27.2
340	$[\text{Gapz}\cdot\text{O}(\text{C}_5\text{H}_3\text{N})\text{CNMe}_2\text{Mn}]^+$	46.0
319	$[(\text{Me}_2\text{Gapz})_2 - \text{Me} + 2\text{H}]^+$	100.0
272	$[\text{Ga}\cdot\text{O}(\text{C}_5\text{H}_3\text{N})\text{CNMe}_2\text{Mn} - \text{H}]^+$	15.1
251	$[(\text{Me}_2\text{Gapz})_2 - \text{Me} - \text{pz} + \text{H}]^+$	39.1
235	$[\text{MeGaO}(\text{C}_5\text{H}_3\text{N})\text{CH}_2\text{NMe}_2]^+$	60.9
192	$[\text{Me}_2\text{Ga}\cdot\text{O}(\text{C}_5\text{H}_3\text{N})]^+$	73.6
177	$[\text{MeGa}\cdot\text{O}(\text{C}_5\text{H}_3\text{N})]^+$	15.0
151	$[\text{O}(\text{C}_5\text{H}_3\text{N})\text{CH}_2\text{NMe}_2]^+$	21.4
99	$[\text{Me}_2\text{Ga}]^+$	24.2
69	$\text{Ga}^+$	26.2
58	$[-\text{CH}_2\text{NMe}_2]^+$	20.0

† At 120°C.

\* Based on  $^{69}\text{Ga}$ .

Table XIV. <sup>†</sup>Mass Spectral Data of [Me<sub>2</sub>GapzO(C<sub>5</sub>H<sub>3</sub>N)CH<sub>2</sub>NMe<sub>2</sub>]Re(CO)<sub>3</sub>

<u>* m/e</u>	<u>Assignment</u>	<u>Intensity</u>
588	[Me <sub>2</sub> Gapz•O(C <sub>5</sub> H <sub>3</sub> N)CH <sub>2</sub> NMe <sub>2</sub> Re(CO) <sub>3</sub> ] <sup>†</sup>	10.2
573	[MeGapz•O(C <sub>5</sub> H <sub>3</sub> N)CH <sub>2</sub> NMe <sub>2</sub> Re(CO) <sub>3</sub> ] <sup>†</sup>	40.7
556	[Gapz•O(C <sub>5</sub> H <sub>3</sub> N)CNMe <sub>2</sub> Re(CO) <sub>3</sub> ] <sup>†</sup>	16.8
528	[Gapz•O(C <sub>5</sub> H <sub>3</sub> N)CNMe <sub>2</sub> Re(CO) <sub>2</sub> ] <sup>†</sup>	10.9
500	[Gapz•O(C <sub>5</sub> H <sub>3</sub> N)CNMe <sub>2</sub> Re(CO)] <sup>†</sup>	10.6
472	[Gapz•O(C <sub>5</sub> H <sub>3</sub> N)CNMe <sub>2</sub> Re] <sup>†</sup>	42.2
319	[(Me <sub>2</sub> Gapz) <sub>2</sub> - Me + 2H] <sup>†</sup>	24.8
251	[(Me <sub>2</sub> Gapz) <sub>2</sub> - Me - pz + H] <sup>†</sup>	24.9
235	[MeGa•O(C <sub>5</sub> H <sub>3</sub> N)CH <sub>2</sub> NMe <sub>2</sub> ] <sup>†</sup>	94.8
192	[Me <sub>2</sub> Ga•O(C <sub>5</sub> H <sub>3</sub> N)] <sup>†</sup>	100.0
177	[MeGa•O(C <sub>5</sub> H <sub>3</sub> N)] <sup>†</sup>	16.5
151	[O(C <sub>5</sub> H <sub>3</sub> N)CH <sub>2</sub> NMe <sub>2</sub> ] <sup>†</sup>	8.4
99	[Me <sub>2</sub> Ga] <sup>†</sup>	28.0
69	Ga <sup>†</sup>	46.5
58	[-CH <sub>2</sub> NMe <sub>2</sub> ] <sup>†</sup>	38.0

<sup>†</sup> At 120°C.

\* Based on <sup>69</sup>Ga and <sup>187</sup>Re.

#### 5.3.4 $L_a Ni(NO)$

Infrared measurements of the  $L_a Ni(NO)$  complex in solution indicated the presence of a coordinated NO group ( $\nu_{NO}$ : 1770  $cm^{-1}$  THF; 1775  $cm^{-1}$   $CH_2Cl_2$ ) clearly in the nitrosyl stretching frequency region ( $\sim 1500$ - $2000$   $cm^{-1}$ ) typical of metal nitrosyl complexes [190]. The  $\nu_{NO}$  value observed for this complex is indicative of a considerably weakened N-O bond in comparison to that of free NO which absorbs in the range 1840-1833  $cm^{-1}$  [189,191].

The room temperature  $^1H$  nmr spectrum of this compound in  $CDCl_3$  solution is interesting in that it displays sharp singlets for the ' $GaMe_2$ ', ' $NMe_2$ ' and  $CH_2$  groups respectively (figure 50). This is suggestive of a square planar arrangement about the Ni center with a pseudo-meridionally coordinated organogallate ligand. However, the unlikelihood of such an arrangement for this complex in light of previous studies which have shown that square planar  $\{MNO\}^{10}$  (i.e., 10 d electrons on the metal M, when the nitrosyl ligand is formally considered to be bound as  $NO^+$ ), complexes should have an M-N-O bond angle of  $120^\circ$  [192,193] (contrary to the linear M-N-O grouping suggested by the observed ir results); led us to suspect that a fluxional process was probably responsible for the observed room temperature  $^1H$  nmr spectrum. The closely related  $[Me_2Ga(3,5-Me_2pz)(OCH_2CH_2NMe_2)]Ni(NO)$  has been shown to be stereochemically non-rigid at room temperature in solution and to possess a tetrahedral conformation about the Ni center in the solid state [194].

A variable temperature  $^1H$  nmr in both  $d_6$ -acetone and toluene- $d_8$  did indeed reveal a fluxional process to be operative in solution. In this experiment the sharp  $-GaMe_2$  signal was monitored. As the solution was

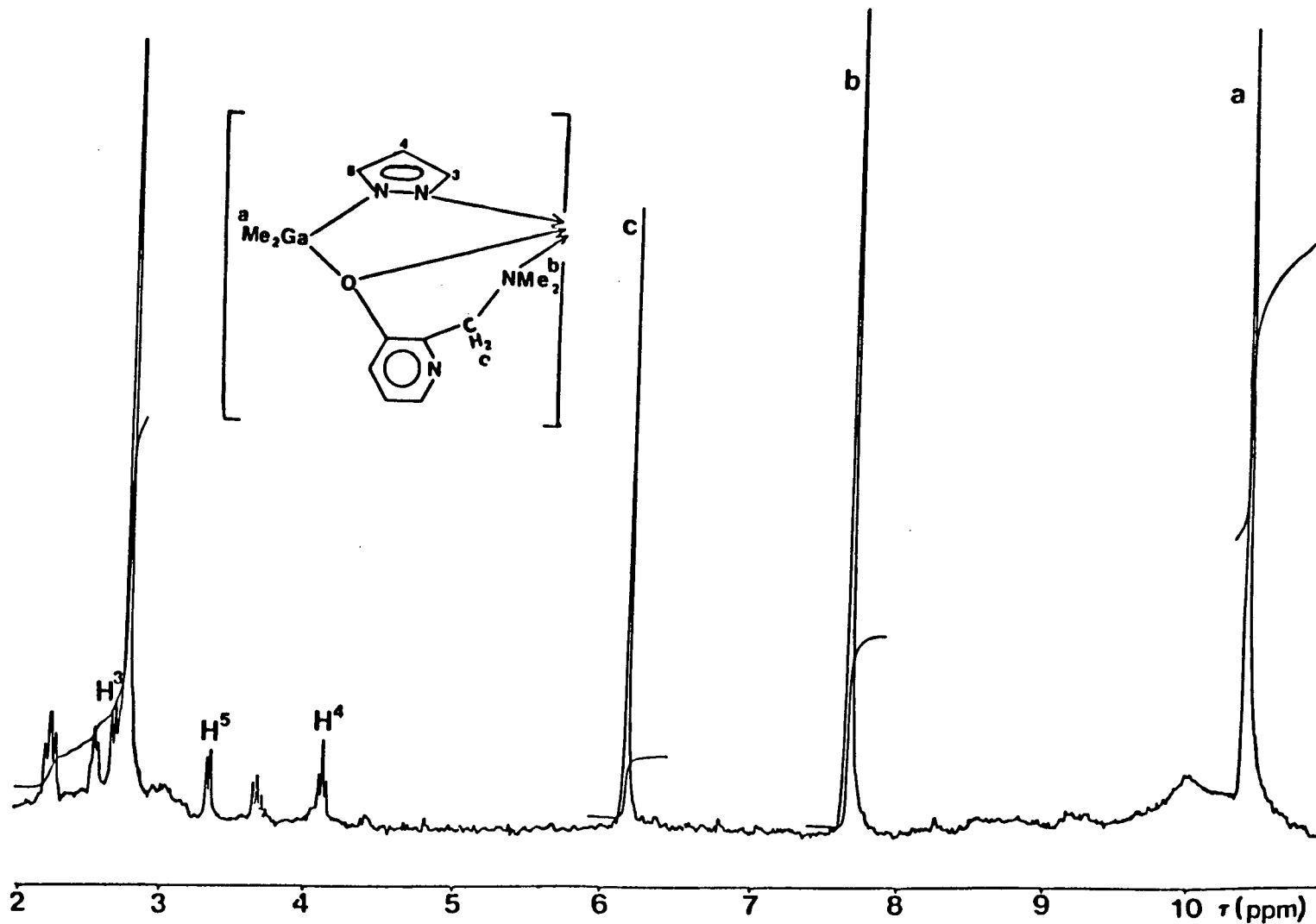


Figure 50. 80 MHz room temperature  $^1\text{H}$  nmr spectrum of  $[\text{Me}_2\text{GapzO}(\text{C}_5\text{H}_3\text{N})\text{CH}_2\text{NMe}_2]\text{Ni}(\text{NO})$  in  $\text{CDCl}_3$  solution.

cooled, marked broadening of the  $-\text{GaMe}_2$  signal was observed. At  $-85^\circ\text{C}$  (the lowest temperature attainable), it was still not possible to collapse the original signal and observe new signals in this region. Evidently, at these lower temperatures, the tetrahedral conformation was becoming established due to a slowing down of the fluxional process.

Unfortunately, instrumental limitations precluded the attainment of temperatures low enough to observe splitting of the signals.

The ir result, together with ir data reported for some  $\{\text{MNO}\}^{10}$  complexes (see Table XV below), as well as the  $^1\text{H}$  nmr results discussed above, led to the conclusion of a facially coordinated  $L_a$  ligand in the present  $L_a\text{Ni}(\text{NO})$  complex with the coordination geometry about Ni being tetrahedral.

Table XV. Comparison of  $\nu_{\text{NO}}$  Values in Selected Four-coordinate  $\{\text{MNO}\}^{10}$  Complexes.

<u>Compound</u>	<u><math>\nu_{\text{NO}}</math> (<math>\text{cm}^{-1}</math>)</u>	<u>Reference</u>
$[\text{Me}_2\text{Gapz} \cdot \text{O}(\text{C}_5\text{H}_3\text{N})\text{CH}_2\text{NMe}_2]\text{Ni}(\text{NO})$	1775 ( $\text{CH}_2\text{Cl}_2$ )	This work
$[\text{Me}_2\text{Ga}(3,5\text{-Me}_2\text{pz})(\text{OCH}_2\text{CH}_2\text{NMe}_2)]\text{Ni}(\text{NO})$	1770 ( $\text{C}_6\text{H}_{12}$ )	194
$[\text{MeGa}(3,5\text{-Me}_2\text{pz})_3]\text{Ni}(\text{NO})$	1785 ( $\text{C}_6\text{H}_{12}$ )	194
$[\text{MeGapz}_3]\text{Ni}(\text{NO})$	1786 ( $\text{C}_6\text{H}_{12}$ )	194
$[\text{Me}_2\text{Ga}(3,5\text{-Me}_2\text{pz}) \cdot \text{OCH}_2(\text{C}_5\text{H}_4\text{N})]\text{Ni}(\text{NO})$	1783 ( $\text{C}_6\text{H}_{12}$ )	173
$(\eta\text{-C}_5\text{H}_5)\text{Ni}(\text{NO})$	1833	196
$[\text{Ni}(\text{CH}_3\text{C}(\text{CH}_2\text{PPh}_2)_3)\text{NO}]^+\text{BF}_4^-$	1750 (Nujol)	195

Possible mechanisms for the proposed fluxional process are shown in figure 51. Two possibilities may be envisaged. First, a trigonal planar intermediate (A) is formed by breaking the Ni-N(amino) bond, followed by inversion at the pyramidal oxygen and reformation of the Ni-N(amino) bond. A second alternative is via a square-planar intermediate (B) with inversion at the Ni center through the plane.

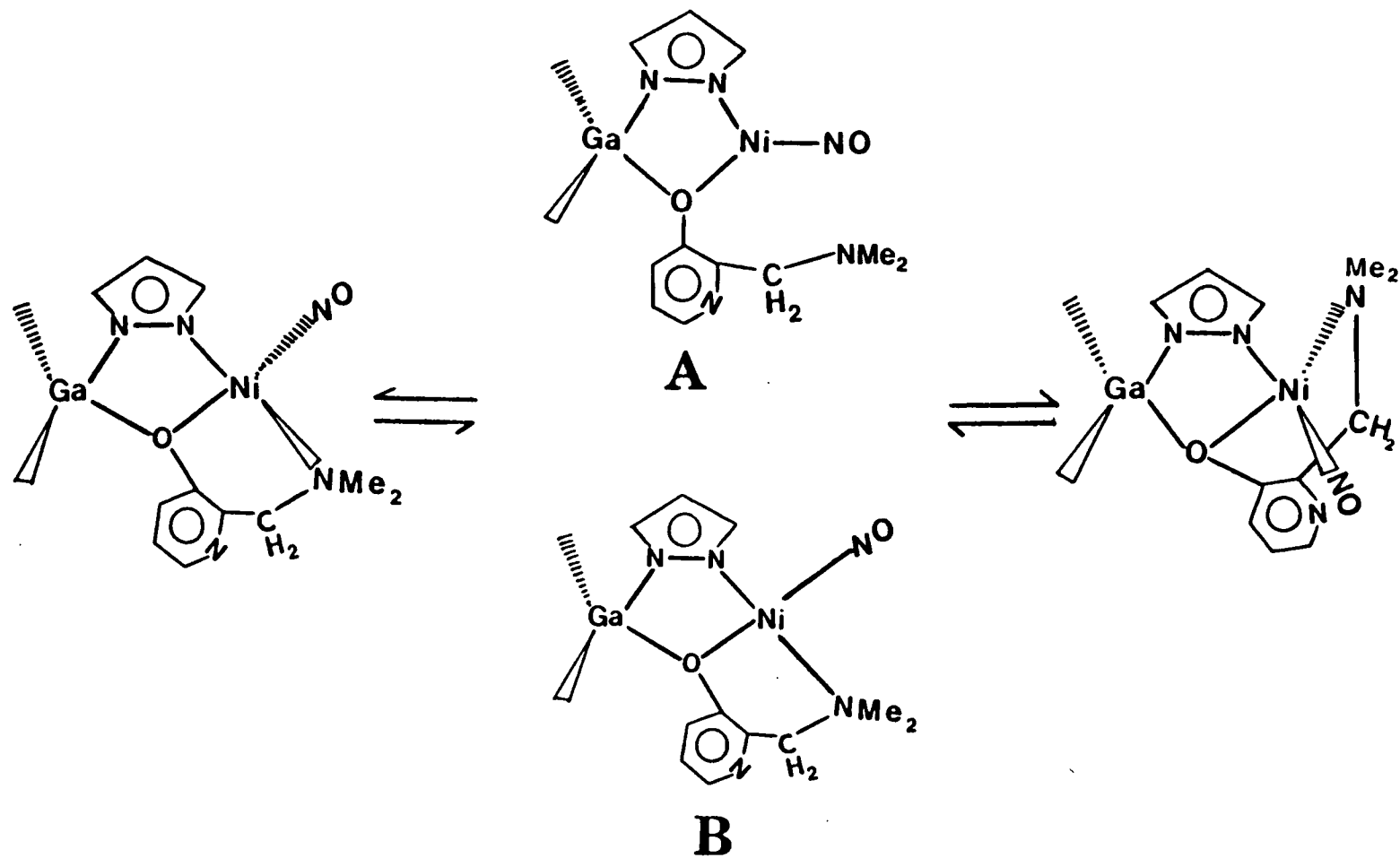


Figure 51. Proposed mechanisms for the fluxional process observed for  $[\text{Me}_2\text{Ga}\mu\text{zO}(\text{C}_5\text{H}_3\text{N})\text{CH}_2\text{NMe}_2]\text{Ni}(\text{NO})$  in  $\text{CDCl}_3$  solution. A = trigonal planar; B = square planar.

### 5.3.5 $L_qM(CO)_3$ (M = Mn, Re)

Both of these tricarbonyl complexes gave three strong  $\nu_{CO}$  bands in their respective ir spectra, indicative of a facial arrangement of the tridentate ligand (see Figure 52).

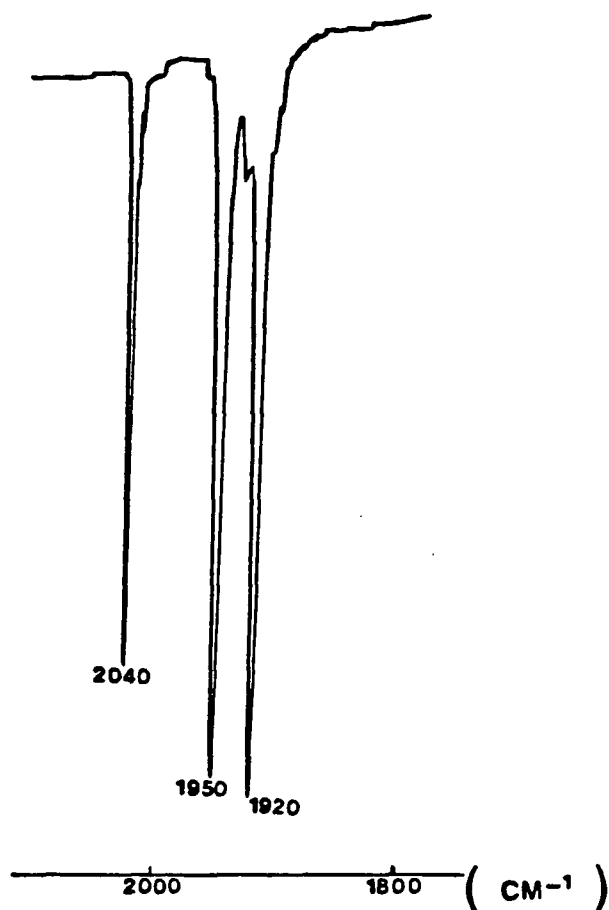


Figure 52. Ir spectrum in the  $\nu_{CO}$  region of  $[Me_2Gapz \cdot O(C_9H_6N)]Mn(CO)_3$  in cyclohexane solution.

As evident from Table XVI, p. 174, the  $\nu_{\text{CO}}$  values for the Re species are consistently lower than those of the Mn complex, again a reflection of the stronger 'M-CO'  $d\pi-\pi^*$  backbonding component in the Re species compared to the valence-isoelectronic Mn compound.

Further confirmation of a facial tridentate organogallate ligand in these  $L_qM(\text{CO})_3$  compounds is provided by the  $^1\text{H}$  nmr results. A typical spectrum is shown for the  $[\text{Me}_2\text{Gapz}\cdot\text{O}(\text{C}_9\text{H}_6\text{N})]\text{Re}(\text{CO})_3$  species in figure 53. Of significance in the spectrum is the gallium alkyl region ( $\sim 9-11 \tau$ ), where two sharp singlets were observed for the 'GaMe<sub>2</sub>' moiety as expected for inequivalent methyl groups on gallium in a facial arrangement of the ligand. A meridionally coordinated ligand, on the other hand, would lead to equivalent Ga-Me groups, and therefore a singlet in this region of the spectrum.

The mass spectral data for both the Mn and Re species are listed in Tables XVII, p. 176 and XVIII, p. 177, respectively. In both compounds, the most intense signals were those attributable to the  $[\text{MeGaO}(\text{C}_9\text{H}_6\text{N})]^+$  ion fragment. While the mass spectrum of the Re species displayed prominent parent ( $\text{P}^+$ ), and  $\text{P-Me}^+$  ion signals, the strongest signals observed for the Mn species were those corresponding to the  $\text{P-3CO}^+$  ion fragment. This observation lends further support for a stronger 'M-CO'  $\pi$ -backbonding component in the Re compound than in the Mn analog as expected when comparing valence isoelectronic first and third row transition metal carbonyl compounds in the same group.

Table XVI. Physical Data for the Complexes  $L_qMT$  (where  $L_q = Me_2Gapz \cdot O(C_6H_6N)$ )

M	T	ANALYSIS CALCD/FOUND			$\nu_{CO} (cm^{-1})$ $C_6H_{12}$ (Nujol)	$^1H$ nmr				
		C	H	N		$GaMe_2$	$H^4$	$H^5$	$H^3$	' $\eta^3-C_3H_5$ '
Re	$(CO)_3$	36.36 36.21	2.69 2.93	7.07 7.06	2025, 1927, 1901 2030, 1925, 1900 ( $CCl_4$ ) (2025, 1915, 1895)	<sup>a</sup> 10.33s 9.48s	4.05t	3.19d	2.23d	
Mn	$(CO)_3$	45.37 46.05	3.34 3.55	9.34 8.86	2040, 1950, 1920 2035, 1948, 1915 (THF)	<sup>a</sup> 10.35s 9.46s	3.86t	3.13d	2.14d	
Mo	$(CO)_2$ $\eta^3-C_3H_5$	45.27 46.03	3.97 3.91	8.34 8.33	1955, 1863 1950, 1858 ( $CCl_4$ )	<sup>a</sup> 10.28s 9.46s	3.85t	3.16d	1.66d	8.41d, 8.31d <sub>A</sub> ( $J = 9.0$ Hz) 7.06 br $H_S$ 6.50 br $H_U$
Rh $\cdot^{13}C_6H_6$	CO	43.62 43.22	3.64 3.63	8.98 9.34	(1968)	<sup>a</sup> 9.80s	3.84t	2.69d	2.28d	

<sup>a</sup> $C_6D_6$ ;  $\tau_{C_6H_6} = 2.84$  ppm;  $J_{HCCH} = 2.0$  Hz for pz protons.

s = singlet, d = doublet, t = triplet, br = broad, dd = doublet of doublets.

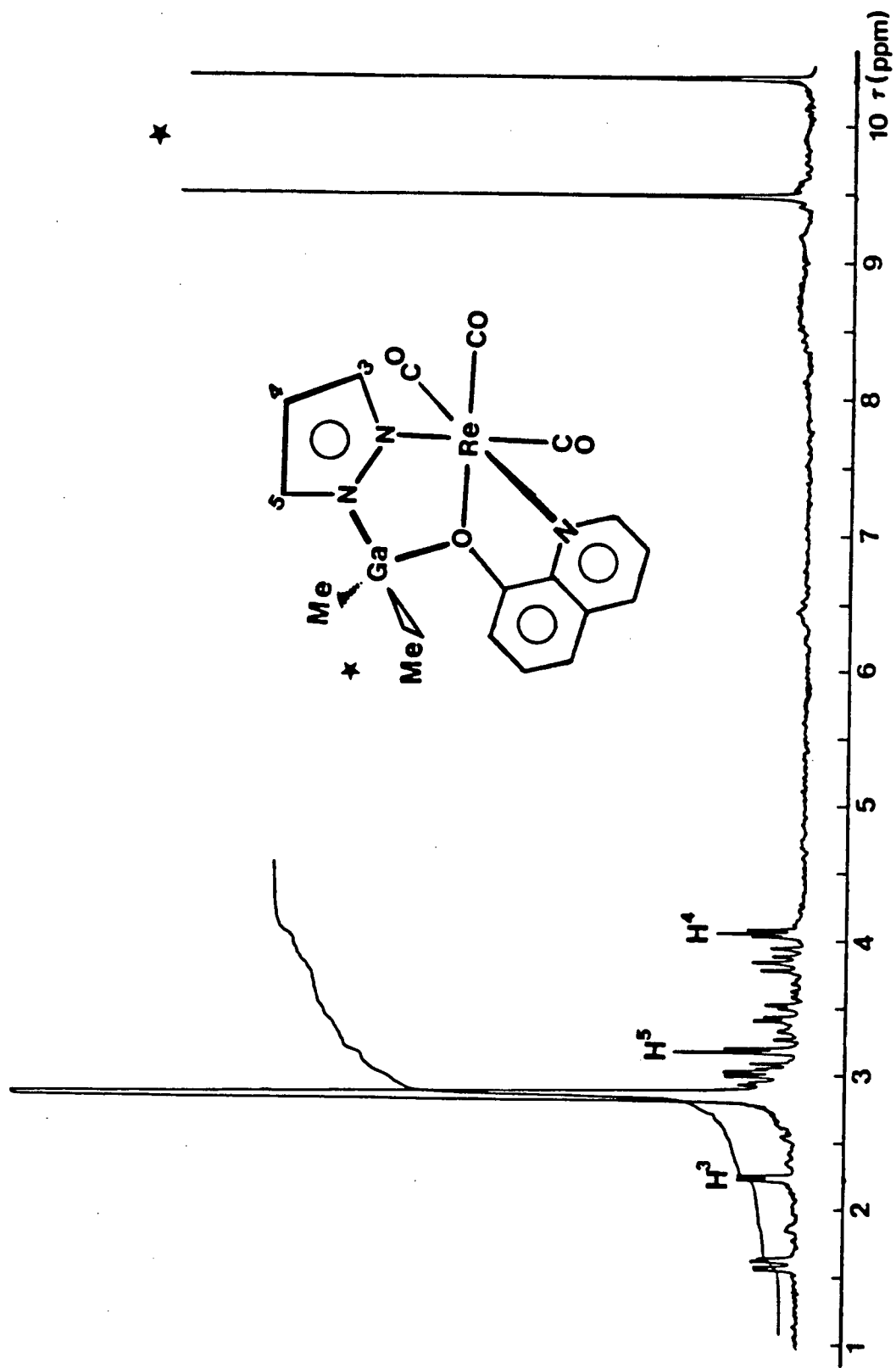


Figure 53. 80 MHz  $^1\text{H}$  nmr spectrum of  $[\text{Me}_2\text{Ga}\zeta\text{O}(\text{C}_9\text{H}_6\text{N})]\text{Re}(\text{CO})_3$  in  $\text{C}_6\text{D}_6$  solution.

Table XVII. † Mass Spectral Data of  $[\text{Me}_2\text{Gapz}\cdot\text{O}(\text{C}_9\text{H}_6\text{N})]\text{Mn}(\text{CO})_3$ 

<u>* m/e</u>	<u>Assignment</u>	<u>Intensity</u>
419	$[\text{Gapz}\cdot\text{O}(\text{C}_9\text{H}_6\text{N})\text{Mn}(\text{CO})_3]^+$	0.1
378	$[\text{MeGapz}\cdot\text{O}(\text{C}_9\text{H}_6\text{N})\text{Mn}(\text{CO})_2]^+$	0.4
365	$[\text{Me}_2\text{Gapz}\cdot\text{O}(\text{C}_9\text{H}_6\text{N})\text{Mn}]^+$	22.4
335	$[\text{Gapz}\cdot\text{O}(\text{C}_9\text{H}_6\text{N})\text{Mn}]^+$	2.4
319	$[(\text{Me}_2\text{Gapz})_2 - \text{Me}]^+$	5.4
251	$[(\text{Me}_2\text{Gapz})_2 - \text{Me} - \text{pzH}]^+$	7.9
243	$[\text{Me}_2\text{Ga}\cdot\text{O}(\text{C}_9\text{H}_6\text{N})]^+$	6.5
228	$[\text{MeGa}\cdot\text{O}(\text{C}_9\text{H}_6\text{N})]^+$	100.0
213	$[\text{Ga}\cdot\text{O}(\text{C}_9\text{H}_6\text{N})]^+$	0.1
199	$[\text{O}\cdot(\text{C}_9\text{H}_6\text{N})\text{Mn}]^+$	18.3
151	$[\text{pzHMn}(\text{CO})]^+$	3.0
99	$[\text{Me}_2\text{Ga}]^+$	13.8
84	$[\text{MeGa}]^+$	1.8
69	$\text{Ga}^+$	64.5

† At 180°C.

\* Based on  $^{69}\text{Ga}$ .

Table XVIII. † Mass Spectral Data of  $[\text{Me}_2\text{Gapz}\cdot\text{O}(\text{C}_9\text{H}_6\text{N})]\text{Re}(\text{CO})_3$ 

<u>* m/e</u>	<u>Assignment</u>	<u>Intensity</u>
581	$[\text{Me}_2\text{Gapz}\cdot\text{O}(\text{C}_9\text{H}_6\text{N})\text{Re}(\text{CO})_3]^+$	17.3
566	$[\text{MeGapz}\cdot\text{O}(\text{C}_9\text{H}_6\text{N})\text{Re}(\text{CO})_3]^+$	48.4
553	$[\text{Me}_2\text{Gapz}\cdot\text{O}(\text{C}_9\text{H}_6\text{N})\text{Re}(\text{CO})_2]^+$	9.5
510	$[\text{MeGapz}\cdot\text{O}(\text{C}_9\text{H}_6\text{N})\text{Re}(\text{CO})]^+$	5.8
497	$[\text{Me}_2\text{Gapz}\cdot\text{O}(\text{C}_9\text{H}_6\text{N})\text{Re}]^+$	33.5
482	$[\text{MeGapz}\cdot\text{O}(\text{C}_9\text{H}_6\text{N})\text{Re}]^+$	12.3
467	$[\text{Gapz}\cdot\text{O}(\text{C}_9\text{H}_6\text{N})\text{Re}]^+$	6.9
331	$[\text{O}\cdot(\text{C}_9\text{H}_6\text{N})\text{Re}]^+$	3.4
228	$[\text{MeGa}\cdot\text{O}(\text{C}_9\text{H}_6\text{N})]^+$	100.0
213	$[\text{Ga}\cdot\text{O}(\text{C}_9\text{H}_6\text{N})]^+$	14.5
99	$[\text{Me}_2\text{Ga}]^+$	3.5
78	$\text{C}_6\text{H}_6^+$	2.4
69	$\text{Ga}^+$	25.1

† At 80°C.

\* Based on  $^{69}\text{Ga}$  and  $^{187}\text{Re}$ .

5.3.6  $L^*Mo(CO)_2(\eta^3-C_3H_5)$  ( $L^* = L_a, L_q$ )

The  $L^*Mo(CO)_2(\eta^3-C_3H_5)$  compounds displayed two strong  $\nu_{CO}$  bands in their ir spectra, similar to those reported for related molybdenum dicarbonyl ' $\eta^3-C_3H_5$ ' complexes (see Table XIX below), and this is indicative of a cis-arrangement of the CO ligands about the Mo atom.

Table XIX. Comparison of  $\nu_{CO}$  values in some  $LMo(CO)_2(\eta^3-C_3H_5)$  complexes.

<u>L</u>	<u><math>\nu_{CO}</math> (cm<sup>-1</sup>) in C<sub>6</sub>H<sub>12</sub></u>	<u>Reference</u>
[Me <sub>2</sub> GapzO(C <sub>5</sub> H <sub>3</sub> N)CH <sub>2</sub> NMe <sub>2</sub> ]	1950,1805	This work
[Me <sub>2</sub> Gapz•O(C <sub>9</sub> H <sub>6</sub> N)]	1955,1863	This work
[Me <sub>2</sub> GapzOCH <sub>2</sub> (C <sub>5</sub> H <sub>4</sub> N)]	1942,1855	173
[Me <sub>2</sub> Gapz•(OCH <sub>2</sub> CH <sub>2</sub> NMe <sub>2</sub> )]	1934,1848	197
[MeGapz <sub>3</sub> ]	1948, 1860	34
[HBpz <sub>3</sub> ]	1958,1874	53
[( $\eta$ -C <sub>5</sub> H <sub>5</sub> )]	*1970,1963,1903,1889	198

\* Interpreted as indicative of the presence of two different species in solution.

The higher  $\nu_{CO}$  values observed when  $L^* = L_q$  (see Table XVI, p. 174) is suggestive of weaker backbonding to the ancillary ligand in this complex due to competitive backbonding to the  $\pi$ -system of the pyridyl ring in the

$L_q^-$  ligand. The ir data recorded for the present complexes, together with results from related molybdenum dicarbonyl ' $\eta^3-C_3H_5$ ' complexes tabulated above, in addition to the  $^1H$  nmr results discussed below, provide strong evidence for facially coordinated tridentate organogallate ligands in the present  $L^*Mo(CO)_2(\eta^3-C_3H_5)$  complexes.

The solution  $^1H$  nmr spectra of the  $L^*Mo(CO)_2(\eta^3-C_3H_5)$  complexes typified by the spectrum of  $[Me_2Gapz \cdot O(C_9H_6N)]Mo(CO)_2(\eta^3-C_3H_5)$  complex in  $C_6D_6$  solution (figure 54), clearly show the methyl groups on gallium to be inequivalent, thereby providing more supportive evidence for a facial unsymmetric tridentate organogallate ligand in these complexes. A mer conformation of the unsymmetric tridentate ligand would render the methyl groups on gallium equivalent and hence a singlet would be observed for the '-GaMe<sub>2</sub>' grouping. Positional isomerism cannot be ruled out in the above complexes, since substitution of the  $\eta^3-C_3H_5$  group for a CO in the  $L^*Mo(CO)_3^-$  ( $L^* = L_a, L_q$ ) precursor could potentially occur at any one of three positions. It is clear, however, from the  $^1H$  nmr spectrum, that substitution of the ' $\eta^3-C_3H_5$ ' group occurs exclusively at one position. Substitution of this group in more than one position would lead to more than one set of Ga-Me signals in the spectra. Molecular models indicate that substitution opposite the "pyrazolyl" moiety is most favored sterically, a position confirmed by X-ray structural determination for the related complex  $[Me_2Ga(3,5-Me_2pz(OCH_2CH_2NH_2))]Mo(CO)_2(\eta^3-C_4H_7)$  [98]. It is noteworthy, however, that in the related  $[Me_2Ga(3,5-Me_2pz)(OCH_2CH_2NH_2)]-$

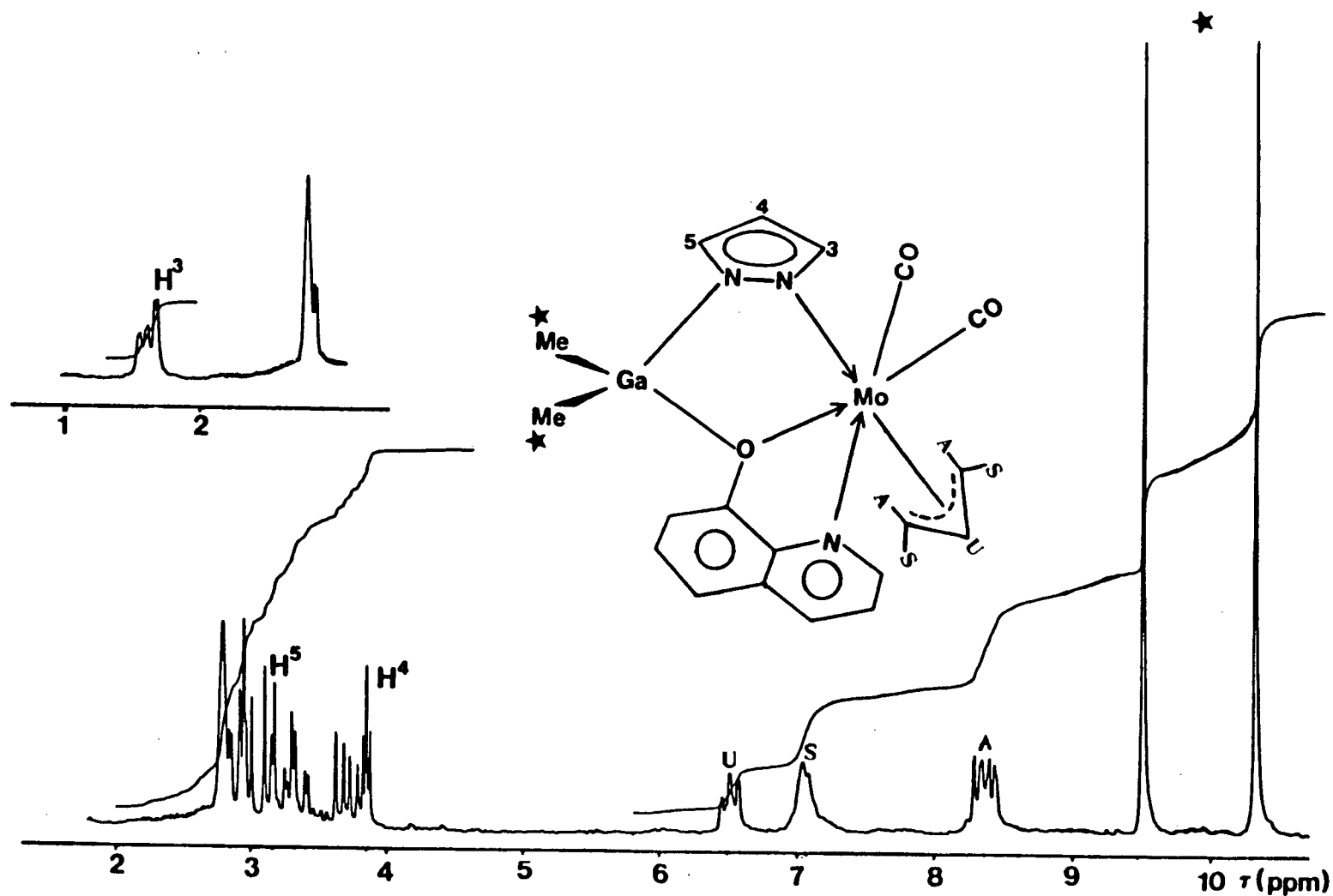


Figure 54. 80 MHz  $^1\text{H}$  nmr spectrum of  $[\text{Me}_2\text{Gapz}'\text{O}(\text{C}_9\text{H}_6\text{N})]\text{Mo}(\text{CO})_2(\eta^3\text{-C}_3\text{H}_5)$  in  $\text{C}_6\text{D}_6$  solution.

$\text{Mo}(\text{CO})_2(\eta^3\text{-C}_7\text{H}_7)$  [199], and  $[\text{Me}_2\text{Ga}(3,5\text{-Me}_2\text{pz})(\text{OCH}_2\text{CH}_2\text{SEt})]\text{Mo}(\text{CO})_2(\eta^3\text{-C}_7\text{H}_7)$  [200], the  $\eta^3\text{-C}_7\text{H}_7$  moiety occupies a position opposite the amino nitrogen and the alkyl sulfur donor atoms, respectively. This positional preference of the  $\eta^3\text{-C}_7\text{H}_7$  ligand was rationalized using structural trans effect arguments i.e., an  $\eta^3\text{-C}_7\text{H}_7$  group occupying a position trans to the pyrazolyl nitrogen would result in close contacts with the amino group or alkyl sulfido group in the latter complexes. In the  $^1\text{H}$  nmr spectrum of the  $\text{L}_a\text{Mo}(\text{CO})_2(\eta^3\text{-C}_3\text{H}_5)$  complex in  $\text{CDCl}_3$ , even though two sharp singlets were observed for the  $\text{GaMe}_2$  moiety indicating inequivalent methyl groups on gallium, the methyl groups of the  $\text{NMe}_2$  moiety seemingly remained equivalent displaying only one sharp singlet. This unusual behaviour is difficult to rationalize. The presence of only two  $\nu_{\text{CO}}$  bands in  $\text{CH}_2\text{Cl}_2$  or cyclohexane for this species indicates the presence of only one isomer, fac, in solution. Apparently some sort of configurational change involving the amino pyridyl moiety of the ligand  $\text{L}_a^-$  must be operative to explain the nmr result. The two anti protons ( $\text{H}_A$ ) for the  $\text{C}_3\text{H}_5$  group appeared as two doublets, while the syn protons ( $\text{H}_S$ ) collapsed into a broad unresolved singlet rather than the expected doublet of doublets for a syn proton coupled to two different protons, the anti ( $\text{H}_A$ ) and the unique proton ( $\text{H}_U$ ). The unique proton ( $\text{H}_U$ ) appeared as a broad unresolved triplet rather than the more complicated triplet of triplets expected for an ' $\eta^3\text{-C}_3\text{H}_5$ ' group in an unsymmetrical environment.

### 5.3.7 $L^*Rh(CO) (L^* = L_a, L_q)$

The uninegative, electronically tridentate cyclopentadienyl,  $C_5H_5^-$ , and the analogous six-electron donor ligand  $HB(3,5-Me_2pz)_3^-$ , are known to react with  $[Rh(CO)_2Cl]_2$  to give the  $(\eta-C_5H_5)Rh(CO)_2$  [201], and  $[HB(3,5-Me_2pz)_3]Rh(CO)_2$  [202,203] complexes respectively. However the introduction of the similar  $HBpz_3^-$  and  $MeGapz_3^-$  ligand systems led to the dinuclear rhodium species  $[HBpz_3]_2Rh_2(\mu-CO)_3$  [102], and  $[MeGapz_3]_2Rh_2(\mu-CO)_3$  [101]. Recently, attempts at isolating rhodium dicarbonyl complexes incorporating the uninegative, unsymmetrical, tridentate  $[Me_2Gapz(OCH_2CH_2NR_2)]^-$  ( $R = H, Me$ ), and the  $[Me_2Gapz \cdot OCH_2(C_5H_4N)]^-$  ligand systems resulted in the isolation of stable, four-coordinate, square-planar Rh(I) monocarbonyl complexes. In the complexes, structurally characterized by X-ray crystallography as  $[Me_2Gapz(OCH_2CH_2NH_2)]Rh(CO)$  [175], and  $[Me_2Gapz \cdot OCH_2(C_5H_4N)]Rh(CO)$  [176], the coordination mode of the tridentate organogallate ligands about the Rh(I) center was unequivocally demonstrated to be meridional.

The reaction of the sterically more bulky  $L_a^-$  and  $L_q^-$  ligands with  $[Rh(CO)_2Cl]_2$  dimeric species afforded orange to dark orange crystals of Rh(I) monocarbonyl compounds via transient dicarbonyl species  $L^*Rh(CO)_2$  as evident from ir monitoring of the reaction mixture during the course of the reactions. A proposed sequence for the formation of the  $L^*Rh(CO)$  complexes is shown in figure 55. The  $\nu_{CO}$  values obtained for the present complexes compare quite well with those reported for related Rh(I) monocarbonyl complexes (Table XX).



Table XX. Comparison of  $\nu_{\text{CO}}$  values in some LRh(CO) complexes.

<u>L</u>	$\nu_{\text{CO}}$ ( $\text{cm}^{-1}$ ) in $\text{CH}_2\text{Cl}_2$	Reference
$[\text{Me}_2\text{Gapz}\cdot\text{O}(\text{C}_5\text{H}_3\text{N})\text{CH}_2\text{NMe}_2]$	1970	This work
$[\text{Me}_2\text{Gapz}\cdot\text{O}(\text{C}_9\text{H}_6\text{N})]$	1968	This work
$[\text{Me}_2\text{Gapz}(\text{OCH}_2\text{CH}_2\text{NR}_2)]$	1957 (R = Me)	175
	1955 (R = H)	175
$[\text{Me}_2\text{Gapz}\cdot\text{OCH}_2(\text{C}_5\text{H}_4\text{N})]$	1962	176
$[\text{Me}(\text{Cl})\text{Gapz}\cdot\text{OCH}_2(\text{C}_5\text{H}_4\text{N})]$	1968	176

The higher  $\nu_{\text{CO}}$  value observed for  $[\text{Me}_2\text{Gapz}\cdot\text{O}(\text{C}_9\text{H}_6\text{N})]\text{Rh}(\text{CO})$  ( $1968\text{ cm}^{-1}$ ), in comparison to those observed for  $[\text{Me}_2\text{Gapz}(\text{OCH}_2\text{CH}_2\text{NR}_2)]\text{Rh}(\text{CO})$  ( $1957\text{ cm}^{-1}$ , R = Me;  $1955\text{ cm}^{-1}$ , R = H), may well result from the  $\pi$ -acidity of the pyridyl ring in the  $[\text{Me}_2\text{Gapz}\cdot\text{O}(\text{C}_9\text{H}_6\text{N})]^-$  ligand. The slightly higher  $\nu_{\text{CO}}$  value recorded for  $[\text{Me}_2\text{Gapz}\cdot\text{O}(\text{C}_5\text{H}_3\text{N})\text{CH}_2\text{NMe}_2]\text{Rh}(\text{CO})$  ( $1970\text{ cm}^{-1}$ ) may be reflective of the poor electron-donating ability of the  $[\text{Me}_2\text{Gapz}\cdot\text{O}(\text{C}_5\text{H}_3\text{N})\text{CH}_2\text{NMe}_2]^-$  ligand.

The  $^1\text{H}$  nmr spectrum of the  $\text{L}_q\text{Rh}(\text{CO})$  complex in  $\text{C}_6\text{D}_6$  solution shown in figure 56 clearly established the presence of a square planar Rh(I) species in solution for this complex. The sharp singlet observed for the  $-\text{GaMe}_2$  group is consistent with a meridionally coordinated organogallate ligand in the complex. Similarly, with the  $\text{L}_a\text{Rh}(\text{CO})$  compound, sharp singlets were displayed for the  $-\text{GaMe}_2$ ,  $-\text{NMe}_2$  and  $-\text{CH}_2-$  moieties in

conformity with a mer configuration of the ligand in this square-planar Rh(I) monocarbonyl compound.

The mass spectrum of the  $L_a$ Rh(CO) species showed trace signals (<0.5%) attributable to the  $P-3Me^+$  and  $P-2Me-CO^+$  ions. The parent ( $P^+$ ) ion was not observed and the most intense signal in the spectrum was assigned to the  $C_5H_4N^+$  ion fragments. In contrast, the mass spectrum of the  $L_q$ Rh(CO) species displayed prominent signals due to the parent ( $P^+$ ) ion, in addition to signals corresponding to the  $P-Me^+$ ,  $P-CO^+$ , and  $P-Me-CO^+$  ions. The mass spectral data for the  $[Me_2GapzO(C_9H_6N)]Rh(CO)$  complex are compiled in Table XXI on p. 187. It is interesting to note that signals were displayed at  $\sim 172$  in the mass spectrum, suggesting the presence of  $GaRh^+$  ions.

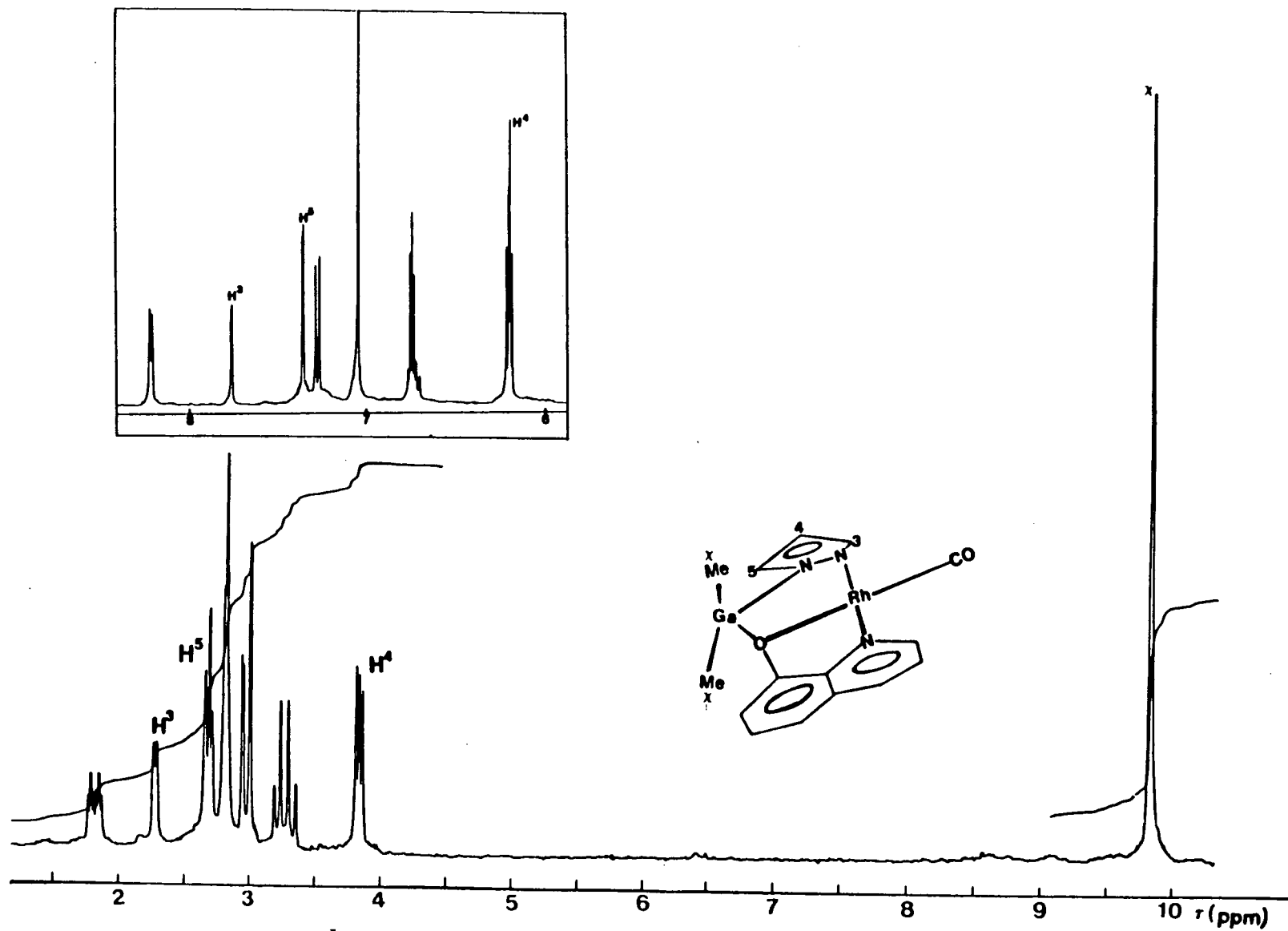


Figure 56. 80 MHz  $^1\text{H}$  nmr spectrum of  $[\text{Me}_2\text{Gapz}'\text{O}(\text{C}_9\text{H}_6\text{N})]\text{Rh}(\text{CO})$  in  $\text{C}_6\text{D}_6$  solution. (400 MHz inset.)

Table XXI. † Mass Spectral Data of  $[\text{Me}_2\text{Gapz}\cdot\text{O}(\text{C}_9\text{H}_6\text{N})]\text{Rh}(\text{CO})$ 

<u>* m/e</u>	<u>Assignment</u>	<u>Intensity</u>
441	$[\text{Me}_2\text{Gapz}\cdot\text{O}(\text{C}_9\text{H}_6\text{N})\text{Rh}(\text{CO})]^+$	16.0
426	$[\text{MeGapz}\cdot\text{O}(\text{C}_9\text{H}_6\text{N})\text{Rh}(\text{CO})]^+$	28.9
413	$[\text{Me}_2\text{Gapz}\cdot\text{O}(\text{C}_9\text{H}_6\text{N})\text{Rh}]^+$	22.2
398	$[\text{MeGapz}\cdot\text{O}(\text{C}_9\text{H}_6\text{N})\text{Rh}]^+$	100.0
383	$[\text{Gapz}\cdot\text{O}(\text{C}_9\text{H}_6\text{N})\text{Rh}]^+$	5.7
316	$[\text{Ga}\cdot\text{O}(\text{C}_9\text{H}_6\text{N})\text{Rh}]^+$	16.0
228	$[\text{MeGa}\cdot\text{O}(\text{C}_9\text{H}_6\text{N})]^+$	68.0
213	$[\text{Ga}\cdot\text{O}(\text{C}_9\text{H}_6\text{N})]^+$	34.3
199	$[\text{pzHRh}(\text{CO})]^+$	10.6
172	$[\text{GaRh}]^+$	11.0
145	$[\text{HO}(\text{C}_9\text{H}_6\text{N})]^+$	8.3
115	$[\text{Me}_2\text{Ga}\cdot\text{O}]^+$	2.5
103	$\text{Rh}^+$	12.4
78	$\text{C}_6\text{H}_6^+$	92.4
69	$\text{Ga}^+$	69.9

† At 120°C.

\* Based on  $^{69}\text{Ga}$ .

### 5.3.8 Reactivity of $L^*Rh(CO)$ ( $L^* = L_a, L_q$ )

#### i) With MeI:

The reaction of  $L_qRh(CO)$  with methyl iodide resulted in the isolation of a five-coordinate Rh(III) acetyl complex  $[Me_2GapzO(C_9H_6N)]Rh(COMe)I$ , presumably via a six-coordinate Rh(III) oxidative addition intermediate. Thus, the  $\nu_{CO}$  band of the Rh(I) monocarbonyl starting material at  $1968\text{ cm}^{-1}$  slowly disappeared upon addition of MeI, and was gradually replaced by two new bands at  $2070$  and  $1700\text{ cm}^{-1}$  which intensified with time. Attempts at isolating the species responsible for the  $\nu_{CO}$  band at  $2070\text{ cm}^{-1}$  failed, and instead crystals of the Rh(III) acetyl complex  $L_qRh(COMe)I$  ( $\nu_{CO}$ :  $1710\text{ cm}^{-1}$ , Nujol) were obtained. A proposed reaction sequence for the formation of the Rh(III) acetyl species is shown in figure 57. It is postulated that the  $\nu_{CO}$  band at  $2070\text{ cm}^{-1}$ , observed in solution during the reaction in the above sequence, is probably due to the presence of a labile six-coordinate Rh(III) product. Thus, alkyl halides are generally known to oxidatively add to square-planar  $d^8$  Rh(I) and Ir(I) centers via this mode [204,205]. This six-coordinate Rh(III) intermediate subsequently undergoes a methyl migration reaction to form the five-coordinate Rh(III) complex  $L_qRh(COMe)I$ , containing a terminal acetyl group. The solution ir spectrum of the Rh(III) acetyl product isolated is interesting in that it shows two bands at  $\sim 2070\text{ cm}^{-1}$  and  $1700\text{ cm}^{-1}$  in  $CH_2Cl_2$ , but in Nujol mull, only one strong  $\nu_{CO}$  band was observed at  $\sim 1710\text{ cm}^{-1}$ . This observation reveals the presence of both the six-coordinate Rh(III), and the five-coordinate Rh(III) acetyl species in solution. A

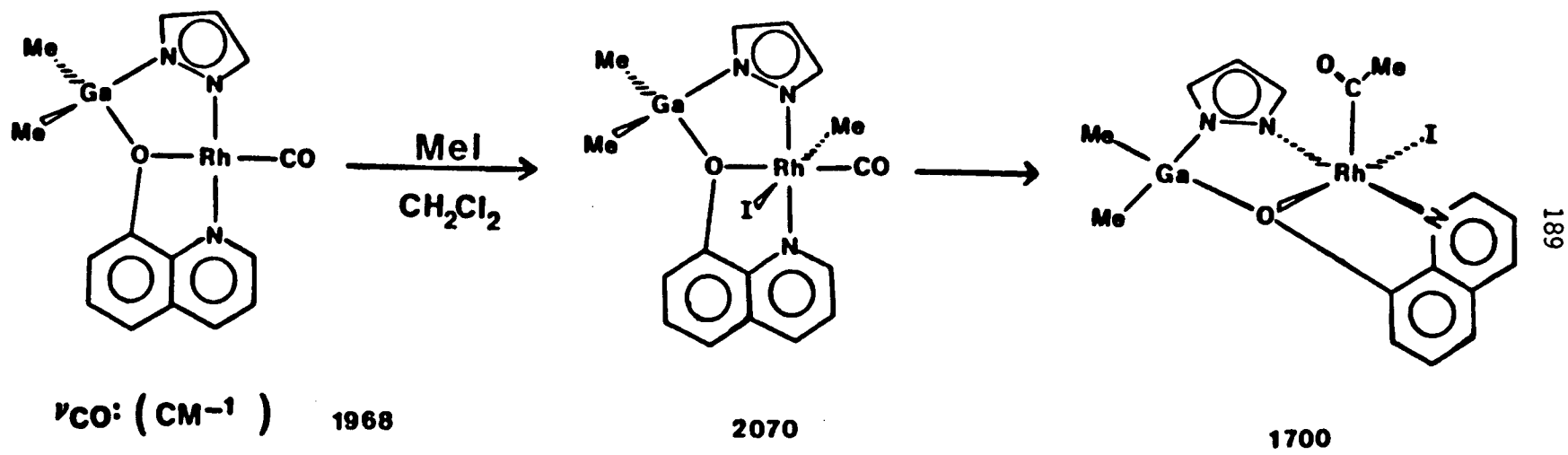


Figure 57. Proposed reaction sequence for the formation of  $[\text{Me}_2\text{Gapz}'\text{O}(\text{C}_9\text{H}_6\text{N})]\text{Rh}(\text{COMe})\text{I}$ .

similar observation has been reported for the compound  $[\text{Ru}(\eta^2\text{-COMe})\text{I}(\text{CO})\text{-}(\text{PMe}_3)_2]$ , an  $\eta^2$ -acyl complex which exists in equilibrium with its carbonyl  $\sigma$ -alkyl isomer,  $[\text{Ru}(\text{CO})_2(\text{Me})\text{I}(\text{PMe}_3)_2]$ , in solution [206].

The  $^1\text{H}$  nmr spectrum of the present  $\text{L}_q\text{Rh}(\text{COMe})\text{I}$  complex in  $\text{CDCl}_3$  solution (figure 58) is consistent with a square pyramidal arrangement about the Rh center, since such a non-planar arrangement would render the methyl groups on gallium inequivalent. The presence of two sharp singlets for the ' $\text{GaMe}_2$ ' moiety in the spectrum is in agreement with the above arrangement. The position of the COMe signal (7.58 $\tau$ ,  $\text{CDCl}_3$ ) compares nicely with those reported for similar rhodium acetyl compounds [17,176,207]; and the square pyramidal arrangement proposed has been established by X-ray crystallography for the closely related  $[\text{Me}_2\text{Gapz}(\text{OCH}_2\text{CH}_2\text{NMe}_2)]\text{Rh}(\text{COMe})\text{I}$  complex [175].

The mass spectral data for the  $[\text{Me}_2\text{Gapz}\cdot\text{O}(\text{C}_9\text{H}_6\text{N})]\text{Rh}(\text{COMe})\text{I}$  complex are collected in Table XXII, p. 192. Signals corresponding to the parent,  $\text{P}^+$ ,  $\text{P-Me}^+$ ,  $\text{P-Me-I}^+$ ,  $\text{P-2Me-I}^+$ , and  $\text{P-Me-CO}^+$  ions were observed in the mass spectrum of this compound, but no  $\text{P-CO}^+$  signals were observed. Signals arising from the latter ion are usually characteristic of transition metal carbonyl compounds containing terminally bound CO groups.

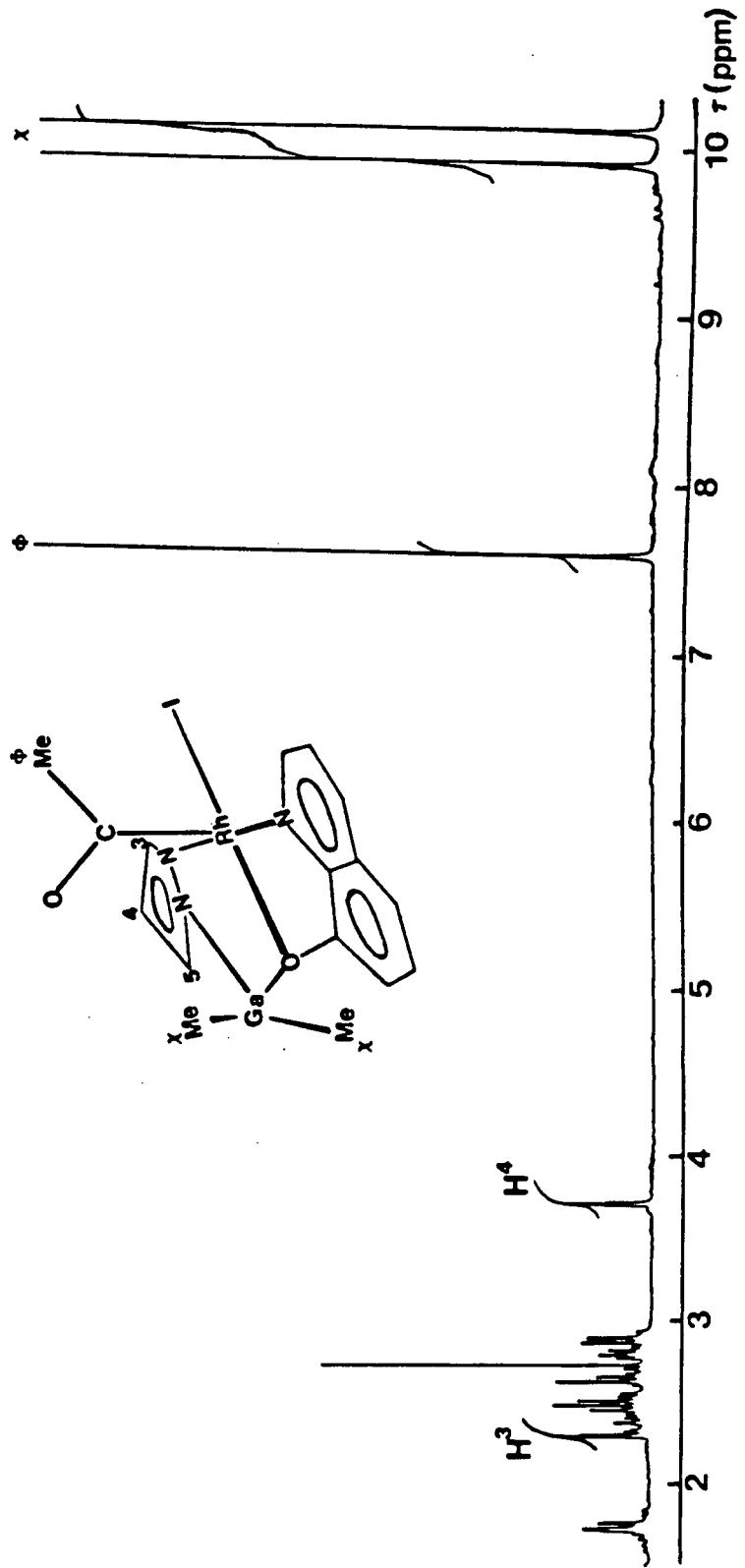


Figure 58. 270 MHz  $^1\text{H}$  nmr spectrum of  $[\text{Me}_2\text{Gapz}\cdot\text{O}(\text{C}_9\text{H}_6\text{N})]\text{Rh}(\text{COMe})\text{I}$  in  $\text{CDCl}_3$  solution.

Table XXII. <sup>†</sup>Mass Spectral Data of [Me<sub>2</sub>Gapz·O(C<sub>9</sub>H<sub>6</sub>N)]Rh(COMe)I

<u>* m/e</u>	<u>Assignment</u>	<u>Intensity</u>
583	[Me <sub>2</sub> Gapz·O(C <sub>9</sub> H <sub>6</sub> N)Rh(COMe)I] <sup>†</sup>	1.3
568	[MeGapz·O(C <sub>9</sub> H <sub>6</sub> N)Rh(COMe)I] <sup>†</sup>	15.2
553	[Gapz·O(C <sub>9</sub> H <sub>6</sub> N)Rh(COMe)I] <sup>†</sup>	0.9
540	[MeGapz·O(C <sub>9</sub> H <sub>6</sub> N)RhMeI] <sup>†</sup>	4.5
525	[Gapz·O(C <sub>9</sub> H <sub>6</sub> N)RhMeI] <sup>†</sup>	9.8
510	[Gapz·O(C <sub>9</sub> H <sub>6</sub> N)RhI] <sup>†</sup>	4.9
456	[pzO(C <sub>9</sub> H <sub>6</sub> N)RhMeI] <sup>†</sup>	8.5
441	[Me <sub>2</sub> Gapz·O(C <sub>9</sub> H <sub>6</sub> N)Rh(CO)] <sup>†</sup>	8.0
426	[MeGapz·O(C <sub>9</sub> H <sub>6</sub> N)Rh(CO)] <sup>†</sup>	14.3
413	[Me <sub>2</sub> Gapz·O(C <sub>9</sub> H <sub>6</sub> N)Rh] <sup>†</sup>	12.1
398	[MeGapz·O(C <sub>9</sub> H <sub>6</sub> N)Rh] <sup>†</sup>	100.0
383	[Gapz·O(C <sub>9</sub> H <sub>6</sub> N)Rh] <sup>†</sup>	4.9
316	[Ga·O(C <sub>9</sub> H <sub>6</sub> N)Rh] <sup>†</sup>	14.7
288	[{O(C <sub>9</sub> H <sub>6</sub> N)} <sub>2</sub> ] <sup>†</sup>	8.0
247	[O(C <sub>9</sub> H <sub>6</sub> N)Rh] <sup>†</sup>	6.7
228	[MeGa·O(C <sub>9</sub> H <sub>6</sub> N)] <sup>†</sup>	77.2
213	[Ga·O(C <sub>9</sub> H <sub>6</sub> N)] <sup>†</sup>	38.4
199	[pzHRh(CO)] <sup>†</sup>	9.8
142	[MeI] <sup>†</sup>	21.9

Table XXIII. † Mass Spectral Data of  $[\text{Me}_2\text{Gapz}\cdot\text{O}(\text{C}_9\text{H}_6\text{N})]\text{Rh}(\text{COMe})\text{I}$  (Cont'd)

<u>* m/e</u>	<u>Assignment</u>	<u>Intensity</u>
127	$\text{I}^+$	8.0
115	$[\text{Me}_2\text{Ga}\cdot\text{O}]^+$	4.5
103	$\text{Rh}^+$	11.6
84	$[\text{MeGa}]^+$	31.7
78	$\text{C}_6\text{H}_6^+$	22.3
69	$\text{Ga}^+$	55.8
58	$\text{Me}_2\text{CO}^+$	72.3
51		

† At 150°C.

\* Based on  $^{69}\text{Ga}$ .

In contrast to the mode of reactivity discussed above for the  $\text{L}_q\text{Rh}(\text{CO})$  complex, the reaction of the  $\text{L}_a\text{Rh}(\text{CO})$  monocarbonyl complex with  $\text{MeI}$  proceeds directly to the formation of what is thought to be a six-coordinate  $\text{Rh}(\text{III})$  oxidative trans-addition product  $\text{L}_a\text{Rh}(\text{Me})(\text{I})\text{CO}$ . Quite interestingly, such six-coordinate addition products containing  $\sigma$ -bonded methyl groups have not been observed either as intermediates or as the net reaction products in the analogous reaction of the related cyclopentadienyl rhodium carbonyl compounds with  $\text{MeI}$ . For example, reaction of  $(\eta\text{-C}_5\text{Me}_5)\text{Rh}(\text{CO})_2$  with  $\text{MeI}$  proceeds directly to the  $(\eta\text{-C}_5\text{Me}_5)\text{Rh}(\text{CO})(\text{COMe})\text{I}$  acetyl complex at 50°C [208]. Thus, the diagnostic terminal  $\nu_{\text{CO}}$  band at

2060  $\text{cm}^{-1}$ , observed during the reaction of  $L_a\text{Rh}(\text{CO})$  with MeI, provided strong evidence for the presence of a six-coordinate Rh(III) species in solution.

The only crystalline product isolated from the reaction of  $L_a\text{Rh}(\text{CO})$  with MeI was identified as the six-coordinate trans-addition Rh(III) derivative, since only a single band was observed in the carbonyl stretching frequency region, and no band was seen in the acetyl stretching frequency regions of the spectrum ( $\nu_{\text{CO}}$ : 2060  $\text{cm}^{-1}$ ,  $\text{CH}_2\text{Cl}_2$ ; 2055  $\text{cm}^{-1}$ , Nujol). These ir results are consistent with a six-coordinate Rh(III) species formulated as  $[\text{Me}_2\text{Gapz}\cdot\text{O}(\text{C}_5\text{H}_3\text{N})\text{CH}_2\text{NMe}_2]\text{Rh}(\text{Me})(\text{I})\text{CO}$ .

The room temperature  $^1\text{H}$  nmr data for the present  $L_a\text{Rh}(\text{Me})(\text{I})\text{CO}$  compound displaying two sharp singlets for the ' $\text{GaMe}_2$ ' and ' $\text{NMe}_2$ ' groupings were consistent with a facial coordination of the organogallate ligand. A sharp singlet was observed for the Rh-Me resonance at  $\sim 9.3\tau$ ; signals attributable to a -COMe resonance were not observed in the spectrum.

A mass spectral study of the  $L_a\text{Rh}(\text{Me})(\text{I})\text{CO}$  complex under electron impact (EI) conditions did not give a spectrum of any worth probably due to thermal lability or non-volatility of the compound. However, with the Fast Atom Bombardment (FAB) technique, signals corresponding to the  $[\text{P-Me}]^+$ ,  $[\text{P+H}]^+$  and  $[\text{P-H}]^+$  ions were observed. The  $[\text{P+H}]^+$  and  $[\text{P-H}]^+$  ions are generally characteristic for molecules ionized by the FAB technique [209]. The presence of signals corresponding to the  $[\text{P+H}]^+$ , and  $[\text{P-H}]^+$

ions in the mass spectrum is an indirect confirmation of the molecular weight of this compound at ~590, and the formulation is further supported by elemental analyses data (see section 5.2.17, p. 146). It is noteworthy however, that the FAB technique was recently used successfully to determine the molecular weight of the silyl rhodium species,  $(\eta\text{-C}_5\text{H}_5)\text{RhCODSi}(\text{CH}_2)_3(\text{MeO})_3$  [210], an organometallic compound that is highly intractable, oily, thermally labile, and moisture-sensitive.

In order to establish the correct structure of the present complex unequivocally, crystals of the  $[\text{Me}_2\text{Gapz}\cdot\text{O}(\text{C}_5\text{H}_3\text{N})\text{CH}_2\text{NMe}_2]\text{Rh}(\text{Me})(\text{I})\text{CO}$  compound have been submitted for X-ray crystal structure determination which is currently in progress.

ii) With  $\text{I}_2$ :

Addition of molecular iodine to a  $\text{CH}_2\text{Cl}_2$  solution of  $\text{L}^*\text{Rh}(\text{CO})$  ( $\text{L}^* = \text{L}_a, \text{L}_q$ ) resulted in the immediate disappearance of the  $\nu_{\text{CO}}$  band attributable to the appropriate Rh(I) monocarbonyl starting material with concomitant appearance of a new  $\nu_{\text{CO}}$  band at  $2090\text{ cm}^{-1}$  ( $\text{L}^* = \text{L}_a$ ), or  $2085\text{ cm}^{-1}$  ( $\text{L}^* = \text{L}_q$ ). The new bands suggest a weakly-bound CO ligand to the Rh metal center in the products. Oxidation of the rhodium center ( $\text{Rh}(\text{I})(\text{d}^8) \rightarrow \text{Rh}(\text{III})(\text{d}^6)$ ) would lead to weaker backbonding contribution from the metal, a strengthening of the C-O bond and consequently an increased  $\nu_{\text{CO}}$  value. Based on this observation, it does appear that a six-coordinate Rh(III) diiodide species  $\text{L}^*\text{RhI}_2(\text{CO})$  had formed, although analytically pure samples of the product could not be isolated. The  $\nu_{\text{CO}}$  values of the present  $\text{L}^*\text{RhI}_2(\text{CO})$  species are in good agreement with those reported for some related Rh(III) diiodides (see Table XXIV below).

Table XXIV. Comparison of  $\nu_{\text{CO}}$  values in  $\text{LRhI}_2(\text{CO})$  complexes.

<u>L</u>	<u><math>\nu_{\text{CO}}(\text{cm}^{-1})</math> in <math>\text{CH}_2\text{Cl}_2</math></u>	<u>Reference</u>
$[\text{Me}_2\text{Gapz}\cdot\text{O}(\text{C}_5\text{H}_3\text{N})\text{CH}_2\text{NMe}_2]$	2090	This work
$[\text{Me}_2\text{Gapz}\cdot\text{O}(\text{C}_9\text{H}_6\text{N})]$	2085	This work
$[\text{Me}_2\text{Gapz}(\text{OCH}_2\text{CH}_2\text{NR}_2)]$ (R = H, Me)	2090	175
$[\text{Me}_2\text{Gapz}\cdot\text{OCH}_2(\text{C}_5\text{H}_4\text{N})]$	2095	176
$[\text{HB}(3,5\text{-Me}_2\text{pz})_3]$	2090	203
$[\text{HBpz}_3]$	2112	102
$[\text{Bpz}_4]$	2100	102
$[(\eta\text{-C}_5\text{H}_5)]$	2065 (Nujol)	211
$[(\eta\text{-C}_5\text{Me}_5)]$	2035	212

It is interesting, however, that the  $\nu_{\text{CO}}$  values for the pyrazolylgallate/-borate-containing species are consistently higher than the values reported for the analogous cyclopentadienyl-containing rhodium diiodide species. This is rather unusual since they oppose the trend previously established for complexes incorporating these ligands [34,53]. That is, pyrazolylgallate tridentate ligands, and the related isoelectronic tridentate pyrazolylborate anions, are generally stronger net electron donors compared to the tridentate cyclopentadienyl ligand and give rise to lower  $\nu_{\text{CO}}$  values in analogous transition metal carbonyl complexes.

#### 5.4 Summary

The coordination compounds  $[\text{Me}_2\text{GaO}(\text{C}_5\text{H}_3\text{N})\text{CH}_2\text{NMe}_2]$ , and  $[\text{Me}_2\text{Ga}\cdot\text{O}(\text{C}_9\text{H}_6\text{N})]_2$  have been isolated and structurally characterized by X-ray crystal structure analyses. The latter compound is dimeric with each gallium atom assuming a distorted trigonal bipyramidal geometry. Steric constraints prevented dimerization of the  $[\text{Me}_2\text{GaO}(\text{C}_5\text{H}_3\text{N})\text{CH}_2\text{NMe}_2]$  compound, which consists of monomeric units containing tetrahedrally coordinated gallium atoms.

Facial coordination of the  $[\text{Me}_2\text{Gapz}\cdot\text{O}(\text{C}_9\text{H}_6\text{N})]^- (\text{L}_q^-)$  ligand has been demonstrated for a variety of transition metal complexes. The versatility of the  $[\text{Me}_2\text{Gapz}\cdot\text{O}(\text{C}_5\text{H}_3\text{N})\text{CH}_2\text{NMe}_2]^- (\text{L}_a^-)$  ligand has been demonstrated by the successful isolation of the  $\text{L}_a\text{M}(\text{CO})_3$  ( $\text{M} = \text{Mn}, \text{Re}$ ) octahedral complexes which exist in both fac and mer conformations in solution. The latter complexes represent the first and the only transition metal carbonyl complexes in which both the fac and mer isomers, incorporating the tridentate ligand, have been shown to co-exist in solution. The four-coordinate nickel nitrosyl complex  $\text{L}_a\text{Ni}(\text{NO})$  is believed to possess a tetrahedral transition metal center, although stereochemical nonrigidity of the complex in solution must be operative to explain the square-planar arrangement suggested by the room temperature  $^1\text{H}$  nmr spectral data.

Meridional coordination has also been demonstrated for the  $\text{L}_a^-$ , and  $\text{L}_q^-$  ligands in the formation of the four-coordinate square-planar Rh(I) monocarbonyl species,  $\text{L}^*\text{Rh}(\text{CO})$  ( $\text{L}^* = \text{L}_a, \text{L}_q$ ). These compounds undergo facile oxidative addition reaction with molecular iodine to give Rh(III)

diodide  $L^*RhI_2(CO)$  species. However, with methyl iodide,  $L_qRh(CO)$  undergoes facile oxidative addition, followed by methyl migration to give a five-coordinate Rh(III) acetyl species  $L_qRh(COMe)I$ . In contrast,  $L_qRh(CO)$  oxidatively adds methyl iodide to give what is thought to be a six-coordinate Rh(III) trans-addition species  $L_aRh(Me)(I)CO$  as the net reaction product.

## CHAPTER VI

## CONCLUSION AND PERSPECTIVES

The  $\text{MeGapz}_3^-$  and  $\text{HBpz}_3^-$  ligands can, on the one hand, successfully mimic the behaviour of the  $\eta\text{-C}_5\text{H}_5^-$  ligand system but, more importantly, on the other hand they can display significantly different behaviour. This versatility has been demonstrated in the present work by exploring the reactivity of the  $\text{LMo(CO)}_3^-$  anions towards (i) alkyl halides and protonating species ( $\text{L} = \text{MeGapz}_3$ ), (ii) a variety of transition metal halide species ( $\text{L} = \text{MeGapz}_3$  or  $\text{HBpz}_3$ ) and (iii) group 14 (Si, Ge, Sn) alkyl or aryl halide species ( $\text{L} = \text{MeGapz}_3$ ).

The successful isolation of the  $\text{M}^+\text{MeGapz}_3\text{Mo(CO)}_3^-$  ( $\text{M}^+ = \text{Na}^+$ ,  $\text{Et}_4\text{N}^+$ ,  $\text{HAsPh}_3^+$ ) salts, the requirement of a strong acid to fully protonate the  $\text{MeGapz}_3\text{Mo(CO)}_3^-$  anion, the dissociation of the Mo-H bond in the hydride  $[\text{MeGapz}_3]\text{Mo(CO)}_3\text{H}$ , and the transformation of the ' $[\text{MeGapz}_3]\text{Mo(CO)}_3\text{Me}$ '  $\sigma$ -methyl complex to the quasi-six-coordinate  $[\text{MeGapz}_3]\text{Mo(CO)}_2(\eta^2\text{-COMe})$  taken together suggests a strong preference for six-coordination by the Mo centre in complexes containing the  $\text{MeGapz}_3^-$  ligand. The transformation of the  $[\text{MeGapz}_3]\text{Mo(CO)}_3\text{R}$  species and the related  $[\text{HBpz}_3]\text{Mo(CO)}_3\text{R}$  ( $\text{R} = \text{Me}, \text{Ph}$ ) compounds to the  $\text{LMo(CO)}_2(\eta^2\text{-COR})$  complexes ( $\text{L} = \text{MeGapz}_3$  or  $\text{HBpz}_3$ ;  $\text{R} = \text{Me}$  or  $\text{Ph}$ ) has never been duplicated in the chemistry of the analogous

$(\eta\text{-C}_5\text{H}_5)\text{Mo}(\text{CO})_3\text{R}$  or  $(\eta\text{-C}_5\text{Me}_5)\text{Mo}(\text{CO})_3\text{R}$  complexes. However, the lack of success in forming an  $\eta^2\text{-COEt}$  product in the present study is probably related to the instability of the  $\sigma\text{-ethyl}$   $[\text{MeGapz}_3]\text{Mo}(\text{CO})_3\text{Et}$  precursor and its tendency to decompose. In fact, the pronounced instability, difficulty in purification, and decomposition accompanied by the formation of ethylene has been noted previously by McCleverty and Wilkinson for the analogous  $(\eta\text{-C}_5\text{H}_5)\text{Mo}(\text{CO})_3\text{Et}$  compound [213]. Similar difficulty may have been encountered by Curtis et al. who provided structural information for the  $[\text{HBpz}_3]\text{Mo}(\text{CO})_2(\eta^2\text{-COR})$  ( $\text{R} = \text{Me}, \text{Ph}$ ) compounds [65] with no data for the corresponding  $\eta^2\text{-COEt}$  derivative. In any event, mechanistic studies as well as thermodynamic data for these  $\text{LMo}(\text{CO})_2(\eta^2\text{-COR})$  ( $\text{L} = \text{MeGapz}_3$  or  $\text{HBpz}_3$ ;  $\text{R} = \text{alkyl or aryl}$ ) complexes should provide some clues as to the factors governing the stability of the above  $\eta^2\text{-acyl}$  compounds over the seven-coordinate  $\text{LMo}(\text{CO})_3\text{R}$  precursors. Such information may provide useful insights into the possibility of promoting hydride migration from a metal hydride to a coordinated CO group in the same metal to form an  $\eta^2\text{-fomyl}$  complex. The above reaction has never been directly observed but the reverse reaction is well established [96].

One of the primary objectives of this work was to develop a synthetic route to heterobimetallic complexes incorporating the tridentate pyrazolyl gallate/borate ligands in which direct metal-metal bonds are featured and to provide insights into the structural, spectroscopic and bonding properties of these compounds. This objective has largely been fulfilled. The 3:3:1 structure demonstrated for the  $[\text{MeGapz}_3]\text{Mo}(\text{CO})_3\text{X}$  ( $\text{X} = \text{CuPPh}_3$  or  $\text{SnPh}_3$ ) complexes represents the first and the only known examples of this

geometry for  $\text{LMo}(\text{CO})_3\text{X}$  ( $\text{L} = \eta\text{-C}_5\text{H}_5$ ,  $\text{HBpz}_3$  or  $\text{MeGapz}_3$ ;  $\text{X} =$  two electron donor ligand) type complexes. It appears from this study, that the 3:3:1 structure is most favoured by a substituent pattern which include an ancillary ligand with low energy vacant orbitals of appropriate symmetry, and a single substituent that is both a good  $\sigma$  donor and a good  $\pi$  donor, yet small in size, occupying the axial position. The above factors are in accord with the theoretical predictions of Kubacek et al. [141], and Hoffmann et al. [214]. As noted by the former authors, an axial halide (even though a good  $\pi$  donor), destabilizes the 3:3:1 structure. This is borne out by the adoption of a 3:4 structure by Curtis 'bromo' derivative  $\text{HBpz}_3\text{Mo}(\text{CO})_3\text{Br}$  [60], and also the fluxional behaviour of the ' $\text{SnMe}_2\text{Cl}$ ' derivative discussed in Chapter IV. The similarity in spectroscopic properties of the  $\text{Mo-M}'$  ( $\text{M}' = \text{Zr}$  or  $\text{Hf}$ ) compounds to those of the  $\text{Mo-M}'$  ( $\text{M}' = \text{Si}$ ,  $\text{Ge}$  or  $\text{Sn}$ ) complexes is a reflection of the tendency of highly electron deficient transition metals in high oxidation states to behave like main group elements (Lewis acids).

The general chemical reactivity of the heterobimetallic compounds reported in this thesis needs further investigation. Preliminary studies in this regard, indicated the formation of unidentified mixture of compounds. It may well be that the steric bulk of the tridentate pyrazolyl gallate/borate ligand is an inhibiting factor in the reactivity of these compounds. In fact the related homobimetallic  $[\text{HBpz}_3]_2\text{Mo}_2(\text{CO})_4$  ( $\text{Mo}\equiv\text{Mo}$ ) dimer has been reported as unreactive toward acetylenes,  $\text{Ph}_2\text{CN}_2$ ,  $\text{CH}_2\text{N}_2$ ,  $\text{P}(\text{OMe})_3$  and  $\text{CO}$  by Curtis et al. [38]. Further studies into the catalytic potential of these heterobimetallic complexes is needed especially for complexes of the type  $\text{LMM}'$  (where  $\text{L} = \text{MeGapz}_3$ , or  $\text{HBpz}_3$ ;

M = Ti-Hf or V-Ta; and M' = Ru, Rh, Ir, Pd or Pt). One obvious problem in this regard, is to ensure that the initial complex remains intact during the catalytic cycle.

In Chapter V, the ligand  $L_q^-$  gave the dimer  $[Me_2GaO(C_9H_6N)]_2$ , and the fac  $L_qM(CO)_3$  (M = Mn or Re) complexes. In contrast, the  $L_a$  ligand yielded the monomer  $Me_2GaO(C_5H_3N)CH_2NMe_2$  and both the fac and mer isomers of  $L_aM(CO)_3$  (M = Mn or Re) complexes. The latter octahedral tricarbonyl complexes are the only examples of such complexes incorporating the unsymmetric tridentate ligand in both the fac and mer conformations. It is difficult to rationalize the difference in reactivity toward MeI observed for the  $L_aRh(CO)$  and  $L_qRh(CO)$  complexes. It is probable, however, that the Rh-Me bond is stronger in the  $L_aRh(Me)(I)CO$  species compared to the  $L_qRh(Me)(I)CO$  species, hence methyl migration is discouraged in the former compound. These observations illustrate how a slight change in the design of the unsymmetric ligands can lead to significantly different behaviour.

References

1. E. Buchner, Ber. 22, 842 (1889).
2. J.J. Kaufman, H.J.T. Preston, E. Kernman and C.L. Cusachs, Int. J. Quantum Chem., Symp 7, 249 (1973).
3. G. Dedichen, Ber. 39, 1831 (1906).
4. G. Minghetti, G. Banditelli and F. Bonati, J. Chem. Soc., Dalton Trans., 1851 (1979).
5. A.L. Bandini, G. Banditelli, F. Bonati, F. Demartin, M. Manassero and G. Minghetti, J. Organomet. Chem. 238, C9 (1982).
6. C.W. Eignbrot, Jr. and K.N. Raymond, Inorg. Chem. 20, 1553 (1981).
7. S. Trofimenko, Chem. Rev. 72, 497 (1972).
8. R.B. King and A. Bond, J. Organomet. Chem. 73, 115 (1974).
9. K.S. Chong, S.J. Rettig, A. Storr and J. Trotter, Can. J. Chem. 57, 3090 (1979).
10. R. Usón, L.A. Oro, M.A. Ciriano, M.T. Pinillos, A. Tiripicchio and M. Tiripicchio Camellini, J. Organomet. Chem. 205, 247 (1981).
11. K.A. Beveridge, G.W. Bushnell and S.R. Stobart, Organometallics 2, 1447 (1983).
12. S. Trofimenko, J. Am. Chem. Soc. 89, 3170 (1967).
13. S. Trofimenko, J. Am. Chem. Soc. 92, 5118 (1970).
14. K.R. Breakell, D.J. Patmore and A. Storr, J. Chem. Soc., Dalton Trans. 749 (1975).
15. M. DiVaira and F. Mani, Inorg. Chim. Acta 70, 99 (1983).
16. S. Trofimenko, Accts. Chem. Res. 4, 17 (1971).
17. A. Shaver, J. Organomet. Chem. Libr. 3, 157 (1977).
18. S. Trofimenko, Inorg. Synth. 12, 99 (1970).
19. C.A. Kosky, P. Ganis and G. Avitabile, Acta Cryst. Sect. B 27, 1859 (1971).
20. G.J. Bullen, R. Mason and P. Pauling, Inorg. Chem. 4, 456 (1965), and references therein.

21. F.A. Cotton, M. Jeremic and A. Shaver, *Inorg. Chim. Acta* 6, 543 (1972).
22. M.I. Bruce and A.P.P. Ostazewski, *J. Chem. Soc., Chem. Commun.*, 1124 (1972).
23. F.A. Cotton and T.J. Marks, *J. Am. Chem. Soc.* 92, 5114 (1970).
24. H.C. Clark and L.E. Manzer, *Inorg. Chem.* 13, 1291 (1974).
25. H.C. Clark and L.E. Manzer, *J. Am. Chem. Soc.* 95, 3812 (1973).
26. P.M. Treichel, W.J. Knebel and R.W. Hess, *J. Am. Chem. Soc.* 93, 5424 (1971).
27. A.D. Westland, *J. Chem. Soc.*, 3060 (1965).
28. D.H. Gerlack, A.R. Kane, G.W. Parshall, J.P. Jesson and E.L. Muetterties, *J. Am. Chem. Soc.* 93, 3543 (1971).
29. G.A. Larkin, R. Mason and M.G.H. Wallbridge, *J. Chem. Soc. (D)*, 1054 (1971).
30. H.C. Clark and R.J. Puddephatt, *Inorg. Chem.* 10, 18 (1971).
31. S. Trofimenko, *Inorg. Chem.* 8, 2675 (1969).
32. T. Desmond, F.J. Lalor, G. Ferguson, B. Ruhl and M. Parvez, *J. Chem. Soc., Chem. Commun.*, 55 (1983).
33. T. Desmond, F.J. Lalor, G. Ferguson and M. Parvez, *J. Chem. Soc., Chem. Commun.*, 457 (1983).
34. K.R. Breakell, S.J. Rettig, D.L. Singbeil, A. Storr and J. Trotter, *Can. J. Chem.* 56, 2099 (1978).
35. K.R. Breakell, S.J. Rettig, A. Storr and J. Trotter, *Can. J. Chem.* 57, 139 (1979).
36. M.R. Churchill, K. Gold and C.E. Maw, Jr., *Inorg. Chem.* 9, 1597 (1970).
37. B.K. Nicholson, *J. Organomet. Chem.* 265, 153 (1984).
38. M.D. Curtis, K. Shui, W.M. Butler and J.C. Huffman, *J. Am. Chem. Soc.* 108, 3335 (1986).
39. S.J. Rettig, A. Storr and J. Trotter, *Can. J. Chem.* 57, 1823 (1979).
40. W.J. Kasowski and J.C. Bailar, Jr., *J. Am. Chem. Soc.* 91, 3212 (1969).

41. K.S. Chong, S.J. Rettig, A. Storr and J. Trotter, *Can. J. Chem.* 55, 4166 (1977).
42. J.S. Thompson, J.L. Zitzman, T.J. Marks and J.A. Ibers, *Inorg. Chim. Acta* 46, L101 (1980).
43. K.S. Chong, S.J. Rettig, A. Storr and J. Trotter, *Can. J. Chem.* 56, 1212 (1978).
44. K.S. Chong, S.J. Rettig, A. Storr and J. Trotter, *Can. J. Chem.* 57, 1335; 3113 (1979).
45. W.L. Jolly, *The Synthesis and Characterization of Inorganic Compounds*, Prentice-Hall, Inc., New Jersey (1970).
46. J.A. Riddick and W.B. Bunger, *Organic Solvents, Physical Properties and Methods of Purification*, 3rd. edition, *Techniques of Chemistry Vol. II*, John Wiley and Sons, Inc., New York (1970).
47. A. Storr and B.S. Thomas, *Can. J. Chem.* 48, 3667 (1970).
48. N.N. Greenwood and K. Wade, *J. Chem. Soc.*, 1527 (1956).
49. H. Schmidbaur and W. Findeiss, *Angew. Chem., Int. Ed.* 3, 696 (1964).
50. D.P. Tate, W.R. Knipple and J.M. Augl, *Inorg. Chem.* 1, 433 (1962).
51. F.A. Cotton, *Inorg. Chem.* 3, 702 (1964).
52. K.F. Purcell and J.C. Kotz, *Inorganic Chemistry*, W.B. Saunders Company, Philadelphia (1977).
53. S. Trofimenko, *J. Am. Chem. Soc.* 91, 588 (1969).
54. F.A. Cotton, C.A. Murillo and B.R. Stults, *Inorg. Chim. Acta* 22, 75 (1977).
55. T.S. Piper and G. Wilkinson, *J. Inorg. Nucl. Chem.* 3, 104 (1956).
56. M. Cousins and M.L.H. Green, *J. Chem. Soc.*, 889 (1963).
57. R. Davis and L.A.P. Kane-Maguire. In *Comprehensive Organometallic Chemistry*, Vol 3; Pergamon Press; Oxford, England (1982).
58. W.W. Greaves and R.J. Angelici, *J. Organomet. Chem.* 191, 49 (1980).
59. D.L. Reger, C.A. Swift and L. Lebioda, *Inorg. Chem.* 23, 349 (1984).
60. M.D. Curtis and K. Shiu, *Inorg. Chem.* 24, 1213 (1985).
61. M.D. Curtis and R.J. Klingler, *J. Organomet. Chem.* 161, 23 (1978).

62. D.S. Ginley, C.R. Bock and M.S. Wrighton, *Inorg. Chim. Acta* 23, 85 (1977).
63. K.W. Barnett, D.W. Slocum, *J. Organomet. Chem.* 44, 1 (1972).
64. M.D. Curtis, K. Shiu and W.M. Butler, *Organometallics* 2, 1475 (1983).
65. M.D. Curtis, K. Shiu and W.M. Butler, *J. Am. Chem. Soc.* 108, 1550 (1986).
66. E.C. Onyiriuka and A. Storr, *Can. J. Chem.*, submitted.
67. S.W. Ulmer, P.M. Skarstad, J.M. Burlitch and R.E. Hughes, *J. Am. Chem. Soc.* 95, 4469 (1973).
68. G. Fachinetti, C. Floriani, P.F. Zanazzi and A.R. Zanazari, *Inorg. Chem.* 17, 3002 (1978).
69. W.F. Edgell, M.T. Yang and N. Koizumi, *J. Am. Chem. Soc.* 87, 2563 (1965).
70. W.F. Edgell and J. Lyford, *J. Am. Chem. Soc.* 93, 6407 (1971).
71. K.H. Pannel and D. Jackson, *J. Am. Chem. Soc.* 98, 4443 (1976).
72. M. Nitay and M. Rosenblum, *J. Organomet. Chem.* 136, C23 (1977).
73. M.Y. Darensbourg, P. Jimenez, J.R. Sackett, J.M. Hanckell and R.L. Kump, *J. Am. Chem. Soc.* 104, 1521 (1982).
74. P. Politzer and P.H. Reggio, *J. Am. Chem. Soc.* 94, 8308 (1972).
75. V.R. Feld, E. Hellner, A. Klopch and K. Dehnicke, *Z. Anorg. Allg. Chem.* 442, 173 (1978).
76. C.P. Horwitz and D.F. Shriver, *Adv. Organomet. Chem.* 23, 219 (1984).
77. M.Y. Darensbourg, *Prog. Inorg. Chem.* 33, 221 (1985).
78. S.W. Benson. The Foundations of Chemical Kinetics, McGraw-Hill; New York (1960) pp. 495, 496.
79. R.S. Drago. Physical Methods in Chemistry, W.B. Saunders Company; Philadelphia (1977).
80. D.M. Adams. Metal-ligand and Related Vibrations, Edward Arnold (Publishers) Ltd., London (1967).
81. P. Leoni, E. Grilli, M. Pasquali and M. Tomassini, *J. Chem. Soc., Dalton Trans.*, 1041 (1986).

82. R.B. King and M.B. Bisnette, *J. Organomet. Chem.* 8, 287 (1967).
83. R.B. King and M.B. Bisnette, *Inorg. Chem.* 4, 475 (1965).
84. F. Calderazzo, *Angew. Chem.* 89, 305 (1977).
85. F. Calderazzo, *Angew. Chem., Int. Ed. Engl.* 16, 299 (1977).
86. C.R. Jablonski and Y. Wang, *Inorg. Chem.* 21, 4037 (1982).
87. C. Masters, *Adv. Organomet. Chem.* 17, 61 (1979).
88. C.K. Rofer-De Poorter, *Chem. Rev.* 81, 447 (1981).
89. W.A. Herrman, *Angew. Chem., Int. Ed. Eng.* 21, 117 (1982).
90. H.G. Alt, *J. Organomet. Chem.* 127, 349 (1977).
91. R.M. Medina and J.R. Masaguer, *J. Organomet. Chem.* 299, 341 (1986).
92. E.C. Onyiriuka, S.J. Rettig and A. Storr, *Can. J. Chem.* 64, 321 (1986).
93. M.J. Bennett and R. Mason, *Proc. Chem. Soc.*, 273 (1963).
94. S.P. Nolan, R. Lopez de la Vega, S.L. Mukerjee and C.D. Hoff, *Inorg. Chem.* 25, 1160 (1986).
95. M.J. Wax and R.G. Bergman, *J. Am. Chem. Soc.* 103, 7028 (1981).
96. J.P. Collman and L.S. Hegeudus. Principles and Applications of Organotransition Metal Chemistry, University Science Books; Mill Valley, California (1980).
97. P.J. Craig and M. Green, *J. Chem. Soc. (A)*, 1978 (1968).
98. K.S. Chong, S.J. Rettig, A. Storr and J. Trotter, *Can. J. Chem.* 57, 1335 (1979).
99. K.S. Chong and A. Storr, *Can. J. Chem.* 58, 2278 (1980).
100. K.S. Chong, S.J. Rettig, A. Storr and J. Trotter, *Can. J. Chem.* 59, 2391 (1981).
101. B.M. Louie, S.J. Rettig, A. Storr and J. Trotter, *Can. J. Chem.* 62, 633 (1984).
102. M. Cocivera, T.J. Desmond, G. Ferguson, B. Kaitner, F.J. Lalor and D.J. O'Sullivan, *Organometallics* 1, 1125 (1982).

103. O.S. Mills and J.P. Nice, *J. Organomet. Chem.* 10, 337 (1967).
104. L. Carlton, W.E. Lindsell, K.J. McCullough and P.N. Preston, *J. Chem. Soc., Dalton Trans.*, 1693 (1984).
105. R.D. Barr, T.B. Marder, A.G. Orpen and I.D. Williams, *J. Chem. Soc., Chem. Commun.*, 112 (1984).
106. M. Green, J.A.K. Howard, A.P. James, C.M. Nunn and F.G.A. Stone, *J. Chem. Soc., Chem. Commun.*, 1113 (1984).
107. R.D. Barr, M. Green, K. Marsden, F.G.A. Stone and P. Woodward, *J. Chem. Soc., Dalton Trans.*, 507 (1983).
108. L.J. Farraguia, A.D. Miles and F.G.A. Stone, *J. Chem. Soc., Dalton Trans.*, 2415 (1984).
109. R.D. Barr, M. Green, J.A.K. Howard, T.B. Marder, A.G. Orpen and F.G.A. Stone, *J. Chem. Soc., Dalton Trans.*, 2757 (1984).
110. C.P. Casey, R.M. Bullock and F. Nief, *J. Am. Chem. Soc.* 105, 7574 (1983).
111. R.G. Finke, G. Gaughan, C. Pierpont and M.E. Cass, *J. Am. Chem. Soc.* 103, 1394 (1981).
112. O. Bars and P. Braunstein, *Angew Chem. Int. Ed. Engl.* 21, 308 (1982).
113. D.A. Roberts, W.C. Mercer, S.M. Zahurak, G.L. Geoffroy, C.W. DeBrosse, M.E. Cass and C.G. Pierpont, *J. Am. Chem. Soc.* 104, 910 (1982).
114. D.A. Roberts and G.L. Geoffroy, In Comprehensive Organometallic Chemistry, Vol. 6, G. Wilkinson, F.G.A. Stone and E.W. Abel Eds. Pergamon Press, Oxford, England (1982) p. 763.
115. G.S. White and D.W. Stephan, *Inorg. Chem.* 24, 1499 (1985).
116. O. Stelzer and E. Unger, *Chem. Ber.* 110, 3430, 3438 (1977).
117. T.S. Targos, R.P. Rosen, R.R. Whittle and G.L. Geoffroy, *Inorg. Chem.* 24, 1375 (1985).
118. R.T. Baker, T.H. Tulip and S.S. Wreford, *Inorg. Chem.* 24, 1379 (1985).
119. G.L. Geoffroy, *Acc. Chem. Res.* 13, 469 (1980).
120. W.L. Gladfelter and G.L. Geoffroy, *Adv. Organomet. Chem.* 18, 207 (1980).

121. F.A. Cotton, *Prog. Inorg. Chem.* 21, 1 (1976).
122. R. Colton and M.J. McCormick, *Coord. Chem. Rev.* 31, 1 (1980).
123. A. Bino, F.A. Cotton, P. Lahuerta, P. Puebla and R. Uson, *Inorg. Chem.* 19, 2357 (1980).
124. G.A. Banta, B.M. Louie, E. Onyiriuka, S.J. Rettig and A. Storr, *Can. J. Chem.* 64, 373 (1986).
125. S. Trofimenko, *Inorg. Synth.* 12, 102 (1970).
126. G. Costa, E. Reisenhofer and L. Stefani, *J. Inorg. Nucl. Chem.* 27, 2581 (1965).
127. H.C. Clark and L. Manzer, *J. Organomet. Chem.* 59, 411 (1973).
128. B. Haymore and R.D. Feltham, *Inorg. Synth.* 14, 81 (1973).
129. M.H. Quick and R.J. Angelici, *Inorg. Synth.* 19, 160 (1979).
130. F. Bonati and G. Wilkinson, *J. Chem. Soc.*, 179 (1964).
131. D.J. Patmore and W.A.G. Graham, *Inorg. Chem.* 5, 1405 (1966).
132. C. Lee, G. Besenyei, B.R. James, D.A. Nelson and M.A. Lilga, *J. Chem. Soc., Chem. Commun.*, 1175 (1985).
133. R.G. Finke, G. Gaughan, C. Pierpont and J.H. Noordik, *Organometallics* 2, 1481 (1983).
134. M.L. Aldridge, M. Green, J.A.K. Howard, G.N. Pain, S.J. Porter, F.G.A. Stone and P. Woodward, *J. Chem. Soc., Dalton Trans.*, 1333 (1982).
135. R.H. Crabtree and M. Lavin, *Inorg. Chem.* 25, 805 (1986).
136. R.J. Klinger, W.M. Butler and M.D. Curtis, *J. Am. Chem. Soc.* 100, 5034 (1978).
137. F.C. Wilson and D.P. Shoemaker, *J. Chem. Phys.* 27, 809 (1957).
138. F.C. Wilson and D.P. Shoemaker, *Naturwiss* 43, 57 (1956).
139. G. Doyle, K.A. Eriksen and D. Van Engen, *Organometallics* 4, 2201 (1985).
140. J.B. Wilford and H.M. Powell, *J. Chem. Soc. (A)*, 8 (1969).
141. P. Kubacek, R. Hoffmann and Z. Havlas, *Organometallics* 1, 180 (1982).

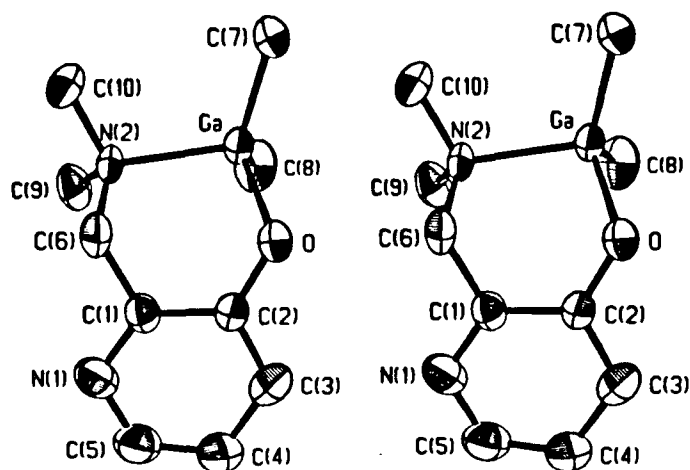
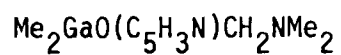
142. F.E. Simon and J.W. Lauher, *Inorg. Chem.* 19, 2338 (1980).
143. M.I. Bruce and A.P.P. Ostaszewski, *J. Chem. Soc., Dalton Trans.*, 2433 (1973).
144. K.R. Breakell, M.Sc. Thesis, U.B.C., (1978) p. 137
145. H.C. Clark and K. von Werner, *J. Organomet. Chem.* 101, 347 (1975).
146. S. Nussbaum and A. Storr, *Can. J. Chem.* 63, 2550 (1985).
147. R.D. Fischer and K. Noack, *J. Organomet. Chem.* 16, 125 (1969).
148. J.M. Burlitch and A. Ferrari, *Inorg. Chem.* 9, 563 (1970).
149. R.B. King, *J. Am. Chem. Soc.* 88, 2075 (1966).
150. M.S. Wrighton and D.S. Ginley, *J. Am. Chem. Soc.* 97, 4246 (1975).
151. A.N. Nesmeyanov, K.N. Anisimov, N.E. Kolobova and A.S. Beschastnov, *Dokl. Akad. Nauk. SSSR*, 159, 377 (1964).
152. B.P. Bir'yukov, Y.T. Struchkov, K.N. Anisimov, N.E. Kolobova and A.S. Beschastnov, *J. Chem. Soc., Chem. Commun.*, 667 (1968).
153. E.H. Brooks and R.J. Cross, *Organomet. Chem. Rev. Sect. A*, 6, 227 (1970).
154. K.M. Mackay and B.K. Nicholson, In *Comprehensive Organometallic Chemistry*, G. Wilkinson, F.G.A. Stone and E.W. Abel Eds. Vol. 6, Pergamon Press, Oxford, England (1982) p. 1043.
155. E.W. Abel and F.G.A. Stone, *Quart. Rev.* 24, 498 (1970).
156. J. Chatt, *Proc. Chem. Soc.*, 318 (1962).
157. H.R.H. Patil and W.A.G. Graham, *Inorg. Chem.* 5, 1401 (1966).
158. D.J. Cardin, S.A. Keppie, B.M. Kingston and M.F. Lappert, *J. Chem. Soc., Chem. Commun.*, 1035 (1967).
159. D.J. Cardin, S.A. Keppie and M.F. Lappert, *J. Chem. Soc. (A)*, 2594 (1970).
160. W. Malisch, H. Schmidbaur and M. Kuhn, *Angew. Chem.* 84, 538 (1972).
161. W. Malisch, *J. Organomet. Chem.* 39, C28 (1972).
162. F. Höfler, *Top. Curr. Chem.* 50, 129 (1974).
163. A. Carrick and F. Glockling, *J. Chem. Soc. (A)*, 913 (1968).

164. J.E. O'Connor and E.R. Corey, *J. Am. Chem. Soc.* 89, 3930 (1967).
165. R.J. Doedens and L.F. Dahl, *J. Am. Chem. Soc.* 87, 2576 (1965).
166. D.H. Olsen and R.E. Rundle, *Inorg. Chem.* 2, 1310 (1963).
167. T.S. Cameron and C.K. Prout, *J. Chem. Soc., Dalton Trans.*, 1447 (1972).
168. M. Elder and D. Hall, *Inorg. Chem.* 8, 1268 (1969).
169. M. Elder and D. Hall, *Inorg. Chem.* 8, 1273 (1969).
170. P. Meakin, S. Trofimenko and J.P. Jesson, *J. Am. Chem. Soc.* 94, 5677 (1972).
171. O.M.A. Salah and M.I. Bruce, *Aust. J. Chem.* 30, 2292 (1977).
172. K.S. Chong and A. Storr, *Can. J. Chem.* 59, 1331 (1981).
173. S.J. Rettig, A. Storr, J. Trotter and K. Urich, *Can. J. Chem.* 62, 2783 (1984).
174. B.M. Louie, S.J. Rettig, A. Storr and J. Trotter, *Can. J. Chem.* 63, 2261 (1985).
175. B.M. Louie, S.J. Rettig, A. Storr and J. Trotter, *Can. J. Chem.* 63, 3019 (1985).
176. D.A. Cooper, S.J. Rettig, A. Storr and J. Trotter, *Can. J. Chem.* 64, 566 (1986).
177. A.J. Canty and C.V. Lee, *Organometallics* 1, 1063 (1982).
178. P.J. Steel, F. Lahouse, D. Lerner and C. Martin, *Inorg. Chem.* 22, 1488 (1983).
179. P. Sullivan, D.J. Salmon, T.J. Meyer and J. Peedin, *Inorg. Chem.* 18, 3369 (1979).
180. E.C. Onyiriuka and A. Storr, *Can. J. Chem.*, Submitted.
181. E.C. Onyiriuka, S.J. Rettig, A. Storr and J. Trotter, *Can. J. Chem.*, Submitted.
182. R.B. King, In Organometallic Synthesis, Vol 1, Academic Press, New York (1965) p. 174.
183. G. Dolcetti and G.R. Norton, *Inorg. Synth.* 16, 35 (1976).
184. R.G. Hayter, *J. Organomet. Chem.* 13, P1-P3 (1968).

185. S.J. Rettig, A. Storr and J. Trotter, *Can. J. Chem.* 53, 58 (1975).
186. K.S. Chong, S.J. Rettig, A. Storr and J. Trotter, *Can. J. Chem.* 57, 586 (1979).
187. K. Dymock and G.J. Palenik, *J. Chem. Soc., Chem. Commun.*, 884 (1973).
188. S.J. Rettig, A. Storr and J. Trotter, *Can. J. Chem.* 52, 2206 (1974).
189. F.A. Cotton and G. Wilkinson, *Advanced Inorganic Chemistry*, 4th ed., John Wiley and Sons Inc., New York (1980).
190. R.D. Feltham and J.H. Enemark, In *Topics in Stereochemistry*, G. Geoffroy, Ed., Vol 12, John Wiley and Sons, New York (1981) p. 155.
191. W.G. Fateley, H.A. Bent and B.L. Crawford, *J. Chem. Phys.* 31, 204 (1959).
192. K.J. Haller and J.H. Enemark, *Inorg. Chem.* 17, 3552 (1978).
193. J.H. Enemark and R.D. Feltham, *Coord. Chem. Rev.* 13, 339 (1974).
194. K.S. Chong, S.J. Rettig, A. Storr and J. Trotter, *Can. J. Chem.* 57, 3107 (1979).
195. D. Berglund and D.W. Meek, *Inorg. Chem.* 11, 1493 (1972).
196. R.B. King, In *Organometallic Synthesis*, Vol 1, Academic Press, New York (1965) p. 169.
197. K.S. Chong and A. Storr, *Can. J. Chem.* 57, 167 (1979).
198. R.B. King, *Inorg. Chem.* 5, 2242 (1966).
199. K.S. Chong, S.J. Rettig, A. Storr and J. Trotter, *Can. J. Chem.* 59, 1665 (1981).
200. S.J. Rettig, A. Storr and J. Trotter, *Can. J. Chem.* 59, 2391 (1981).
201. E.O. Fischer and K. Bittler, *Z. Naturforsch* 16b, 225 (1961).
202. S. Trofimenko, *Inorg. Chem.* 10, 1372 (1971).
203. S. May, P. Reinsalu and J. Powell, *Inorg. Chem.* 19, 1582 (1980).
204. I.C. Douek and G. Wilkinson, *J. Chem. Soc. (A)*, 2605 (1969).
205. P. Uguagliati, A. Palazzi, G. Deganello and U. Belluco, *Inorg. Chem.* 9, 724 (1970).

206. W.R. Roper, G.E. Taylor, J.M. Waters and L.J. Wright, *J. Organomet. Chem.* 182, C46 (1979).
207. M.C. Baird, J.T. Mague, J.A. Osborn and G. Wilkinson, *J. Chem. Soc. (A)*, 1347 (1967).
208. J.W. Kang and P.M. Maitlis, *J. Organomet. Chem.* 26, 393 (1971).
209. M. Barber, R.S. Bordoli, R.D. Sedgwick, A.N. Tyler and E.T. Whalley, *Biomed. Mass Spectrom.* 8, 337 (1981).
210. M. Barber, R.S. Bordoli, R.D. Sedgwick and A.N. Tyler, *Nature* 293, 270 (1981).
211. R.B. King, *Inorg. Chem.* 5, 82 (1966).
212. J.W. Kang, K. Moseley and P.M. Maitlis, *J. Am. Chem. Soc.* 91, 5972 (1969).
213. J.A. McCleverty and G. Wilkinson, *J. Chem. Soc.*, 4096 (1963).
214. R. Hoffmann, B.F. Beier, E.L. Muetterties and A.R. Rossi, *Inorg. Chem.* 16, 511 (1977).

## APPENDIX I

STEREO DIAGRAMS, BOND LENGTHS AND BOND ANGLES  
OF SOME OF THE PREPARED DERIVATIVES

Intra-annular torsion angles (deg)  
standard deviations in parentheses

Atoms	Value(deg)
N(2)-Ga -O -C(2)	41.7(3)
Ga -O -C(2)-C(1)	-49.5(5)
C(6)-C(1)-C(2)-O	-5.0(7)
C(2)-C(1)-C(6)-N(2)	64.9(6)
Ga -N(2)-C(6)-C(1)	-56.1(5)
O -Ga -N(2)-C(6)	9.8(3)

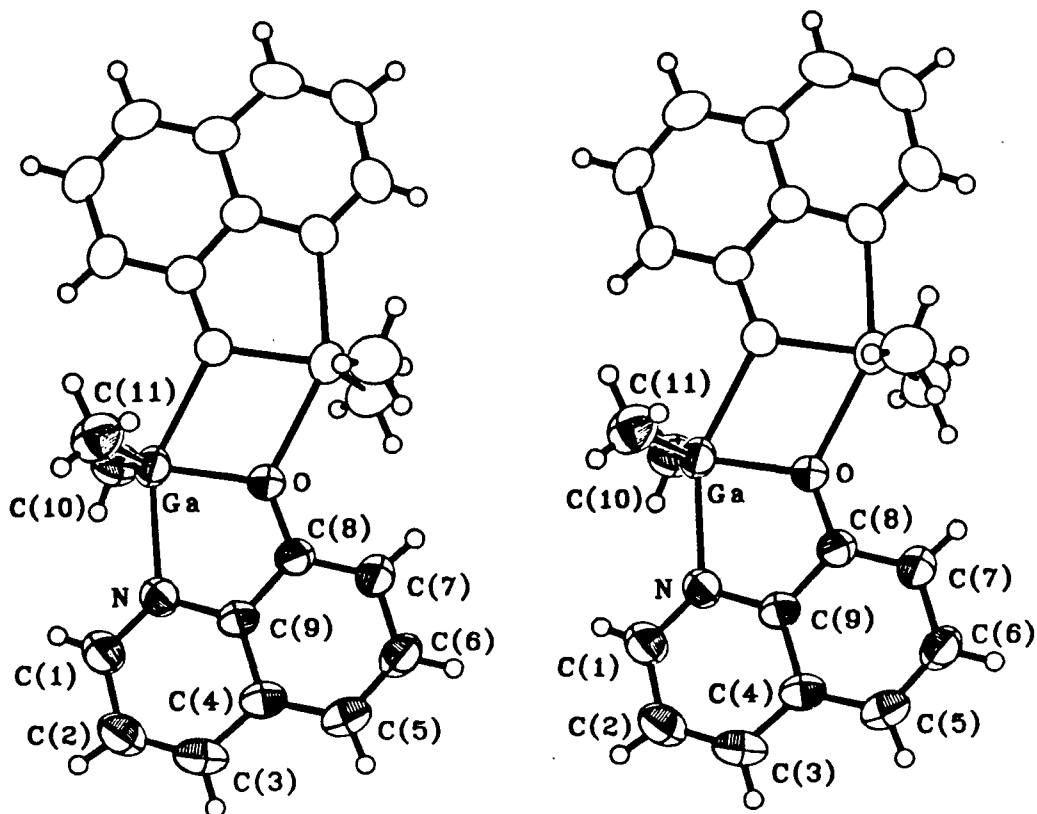
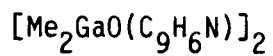
$\text{Me}_2\text{GaO}(\text{C}_5\text{H}_3\text{N})\text{CH}_2\text{NMe}_2$ , cont'd

Bond lengths (Å) with estimated  
standard deviations in parentheses

Bond	uncorr.	corr.	Bond	uncorr.	corr.
Ga -O	1.892(3)	1.897	N(2)-C(9)	1.477(6)	1.481
Ga -N(2)	2.127(4)	2.135	N(2)-C(10)	1.480(6)	1.480
Ga -C(7)	1.950(5)	1.956	C(1)-C(2)	1.415(8)	1.420
Ga -C(8)	1.939(6)	1.947	C(1)-C(6)	1.498(7)	1.503
O -C(2)	1.328(5)	1.332	C(2)-C(3)	1.389(8)	1.393
N(1)-C(1)	1.325(7)	1.329	C(3)-C(4)	1.423(14)	1.427
N(1)-C(5)	1.324(13)	1.327	C(4)-C(5)	1.353(15)	1.358
N(2)-C(6)	1.492(6)	1.496			

Bond angles (deg) with estimated  
standard deviations in parentheses

Bonds	Angle(deg)	Bonds	Angle(deg)
O -Ga -N(2)	95.24(15)	C(6)-N(2)-C(10)	107.8(4)
O -Ga -C(7)	110.3(2)	C(9)-N(2)-C(10)	107.7(4)
O -Ga -C(8)	108.3(2)	N(1)-C(1)-C(2)	124.2(5)
N(2)-Ga -C(7)	107.3(2)	N(1)-C(1)-C(6)	117.2(6)
N(2)-Ga -C(8)	107.4(2)	C(2)-C(1)-C(6)	118.6(5)
C(7)-Ga -C(8)	124.3(3)	O -C(2)-C(1)	120.3(4)
Ga -O -C(2)	118.8(3)	O -C(2)-C(3)	122.2(5)
C(1)-N(1)-C(5)	116.5(7)	C(1)-C(2)-C(3)	117.4(5)
Ga -N(2)-C(6)	107.8(3)	C(2)-C(3)-C(4)	117.8(7)
Ga -N(2)-C(9)	112.4(3)	C(3)-C(4)-C(5)	118.2(12)
Ga -N(2)-C(10)	111.1(3)	N(1)-C(5)-C(4)	125.7(13)
C(6)-N(2)-C(9)	109.8(4)	N(2)-C(6)-C(1)	113.0(4)



Bond lengths (Å) with estimated  
standard deviations in parentheses\*

Bond	Length(Å)	Bond	Length(Å)
Ga -O	1.937(3)	C(2)-C(3)	1.356(7)
Ga -N	2.211(3)	C(3)-C(4)	1.411(6)
Ga -C(10)	1.948(6)	C(4)-C(5)	1.400(6)
Ga -C(11)	1.945(5)	C(4)-C(9)	1.419(5)
O -O'	2.297(3)	C(5)-C(6)	1.367(7)
O -C(8)	1.336(5)	C(6)-C(7)	1.403(6)
N -C(1)	1.319(5)	C(7)-C(8)	1.369(5)
N -C(9)	1.362(5)	C(8)-C(9)	1.415(5)
C(1)-C(2)	1.397(7)		

\*Primed atoms related by inversion through the centre at (1/2,1/2,1/2).

$[\text{Me}_2\text{GaO}(\text{C}_9\text{H}_6\text{N})]_2$ , cont'd

Bond angles (deg) with estimated  
standard deviations in parentheses

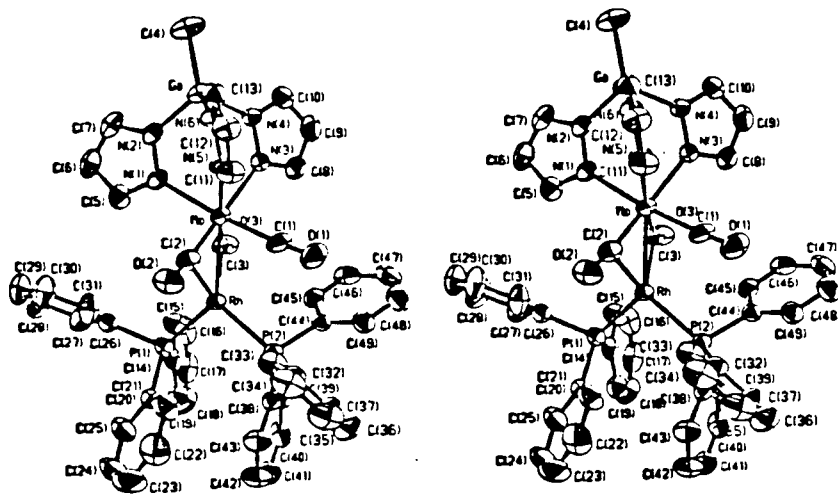
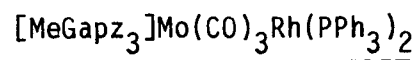
Bonds			Angle(deg)	Bonds			Angle(deg)
O	-Ga	-N	78.37(11)	N	-C(1)-C(2)	122.4(5)	
O	-Ga	-C(10)	114.0(2)	C(1)-C(2)-C(3)	119.6(4)		
O	-Ga	-C(11)	113.6(2)	C(2)-C(3)-C(4)	120.7(4)		
O	-Ga	-O'	71.29(12)	C(3)-C(4)-C(5)	125.5(4)		
N	-Ga	-C(10)	100.1(2)	C(3)-C(4)-C(9)	115.9(4)		
N	-Ga	-C(11)	98.2(2)	C(5)-C(4)-C(9)	118.5(4)		
N	-Ga	-O'	149.65(11)	C(4)-C(5)-C(6)	119.7(4)		
C(10)-Ga	-C(11)	131.5(3)	C(5)-C(6)-C(7)	121.7(4)			
C(10)-Ga	-O'	92.9(2)	C(6)-C(7)-C(8)	120.6(4)			
C(11)-Ga	-O'	93.2(2)	O	-C(8)-C(7)	124.4(4)		
Ga	-O	-C(8)	118.9(2)	O	-C(8)-C(9)	117.2(3)	
Ga	-O	-Ga'	108.71(12)	C(7)-C(8)-C(9)	118.3(4)		
C(8)-O	-Ga'	132.3(2)	N	-C(9)-C(4)	122.6(3)		
Ga	-N	-C(1)	132.0(3)	N	-C(9)-C(8)	116.3(3)	
Ga	-N	-C(9)	109.1(2)	C(4)-C(9)-C(8)	121.1(3)		
C(1)-N	-C(9)	118.9(4)					

Bond lengths involving hydrogen atoms (A) with  
estimated standard deviations in parentheses

Bond	Length(A)	Bond	Length(A)
C(1)-H(1)	0.81(5)	C(10)-H(10a)	0.76(11)
C(2)-H(2)	0.89(7)	C(10)-H(10b)	0.92(7)
C(3)-H(3)	0.89(5)	C(10)-H(10c)	0.85(6)
C(5)-H(5)	0.88(5)	C(11)-H(11a)	0.97(7)
C(6)-H(6)	0.91(6)	C(11)-H(11b)	0.77(8)
C(7)-H(7)	0.92(5)	C(11)-H(11c)	1.00(12)

Bond angles involving hydrogen atoms (deg) with  
estimated standard deviations in parentheses

Bonds			Angle(deg)	Bonds			Angle(deg)
N	-C(1)-H(1)	115(3)	Ga	-C(10)-H(10a)	113(7)		
C(2)-C(1)-H(1)	123(3)	Ga	-C(10)-H(10b)	105(4)			
C(1)-C(2)-H(2)	112(5)	Ga	-C(10)-H(10c)	97(4)			
C(3)-C(2)-H(2)	128(5)	H(10a)-C(10)-H(10b)	104(8)				
C(2)-C(3)-H(3)	122(3)	H(10a)-C(10)-H(10c)	109(8)				
C(4)-C(3)-H(3)	117(3)	H(10b)-C(10)-H(10c)	128(6)				
C(4)-C(5)-H(5)	122(4)	Ga	-C(11)-H(11a)	117(4)			
C(6)-C(5)-H(5)	117(4)	Ga	-C(11)-H(11b)	108(7)			
C(5)-C(6)-H(6)	118(4)	Ga	-C(11)-H(11c)	122(6)			
C(7)-C(6)-H(6)	120(4)	H(11a)-C(11)-H(11b)	106(7)				
C(6)-C(7)-H(7)	116(4)	H(11a)-C(11)-H(11c)	86(6)				
C(8)-C(7)-H(7)	123(4)	H(11b)-C(11)-H(11c)	116(9)				



[MeGap<sub>3</sub>]Mo(CO)<sub>3</sub>Rh(PPh<sub>3</sub>)<sub>2</sub>, cont'd

Bond lengths (Å) with estimated  
standard deviations in parentheses

Bond	Length(Å)	Bond	Length(Å)
(MeGap <sub>3</sub> )Mo(CO) <sub>3</sub> Rh(PPh <sub>3</sub> ) <sub>2</sub>			
Rh -Mo	2.6066(5)	C(11)-C(12)	1.383(7)
Rh -P(1)	2.2491(13)	C(12)-C(13)	1.357(7)
Rh -P(2)	2.2836(12)	C(14)-C(15)	1.383(7)
Rh -C(1)	2.845(5)	C(14)-C(19)	1.374(7)
Rh -C(2)	2.334(5)	C(15)-C(16)	1.411(8)
Rh -C(3)	2.079(5)	C(16)-C(17)	1.355(9)
Mo -N(1)	2.249(4)	C(17)-C(18)	1.377(9)
Mo -N(3)	2.273(4)	C(18)-C(19)	1.396(8)
Mo -N(5)	2.247(4)	C(20)-C(21)	1.383(7)
Mo -C(1)	1.982(5)	C(20)-C(25)	1.366(7)
Mo -C(2)	1.971(6)	C(21)-C(22)	1.397(8)
Mo -C(3)	2.034(5)	C(22)-C(23)	1.348(10)
Ga -N(2)	1.915(4)	C(23)-C(24)	1.364(11)
Ga -N(4)	1.924(4)	C(24)-C(25)	1.388(9)
Ga -N(6)	1.927(4)	C(26)-C(27)	1.377(7)
Ga -C(4)	1.931(5)	C(26)-C(31)	1.393(7)
P(1)-C(14)	1.840(5)	C(27)-C(28)	1.399(8)
P(1)-C(20)	1.834(5)	C(28)-C(29)	1.344(9)
P(1)-C(26)	1.839(5)	C(29)-C(30)	1.368(9)
P(2)-C(32)	1.837(5)	C(30)-C(31)	1.380(8)
P(2)-C(38)	1.836(5)	C(32)-C(33)	1.381(7)
P(2)-C(44)	1.848(5)	C(32)-C(37)	1.400(7)
O(1)-C(1)	1.154(6)	C(33)-C(34)	1.385(7)
O(2)-C(2)	1.175(6)	C(34)-C(35)	1.353(9)
O(3)-C(3)	1.190(5)	C(35)-C(36)	1.376(9)
N(1)-N(2)	1.367(5)	C(36)-C(37)	1.378(8)
N(1)-C(5)	1.327(6)	C(38)-C(39)	1.386(7)
N(2)-C(7)	1.344(6)	C(38)-C(43)	1.396(7)
N(3)-N(4)	1.364(5)	C(39)-C(40)	1.385(7)
N(3)-C(8)	1.328(6)	C(40)-C(41)	1.369(8)
N(4)-C(10)	1.337(6)	C(41)-C(42)	1.369(9)
N(5)-N(6)	1.369(5)	C(42)-C(43)	1.382(8)
N(5)-C(11)	1.326(6)	C(44)-C(45)	1.383(7)
N(6)-C(13)	1.344(6)	C(44)-C(49)	1.383(7)
C(5)-C(6)	1.376(7)	C(45)-C(46)	1.387(7)
C(6)-C(7)	1.355(8)	C(46)-C(47)	1.385(9)
C(8)-C(9)	1.383(7)	C(47)-C(48)	1.364(8)
C(9)-C(10)	1.347(7)	C(48)-C(49)	1.390(8)

[MeGapz<sub>3</sub>]Mo(CO)<sub>3</sub>Rh(PPh<sub>3</sub>)<sub>2</sub>, cont'd

Bond angles (deg) with estimated  
standard deviations in parentheses

Bonds	Angle(deg)	Bonds	Angle(deg)
(MeGapz <sub>3</sub> )Mo(CO) <sub>3</sub> Rh(PPh <sub>3</sub> ) <sub>2</sub>			
Mo -Rh -P(1)	135.80(4)	Ga -N(6)-N(5)	120.5(3)
Mo -Rh -P(2)	128.70(4)	Ga -N(6)-C(13)	130.8(3)
Mo -Rh -C(1)	42.35(10)	N(5)-N(6)-C(13)	108.8(4)
Mo -Rh -C(2)	46.61(13)	Rh -C(1)-Mo	62.37(15)
Mo -Rh -C(3)	49.91(14)	Rh -C(1)-O(1)	122.5(4)
P(1)-Rh -P(2)	95.27(5)	Mo -C(1)-O(1)	173.9(5)
P(1)-Rh -C(1)	172.17(12)	Rh -C(2)-Mo	74.0(2)
P(1)-Rh -C(2)	110.97(14)	Rh -C(2)-O(2)	117.9(4)
P(1)-Rh -C(3)	110.90(14)	Mo -C(2)-O(2)	167.4(4)
P(2)-Rh -C(1)	87.84(11)	Rh -C(3)-Mo	78.6(2)
P(2)-Rh -C(2)	130.20(13)	Rh -C(3)-O(3)	128.1(4)
P(2)-Rh -C(3)	116.64(14)	Mo -C(3)-O(3)	153.2(4)
C(1)-Rh -C(2)	61.9(2)	N(1)-C(5)-C(6)	110.6(5)
C(1)-Rh -C(3)	73.8(2)	C(5)-C(6)-C(7)	105.5(5)
C(2)-Rh -C(3)	93.1(2)	N(2)-C(7)-C(6)	108.8(5)
Rh -Mo -N(1)	111.64(11)	N(3)-C(8)-C(9)	110.6(5)
Rh -Mo -N(3)	128.38(10)	C(8)-C(9)-C(10)	105.1(5)
Rh -Mo -N(5)	142.50(10)	N(4)-C(10)-C(9)	109.3(5)
Rh -Mo -C(1)	75.27(14)	N(5)-C(11)-C(12)	111.4(4)
Rh -Mo -C(2)	59.40(14)	C(11)-C(12)-C(13)	104.4(4)
Rh -Mo -C(3)	51.45(13)	N(6)-C(13)-C(12)	109.5(4)
N(1)-Mo -N(3)	86.92(14)	P(1)-C(14)-C(15)	115.7(4)
N(1)-Mo -N(5)	85.69(14)	P(1)-C(14)-C(19)	125.3(4)
N(1)-Mo -C(1)	172.9(2)	C(15)-C(14)-C(19)	118.8(5)
N(1)-Mo -C(2)	96.1(2)	C(14)-C(15)-C(16)	120.5(5)
N(1)-Mo -C(3)	88.2(2)	C(15)-C(16)-C(17)	120.0(6)
N(3)-Mo -N(5)	83.74(14)	C(16)-C(17)-C(18)	119.7(6)
N(3)-Mo -C(1)	89.7(2)	C(17)-C(18)-C(19)	120.7(6)
N(3)-Mo -C(2)	169.7(2)	C(14)-C(19)-C(18)	120.2(5)
N(3)-Mo -C(3)	83.3(2)	P(1)-C(20)-C(21)	117.7(4)
N(5)-Mo -C(1)	87.8(2)	P(1)-C(20)-C(25)	122.9(4)
N(5)-Mo -C(2)	86.7(2)	C(21)-C(20)-C(25)	119.2(5)
N(5)-Mo -C(3)	166.0(2)	C(20)-C(21)-C(22)	119.8(6)
C(1)-Mo -C(2)	86.1(2)	C(21)-C(22)-C(23)	120.3(7)
C(1)-Mo -C(3)	97.5(2)	C(22)-C(23)-C(24)	120.0(6)
C(2)-Mo -C(3)	106.5(2)	C(23)-C(24)-C(25)	120.5(7)
N(2)-Ga -N(4)	103.0(2)	C(20)-C(25)-C(24)	120.0(6)
N(2)-Ga -N(6)	100.5(2)	P(1)-C(26)-C(27)	125.4(4)
N(2)-Ga -C(4)	116.3(2)	P(1)-C(26)-C(31)	117.3(4)
N(4)-Ga -N(6)	98.0(2)	C(27)-C(26)-C(31)	117.3(5)
N(4)-Ga -C(4)	116.5(2)	C(26)-C(27)-C(28)	121.1(6)
N(6)-Ga -C(4)	119.4(2)	C(27)-C(28)-C(29)	120.8(6)
Rh -P(1)-C(14)	114.8(2)	C(28)-C(29)-C(30)	119.0(6)
Rh -P(1)-C(20)	118.9(2)	C(29)-C(30)-C(31)	121.4(6)

continued...

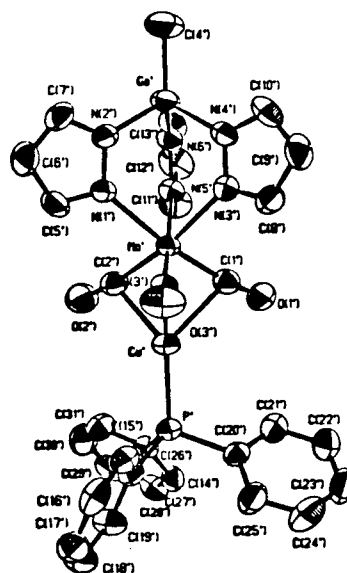
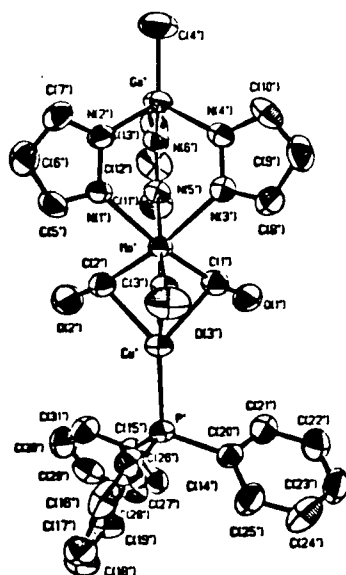
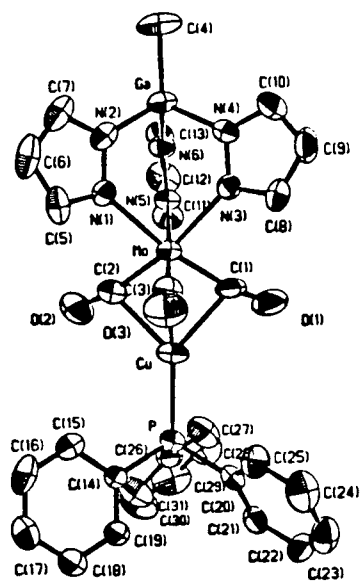
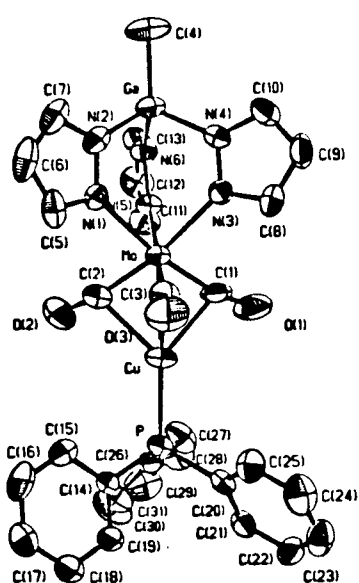
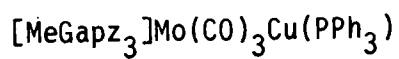
[MeGapz<sub>3</sub>]Mo(CO)<sub>3</sub>Rh(PPh<sub>3</sub>)<sub>2</sub>, cont'd

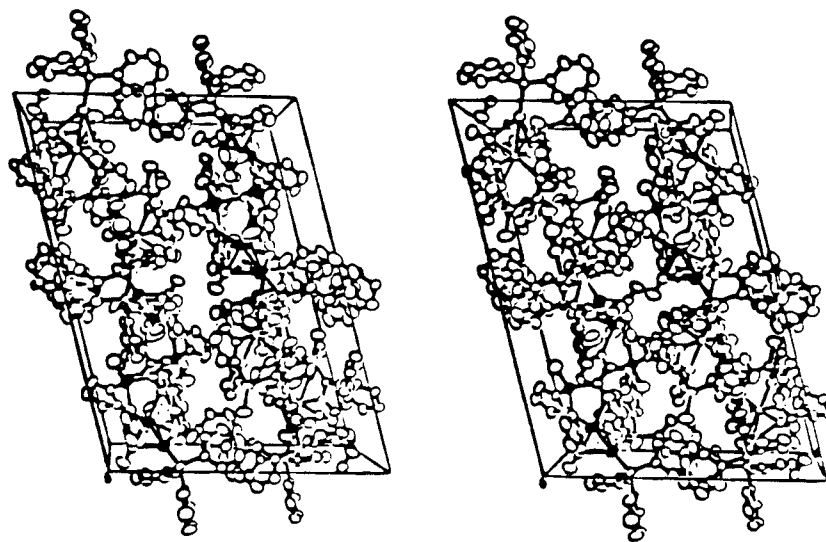
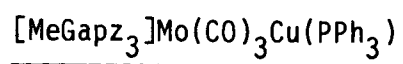
Rh -P(1)-C(26)	113.5(2)	C(26)-C(31)-C(30)	120.4(5)
C(14)-P(1)-C(20)	106.5(2)	P(2)-C(32)-C(33)	120.0(4)
C(14)-P(1)-C(26)	103.3(2)	P(2)-C(32)-C(37)	121.5(4)
C(20)-P(1)-C(26)	97.5(2)	C(33)-C(32)-C(37)	118.5(5)
Rh -P(2)-C(32)	112.6(2)	C(32)-C(33)-C(34)	120.3(5)
Rh -P(2)-C(38)	126.2(2)	C(33)-C(34)-C(35)	120.7(6)
Rh -P(2)-C(44)	107.41(15)	C(34)-C(35)-C(36)	120.3(5)
C(32)-P(2)-C(38)	101.1(2)	C(35)-C(36)-C(37)	120.0(6)
C(32)-P(2)-C(44)	104.5(2)	C(32)-C(37)-C(36)	120.2(6)
C(38)-P(2)-C(44)	102.9(2)	P(2)-C(38)-C(39)	122.5(4)
Mo -N(1)-N(2)	125.6(3)	P(2)-C(38)-C(43)	119.6(4)
Mo -N(1)-C(5)	128.1(3)	C(39)-C(38)-C(43)	117.8(4)
N(2)-N(1)-C(5)	106.3(4)	C(38)-C(39)-C(40)	120.7(5)
Ga -N(2)-N(1)	120.4(3)	C(39)-C(40)-C(41)	120.6(5)
Ga -N(2)-C(7)	130.6(4)	C(40)-C(41)-C(42)	119.6(5)
N(1)-N(2)-C(7)	108.9(4)	C(41)-C(42)-C(43)	120.4(6)
Mo -N(3)-N(4)	126.5(3)	C(38)-C(43)-C(42)	120.7(5)
Mo -N(3)-C(8)	127.5(3)	P(2)-C(44)-C(45)	118.2(4)
N(4)-N(3)-C(8)	106.0(4)	P(2)-C(44)-C(49)	122.2(4)
Ga -N(4)-N(3)	118.9(3)	C(45)-C(44)-C(49)	119.5(5)
Ga -N(4)-C(10)	132.0(3)	C(44)-C(45)-C(46)	120.0(5)
N(3)-N(4)-C(10)	109.1(4)	C(45)-C(46)-C(47)	120.0(5)
Mo -N(5)-N(6)	125.3(3)	C(46)-C(47)-C(48)	120.1(5)
Mo -N(5)-C(11)	128.7(3)	C(47)-C(48)-C(49)	120.2(6)
N(6)-N(5)-C(11)	105.9(4)	C(44)-C(49)-C(48)	120.2(5)

## Intra-annular torsion angles (deg)

standard deviations in parentheses

Atoms	Value(deg)
(MeGapz <sub>3</sub> )Mo(CO) <sub>3</sub> Rh(PPh <sub>3</sub> ) <sub>2</sub>	
N(3)-Mo -N(1)-N(2)	-38.5(4)
Mo -N(1)-N(2)-Ga	-3.9(5)
N(4)-Ga -N(2)-N(1)	52.3(4)
N(2)-Ga -N(4)-N(3)	-47.4(4)
Mo -N(3)-N(4)-Ga	-3.8(5)
N(1)-Mo -N(3)-N(4)	43.3(4)
N(5)-Mo -N(1)-N(2)	45.4(4)
Mo -N(1)-N(2)-Ga	-3.9(5)
N(6)-Ga -N(2)-N(1)	-48.6(4)
N(2)-Ga -N(6)-N(5)	52.1(4)
Mo -N(5)-N(6)-Ga	-2.2(5)
N(1)-Mo -N(5)-N(6)	-41.7(4)
N(5)-Mo -N(3)-N(4)	-42.7(4)
Mo -N(3)-N(4)-Ga	-3.8(5)
N(6)-Ga -N(4)-N(3)	55.4(4)
N(4)-Ga -N(6)-N(5)	-52.8(4)
Mo -N(5)-N(6)-Ga	-2.2(5)
N(3)-Mo -N(5)-N(6)	45.7(4)





[MeGapz<sub>3</sub>]Mo(CO)<sub>3</sub>Cu(PPh<sub>3</sub>), cont'd

Bond lengths (Å) with estimated  
standard deviations in parentheses

Bond	Length(Å)	Bond	Length(Å)
(MeGapz <sub>3</sub> )Mo(CO) <sub>3</sub> Cu(PPh <sub>3</sub> )			
Mo -Cu	2.5041(8)	N(3')-N(4')	1.358(6)
Mo -N(1)	2.254(5)	N(3')-C(8')	1.323(7)
Mo -N(3)	2.257(4)	N(4')-C(10')	1.348(7)
Mo -N(5)	2.246(4)	N(5')-N(6')	1.366(6)
Mo -C(1)	1.966(7)	N(5')-C(11')	1.336(7)
Mo -C(2)	1.958(7)	N(6')-C(13')	1.339(7)
Mo -C(3)	1.971(7)	C(5)-C(6)	1.375(9)
Mo' -Cu'	2.5216(8)	C(6)-C(7)	1.366(9)
Mo' -N(1')	2.253(5)	C(8)-C(9)	1.367(8)
Mo' -N(3')	2.273(5)	C(9)-C(10)	1.361(8)
Mo' -N(5')	2.257(5)	C(11)-C(12)	1.385(8)
Mo' -C(1')	1.958(7)	C(12)-C(13)	1.353(8)
Mo' -C(2')	1.970(7)	C(14)-C(15)	1.383(7)
Mo' -C(3')	1.980(7)	C(14)-C(19)	1.372(7)
Ga -N(2)	1.922(5)	C(15)-C(16)	1.379(8)
Ga -N(4)	1.929(5)	C(16)-C(17)	1.378(9)
Ga -N(6)	1.917(5)	C(17)-C(18)	1.361(8)
Ga -C(4)	1.943(6)	C(18)-C(19)	1.376(8)
Ga' -N(2')	1.924(5)	C(20)-C(21)	1.378(7)
Ga' -N(4')	1.926(5)	C(20)-C(25)	1.378(7)
Ga' -N(6')	1.928(5)	C(21)-C(22)	1.375(8)
Ga' -C(4')	1.935(6)	C(22)-C(23)	1.374(9)
Cu -P	2.193(2)	C(23)-C(24)	1.383(9)
Cu -C(1)	2.259(6)	C(24)-C(25)	1.383(9)
Cu -C(2)	2.274(7)	C(26)-C(27)	1.383(8)
Cu -C(3)	2.419(6)	C(26)-C(31)	1.365(8)
Cu' -P'	2.199(2)	C(27)-C(28)	1.371(9)
Cu' -C(1')	2.410(6)	C(28)-C(29)	1.371(10)
Cu' -C(2')	2.322(6)	C(29)-C(30)	1.341(10)
Cu' -C(3')	2.234(6)	C(30)-C(31)	1.378(9)
P -C(14)	1.819(6)	C(5')-C(6')	1.361(8)
P -C(20)	1.826(6)	C(6')-C(7')	1.375(8)
P -C(26)	1.833(6)	C(8')-C(9')	1.395(8)
P' -C(14')	1.811(6)	C(9')-C(10')	1.347(8)
P' -C(20')	1.812(6)	C(11')-C(12')	1.368(9)
P' -C(26')	1.817(6)	C(12')-C(13')	1.348(9)
O(1)-C(1)	1.160(7)	C(14')-C(15')	1.388(8)
O(2)-C(2)	1.174(7)	C(14')-C(19')	1.374(7)
O(3)-C(3)	1.159(6)	C(15')-C(16')	1.381(8)
O(1')-C(1')	1.169(6)	C(16')-C(17')	1.375(8)
O(2')-C(2')	1.164(7)	C(17')-C(18')	1.359(8)
O(3')-C(3')	1.155(6)	C(18')-C(19')	1.386(8)
N(1)-N(2)	1.373(6)	C(20')-C(21')	1.374(8)
N(1)-C(5)	1.332(7)	C(20')-C(25')	1.384(8)
N(2)-C(7)	1.347(7)	C(21')-C(22')	1.392(8)
N(3)-N(4)	1.367(6)	C(22')-C(23')	1.354(9)
N(3)-C(8)	1.345(7)	C(23')-C(24')	1.361(10)
N(4)-C(10)	1.347(7)	C(24')-C(25')	1.391(9)

continued /...

[MeGapz<sub>3</sub>]Mo(CO)<sub>3</sub>Cu(PPh<sub>3</sub>), cont'd

N(5)-N(6)	1.371(6)	C(26')-C(27')	1.385(7)
N(5)-C(11)	1.334(7)	C(26')-C(31')	1.385(8)
N(6)-C(13)	1.343(7)	C(27')-C(28')	1.384(8)
N(1')-N(2')	1.364(6)	C(28')-C(29')	1.358(8)
N(1')-C(5')	1.323(7)	C(29')-C(30')	1.365(9)
N(2')-C(7')	1.316(7)	C(30')-C(31')	1.384(8)

Bond angles (deg) with estimated  
standard deviations in parentheses

Bonds	Angle(deg)	Bonds	Angle(deg)
(MeGapz <sub>3</sub> )Mo(CO) <sub>3</sub> Cu(PPh <sub>3</sub> )			
Cu -Mo -N(1)	130.52(12)	N(5)-N(6)-C(13)	108.5(5)
Cu -Mo -N(3)	131.46(12)	Mo' -N(1')-N(2')	126.4(3)
Cu -Mo -N(5)	123.55(12)	Mo' -N(1')-C(5')	128.3(4)
Cu -Mo -C(1)	59.3(2)	N(2')-N(1')-C(5')	105.3(5)
Cu -Mo -C(2)	59.8(2)	Ga' -N(2')-N(1')	120.0(4)
Cu -Mo -C(3)	64.1(2)	Ga' -N(2')-C(7')	130.7(4)
N(1)-Mo -N(3)	84.1(2)	N(1')-N(2')-C(7')	109.3(5)
N(1)-Mo -N(5)	86.4(2)	Mo' -N(3')-N(4')	126.0(4)
N(1)-Mo -C(1)	170.0(2)	Mo' -N(3')-C(8')	127.4(4)
N(1)-Mo -C(2)	88.6(2)	N(4')-N(3')-C(8')	106.5(5)
N(1)-Mo -C(3)	86.7(2)	Ga' -N(4')-N(3')	120.1(4)
N(3)-Mo -N(5)	85.3(2)	Ga' -N(4')-C(10')	131.3(5)
N(3)-Mo -C(1)	87.0(2)	N(3')-N(4')-C(10')	108.3(5)
N(3)-Mo -C(2)	168.5(2)	Mo' -N(5')-N(6')	127.0(4)
N(3)-Mo -C(3)	90.2(2)	Mo' -N(5')-C(11')	127.6(4)
N(5)-Mo -C(1)	88.4(2)	N(6')-N(5')-C(11')	105.4(5)
N(5)-Mo -C(2)	85.4(2)	Ga' -N(6')-N(5')	119.2(4)
N(5)-Mo -C(3)	172.1(2)	Ga' -N(6')-C(13')	132.0(5)
C(1)-Mo -C(2)	99.4(3)	N(5')-N(6')-C(13')	108.7(5)
C(1)-Mo -C(3)	97.8(3)	Mo -C(1)-Cu	72.3(2)
C(2)-Mo -C(3)	98.3(3)	Mo -C(1)-O(1)	170.6(5)
Cu' -Mo' -N(1')	125.14(11)	Cu -C(1)-O(1)	116.9(4)
Cu' -Mo' -N(3')	128.36(12)	Mo -C(2)-Cu	72.1(2)
Cu' -Mo' -N(5')	132.68(13)	Mo -C(2)-O(2)	170.6(6)
Cu' -Mo' -C(1')	63.7(2)	Cu -C(2)-O(2)	117.2(5)
Cu' -Mo' -C(2')	60.8(2)	Mo -C(3)-Cu	68.7(2)
Cu' -Mo' -C(3')	58.0(2)	Mo -C(3)-O(3)	172.6(6)
N(1')-Mo' -N(3')	84.5(2)	Cu -C(3)-O(3)	118.6(5)
N(1')-Mo' -N(5')	85.2(2)	N(1)-C(5)-C(6)	111.8(6)
N(1')-Mo' -C(1')	171.1(2)	C(5)-C(6)-C(7)	104.4(6)
N(1')-Mo' -C(2')	89.1(2)	N(2)-C(7)-C(6)	109.4(6)
N(1')-Mo' -C(3')	87.2(2)	N(3)-C(8)-C(9)	110.9(6)
N(3')-Mo' -N(5')	85.0(2)	C(8)-C(9)-C(10)	104.9(5)
N(3')-Mo' -C(1')	90.4(2)	N(4)-C(10)-C(9)	109.8(5)
N(3')-Mo' -C(2')	170.8(2)	N(5)-C(11)-C(12)	111.7(6)
N(3')-Mo' -C(3')	86.8(2)	C(11)-C(12)-C(13)	103.7(5)
N(5')-Mo' -C(1')	87.1(2)	N(6)-C(13)-C(12)	110.5(5)
N(5')-Mo' -C(2')	88.0(2)	P -C(14)-C(15)	119.2(5)
N(5')-Mo' -C(3')	169.3(2)	P -C(14)-C(19)	121.9(4)
C(1')-Mo' -C(2')	95.1(2)	C(15)-C(14)-C(19)	118.9(6)
C(1')-Mo' -C(3')	99.8(2)	C(14)-C(15)-C(16)	119.1(6)
C(2')-Mo' -C(3')	99.4(2)	C(15)-C(16)-C(17)	121.1(6)
N(2)-Ga -N(4)	100.2(2)	C(16)-C(17)-C(18)	119.7(6)

continued /...

[MeGap<sub>3</sub>]Mo(CO)<sub>3</sub>Cu(PPh<sub>3</sub>), cont'd

N(2)-Ga -N(6)	101.7(2)	C(17)-C(18)-C(19)	119.4(6)
N(2)-Ga -C(4)	116.7(3)	C(14)-C(19)-C(18)	121.8(6)
N(4)-Ga -N(6)	100.3(2)	P -C(20)-C(21)	123.6(4)
N(4)-Ga -C(4)	115.7(3)	P -C(20)-C(25)	116.7(5)
N(6)-Ga -C(4)	119.1(3)	C(21)-C(20)-C(25)	119.6(6)
N(2')-Ga' -N(4')	100.0(2)	C(20)-C(21)-C(22)	120.6(6)
N(2')-Ga' -N(6')	101.3(2)	C(21)-C(22)-C(23)	119.8(6)
N(2')-Ga' -C(4')	117.1(3)	C(22)-C(23)-C(24)	120.0(6)
N(4')-Ga' -N(6')	99.7(2)	C(23)-C(24)-C(25)	120.0(6)
N(4')-Ga' -C(4')	116.4(3)	C(20)-C(25)-C(24)	119.9(6)
N(6')-Ga' -C(4')	119.1(3)	P -C(26)-C(27)	118.5(5)
Mo -Cu -P	177.02(6)	P -C(26)-C(31)	123.3(5)
Mo -Cu -C(1)	48.4(2)	C(27)-C(26)-C(31)	118.2(6)
Mo -Cu -C(2)	48.1(2)	C(26)-C(27)-C(28)	120.6(6)
Mo -Cu -C(3)	47.2(2)	C(27)-C(28)-C(29)	120.7(7)
P -Cu -C(1)	132.7(2)	C(28)-C(29)-C(30)	118.2(7)
P -Cu -C(2)	129.0(2)	C(29)-C(30)-C(31)	122.3(7)
P -Cu -C(3)	134.7(2)	C(26)-C(31)-C(30)	119.9(6)
C(1)-Cu -C(2)	82.6(2)	Mo' -C(1')-Cu'	69.6(2)
C(1)-Cu -C(3)	78.6(2)	Mo' -C(1')-O(1')	171.5(5)
C(2)-Cu -C(3)	78.5(2)	Cu' -C(1')-O(1')	118.4(4)
Mo' -Cu' -P'	175.17(6)	Mo' -C(2')-Cu'	71.4(2)
Mo' -Cu' -C(1')	46.72(15)	Mo' -C(2')-O(2')	170.7(5)
Mo' -Cu' -C(2')	47.8(2)	Cu' -C(2')-O(2')	117.8(5)
Mo' -Cu' -C(3')	48.8(2)	Mo' -C(3')-Cu'	73.2(2)
P' -Cu' -C(1')	128.8(2)	Mo' -C(3')-O(3')	169.6(5)
P' -Cu' -C(2')	132.0(2)	Cu' -C(3')-O(3')	117.1(4)
P' -Cu' -C(3')	135.2(2)	N(1')-C(5')-C(6')	112.3(5)
C(1')-Cu' -C(2')	75.5(2)	C(5')-C(6')-C(7')	103.5(5)
C(1')-Cu' -C(3')	80.8(2)	N(2')-C(7')-C(6')	109.7(6)
C(2')-Cu' -C(3')	82.8(2)	N(3')-C(8')-C(9')	111.0(6)
Cu -P -C(14)	113.0(2)	C(8')-C(9')-C(10')	103.8(5)
Cu -P -C(20)	114.9(2)	N(4')-C(10')-C(9')	110.2(6)
Cu -P -C(26)	113.3(2)	N(5')-C(11')-C(12')	111.4(6)
C(14)-P -C(20)	102.7(2)	C(11')-C(12')-C(13')	104.7(6)
C(14)-P -C(26)	107.3(3)	N(6')-C(13')-C(12')	109.8(6)
C(20)-P -C(26)	104.7(3)	P' -C(14')-C(15')	119.4(5)
Cu' -P' -C(14')	119.1(2)	P' -C(14')-C(19')	121.7(5)
Cu' -P' -C(20')	111.3(2)	C(15')-C(14')-C(19')	118.9(5)
Cu' -P' -C(26')	111.1(2)	C(14')-C(15')-C(16')	120.3(6)
C(14')-P' -C(20')	104.3(3)	C(15')-C(16')-C(17')	119.7(6)
C(14')-P' -C(26')	104.6(3)	C(16')-C(17')-C(18')	120.7(6)
C(20')-P' -C(26')	105.5(3)	C(17')-C(18')-C(19')	119.7(6)
Mo -N(1)-N(2)	125.9(3)	C(14')-C(19')-C(18')	120.7(6)
Mo -N(1)-C(5)	128.3(4)	P' -C(20')-C(21')	119.0(5)
N(2)-N(1)-C(5)	105.7(5)	P' -C(20')-C(25')	122.1(5)
Ga -N(2)-N(1)	119.7(4)	C(21')-C(20')-C(25')	118.9(6)
Ga -N(2)-C(7)	131.5(5)	C(20')-C(21')-C(22')	121.3(6)
N(1)-N(2)-C(7)	108.7(5)	C(21')-C(22')-C(23')	118.4(6)
Mo -N(3)-N(4)	125.9(3)	C(22')-C(23')-C(24')	122.0(7)
Mo -N(3)-C(8)	127.8(4)	C(23')-C(24')-C(25')	119.5(7)
N(4)-N(3)-C(8)	106.2(4)	C(20')-C(25')-C(24')	119.8(6)
Ga -N(4)-N(3)	119.5(3)	P' -C(26')-C(27')	123.8(5)
Ga -N(4)-C(10)	132.2(4)	P' -C(26')-C(31')	117.8(5)
N(3)-N(4)-C(10)	108.2(5)	C(27')-C(26')-C(31')	118.4(5)
Mo -N(5)-N(6)	127.1(3)	C(26')-C(27')-C(28')	120.4(5)
Mo -N(5)-C(11)	127.2(4)	C(27')-C(28')-C(29')	120.5(6)
N(6)-N(5)-C(11)	105.6(4)	C(28')-C(29')-C(30')	120.0(6)
Ga -N(6)-N(5)	118.6(3)	C(29')-C(30')-C(31')	120.3(6)
Ga -N(6)-C(13)	132.9(4)	C(26')-C(31')-C(30')	120.3(6)

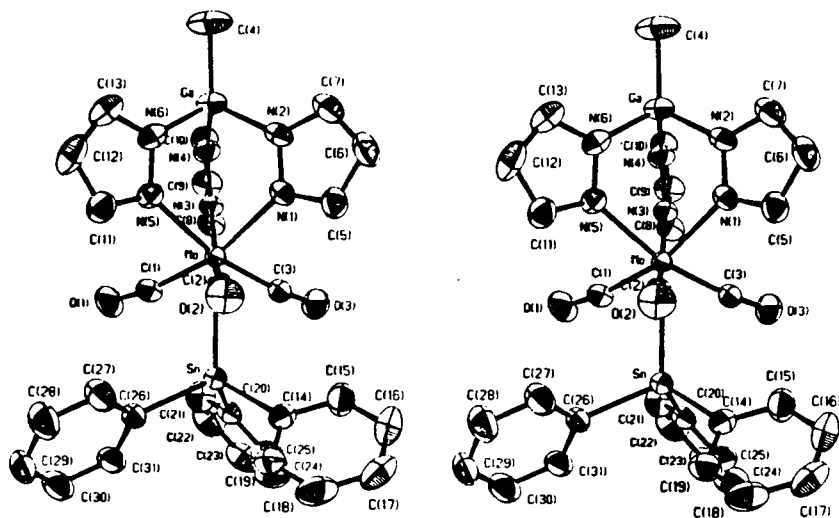
[MeGapz<sub>3</sub>]Mo(CO)<sub>3</sub>Cu(PPh<sub>3</sub>), cont'd

Intra-annular torsion angles (deg)

standard deviations in parentheses

Atoms	Value(deg)
(MeGapz <sub>3</sub> )Mo(CO) <sub>3</sub> Cu(PPh <sub>3</sub> )	
N(3)-Mo -N(1)-N(2)	42.9(4)
Mo -N(1)-N(2)-Ga	2.6(5)
N(4)-Ga -N(2)-N(1)	-53.3(4)
N(2)-Ga -N(4)-N(3)	47.5(4)
Mo -N(3)-N(4)-Ga	7.9(6)
N(1)-Mo -N(3)-N(4)	-49.1(4)
N(5)-Mo -N(1)-N(2)	-42.7(4)
Mo -N(1)-N(2)-Ga	2.6(5)
N(6)-Ga -N(2)-N(1)	49.6(4)
N(2)-Ga -N(6)-N(5)	-53.9(4)
Mo -N(5)-N(6)-Ga	5.4(5)
N(1)-Mo -N(5)-N(6)	38.4(4)
N(5)-Mo -N(3)-N(4)	37.7(4)
Mo -N(5)-N(6)-Ga	5.4(5)
N(6)-Ga -N(4)-N(3)	-56.6(4)
N(4)-Ga -N(6)-N(5)	48.9(4)
Mo -N(3)-N(4)-Ga	7.9(6)
N(3)-Mo -N(5)-N(6)	-46.0(4)
N(3')-Mo' -N(1')-N(2')	41.0(4)
Mo' -N(3')-N(4')-Ga'	5.3(6)
N(4')-Ga' -N(2')-N(1')	-53.6(4)
N(2')-Ga' -N(4')-N(3')	48.3(4)
Mo' -N(1')-N(2')-Ga'	3.8(6)
N(1')-Mo' -N(3')-N(4')	-46.3(4)
N(5')-Mo' -N(1')-N(2')	-44.4(4)
Mo' -N(5')-N(6')-Ga'	1.7(6)
N(6')-Ga' -N(2')-N(1')	48.5(4)
N(2')-Ga' -N(6')-N(5')	-51.3(4)
Mo' -N(1')-N(2')-Ga'	3.8(6)
N(1')-Mo' -N(5')-N(6')	41.4(4)
N(5')-Mo' -N(3')-N(4')	39.3(4)
Mo' -N(5')-N(6')-Ga'	1.7(6)
N(6')-Ga' -N(4')-N(3')	-55.1(4)
N(4')-Ga' -N(6')-N(5')	51.0(4)
Mo' -N(3')-N(4')-Ga'	5.3(6)
N(3')-Mo' -N(5')-N(6')	-43.5(4)

[MeGap<sub>3</sub>]Mo(CO)<sub>3</sub>SnPh<sub>3</sub>



Bond lengths (Å) with estimated  
standard deviations in parentheses

Bond	Length(Å)	Bond	Length(Å)
Sn -Mo	2.8579(3)	N(6)-C(13)	1.346(4)
Sn -C(14)	2.157(3)	C(5)-C(6)	1.377(5)
Sn -C(20)	2.166(3)	C(6)-C(7)	1.370(6)
Sn -C(26)	2.151(3)	C(8)-C(9)	1.380(5)
Mo -N(1)	2.244(2)	C(9)-C(10)	1.356(5)
Mo -N(3)	2.239(2)	C(11)-C(12)	1.380(5)
Mo -N(5)	2.244(2)	C(12)-C(13)	1.362(6)
Mo -C(1)	1.967(3)	C(14)-C(15)	1.384(5)
Mo -C(2)	2.000(3)	C(14)-C(19)	1.385(4)
Mo -C(3)	1.994(3)	C(15)-C(16)	1.386(5)
Ga -N(2)	1.923(3)	C(16)-C(17)	1.362(6)
Ga -N(4)	1.920(3)	C(17)-C(18)	1.379(6)
Ga -N(6)	1.931(3)	C(18)-C(19)	1.382(5)
Ga -C(4)	1.943(4)	C(20)-C(21)	1.372(5)
O(1)-C(1)	1.154(4)	C(20)-C(25)	1.380(5)
O(2)-C(2)	1.139(3)	C(21)-C(22)	1.384(5)
O(3)-C(3)	1.141(3)	C(22)-C(23)	1.386(6)
N(1)-N(2)	1.367(3)	C(23)-C(24)	1.351(6)
N(1)-C(5)	1.327(4)	C(24)-C(25)	1.390(5)
N(2)-C(7)	1.343(4)	C(26)-C(27)	1.380(5)
N(3)-N(4)	1.364(3)	C(26)-C(31)	1.388(4)
N(3)-C(8)	1.331(4)	C(27)-C(28)	1.376(5)
N(4)-C(10)	1.343(4)	C(28)-C(29)	1.384(5)
N(5)-N(6)	1.356(3)	C(29)-C(30)	1.372(5)
N(5)-C(11)	1.344(4)	C(30)-C(31)	1.386(5)

[MeGapz<sub>3</sub>]Mo(CO)<sub>3</sub>SnPh<sub>3</sub>, cont'd

Bond angles (deg) with estimated  
standard deviations in parentheses

Bonds	Angle(deg)	Bonds	Angle(deg)
Mo -Sn -C(14)	112.50(8)	N(3)-N(4)-C(10)	107.9(3)
Mo -Sn -C(20)	113.69(8)	Mo -N(5)-N(6)	125.4(2)
Mo -Sn -C(26)	113.00(8)	Mo -N(5)-C(11)	127.9(2)
C(14)-Sn -C(20)	105.57(11)	N(6)-N(5)-C(11)	106.6(2)
C(14)-Sn -C(26)	106.01(11)	Ga -N(6)-N(5)	120.5(2)
C(20)-Sn -C(26)	105.38(11)	Ga -N(6)-C(13)	130.7(2)
Sn -Mo -N(1)	129.32(6)	N(5)-N(6)-C(13)	108.9(3)
Sn -Mo -N(3)	127.95(6)	Mo -C(1)-O(1)	169.7(3)
Sn -Mo -N(5)	126.83(7)	Mo -C(2)-O(2)	172.1(3)
Sn -Mo -C(1)	67.22(9)	Mo -C(3)-O(3)	172.7(3)
Sn -Mo -C(2)	67.57(8)	N(1)-C(5)-C(6)	111.1(3)
Sn -Mo -C(3)	67.82(8)	C(5)-C(6)-C(7)	104.6(3)
N(1)-Mo -N(3)	85.61(9)	N(2)-C(7)-C(6)	109.2(3)
N(1)-Mo -N(5)	86.02(9)	N(3)-C(8)-C(9)	110.9(3)
N(1)-Mo -C(1)	163.46(11)	C(8)-C(9)-C(10)	104.2(3)
N(1)-Mo -C(2)	82.72(10)	N(4)-C(10)-C(9)	110.3(3)
N(1)-Mo -C(3)	83.38(10)	N(5)-C(11)-C(12)	110.3(3)
N(3)-Mo -N(5)	86.42(9)	C(11)-C(12)-C(13)	104.9(3)
N(3)-Mo -C(1)	82.32(10)	N(6)-C(13)-C(12)	109.4(3)
N(3)-Mo -C(2)	164.47(10)	Sn -C(14)-C(15)	121.9(2)
N(3)-Mo -C(3)	82.72(10)	Sn -C(14)-C(19)	120.2(2)
N(5)-Mo -C(1)	81.98(11)	C(15)-C(14)-C(19)	117.8(3)
N(5)-Mo -C(2)	82.59(10)	C(14)-C(15)-C(16)	120.9(3)
N(5)-Mo -C(3)	165.35(10)	C(15)-C(16)-C(17)	120.5(4)
C(1)-Mo -C(2)	106.84(12)	C(16)-C(17)-C(18)	119.6(3)
C(1)-Mo -C(3)	106.15(12)	C(17)-C(18)-C(19)	120.0(3)
C(2)-Mo -C(3)	105.97(12)	C(14)-C(19)-C(18)	121.1(3)
N(2)-Ga -N(4)	99.99(11)	Sn -C(20)-C(21)	122.7(2)
N(2)-Ga -N(6)	99.47(11)	Sn -C(20)-C(25)	119.6(2)
N(2)-Ga -C(4)	117.9(2)	C(21)-C(20)-C(25)	117.6(3)
N(4)-Ga -N(6)	100.00(11)	C(20)-C(21)-C(22)	122.2(4)
N(4)-Ga -C(4)	117.8(2)	C(21)-C(22)-C(23)	119.0(4)
N(6)-Ga -C(4)	118.1(2)	C(22)-C(23)-C(24)	119.7(3)
Mo -N(1)-N(2)	125.0(2)	C(23)-C(24)-C(25)	120.8(4)
Mo -N(1)-C(5)	128.4(2)	C(20)-C(25)-C(24)	120.7(4)
N(2)-N(1)-C(5)	106.5(2)	Sn -C(26)-C(27)	123.0(2)
Ga -N(2)-N(1)	120.7(2)	Sn -C(26)-C(31)	120.1(2)
Ga -N(2)-C(7)	130.6(2)	C(27)-C(26)-C(31)	116.9(3)
N(1)-N(2)-C(7)	108.6(3)	C(26)-C(27)-C(28)	122.2(3)
Mo -N(3)-N(4)	125.0(2)	C(27)-C(28)-C(29)	120.2(3)
Mo -N(3)-C(8)	128.3(2)	C(28)-C(29)-C(30)	118.7(3)
N(4)-N(3)-C(8)	106.7(2)	C(29)-C(30)-C(31)	120.6(3)
Ga -N(4)-N(3)	120.8(2)	C(26)-C(31)-C(30)	121.4(3)
Ga -N(4)-C(10)	131.0(2)		

## APPENDIX II

THEORETICAL INTENSITY PATTERNS FOR  
MASS SPECTROMETRIC ANALYSIS